HEWLETT-PACKARD
JOURNAL

Articles

© Hewlett-Packard Company 1991 Printed in U.S.A.

Departments

In this Issue

If the modulation bandwidth is 20 gigahertz, how high must the carrier frequency be? For fiber optic communications systems, where the carrier is light, the answer seems to be unspeakably high, since only the wavelength of the light is mentioned, never its frequency. Using carrier wavelengths around 1300 or 1550 nanometers—in the infrared region of the electromagnetic spectrum—today's fiber optic systems typically operate at data rates of hundreds of megabits per second. Gigabit-per-second systems are going into operation, and the components for ten-gigabit-per-second systems are being developed. Naturally, new test instrumentation and techniques are needed to help design, install, and maintain these new systems. This is the purpose of a new family of HP 20-GHz lightwave component analysis products whose members include a lightwave component analyzer, a lightwave test set, several lightwave sources, a lightwave modulator, and a lightwave receiver. Related but separate developments are an optical isolator and a lightwave converter. We're introduced to this family, its design philosophy, and its measurement capabilities in the article on page 6. Lightwave component analysis is similar to microwave network analysis except that the input port and/or the output port of the component being analyzed may be optical. The HP 8703A lightwave component analyzer (page 13) consists of a microwave network analyzer, lightwave and microwave test sets, a lightwave source with 20-GHz modulation capability, a processor, and a display in one integrated, calibrated instrument. Development of the internal lightwave source was a major challenge. The design uses an unmodulated laser followed by an optical modulator. This has the advantage that external lasers of other types and wavelengths can be substituted for the internal laser, but it required the development of the first integrated optical modulator for a commercial instrument (page 41) and a high-performance optical isolator to protect the laser from reflected energy (page 45). The HP 83420A lightwave test set (page 23) is designed for users who already have an HP microwave network analyzer and want to add lightwave component analysis capability. It provides most of the capabilities of the HP 8703A with very similar accuracies. The isolator, modulatable source, modulator, and two unmodulated laser sources are available as separate products. Accuracy considerations in the calibration and use of the HP 8703A analyzer are discussed in the article on page 34.

For those who only need to convert optical energy to electrical signals that can be measured by a spectrum analyzer, a network analyzer, a bit error rate tester, or an oscilloscope, the HP 11982A lightwave converter (page 51) provides an optical front end for these instruments.

Our second major subject this month is also a lightwave instrument. The HP 8153A lightwave multimeter represents an evolutionary design step from an optical power meter. With two plug-in slots added to a power meter mainframe and a selection of plug-in power sensor and optical source modules, the HP 8153A can make not only absolute power measurements on optical sources, but also relative power measurements and loss measurements on active and passive devices. The multimeter, its measurement capabilities, and its mechanical design are described in the article on page 58. The power sensor module design is the subject of the article on page 63. For the firmware design story, see page 77, and for the source modules, see page 73. Power measurement accuracy and how to measure it were major concerns in the multimeter design.

The question of accuracy measurement is being addressed by an emerging international standard for optical power meter calibration, as discussed in the article on page 70. Because the source modules are used for loss measurements, superior stability was the most important design objective for them. To accommodate future modules with unanticipated capabilities, the mainframe firmware looks in the module to find and upload any needed functions that aren't in the mainframe. The firmware automates many common functions so that many measurements can be made and plotted without any user programming.

The Apollo Domain operating system and the HP-UX operating system are both based on the UNIX operating system, a product (and a trademark) of UNIX System Laboratories, Inc. While expert computer programmers and users like the power and flexibility of these operating systems, casual and less technical users can be intimidated by the user interface, which is somewhat cryptic. HP VUE (see page 88) is an easy-to-learn and easy-to-use visual user interface for the Domain and HP-UX operating systems. Using a desktop metaphor, it offers the look and feel of the OSF/Motif graphical user interface along with iconic, point-and-click file manipulation and pull-down menus and dialog boxes that provide a friendly interface to many Domain and HP-UX utilities. The main component of HP VUE is the visual shell, which provides file manipulation and command execution. Several utilities are also included.

R.P. Dolan
Editor

Cover

Superimposed on a photograph of the optical modulator described in the article on page 41 are a simulated light beam (blue) and microwave energy (yellow), interacting in the modulator (green region) to produce a modulated light beam, represented here by a wavy blue line.

What's Ahead

In the April issue, we'll have articles about the design of the HP 8360 series of synthesized sweep oscillators with outputs to 50 GHz, and the design of a pair of millimeter-wave source modules that multiply microwave input signals (12.5 to 18.75 GHz) to V band (50 to 75 GHz) and W band (75 to 110 GHz). An automated test tool for C and C++ programs (HP Branch Validator), an instrument for generating I-Q signals to test North American digital cellular radios (HP 11846A), and a measurement system for verifying the accuracy of North American digital cellular transmitters (HP 11847A) will also have their design stories told.

High-Speed Lightwave Component Analysis to 20 GHz

A new family of instruments—analyzer, test set, sources, receivers, and modulator—characterizes electrical, electrooptical, and optical components of fiber optic communications sysems at modulation rates to 20 GHz.

by Roger W. Wong, Paul R. Hernday, and Daniel R. Harkins

FIBER OPTIC COMMUNICATIONS systems that have emerged over the last decade compete very well with more traditional communications systems as a cost-effective means for information exchange. These systems typically operate at hundreds of megabits per second, and pilot systems being installed work at gigabit-per-second rates. Research laboratories throughout the world are developing devices capable of operating at modulation bandwidths of many tens of gigahertz, and are developing building blocks that would bring reality and practicability to the 10-gigabit-per-second fiber optic communication system.

However, as the technology advances, system speeds exceed many gigabits per second, and the trend toward lowering the effective cost per bit and mile continues, the component designer needs to maximize the performance of each system block and minimize or eliminate adverse interactions among system blocks to optimize overall system performance. New techniques and tools are needed to help in the design, manufacture, and support of these components and systems. A knowledge of the latest concepts in characterizing such components, and of the modern measuring techniques used to quantify a device's performance, simplifies the tasks of design, evaluation, and characterization for the engineer.

The typical communication system (Fig. 1) can be partitioned into several subsystems such as the transmitter, the receiver, and the propagation medium. Individual network components include amplifiers, filters, modulators, and demodulators. All of these need to meet certain performance levels for the overall system to meet its objectives. It is customary to characterize a digital system's overall performance in terms of bit error rate (BER). However, although a bit error rate of 1×10^{-9} (one error per billion bits transmitted) is a meaningful system specification, it is rather difficult to derive from it a modulator or filter specification or characteristic to which the component can be designed. Furthermore, if the system does not meet the given BER specification, such a measurement of error rate provides very little diagnostic information for isolating a faulty assembly or component.

Derivatives of the BER measurements such as eye patterns are more powerful when it comes to detecting signal-to-noise degradations, but these cannot replace the fundamental component measurements like gain, bandwidth, or frequency response. When the bit rates are so high that most of the baseband signal energy is in the microwave frequency range, then reflections and multipath transmission cause major additional performance degradations, which have to be specified and characterized.[1]

Lightwave Component Analysis

In the ultrahigh-speed systems being designed in research laboratories, the modulated signals contain spectral components reaching well into the microwave region. In digital systems, where the information source is an encoded bit stream of high and low states, the information-carrying signal is usually a pulse sequence. The required bandwidth to transmit this sequence is derived from the pulse width of the signal, or conversely, the system's bandwidth defines the pulse shape, rise time, and overshoot of the applied time-domain signal.

With ultrafast gigabit systems, most of the signal energy is no longer propagated by electrons in conductors but rather in electromagnetic fields along transmission lines. Signal scattering caused either by mismatches (reflections) or by multipath transmission significantly degrades system performance.

The component designer needs to have tools to measure
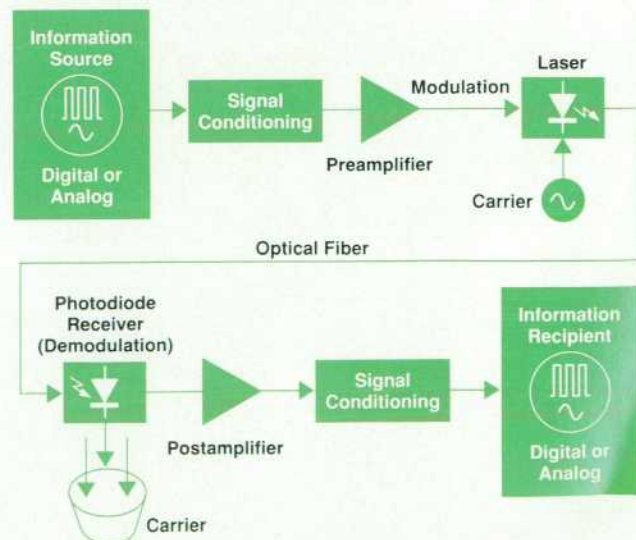
1. *Typical lightwave communications system.*
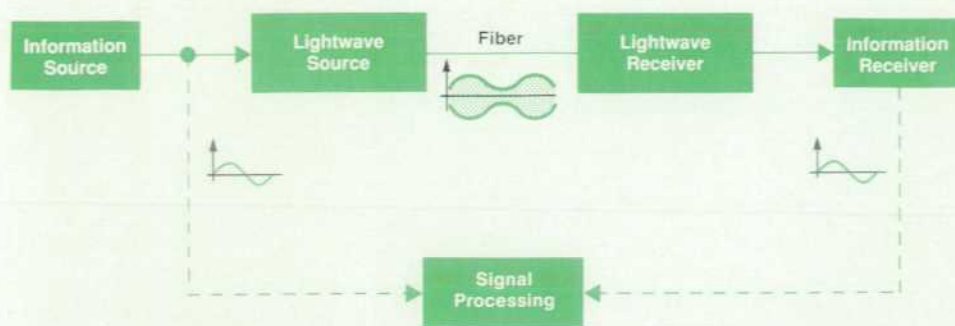
Fig. 2. *Lightwave component analyzer concept. The system compares transmitted and received sine wave modulation superimposed on a 1300-nm or 1550-nm optical carrier.*

and characterize each high-speed device in terms of its modulation frequency response (bandwidth), its microwave impedance, its optical return loss, its propagation time or equivalent electrical length, and its microwave and optical interactions with other high-speed devices. The making of these measurements on electrical, electrooptical, and optical devices is called lightwave component analysis. Typical devices are shown in Table I.

The lightwave component analyzer measurement concept is shown in Fig. 2. The lightwave component analyzer system measures a modulation transfer function of a device under test, providing the amplitude and phase characteristics. The information source is a sine wave signal incident to the transmitter. The sine wave modulation signal is placed on the light carrier to create an amplitude modulated light signal, which is transmitted through an optical device such as an optical fiber. The receiver demodulates the modulated signal after it has been operated upon by the device under test. The signal processing unit forms the complex ratio of the device's input and output (i.e., the modulation transfer function amplitude and phase) and applies the appropriate corrections for the device being measured.[2]

20-GHz Lightwave Measurement Needs

In years past, selected lightwave laboratories have developed their own measurement systems, which typically consisted of a directly modulatable laser diode (bandwidths 10 to 15 GHz), a photodiode detector, and a microwave network analyzer. Typically, these systems had limited dynamic range because of small signal levels either into the laser or from the photodiode, and they required extensive knowledge of the measurement block diagram and extraordinary care when connecting and measuring devices. This alternative of building one's own system did not exist except for a small number of laboratories, for there weren't then nor are there now any commercially available laser diodes with 15-GHz to 20-GHz modulation bandwidths.

To develop 20-GHz lightwave component analysis capability, our investments were focused on the optical modulator and on optical isolator technologies. One of the primary challenges in the 20-GHz lightwave program was to develop a lightwave source capable of 20-GHz modulation rates. More information on the optical modulator and isolator technology developments can be found in the articles on pages 41 and 45, respectively.

The objectives of the 20-GHz lightwave program were to provide lightwave component analysis measurements to customers who may and may not already own HP microwave network analyzers, and to provide lightwave technology to customers in the form of instruments and accessories. Fig. 3 shows the products that have resulted from the 20-GHz lightwave program. They are:

- HP 8703A lightwave component analyzer
- HP 83420A lightwave test set
- HP 83421A lightwave source
- HP 83422A lightwave modulator
- HP 83423A lightwave receiver
- HP 83424A lightwave CW source
- HP 83425A lightwave CW source.

Analyzer Design Objectives

The HP 8703A is the integrated system that combines the 20-GHz microwave and lightwave technologies to provide measurement solutions for high-speed component design and characterization. The key objectives were to provide 20-GHz lightwave component analysis measurement capabilities similar to earlier products,[2] to provide accurate, repeatable, and calibrated measurements, to provide the greatest possible measurement dynamic range with the technology used, and to provide a measurement system that was easy to use from both calibration and measurement standpoints. This system is designed for customers who do not already have HP microwave network analyzers.

The integrated system configuration allows more freedom to optimize system dynamic range by designing microwave components that drive the lightwave components at

Table I
Types of Lightwave Devices

	Electrical (RF) Output	Optical (Modulated) Output
Electrical (RF) Input	**Electrical-to-Electrical Devices** ■ Amplifiers ■ Coaxial Cables and Passive Components ■ Repeater Links	**Electrical-to-Optical Devices** ■ Laser Diodes and LEDs ■ Optical Sources ■ Optical Modulators
Optical (Modulated) Input	**Optical-to-Electrical Devices** ■ PIN Photodiodes ■ Avalanche Photodiodes ■ Optical Receivers	**Optical-to-Optical Devices** ■ Optical Fibers, Passive Components, Attenuators ■ Optical Modulators ■ Regenerators

Fig. 3. *New HP 20-GHz lightwave instruments include the HP 8703A lightwave component analyzer, the HP 83420A lightwave test set, the HP 83421A lightwave source, the HP 83422A lightwave modulator, the HP 83423A lightwave receiver, the HP 83424A lightwave CW source, and the HP 83425A lightwave CW source (not shown).*

their preferred levels and optimize the lightwave and microwave interfaces. Fig. 4 shows the HP 8703A system, which consists of three sections. The top section performs the signal processing and display functions and the user interface function. The middle and lower sections perform the microwave and lightwave test set functions, respectively. They condition and route the appropriate signals through the appropriate RF switches to provide accurate, repeatable, and fast measurements.

The lightwave test set consists of a modulatable optical source, a 3-dB directional coupler, and an optical receiver. The six RF switches in the middle and bottom sections allow a much simplified calibration and measurement process that minimizes the effects of RF cable nonrepeatablity and RF mismatches. A more detailed discussion of the HP 8703A system design issues, trade-offs, and solutions appears in the article on page 13.

Test Set Design Objectives

For those who already have an HP microwave network analyzer but want to add basic 20-GHz lightwave measurement capability, the HP 83420A lightwave test set is the most cost-effective approach. The design objectives for this project were similar to those of the HP 8703A, except that the test set would work with existing HP 8510B, HP 8720B, and HP 8757C network analyzers.

Fig. 5 shows a lightwave component analyzer system configured with the HP 83420A lightwave test set, the HP 8510B network analyzer, and an HP 9000 Series 300 computer acting as system controller. Because the block diagrams of the network analyzers were already defined and fixed, the test set definition had its challenges and constraints. The most severe constraint, fixed network analyzer interfaces, precluded incorporating an RF switch matrix into the measurement system. Consequently, users must effect a few more cable connections and disconnections than are necessary to perform the same device measurements with the HP 8703.

The optical measurement dynamic range of the system of Fig. 5 typically approaches that of the HP 8703A within a few dB. The system provides all basic lightwave device measurements, and the external controller provides the same guided calibration and measurement setup instruc-
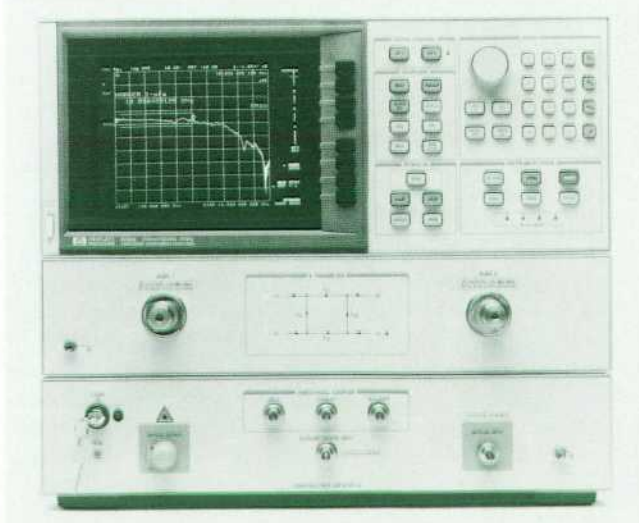

Fig. 4. *HP 8703A lightwave component analyzer.*

Fig. 5. *HP 83420A lightwave test set with the HP 8510B microwave network analyzer.*

tions as the integrated system. More detailed information on the lightwave test set and its development are given in the article on page 23.

Measurements

Table II lists the basic transmission and reflection measurements most useful for the design, evaluation, and characterization of high-frequency components.[3,4] Fig. 6 shows the HP 8703A connections for the four types of devices. A few of the more unusual measurements and their applications will be covered in this article.

1550-nm Chromatic Dispersion Fiber Measurement

Chromatic dispersion in standard single-mode optical fiber crosses through the zero dispersion point in the 1300-nm wavelength band and reaches values of approximately 16 ps/km-nm at 1550 nm. Fig. 7a illustrates the effects of chromatic dispersion on a signal. Consider an intensity modulated signal with upper and lower sidebands spaced f_1 from the carrier. As the signal propagates along the fiber, each component travels at a slightly different velocity, resulting in time delays from one component to another. For a given length of fiber, there exists a set of modulation frequencies at which the sidebands are phase shifted to the extent that the AM component vanishes and nulls occur in the baseband AM response of the fiber. A closed-form expression predicts the frequencies at which this will occur and allows the fiber dispersion value to be calculated.[4,5,6]

The baseband AM response of a 17.7-km single-mode fiber is shown in Fig. 7b. The fiber was measured in the optical transmission configuration shown in Fig. 6. The source was a 1550-nm DFB (distributed feedback) laser. The measurement was done in step sweep mode to provide the most accurate signal detection despite the long transmission delay. It was performed twice, at different values of HP 8703A optical modulator bias voltage, to eliminate the effect of residual phase modulation. The null frequencies of the two measurements are averaged. The dispersion determined in this manner is 16.2 ps/km-nm.

Laser FM Response Measurement

Frequency-shift keying (FSK) systems shift the frequency
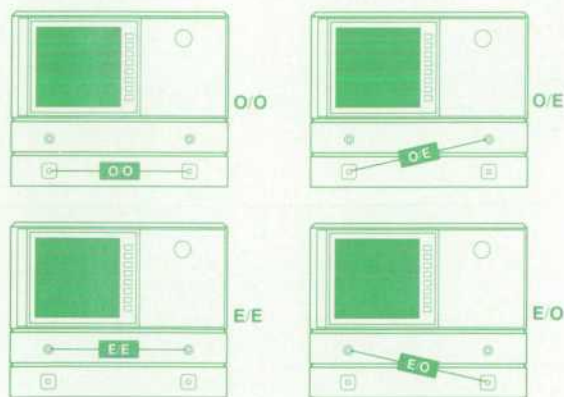
Fig. 6. HP 8703A device connection diagrams for different device types. E/O indicates a device with an electrical input and an optical output (e.g., a laser), and so on. See Table I for device types.

Table II
Lightwave Component Analysis Measurements*

Transmission

Insertion Loss/Gain
Frequency Response
  Modulation Bandwidth
  Flatness
  Slope Responsivity (a)
Time-Domain Analysis
  Rise Time
  Pulse Dispersion
Delay
Length
Insertion Modulation Phase
Group Delay (as applied to the information)
ϵ_r or n (index of refraction)
Reflection Sensitivity (E/O devices)

Reflection

Return Loss
Impedance (electrical/RF)
Reflectometry
  Electrical Time-Domain Reflectometry
  Optical Frequency-Domain Reflectometry (OFDR)
Delay
Length

(a) Conversion efficiency of electrical/optical or optical/electrical devices only

*Apply to electrical/electrical (E/E), electrical/optical (E/O), optical/electrical (O/E), and optical/optical (O/O) devices unless specified otherwise.

of an optical carrier in response to a modulating signal. Since DFB lasers produce carrier frequency shifts of 100 MHz to 2 GHz per milliampere of bias current, they are often chosen as sources in FSK systems. Very high FM rates are achieved by the mechanism of carrier modulation. Thus, there is interest in measuring FM laser response as a function of bias current.

Coherent detection FSK systems typically use a local oscillator laser at the receiving end. Alternatively, an optical frequency discriminator can be used to convert the incoming FM signal to an AM signal, allowing the use of conventional direct detection schemes, which are well understood. The discriminator may be a Mach-Zehnder or Michelson interferometer or a ring resonator. The concerns in such systems are the FM response of the DFB laser and the bandwidth of the receiver electronics.

FM response tests require some form of optical frequency discriminator. As an example, assume that a Mach-Zehnder interferometer is used as the discriminating element. When operated at quadrature, the point halfway between full output and minimum output, the interferometer produces an output optical intensity that varies linearly with changes of carrier frequency. Using an FM discriminator of known sensitivity with a lightwave component analyzer (HP 8703A or HP 83420A + network analyzer), the DFB laser's AM and FM frequency responses can be measured.[4]

Fig. 8 shows measurements of the AM and FM responses

of a 1300-nm DFB laser. The two responses are constructed by adding and subtracting measurements performed at adjacent quadrature points of the discriminator, that is, at discriminator operating slopes of opposite sign but identical magnitude. The relative levels of AM and FM depend upon the differential path length of the discriminator. This measurement can be calibrated with the use of an external modulated optical power reference. Note that the measurement reveals a null in the FM response at 3.7 GHz.

Receiver Optical Launch Measurement

One common application for optical reflection measurements is the design and characterization of optical launches onto a photodiode receiver. Of interest to the designer would be not only the overall return loss of the launch including the optical connector and launch optics, but also the location and return loss value of each individual reflection.

(a)

Fig. 8. *FM laser response measurement.*

By using the lightwave component analyzer technique and its time-domain capabilities, selective reflection measurements—the separation of optical reflections in the distance domain—are easily made on a wide variety of optical sensors, lightwave components, subsystems, and systems. An optical mismatch can be measured by separating the incident test signal from the reflected one by means of a directional coupler. The ratio of reflected to incident signals yields the reflection coefficient magnitude at the optical frequency and can be measured by an optical power meter. However, using the lightwave component analyzer technique and applying a modulated test signal has the advantage that the origin of the reflected signal can be determined by computing the propagation delay and distance from the envelope (modulated) phase shift of the reflected signal. Furthermore, it is possible to apply the same technique to mutliple reflections, thus separating them in the distance or time domain. This method of

(b)

Fig. 7. *(a) Fiber chromatic dispersion concept. (b) Fiber chromatic dispersion measurement.*
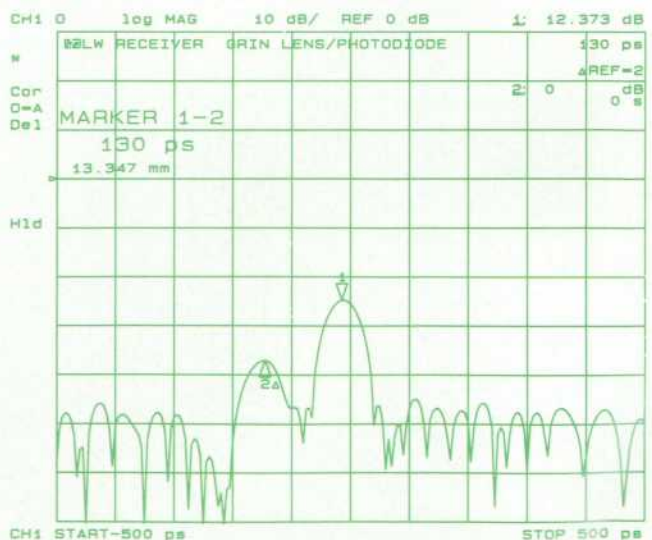
Fig. 9. *Optical reflection measurement of a lightwave receiver GRIN lens optical launch.*
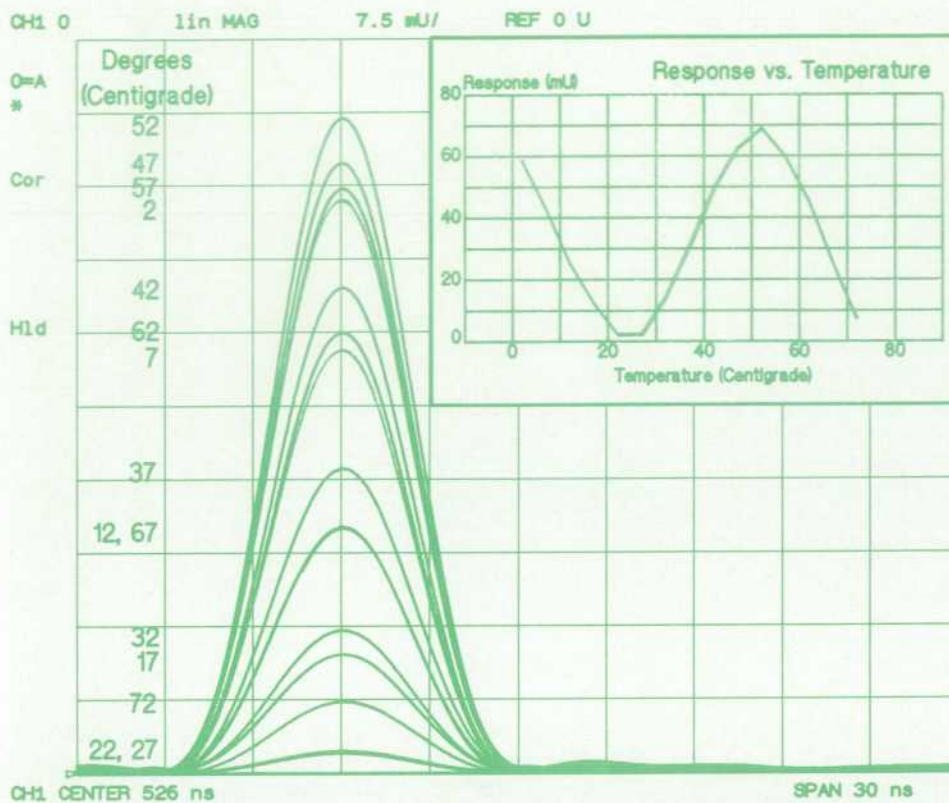
Fig. 10. *Fiber temperature sensor measurement. The test device is a 1-mm Fabry-Perot sensor 50 m away. (Test device courtesy of Texas A&M University Department of Electrical Engineering.)*

measuring optical reflections is far superior to the power meter approach, which yields only an average reflection coefficient with no indication of the number of reflections or their amplitudes or positions.[1]

Fig. 9 shows a selective reflection measurement of a photodiode receiver optical launch using a GRIN (graded-index) lens. Marker 2 shows a return loss of 35 dB created by the interface of a fiber to the first surface of the GRIN lens with index matching compound. Marker 1 shows the combination of the reflection from the second GRIN lens surface, which is antireflection-coated, and the photodiode surface (25 dB return loss). The two responses are spaced about 14 mm apart, which corresponds to the length of the GRIN lens used.

The lightwave component analyzer system has a maximum modulation frequency range of 20 GHz. The inverse of the maximum frequency range, in this case 50 ps, determines the theoretical limit for resolving two closely spaced and equal reflections. In other words, the system can resolve two closely spaced reflections whose round-trip signal travel time is equal to or greater than 50 ps, which corresponds to two reflections spaced approximately 5 mm apart in optical fiber. This limit is often referred to as the two-event resolution or response resolution of the system.

Temperature Sensor Measurement

In-line Fabry-Perot sensors, currently in development, can be cascaded and are immune to electromagnetic interference, making them ideal candidates for aircraft, ships, and industial plants. They are built by coating a cleaved fiber with a low-reflectance dielectric mirror, then reattach-

ing the fiber with a fusion splice. The process is repeated some small distance down the fiber to create the short Fabry-Perot interferometer. Light incident on the sensor is partially reflected by both mirrors. Since the sensor is shorter than the coherence length of the light source in the measurement, the two reflections will interfere strongly as the sensor expands and contracts with temperature. Such sensors must be individually calibrated. These sensors can be interrogated using either time-domain or frequency-domain reflectometry techniques.

The frequency-domain reflectometry measurement uses
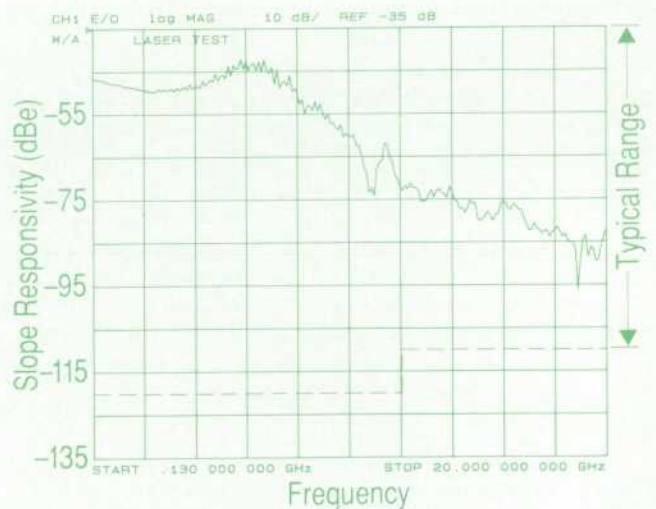
Fig. 11. *Laser frequency response measurement dynamic range. 85 dBe is typical.*
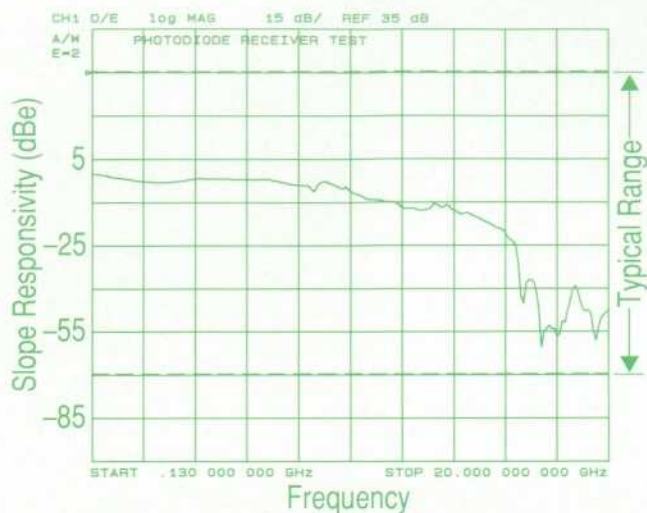
Fig. 12. *Photodiode frequency response measurement dynamic range. 105 dBe is typical.*

Fig. 13. *Optical system dynamic range using an optical attenuator.*

a 1550-nm DFB laser whose linewidth is about 30 MHz. The light from the laser source is coherent over the length of the Fabry-Perot sensor. Measurements are taken at intervals of 5°C, and the data is transformed to the time domain, as shown in Fig. 10. Since the two Fabry-Perot surfaces are separated by less than the distance resolution of the instrument, the combined reflections appear as a single reflection having an amplitude that depends upon temperature.

System Performance

Dynamic range is a common figure of merit for test instrumentation. Typical system performance is dependent upon many factors such as the HP 8703A measurement calibration routine selected (e.g., response, response/isolation, etc.), the signal drive levels used, and the signal processing features selected (e.g., IF bandwidth, signal averaging, signal smoothing). To convey the typical dynamic range performance of the HP 8703A system, three devices were selected: a laser diode (E/O device), a photodiode (O/E device), and an optical attenuator (O/O device), as shown in Figs. 11, 12, and 13, respectively.

Figs. 11 and 12 show the typical slope responsivity or conversion efficiency measurement dynamic ranges for laser/transmitter and photodiode/receiver devices. The dynamic ranges are typically 85 and 105 electrical dB for transmitter and receiver devices, respectively.

Fig. 13 shows the transmission measurement dynamic range for optical devices. An optical step attenuator provided various values of attenuation. The noise floor of the system shown varies from approximately 48 to 44 optical dB over frequency. The response/isolation measurement calibration routine was selected with an IF bandwidth of 10 Hz and an averaging factor of 16 for the 40-dB and 50-dB attenuator steps.

Acknowledgments

Contributions to the development of the lightwave and microwave technologies, hardware components, and system calibration and design that went into the 20-GHz light-

wave component analyzer, test set, and accessories came from many people located in many Hewlett-Packard entities. We would like to thank Waguih Ishak, Steve Newton, Bill Chang, Dave Dolfi, and their teams at HP Laboratories and we certainly appreciate their many contributions in lightwave technology and support. Over the course of the project, the codevelopment efforts, cooperation, and support we enjoyed with Bob Bray, Mark Zurakowski, Roger Jungerman, and their teams at the Microwave Technology Division were greatly appreciated and much welcomed. It was through the joint efforts of both divisions' teams that the optical modulator was developed from a device of notable scientific curiousity to one capable of meeting manufacturing standards of quality, performance, and robustness. Finally, we would especially like to thank the members of our Network Measurements Division lightwave team for their dedication and teamwork in meeting the challenges and rigors of the aggressively scheduled 20-GHz lightwave program. Additionally, we greatly appreciate the help and support we received from our support groups and other R&D personnel during the development and new product introduction phases of the program. And to Hugo Vifian, a special word of thanks and appreciation for his unwavering support, confidence, and commitment during this development program.

References
1. H. Vifian and R. Wong, "Characterizing High-Speed Lightwave Components," *Fiberoptic Product News*, Vol. 4, no. 10, October 1989, pp. 22-28 and 39, and Vol. 4, no. 11, November 1989, pp. 24-26.
2. R. Wong, P. Hernday, M. Hart, and G. Conrad, "High-Speed Lightwave Component Analysis," *Hewlett-Packard Journal*, Vol. 40, no. 3, June 1989, pp. 35-51.
3. R. Wong, P. Hernday, and M. Hart, "Technical Innovations for the Design of a New 20-GHz Lightwave Component Analyzer," *Hewlett-Packard RF and Microwave and Lightwave Measurement Symposium*, October 1989.
4. P. Hernday, R. Wong, and D. Harkins, "Advanced Applications of 20-GHz Lightwave Component Analysis," *Hewlett-Packard RF*

and Microwave and Lightwave Measurement Symposium, July 1990.

5. S. Bahsoun and J. Nagel, AT&T Bell Laboratories, private communication, November 1989.

6. P. Hernday and R. Wong, "20-GHz Lightwave Component Analysis Instrumentation Using an Integrated Optical Modulator," Optical Fiber Communication Conference (OFC), San Francisco, January 1990.

Design of a 20-GHz Lightwave Component Analyzer

The HP 8703A is a fully integrated and calibrated instrument for lightwave component characterization. It offers a choice of wavelengths and laser types, both internal and external.

by Paul R. Hernday, Geraldine A. Conrad, Michael G. Hart, and Rollin F. Rawson

A LIGHTWAVE COMPONENT ANALYZER measures the ratio of a signal incident on a device under test—the stimulus—and a related signal coming from the device under test—the response. The stimulus is a sinusoidal electrical signal or an optical signal with sinusoidal intensity modulation. The response signal may be electrical or optical.

Key elements of such a measurement system are a modulated lightwave source and a lightwave receiver. Accompanying elements, derived from a vector network analyzer, include a synthesized RF/microwave source, a multichannel receiver, a test set, and a signal processing, control, and display section. This combination of instrument blocks, with its array of electrical and optical test ports, allows measurements of the types of components found in lightwave communication systems as well as other types of optical and optical fiber components.

Different product concepts and system configurations were considered during the design of the HP 8703A lightwave component analyzer. Project objectives included 20-GHz measurement capability, versatility, ease of use, measurement accuracy, traceability to respected standards, and system value. The first concept considered was the approach used in the HP 8702B lightwave component analyzer,[1] which had a separate source and receiver. This provides the greatest flexibility in configuring measurements and allows the versatility of using the lightwave source and receiver with other microwave instruments. However, flexibility comes at the price of increased complexity in connections and calibration. In addition, questionable repeatability of measurements at 20-GHz modulation rates may contribute to large measurement errors. Although this approach offered the most flexibility, measurement accuracy and ease of use were considered more important design goals, so this approach was rejected.

The design finally selected is an integrated analyzer system. By integrating the system, the measurement dynamic range and accuracy were optimized and the user interface was simplified. The HP 8703A consists of two subsystems connected as one fully integrated and calibrated system (Fig. 1). The upper box is a modified vector network analyzer and contains the RF test set and the processing and display section. The lightwave components are housed in the lower box. The front panel has a centralized and simple layout making measurements easy to configure. A matrix of RF and optical switches is controlled automatically by the analyzer to distribute electrical and optical signals according to the type of device under test. The RF switches have excellent repeatability, typically a few hundredths of a dB, which greatly improves overall measurement repeatability. Internal signal paths are comprehensively calibrated with respect to the test ports. This allows measurement calibration to be performed with only a few simple connections. A more detailed discussion of measurement calibration is given later in this article. Calibration of internal signal paths is discussed in the article on page 34.

RF Test Set and Signal Processing

The upper box of the HP 8703A lightwave component analyzer is based on the HP 8720B network analyzer. It contains the RF test set, signal processor, and display. The RF source in the HP 8720B was modified for use in the HP 8703A. The receiver, the digital control, the display, and the power supply are the same for both analyzers.

A synthesized source generates a swept or CW signal in

the range of 130 MHz to 20 GHz. The full frequency range is covered in subsweeps harmonically locked to a fractional-N synthesizer. The higher frequency bands are provided by YIG oscillators, while the low band is obtained by heterodyning YIG and fixed oscillators. Some of the electrical source signal is used to establish a magnitude and phase reference and for phase-locking and level control. The HP 8703A uses a four-stage GaAs amplifier to boost the electrical output power available at the front-panel electrical ports. The analyzer's electrical output level is adjustable from +5 dBm to −50 dBm in 5-dB steps.

An RF switch in the test set routes the output of the source either to the lightwave test set or to the RF test ports. Another RF switch selects either RF port 1 or RF port 2 as the output port. Port 1 and port 2 are at the outputs of broadband directional couplers used as signal separation devices for reflection measurements. When port 1 is selected as the output port the signal passes directly through the coupler, and when port 2 is selected the signal is coupled. As a result, the maximum power available at port 2 is approximately 20 dB lower than at port 1.

The receiver measures and processes the input signals for display on the built-in CRT. The receiver has three identical samplers: A, B, and R. The A and B samplers are
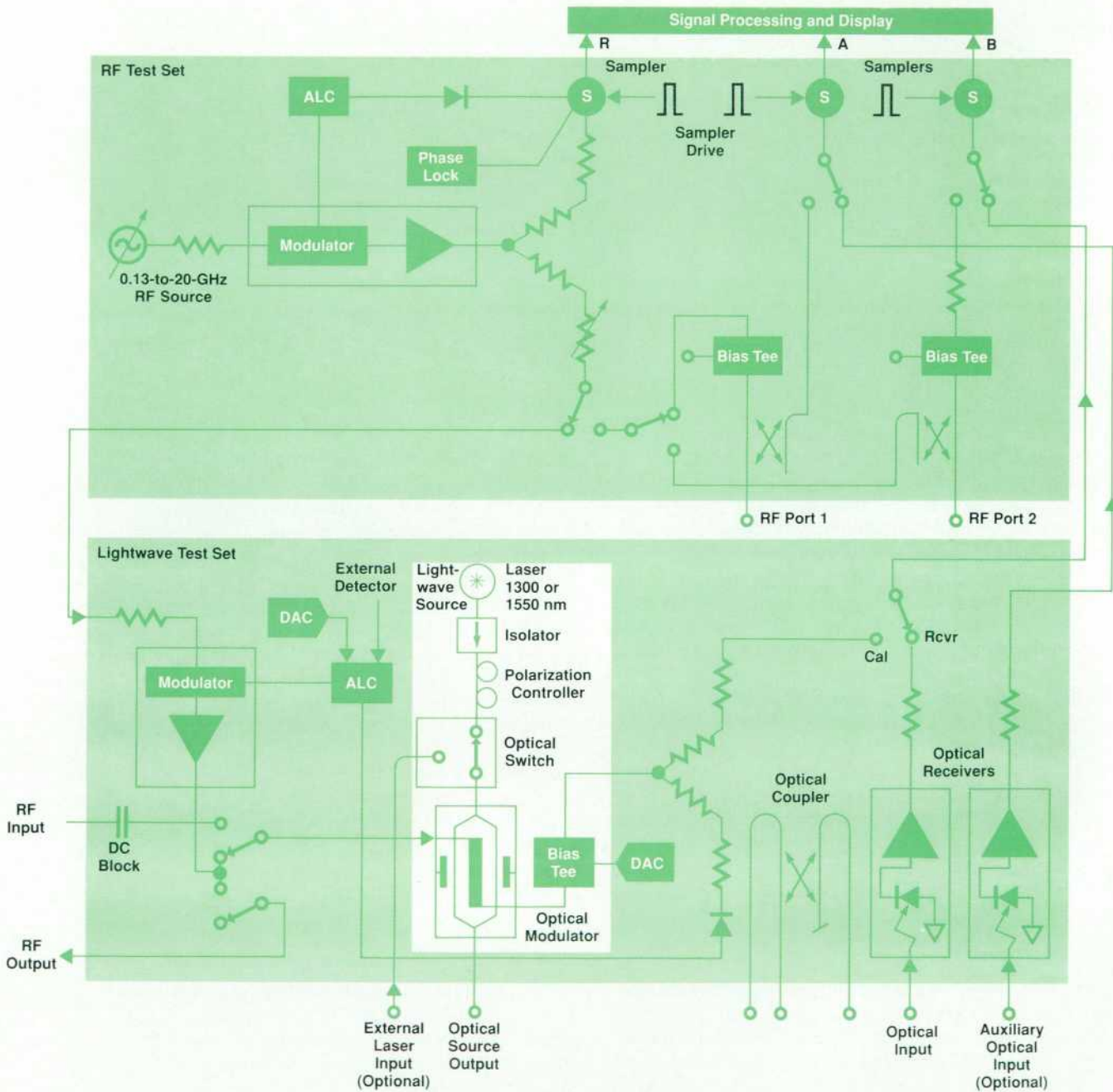

Fig. 1. *HP 8703A lightwave component analyzer block diagram. The top units contain the RF test set and the processing and display module. The bottom unit houses the lightwave test set.*

each preceded by an RF switch. These switches select whether the sampled signal is from the lightwave test set or the RF test set. When the RF test set is selected the A sampler measures either the reflected signal returning to port 1 or the signal transmitted to port 1. Similarly, the B sampler measures either the reflected signal returning to port 2 or the signal transmitted to port 2. The A, B, and R signals are down-converted in two stages to a fixed 4-kHz IF. The digital IF stage converts the 4-kHz IF into digital format and forms the ratios A/R and B/R. These ratios are complex quantities providing magnitude and phase information. These vector measurements offer important signal processing advantages over magnitude-only scalar measurements. Data can be averaged to reduce noise. The accuracy of measurements can be enhanced using error correction techniques. Additional information can be obtained by transforming frequency-domain measurements to the time domain.

Signal processing following the digital IF stage is done in the digital control section by the instrument firmware. Most of the instrument firmware was reused from the HP 8720B. This helped maintain a common user interface with other Hewlett-Packard network and component analyzers and significantly reduced the development effort. The data processing flow includes noise reduction, error correction, time-domain transform, formatting, scaling, and display of measured data. This is the same processing performed in other Hewlett-Packard network analyzers and in the HP 8702B lightwave component analyzer.[1]

Lightwave Test Set

The lightwave test set (Fig. 1) consists of the lightwave source, the RF drive path, printed circuit boards containing the automatic level control (ALC) circuits, laser and modulator bias circuits, and front-panel controls, and the lightwave receiver.

Lightwave Source

The lightwave source produces light that is intensity modulated at microwave frequencies. The source of light is an unmodulated (CW) semiconductor laser. The light is directed through a high-performance isolator to protect the
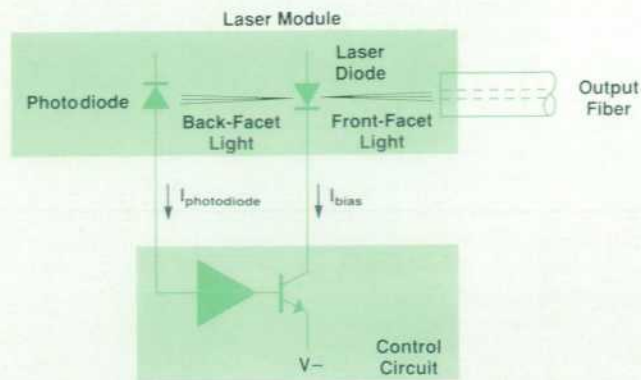
Fig. 2. Laser thermal control loop.

laser from the destabilizing influence of reflected light. Next, the light passes through a polarization controller, which is rotated to create the proper state of polarization at the input of the optical modulator. The modulator operates at maximum efficiency when its light input is linearly polarized and the E-field is in the plane of the modulator circuit. After exiting the modulator, the laser light is routed to the front panel OPTICAL OUTPUT connector.

Modulation Technique

The design goals included developing a lightwave source with 20-GHz modulation capability. This can be achieved by direct current-injection modulation of lasers, or by external intensity modulation using modulator or heterodyne techniques. While direct modulation of diode lasers to 20 GHz has been achieved, the approach suffers from signal-induced degradation of the optical spectrum. Spectral width, modal distribution, and even center wavelength can be affected by the application of a large electrical drive signal.

The optical heterodyne technique, in which two highly stable single-line lasers, slightly offset in frequency, are combined to produce a beat signal, can achieve the desired modulation bandwidth. Typically, the lasers, which are temperature tuned, require precise control of temperature and long measurement times. In addition, modulation

Fig. 3. Laser diode bias control loop.

phase is not well-defined.

The technique used in the HP 8703A is external modulation. The light output of a high-power CW laser diode is intensity modulated by a lithium niobate modulator. This allows the use of a variety of laser sources, such as Fabry-Perot, DFB (distributed feedback) or external cavity, with the same modulator. The drawbacks to this technique over direct modulation are the added components, additional optical insertion loss, and the need for polarization control.

Dual-Wavelength Capability

To meet the need for measurement capabilities at the two telecommunications wavelengths (1300 and 1550 nm), two alternatives were considered: (1) to provide the dual-wavelength capability entirely within the HP 8703A system, or (2) to provide a single laser of either wavelength and allow access to the modulator by other lasers via an external laser input port.

Providing both wavelengths internally restricts laser choices and increases the cost of the instrument for users who do not need the capability. The external laser input alternative was chosen because it offers the best value and flexibility to the user. Option 100 adds the external laser input port and an optical switch to select between internal and external sources. Examples of external lasers include Fabry-Perot, DFB, DBR (distributed Bragg reflector), and various types of external cavity lasers at either wavelength. The external laser must be well-isolated to avoid reflected light effects. Its polarization must be adjusted with an external polarization controller. Two DFB CW laser instruments, the HP 83424A and HP 83425A, are available as companion sources at 1550 nm and 1308 nm, respectively. These lasers typically have greater than 80 dB of optical isolation and a two-section polarization controller to present the appropriate polarized light to the optical modulator in the HP 8703A. As internal lasers, the HP 8703A system offers either a 1308-nm Fabry-Perot laser or a 1308-nm (Option 220) or 1550-nm (Option 210) distributed feedback laser.
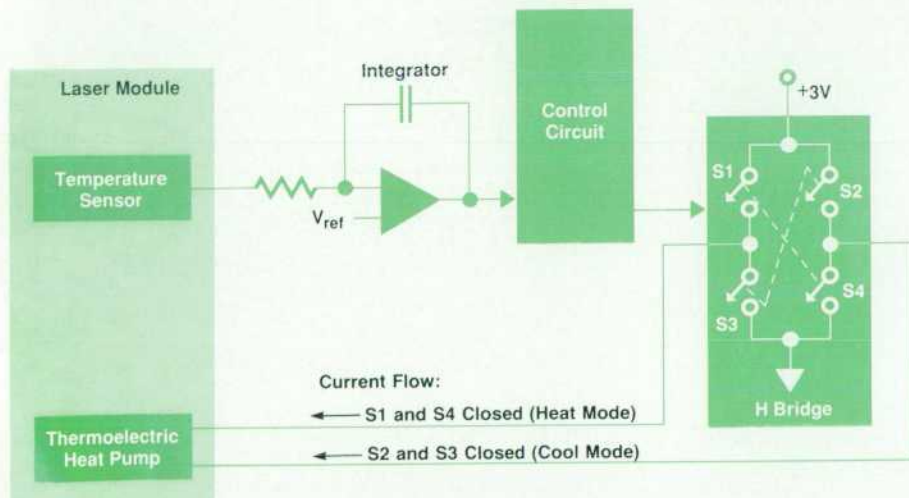
Optical Modulator

The optical modulator within the HP 8703A lightwave source has an optical transfer function that is dependent on both bias and wavelength. Thus, when the user changes wavelength, the bias to the optical modulator must be optimized to ensure proper operation. This is conveniently implemented as an autobias function which automatically adjusts the bias if the wavelength is changed or if an optical measurement calibration is performed. The design of the optical modulator is discussed in the article on page 41.

Source Temperature Control

The source can contain either a Fabry-Perot or an optional DFB laser. In either case, the wavelength and output power vary as a function of temperature.

To minimize the temperature effects, a thermal control loop maintains the temperature of the laser at its specified value. The thermal loop maintains the temperature within 0.1°C over the environmental temperature range of 0°C to +55°C. The laser diode and temperature sensor are both mounted on the surface of the thermoelectric heat pump

inside the laser module. A voltage proportional to the temperature of this surface is generated by the sensor and applied to an integrator as an error signal (Fig. 2). The integrator output serves as a control signal for the 70-kHz pulse width modulated current control circuit consisting of an H-bridge. The H-bridge directs the current through the thermoelectric heat pump in the proper direction to either heat or cool the laser.

Laser bias current is controlled by another loop (Fig. 3) consisting of a photodiode, an amplifier, and the laser bias current source.

The laser diode chip has front and back facets from which light is emitted. The front-facet light is coupled into the fiber and on to the isolator. The back-facet light is coupled into a photodetector which generates a current proportional to the back-facet light. This current is transformed into an error voltage which controls the laser diode current source such that the laser maintains an output power of 5 mW.

Protection from Optical Reflections

Lasers are very sensitive to reflected light reentering the laser cavity. This effect, referred to as reflection sensitivity, changes the linewidth, modal distribution, and transfer characteristics of a laser. The susceptibility of a laser to reflected light depends on many factors, including the magnitude, delay, and polarization of the reflected light. Reflection sensitivity can be reduced with an optical isolator or a well-matched attenuator.

Sources of reflections within the lightwave source include optical modulator input and output transitions, the output connector, the device under test, and the receiver.

To conserve optical power while preserving the integrity of the laser, the optical isolator approach was selected. The isolator is required to have low loss (3.5 dB maximum), high isolation (50 dB minimum) and minimum impact on the degree of polarization. A specially developed HP isolator, described in the article on page 45, meets the above requirements. Fig. 4 shows how the reflection sen-
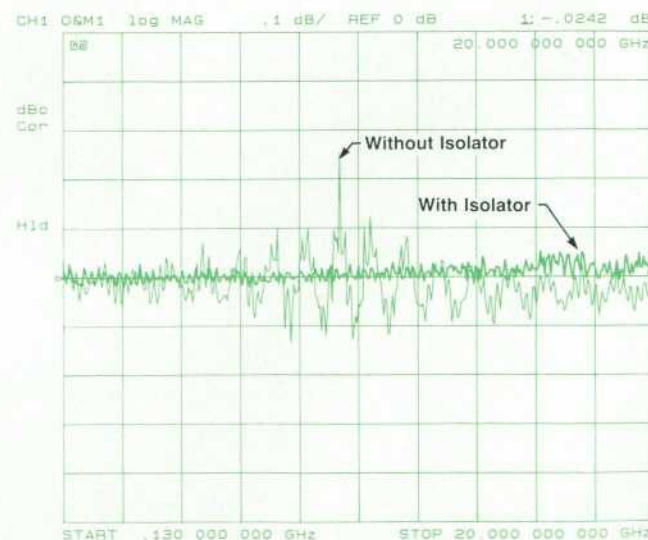

Fig. 4. *Reflection sensitivity of the HP 8703A lightwave source module with and without the isolator, showing improvement from more than 0.3 dB to less than 0.05 dB peak to peak.*

sitivity of the HP 8703A lightwave source is reduced to less than 0.05 dB by the additional isolation.

Optimizing Polarization

The key component of the lightwave source is the optical modulator. It is based on the electrooptic effect in lithium niobate material. Generally, the crystal is cut such that an applied electric field produces the largest possible electrooptic effect. In this case, the optical modulator is an x-cut device. Since the horizontal component of the electric field experiences maximum effect, the polarization of the applied optical signal must be horizontal.

Regular single-mode fiber does not propagate a fixed state of polarization. Two possible solutions were investigated. One was polarization-maintaining fiber, and the other was a polarization controller.

If linearly polarized light is launched along one of the principal axes of polarization-maintaining fiber, its polarization state remains essentially unchanged as it travels down the fiber. Using this technique, the linearly polarized light output of the laser chip could be presented at the correct angle to the optical modulator. However, this solution would have required all components ahead of the optical modulator to have polarization-maintaing fiber pigtails, and this carries a penalty in cost and fabrication com-
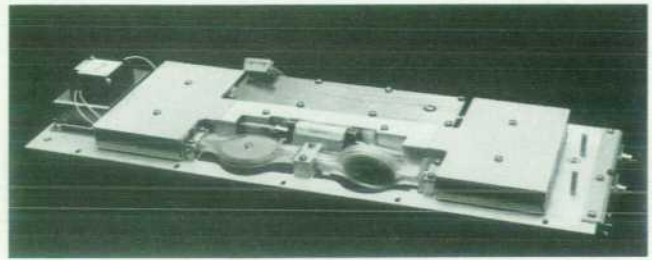

Fig. 5. *Lightwave source, showing axially mounted two-element polarization controller.*

plexity.

The polarization controller used in the HP 8703A is of the fiber type. The fiber is coiled to create physical stress in the plane of the coil. Light with its E-field in the plane of the coil travels at a slightly different velocity than light traveling in the nonstressed axis. This process is controlled by rotating the coil about the axis of the input fiber, thereby changing the way input light is resolved along the stress-induced fiber axes and therefore transforming the polarization state from input to output.[2]

To minimize cost and provide simple adjustment, the HP 8703A lightwave source uses an axially mounted two-

---

Measurement Capabilities of the HP 8703A Lightwave Component Analyzer and the HP 71400C Lightwave Signal Analyzer

Hewlett-Packard Company now offers two analyzers for high-speed lightwave measurements. The HP 8703A lightwave component analyzer featured in this issue and the HP 71400C lightwave signal analyzer[1] have been designed to maximize each instrument's measurement contributions for a particular set of measurements. The two sets of measurements are complementary.

Lightwave Signal Analyzer

The HP 71400C lightwave signal analyzer derives its origins from the HP 70000 modular measurement system, which provides high-sensitivity RF and microwave spectrum analysis measurement capabilities. The HP 71400C's primary function is to resolve and measure the modulation frequency spectrum of an optical signal and noise. Direct measurements of optical modulation index and relative intensity noise are made possible by a built-in power meter. It complements the class of products known as optical spectrum analyzers in that the HP 71400C measures the modulation signal superimposed on the light carrier and not the light carrier's optical spectrum. With the addition of an interferometer, characteristics of an optical signal such as its linewidth or chirp under modulation can be measured with high resolution. With the addition of an electrical tracking generator, simple stimulus-response measurements are possible.

Key characteristics of the lightwave signal analyzer are an extremely wide-bandwidth photodetector and preamplifier to capture both low-frequency and high-frequency components of the signal, a wide dynamic range and a low noise floor to enable the measurement of both the signal and the noise of the modulation simultaneously, and a calibrated lightwave receiver front end and optical power meter to measure the lightwave signal directly.

Lightwave Component Analyzer

The HP 8703A lightwave component analyzer derives its origins from the HP 8720B microwave network analyzer, which provides wide-dynamic-range microwave s-parameter device characterization. The HP 8703A's primary function is to characterize the small-signal transfer and/or reflection characteristics of the device or component under test. The measurement is performed by sending a precisely known stimulus signal (electrical or optical) to the device under test and comparing it with the result of its having been operated upon by the device under test. Measurement results are the modulation transfer function amplitude and phase, electrical impedance, and optical return loss characteristics of the device. Since characterization is required over a range of modulation frequencies, the stimulus frequency is swept, and with built-in Fourier transform capability, transmission information can be displayed as the equivalent step or impulse response of the device. Reflection measurements benefit from the transform because it identifies the locations and relative magnitudes of multiple reflections.

Key characteristics of the lightwave component analyzer are precise, high-power electrical and optical stimulus, precise and sensitive electrical and optical receivers which measure both the magnitude ratio and the relative phase of the transmitted and reflected signal, wide bandwidth and dynamic range, processing algorithms for calculating the equivalent time-domain responses, and the ability to perform measurement calibration, which removes measurement uncertainties resulting from converters, cables, connectors, and other elements in the test system.

Measurement Summary

Summarized below are the primary measurement capabilities

of the lightwave signal and component analyzers by generic device type.

- **Transmitter Devices** (lasers, modulators, etc.):
  - □ Lightwave Signal Analyzer:
    - -Output power
    - -Noise: Noise power spectral density
      - Relative intensity noise (RIN)
      - Signal-to-noise ratio
    - -Modulation signal distortion
    - -Linewidth, chirp, and FM response (a)
    - -Modulation frequency response and responsivity (b)
    - -Pulse modulation spectra
  - □ Lightwave Component Analyzer:
    - -Modulation frequency response and responsivity
    - -Step or impulse response
    - -Modulation phase/delay/length
    - -Electrical impedance
    - -Optical return loss (versus frequency or distance)
    - -Reflection sensitivity

- **Receiver Devices** (photodiodes—pins, APDs, etc.):
  - □ Lightwave Signal Analyzer:
    - -Signal characteristics incident on the device
    - -Signal distortion before and after the device under test
  - □ Lightwave Component Analyzer:
    - -Modulation frequency response
    - -Step or impulse response
    - -Modulation phase/delay/length
    - -Electrical impedance
    - -Optical return loss (versus frequency or distance)

- **Optical Devices** (fiber, connectors, sensors, etc.):
  - □ Lightwave Component Analyzer:
    - -Insertion loss (gain)
    - -Modulation phase/delay/length
    - -Optical return loss (versus frequency or distance)

- **Electrical Devices** (amplifiers, filters, cables, etc.):
  - □ Lightwave Signal Analyzer:
    - -Signal frequency spectrum characterization
    - -Noise response characterization
    - -Modulation frequency response (b)
    - -Signal distortion
  - □ Lightwave Component Analyzer:
    - -Full s-parameter characterization
    - -Step or impulse response
    - -Group delay
    - -Time-domain reflectometry (by transform from frequency domain)

Notes: (a) Used with the HP 11980A Fiber Optic Interferometer
(b) Used with the HP 70300A or HP 70301A Tracking Generator

Jack Dupre
R&D Section Manager
Signal Analysis Division

Roger Wong
R&D Section Manager
Network Measurements Division

References
1. C.M. Miller, "High-Speed Lightwave Signal Analysis," *Hewlett-Packard Journal*, Vol. 41, no. 1, February 1990, pp. 80-91.
2. D.M. Baney and W.V. Sorin, "Linewidth and Power Spectral Measurements of Single-Frequency Lasers," *Ibid*, pp. 92-96.

element polarization controller (Fig. 5). The elements contain one or two turns of unjacketed, buffered fiber. The length of fiber gives a quarter-wavelength phase shift between the principal axes at the operating wavelength. Each element is adjustable through a swing of 180 degrees. One element is set in the factory and can be readjusted by HP service personnel. The other element is adjustable from the front panel by the user.

The light polarization at the output of the polarization controller is quite stable and varied less than ±1 degree in vibration tests. The high stability of the laser source deck virtually eliminates the need for readjustment.

Optical Modulator Stability

The optical modulator used in the lightwave source was developed by HP for this project (see article, page 41). The component consists of a coplanar RF transmission line on top of a lithium niobate substrate. A light guide deposited in the lithium niobate splits and recombines the light beam, forming a Mach-Zehnder interferometer. The velocity of propagation changes in the light guides as an RF signal copropagates along the coplanar line. The two beams of light add and subtract coherently with the RF, providing a phase-coherent, intensity-modulated light signal.

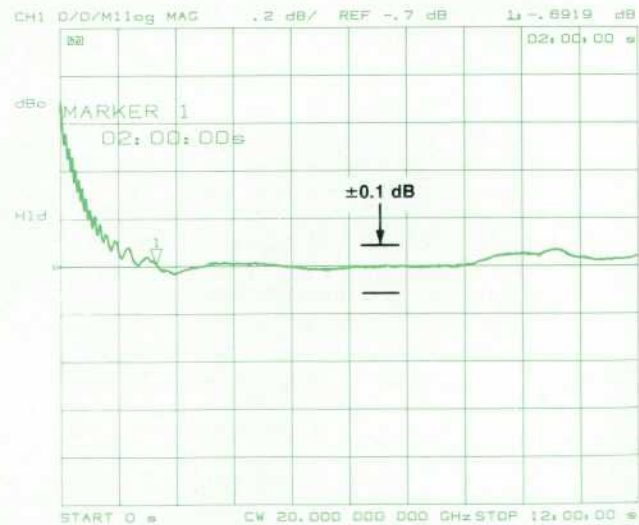For optimum performance, the modulator is biased with

Fig. 6. *Stability of the HP 8703A including warm-up period.*

a dc voltage at a point halfway between maximum and minimum output intensity (the quadrature point). The bias point is affected by the amount of dc voltage applied, time, humidity, temperature, and stresses during packaging. The

packaged devices have been subjected to rigorous environmental tests listed in another article in this issue, and have remained within specifications. Fig. 6 shows that the total instrument drift of the HP 8703A including the modulator is less than 0.10 dB over ten hours after a recommended instrument warm-up period.

To ensure optimum operation, an autobias routine has been implemented in firmware. It is accessible under the calibration or stimulus menu. It is recommended that the autobias routine be used during warm-up, if the wavelength is changed, or if the bias is changed for some reason such as two-tone testing. This routine is automatically performed before each optical measurement calibration unless turned off by the user.

The autobias function requires that at least a minimal optical signal be present at the optical receiver input of the HP 8703A. The instrument automatically measures the modulated signal level at a CW frequency of 1 GHz at the existing bias level and one volt above and below that bias level. It adjusts the bias voltage until the modulation output signal at the current bias level is greater than the signal at both one volt above and one volt below that bias voltage. Then a parabolic curve fit is performed and the maximum point is chosen as the correct quadrature voltage.

RF Drive Path

For lightwave measurements, the RF signal from the upper network analyzer box is routed to the modulator/amplifier in the lightwave test set. The modulator/amplifier was developed as a power driver for the optical modulator. It has about 40 dB of gain control, is capable of delivering 20 dBm of output power, and has a minimum gain of 20 dB to 20 GHz. This performance is made possible by a cascade of two microwave monolithic integrated circuit (MMIC) attenuators followed by four MMIC amplifier chips.

The lithium niobate modulator operates at best efficiency with about +12 dBm of RF at the output. It has about 1 dB of loss at 130 MHz, and about 9 dB of loss at 20 GHz, as shown in Fig. 7. A sample of the RF signal is routed out of the optical modulator to the leveling circuit. This sample is used to set the correct power level drive to the optical modulator.

Lightwave Receiver

The lightwave receiver completes the lightwave path. It is based on the HP 70810A lightwave receiver.[3] Modifica-

Fig. 7. Optical modulator RF insertion loss.

tions include increasing the low-end frequency to 130 MHz and improving the flatness.

A simplified block diagram of the lightwave receiver is shown in Fig. 8. Light from the input fiber is collimated and focused onto a high-speed pin photodetector. The time varying component of the photocurrent represents the demodulated signal. It is fed through a preamplifier with 30 dB of gain to a sampler in the HP 8703A to be processed and displayed. A typical measurement of the lightwave receiver frequency response is shown in Fig. 9.

User Interface

The HP 8703A contains an enhanced version of the guided setup user interface found in the HP 8702B Lightwave Component Analyzer.[1] At power-on and preset, the user is given a choice between normal operation and guided setup. Guided setup is a series of softkey menus, textual instructions, and graphical displays to lead a user through configuring and calibrating a measurement. It provides a subset of the analyzer feature set required for basic measurements. The user of guided setup is able to make a simple measurement without having to choose from among features useful for more advanced measurements. In addition, assistance is given on how to connect the measurement system and how to perform measurement calibration.
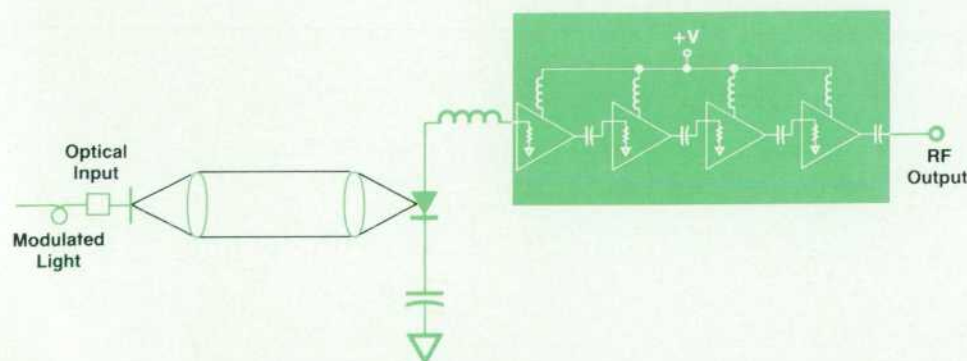

Fig. 8. Lightwave receiver block diagram.

CH1 O/E   log MAG   1 dB/ REF 29 dB   1: 27.182 dB
dB
E-2
×
dBe

H1d

START .130 000 000 GHz   STOP 20.000 000 000 GHz

Fig. 9. *Lightwave receiver frequency response.*

Guided setup was enhanced by increasing the types of measurements that can be performed, adding transmission/reflection measurements for all devices and reflection sensitivity measurements for E/O devices. Additional calibration types and instructions have been implemented. The use of graphics was increased to further simplify the calibration process.

The user is first instructed to select the type of device to be tested. The choices are O/O, O/E, E/O, and E/E. Guided setup next prompts the user to select the type of measurement to be performed. The choices available are dependent on the type of test device and the presence or absence of the optional second lightwave receiver. After the measurement type is selected a block diagram of the measurement configuration is shown (Fig. 10). The user is next instructed to set start and stop frequencies, the sweep time, and the power level of the stimulus signal. With the measurement parameters defined, the user is guided through calibration of the measurement. Calibration is performed by measuring
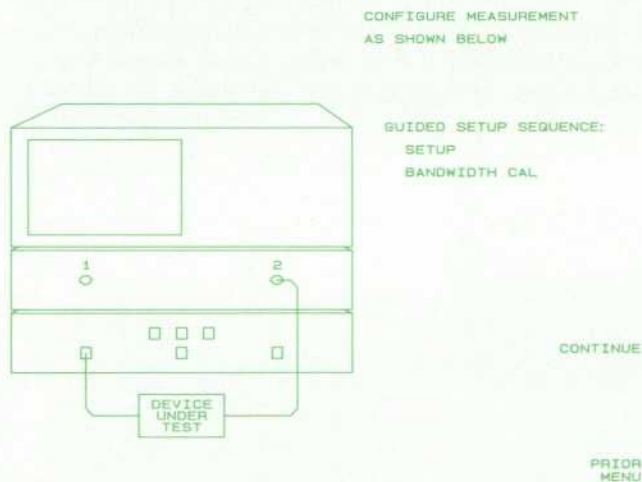
a set of standard devices. The analyzer firmware contains models of these standards as well as calibrated measurements of signal paths within the analyzer. Using the calibration measurements made by the user and the internal calibration data, the analyzer is able to remove systematic errors from measurements of the test device. Several types of correction are available for removing various types of systematic errors. For each type of correction the user is guided through the measurements of the necessary calibration standards. A connection diagram is shown for each standard (Fig. 11). Following calibration the user is instructed to connect the test device. Guided setup assists in formatting the data, producing a printed or plotted copy, and saving the analyzer setup in an internal register.

At any time during the guided setup sequence the user can return to normal operation by pressing any of the labeled function keys on the front panel. Guided setup is always entered from the beginning by pressing the GUIDED SETUP softkey, which is displayed after power on or preset and after pressing the **SYSTEM** key. While using guided setup the user can move forward and backward through the series of menus as needed.

Measurement Calibration

All measurements contain errors caused by the measurement system and by interactions between the measurement system and the device under test. At high frequencies these errors are particularly significant. Measurement errors can be classified as random or systematic. Random errors cannot be eliminated through the calibration process. They include noise, connector repeatability, and the environmental effects of temperature and vibration. These errors are best addressed by controlling the environment and averaging multiple measurements. Systematic errors, on the other hand, are repeatable and stable and therefore can be characterized and greatly reduced using measurement calibration. The HP 8703A lightwave component analyzer has the same capability for error correction as Hewlett-Packard network analyzers, along with the additional ability to make calibrated measurements of lightwave components.

CONFIGURE MEASUREMENT
AS SHOWN BELOW

GUIDED SETUP SEQUENCE:
  SETUP
  BANDWIDTH CAL

CONTINUE

PRIOR
MENU

Fig. 10. *Guided setup—measurement configuration diagram.*

CONNECT THRUS AS SHOWN BELOW   THRUS
PRESS SOFTKEY TO MEASURE
PRESS 'DONE' TO CONTINUE

DONE:
RESPONSE

VIEW
MEASURE

RESTART
CAL
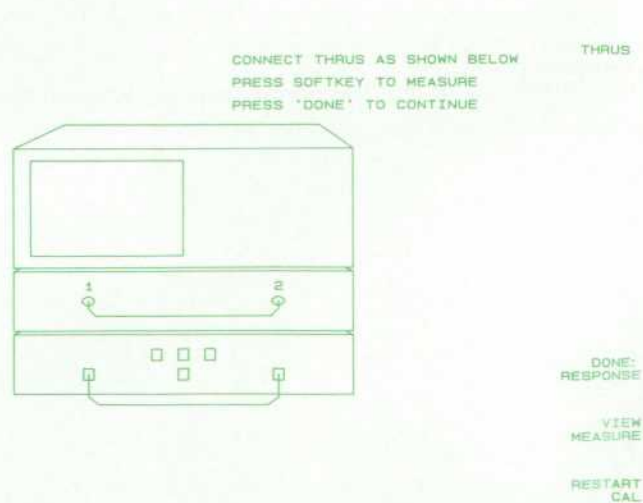
Fig. 11. *Guided setup—calibration configuration diagram.*

$$s_{21a} = \frac{\left(\dfrac{s_{21m} - e_{xf}}{e_{tf}} \right)}{\left[1 + \left(\dfrac{s_{11m} - e_{df}}{e_{rf}} \right)\left(e_{sf} \right) \right]}$$

s_{21a} : Actual Transmission Response
s_{21m} : Measured Transmission Response
s_{11m} : Measured Reflection Response

e_{df} : Directivity
e_{sf} : Source Match
e_{rf} : Reflection Tracking
e_{xf} : Isolation
e_{tf} : Transmission Tracking

Fig. 13. *Response and match calibration routine error model equation for E/O devices.*
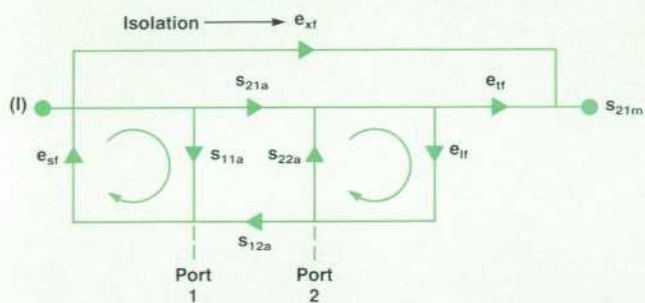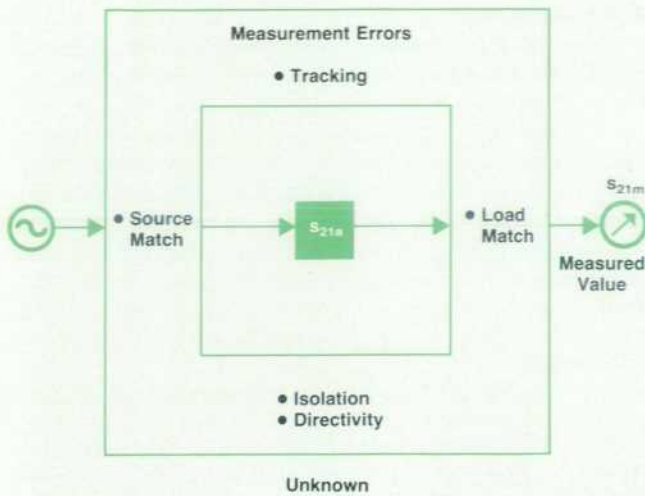

Fig. 12. *Twelve-term error correction model for two-port devices. There are two sets of error terms, forward and reverse, each set consisting of six error terms: (1) directivity, e_{df} (forward) and e_{dr} (reverse), (2) isolation, e_{xf} and e_{xr}, (3) source match, e_{sf} and e_{sr}, (4) load match, e_{lf} and e_{lr}, (5) transmission tracking, e_{tf} and e_{tr}, (6) reflection tracking, e_{rf} and e_{rr}.*

The HP 8703A evolved from a microwave network analyzer, and contains the systematic error correction capabilities found in such instruments. Based upon the signal flow illustrated in Fig. 12, the 12-term error correction process greatly improves the accuracy of most measurements. Six of the error terms are for the forward path and six for the reverse path. The six terms are directivity, source match, reflection tracking, load match, isolation, and transmission tracking. Directivity is a figure of merit for how well the signal separation device separates forward and reverse signals for reflection measurements. Source match is the vector sum of signals at the system input test port arising from impedance mismatches between the system and the input of the test device. Tracking error is the vector sum of all frequency response errors in the system between the reference and the test signal paths. This error is a major factor in transmission and reflection measurements. Load match is the vector sum of signals at the system input test port arising from impedance mismatches between the system and the output of the test device. Isolation is a measure of the amount of stimulus signal that appears at the RF receiver without passing through the device under test.

Often some of the twelve error terms may be insignificant or the full accuracy may not be needed. The HP 8703A has several correction routines to characterize and remove one or more of these errors. The HP 8703A has the same set of RF correction routines as the HP 8720B network analyzer, as well as a new routine for measurements of E/O and O/E devices.

Calibration is performed by measuring standard devices whose nominal characteristics are stored in calibration memory. Electrical standards are devices such as opens, shorts, loads, and RF cables. Optical standards are reflectors, Fresnel reflections at connector/air interfaces, and optical cables. Calibrated lightwave sources and lightwave receivers are used as standards for transmission measurements of E/O and O/E devices. These standards are calibrated in terms of responsivity versus modulation frequency. The signal paths internal to the HP 8703A are calibrated at the factory and calibration data is stored in the analyzer.

E/O devices commonly have input impedances much less than the system impedance of 50 ohms. The HP 8703A match calibration feature is an extended calibration process that backs the mismatch ripple out of the test results. Direc-

$$s_{21a} = \frac{\left[1 + \left(\dfrac{s_{22m} - e_{dr}}{e_{rr}} \right)\left(e_{sr} - e_{lf} \right) \right]\left(\dfrac{s_{21m} - e_{xf}}{e_{tf}} \right)}{\left[1 + \left(\dfrac{s_{22m} - e_{dr}}{e_{rr}} \right)\left(e_{sr} \right) \right]}$$

s_{21a} : Actual Transmission Response
s_{21m} : Measured Transmission Response
s_{22m} : Measured Reflection Response

e_{dr} : Directivity
e_{sr} : Source Match
e_{rr} : Reflection Tracking
e_{lf} : Load match
e_{xf} : Isolation
e_{tf} : Transmission Tracking

Fig. 14. *Response and match calibration routine error model equation for O/E devices.*

tional coupler directivity, source match, and reflection tracking of the electrical test port are determined by measuring an open, a short, and a well-matched termination. Then the electrical input match and the responsivity (transmission response) of the E/O device are measured. The results of the calibration and measurement steps are combined in the equation of Fig. 13 to produce the corrected, displayed measurement result.

Response and match calibration of O/E device measurements is similiar to that for E/O devices. The output impedance of O/E devices is commonly much greater than the 50-ohm system impedance, resulting in mismatch errors. An open, a short, and a load are measured at the test port at the electrical output of the test device to determine reverse directivity, source match, and reflection tracking. An electrical through connection is made between the electrical ports 1 and 2, and s_{11} is measured to determine the load match of the output test port. With the test device connected, reverse reflection is measured and used to correct the transmission measurment using the equation shown in Fig. 14.

More information on accuracy and error correction is given in the article on page 34.

References

1. R.W. Wong, et al, "High-Speed Lightwave Component Analysis," *Hewlett-Packard Journal*, Vol. 40, no. 3, June 1989. pp. 35-51.
2. H.C. Lefevre, "Single-Mode Fibre Fractional Wave Devices and Polarisation Controllers," *Electronics Lettres*, Vol. 16, no. 20, 1980, pp. 778-790.
3. C.M. Miller, "High-Speed Lightwave Signal Analysis," *Hewlett-Packard Journal*, Vol. 41, no. 1, February 1990, pp. 80-91.

20-GHz Lightwave Test Set and Accessories

With this lightwave test set and a compatible HP microwave network analyzer, users have the same key 20-GHz lightwave component analysis capabilities as with the integrated HP 8703A analyzer. The microwave network analyzer can still be used for its normal functions.

by Joel P. Dunsmore and John V. Vallelunga

THE RISE OF LIGHTWAVE TECHNOLOGY has stimulated a need for measuring equipment such as the HP 8703A microwave lightwave component analyzer described in the article on page 13. The HP 8703A has an integrated microwave network analyzer with all the lightwave components and firmware to perform high-quality lightwave modulation frequency response measurements and frequency-domain reflectometry. This product has stimulated interest in this measurement method, and customers have responded with requests to upgrade their existing high-performance microwave network analyzers to add lightwave measuring capabilities. As a result, a project was started with the objective of taking the lightwave technology from the HP 8703A and designing an instrument to bring lightwave measurements to the HP 8510B, HP 8720B, and HP 8757C microwave network analyzers. The result is the HP 83420A lightwave test set.

Many of the lightwave components developed for the HP 8703A are state-of-the-art. There were many customer inquiries for these components for use as laboratory equipment in system experiments. With this in mind, a series of lightwave accessories was developed along with the lightwave test set. Each accessory is a subset of the test set system, so much of the development engineering was leveraged from the test set project. This shared development allowed us to produce six instruments with a single project team.

Fig. 1 shows how a microwave analyzer can be used to measure lightwave components. The information source is the microwave synthesizer, the information receiver is the microwave test set receiver, and the signal processor is the network analyzer processor and display. In this system, the information is the magnitude and phase of the source signal. In any measurement, we are looking for changes in the magnitude and phase of this signal. From these changes we can determine the transfer function of the device under test (DUT). The system is first calibrated by measuring the response using the internal components. This is the reference response. Next, the DUT replaces the equivalent component (for example, a laser diode might replace the lightwave transmitter), and the system response is again measured. The change from the reference response represents the effect of the DUT. The processor determines the response of the DUT and displays the response in a format

chosen by the user.

The lightwave components required for the test set were quite far along in development for the HP 8703A. The major concerns were making the lightwave test set compatible with existing network analyzers, and adding control and calibration software to the system. This required understanding of the signal flow and control of the target network analyzers.

Network Analyzer Considerations

The HP 8510B network analyzer is a widely used high-performance microwave vector network analyzer, and many HP customers who make high-speed measurements have HP 8510B analyzers. Therefore, it was the primary target for the HP 83420A lightwave test set. The test set is designed to take advantage of the HP 8510B system's flexibility. However, the lightwave test set is also compatible with the HP 8720B Option H80 (a special option for use with the HP 83420A) and with the HP 8757C scalar network analyzer.
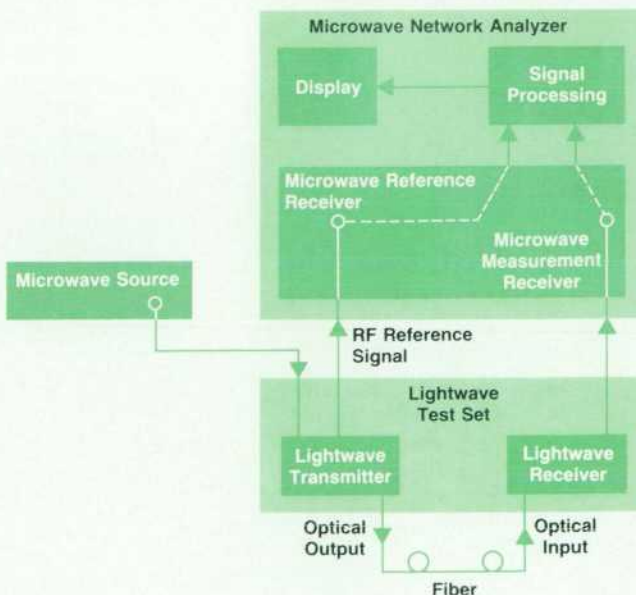

Fig. 1. *Lightwave measurements with a microwave network analyzer.*

In the HP 8510B, the signal flow is from the microwave source to the microwave test set. In the test set, a power splitter divides the signal into a reference path and a test path. The reference path is used to phase-lock the receiver to the source and as a measure of the incident signal to the device under test. The test path routes the signal through a directional device to the front panel. The test signal is measured at either the reflection receiver (for return loss tests) or at the transmission receiver (for gain or loss tests). To use this system to measure lightwave components, it is necessary to use the microwave source for the lightwave modulating signal and the microwave receiver as the detector for demodulated lightwave signals. The microwave analyzer processor contains error correction functions which can be used to remove the system response from the measured response of the DUT to give the correct DUT response. However, as shown later, the simple corrections of the network analyzer must be modified to provide the true DUT response. These changes to the calibration arrays in the microwave analyzer are performed by a computer, which also sets up the measurements and guides the user through each calibration and measurement step.

In addition to measurement correction, the microwave analyzer processor has a fast inverse Fourier transform function which can transform the frequency response information into a time-domain response. This allows measuring equivalent impulse or step responses of components in transmission measurements, such as ringing in a photodiode receiver. In reflection measurements, multiple reflec-tions from fiber connections and splices can be determined, displaying both the magnitude and spacing of individual reflections. Sophisticated gating functions can remove effects of test fixturing, showing only the response of the desired DUT.

The microwave test set characteristics determined many of the requirements of the lightwave test set block diagram. The loss in the microwave test set is substantial, so the drive power from the front panel port is insufficient for many lightwave sources such as laser diodes. The system works best if the reference signal is representative of the drive signal to the device under test. For measuring lightwave receivers, the reference signal should represent the power in the modulated lightwave drive signal. Also, the reference signal to the microwave test set must be at least -3 dBm to provide for phase-locking of the receiver. From these requirements, the lightwave test set block diagram was designed.

Block Diagram

The block diagram of the HP 83420A lightwave test set is shown in Fig. 2. This RF signal topology was chosen to provide superior performance when used with network analyzers. The lightwave test set consists of four major functional blocks:

- The lightwave source deck
- The amplified lightwave receiver
- The RF drive portion
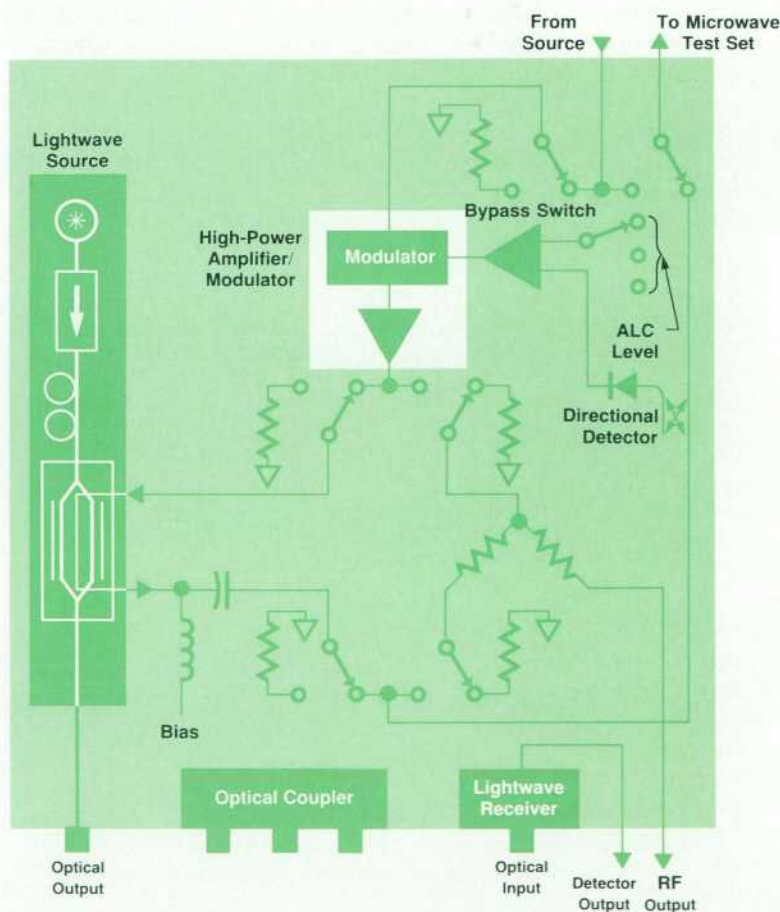- The main printed circuit board, which contains bias,

Fig. 2. HP 83420A lightwave test set block diagram.

automatic level control (ALC), front-panel control, and remote programming control circuitry. The details of the hardware implementation are discussed later.

The test set has four operating modes, depending upon the type of device to be tested. The simplest is the E/E mode, for testing electrical devices such as amplifiers and filters. In this mode, a switch is used to bypass the lightwave test set completely. The HP 8510B system operates as if no test set were present. This is important for systems that are used by different groups, ensuring that the HP 8510B system is not degraded in any way when used in normal operation. In the E/E mode, the only change is a small amount of loss because of the switch.

The three active modes for the lightwave test set are the E/O mode for measuring lightwave sources (electrical drive and optical measurement), the O/E mode for measuring lightwave receivers (optical drive and electrical measurement), and the O/O mode for measuring optical devices such as fiber (optical drive and optical measurement).

In all modes of operation, the source is routed back through a broadband directional detector and out the rear of the instrument as the RF reference output.

E/O Mode

In the E/O mode, the signal source to drive the DUT comes from the front panel of the lightwave test set. The microwave source signal passes through the bypass switch and into a broadband high-power amplifier. This circuit also contains a wide-range modulator to control the power out of the amplifier. The signal from the amplifier is routed to a set of switches which drive either the optical modulator (for O/E and O/O modes) or, in this case, a power splitter. One branch of the power splitter is routed to the front panel and is used to drive the E/O DUT. The amplifier has a +20-dBm drive capability, which provides about +12 dBm of drive at the front panel. This is significantly more than is available from the microwave test set, which is usually less than −10 dBm.

The other branch of the power splitter is routed back to the directional detector. This element has very little loss and produces a detected dc signal proportional to the incident power. The detected signal is used to level the power at the front panel through the ALC loop. The ALC loop responds by driving the RF modulator in the amplifier microcircuit. This loop corrects for changes in signal drive from the source, gain flatness in the amplifier, and other losses in the signal path. One additional requirement of the loop is that it not have power spikes if the source signal is temporarily blanked (such as in retrace). Power spikes can occur when an ALC loop goes to minimum attenuation as the RF signal is blanked. When the RF signal comes back on, the loop takes some time to settle to the proper attenuation, and a large power spike will occur until the attenuation changes. These power spikes can damage sensitive laser diodes. Details of this control circuit are described later.

The signal that passes through the directional detector is routed to the rear of the instrument and is used as the reference signal to the microwave test set. It must be at least −3 dBm to drive the phase-lock circuitry. This sets the minimum RF drive in the E/O mode. Because this signal is proportional to the drive signal, the signal in the reference receiver is a true representation of the incident signal to the E/O DUT.

Two power levels (minimum and maximum) are provided at the front panel. In the E/O drive mode, the minimum power at the front panel is about 0 dBm, and the maximum is about +12 dBm. The output power level varies less then ±2 dB from the nominal output.

To complete the measurement path, the lightwave receiver in the test set is used to detect the modulated lightwave signal from the E/O DUT. This detected signal is a microwave signal of the same frequency as the drive signal, and is measured on the microwave test set.

O/E Mode

In the O/E mode, a modulated lightwave signal from the test set drives an O/E DUT. This modulated lightwave signal is generated by routing the signal from the amplifier microcircuit to the optical modulator. The optical modulator has about 2 dB of loss at 130 MHz and about 10 dB at 20 GHz. The microwave signal passes through the optical modulator and is routed to the directional detector. Here the leveling loop keeps the power at the output of the modulator constant, making up for the sloped loss of the optical modulator. Leveling at the output keeps the modulated optical power fairly constant.

Again, two power levels (minimum and maximum) are available for the optical drive. The average optical power is not changed, but the depth of modulation is. The minimum power level gives more linear modulation with lower distortion and better repeatability. Maximum power is used for best dynamic range. The difference between minimum and maximum optical drive is about 6 dB of optical modulated power. The minimum power is set to provide −3 dBm to the reference channel in the microwave test set.

The reference signal is proportional to the optical modulated signal, so that the signal in the reference receiver in the microwave test set is a true representation of the incident signal to the O/E DUT.

The measurement is completed by measuring the microwave output of the O/E DUT using the microwave test set measuring receiver.

O/O Mode

The O/O mode has the same drive as the O/E mode, with the optical modulated signal coming from the test set. The signal passes through the O/O DUT and is detected by the lightwave receiver in the test set. The microwave signal is then measured by the measuring receiver in the microwave test set.

The O/O mode is also used for making optical reflection measurements. In this measurement, the built-in optical directional coupler is used to separate the incident optical signal from the reflected signal. The reflected signal is routed to the lightwave receiver in the test set, which detects the microwave signal. The signal is measured on the microwave test set measuring receiver.

Calibration and Measurement

One of the more significant contributions of the HP 83420A system is its calibration capability, which allows users to determine the transfer characteristics of DUTs. Previously, the measurements depended upon measuring devices having flat frequency responses (which they did not), and corrections for any slope or ripple were tedious and often not well-founded. With the development of the HP 8703A, the response measurements could be traced back to the very accurate HP dual-heterodyne YAG (yttrium aluminum garnet) system. This background formed an excellent base from which the HP 83420A system could build a calibration method for removing frequency response errors.

Each of the measurement modes can be calibrated to eliminate errors arising from the frequency responses of the components in the lightwave test set. In each mode, a user calibration measurement is performed. This is saved in the microwave analyzer calibration arrays and is then modified by the control software to provide the correct response for the type of device being measured. The modified calibration array is passed back to the microwave analyzer, which can now operate in a local mode without further contact with the control software. This method of operation means that users can make measurements, format data, and produce hard copy output using the network analyzer in its normal operating mode; no new operating systems need be learned. Each of the calibration measurements, with appropriate connections, is displayed graphically by the control software. The user is guided through the calibration and measurement sequence.

O/O Calibration and Measurement. The measurement calibration for an O/O DUT is a response calibration of a through optical cable. The measurement of the O/O DUT is normalized to the through line. When the device is measured, the only response displayed is the DUT's. The analyzer firmware performs the mathematical operations to remove the response of the lightwave test set. Fig. 3 shows the calibration measurement and the device measurement configurations. The calibration measurement includes the following terms:

Calibration Measurement =

(ES)(OS)(LWCABLE1)(LWCABLE2)(OR)(ER),

where:
ES	=	electrical source response
OS	=	optical source response
LWCABLE1	=	source lightwave cable response
LWCABLE2	=	receiver lightwave cable response
ER	=	electrical receiver response
OR	=	optical receiver response.

The device measurement is represented by:

Device Measurement =

(ES)(OS)(LWCABLE1)(O/ODUT)(LWCABLE2)(OR)(ER)

where O/ODUT = O/O DUT response: Therefore,

$$\frac{\text{Device Measurement}}{\text{Calibration Measurement}} =$$

$$\frac{\text{(ES)(OS)(LWCABLE1)(O/ODUT)(LWCABLE2)(OR)(ER)}}{\text{(ES)(OS)(LWCABLE1)(LWCABLE2)(OR)(ER)}} = \text{O/ODUT}$$

O/O Reflection Calibration and Measurement. In the O/O reflection mode, the calibration technique and equations are essentially the same. A calibration measurement is made with a known reflection. The device measurement is then normalized to the calibration measurement. The difference here is that the usual reflection is a Fresnel reflection from an open fiber (3.5% reflection or 14.8-dB return loss). The calibration arrays are modified to show a 14.8-dB return loss for the calibration standard.

Lightwave Reference Receiver. The internal lightwave receiver is used as a calibration standard for O/E and E/O measurements. At the factory, a very careful measurement is performed to determine the magnitude and phase response of the internal lightwave receiver. This measurement can be traced back to the dual-heterodyne YAG measuring system. The response data for the lightwave receiver is stored on a calibration data disk, which is keyed to the serial number of the lightwave test set measured. During an O/E or E/O calibration, the response of the lightwave receiver is read from the disk and used as shown below.
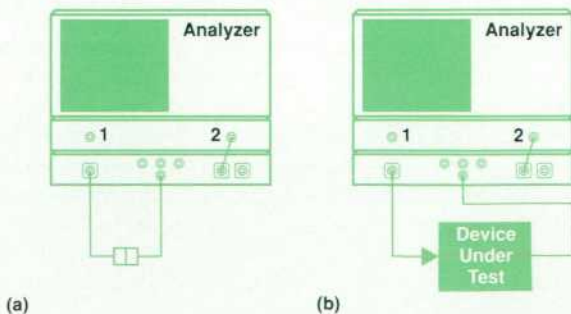

Fig. 3. Optical configurations. (a) Calibration measurement. (b) Device measurement.
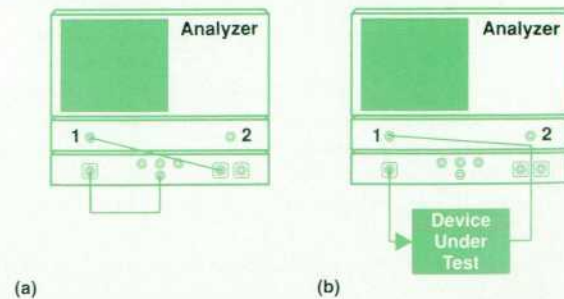
Fig. 4. Optical-to-electrical configurations. (a) Calibration measurement. (b) Device measurement.

O/E Calibration and Measurement. The calibration for an O/E measurement removes the responses of the lightwave source and the microwave receiver. As shown in Fig. 4, a user calibration is first made measuring the internal lightwave receiver. Then, for the device measurement, the O/E DUT is substituted for the internal lightwave receiver. Fig. 5 shows the calibration and measurement signal paths. In the calibration step, a full optical path is measured. The internal lightwave receiver is the only portion of the calibration measurement that is not in the DUT measurement. Therefore, for a proper correction of the system response, the response of the internal lightwave receiver must be subtracted from the calibration measurement. This modified calibration, combined with the user DUT measurement, will yield only the DUT response. The calibration measurement can be expressed as:

Calibration Measurement =

(ES)(OS)(LWCABLE)(OR)(ECABLE)(ER),

where:
ES	=	electrical source response
OS	=	optical source response
LWCABLE	=	source lightwave cable response
ECABLE	=	receiver RF cable response

ER	=	electrical receiver response
OR	=	optical receiver response.

The DUT measurement can be expressed as:

Device Measurement =

(ES)(OS)(LWCABLE)(O/EDUT)(ECABLE)(ER),

where O/EDUT = O/E DUT response.

The calibration measurement is combined with the optical receiver response data ORCAL (contained on the data disk) to form a calibration response:

Calibration Response = Calibration Measurement/(ORCAL).

Therefore,

$$\frac{\text{Device Measurement}}{\text{Calibration Response}} =$$

$$\frac{(ES)(OS)(LWCABLE)(O/EDUT)(ECABLE)(ER)}{(ES)(OS)(LWCABLE)(OR)(ECABLE)(ER)(1/ORCAL)}$$
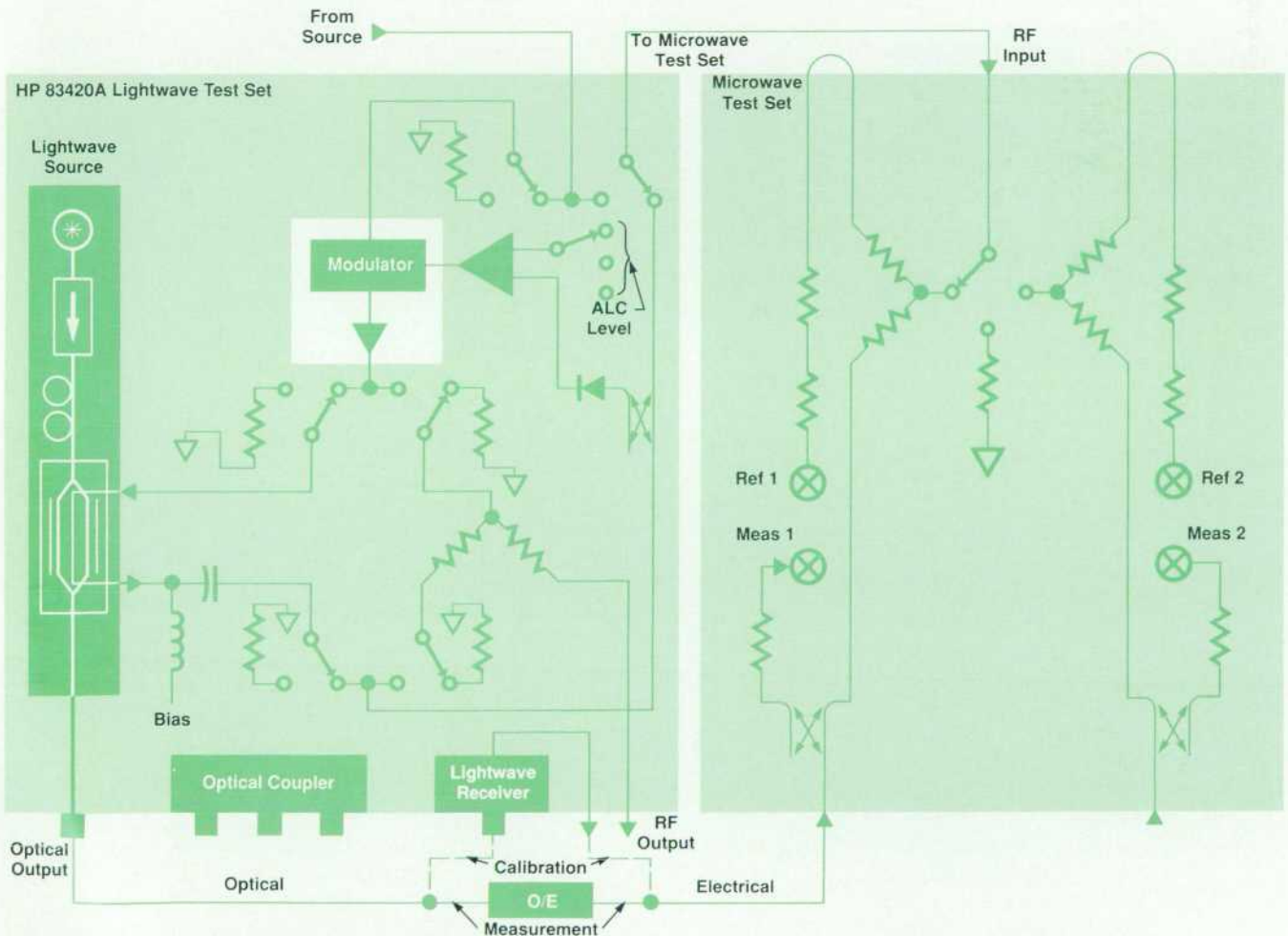
Fig. 5. *Signal paths for optical-to-electrical calibration and measurement.*

$$= (O/EDUT)\ (ORCAL)/(OR).$$

Ideally, OR = ORCAL, that is, the factory-measured response of the optical receiver saved on disk (ORCAL) should be the same as the actual response of the optical receiver (OR) at the time of measurement. If that is true, then the above ratio gives only the O/E DUT response.

E/O Calibration and Measurement. The calibration of an E/O measurement uses the same principle as the O/E measurement. Fig. 6 shows the calibration measurement and device measurement configurations for E/O devices. Fig. 7 shows the signal flow for two different calibration paths. For E/O devices, the drive signal can come from either the lightwave test set (high-power drive) or the microwave test set. The drive from the microwave test set is much lower in power, but can be used to make reflection measurements, such as input impedance or return loss, as well as transmission measurements. Fig. 8 shows the device measurement signal block diagram. In the calibration measurement, only the electrical path is measured. The device measurement path includes the E/O DUT, a lightwave cable, and the internal optical receiver as well as the electrical path. The calibration response is modified to add the response of the optical receiver by adding the response data from the disk to the calibration measurement.

The calibration measurement can be expressed as:

(a)   (b)
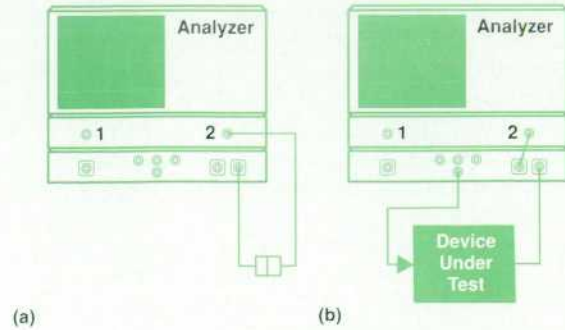
**Fig. 6.** *Electrical-to-optical configurations. (a) Calibration measurement. (b) Device measurement.*

Calibration Measurement = (ES)(ECABLE1)(ECABLE2)(ER),

where: | ES | = electrical source response
| | ECABLE1 | = source RF cable response
| | ECABLE2 | = receiver RF cable response
| | ER | = electrical receiver response

The DUT measurement can be expressed as:

Device Measurement =
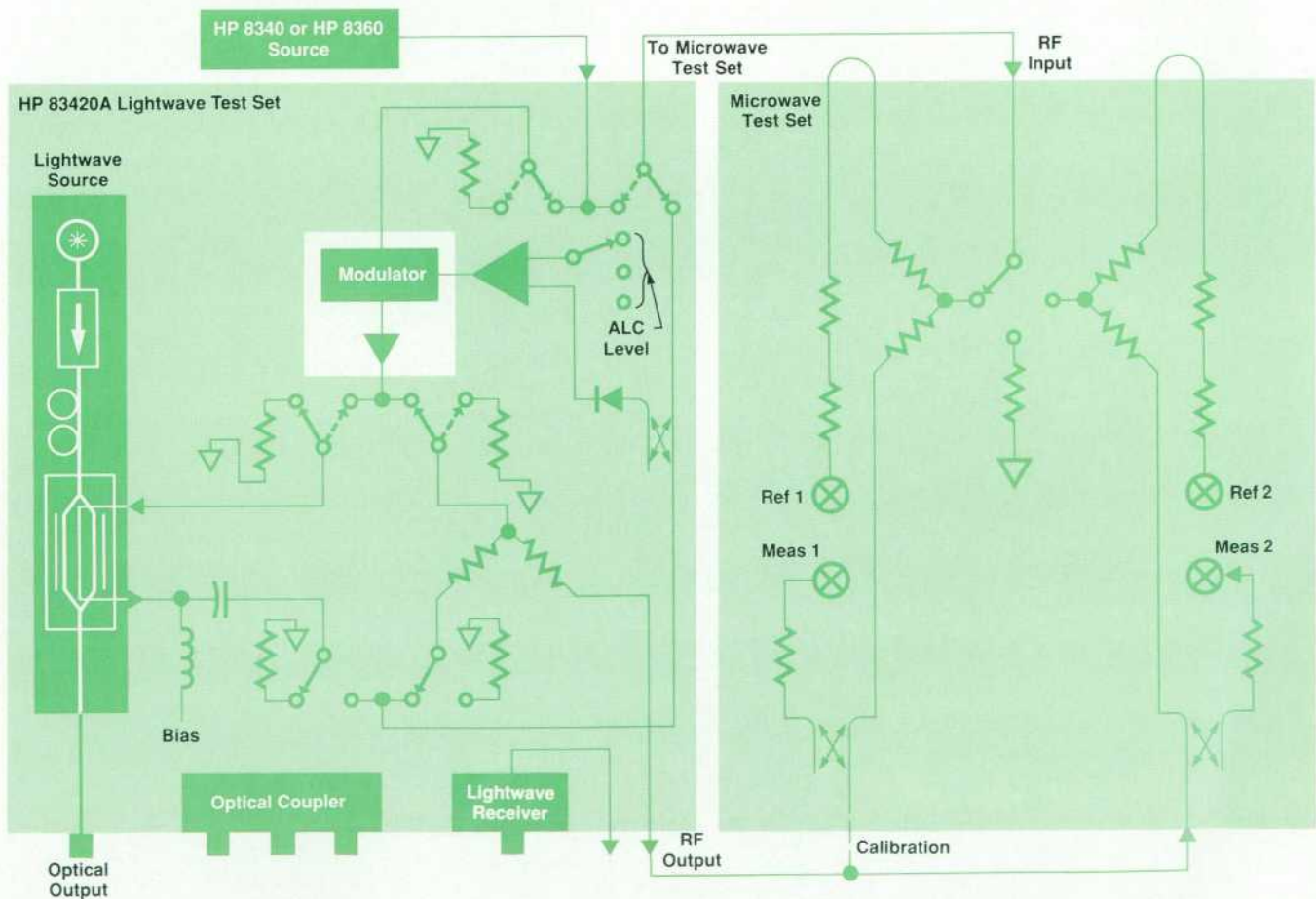
Fig. 7. *Signal paths for two different electrical-to-optical calibration measurements. The RF drive signal can come from either the lightwave test set or the RF test set.*
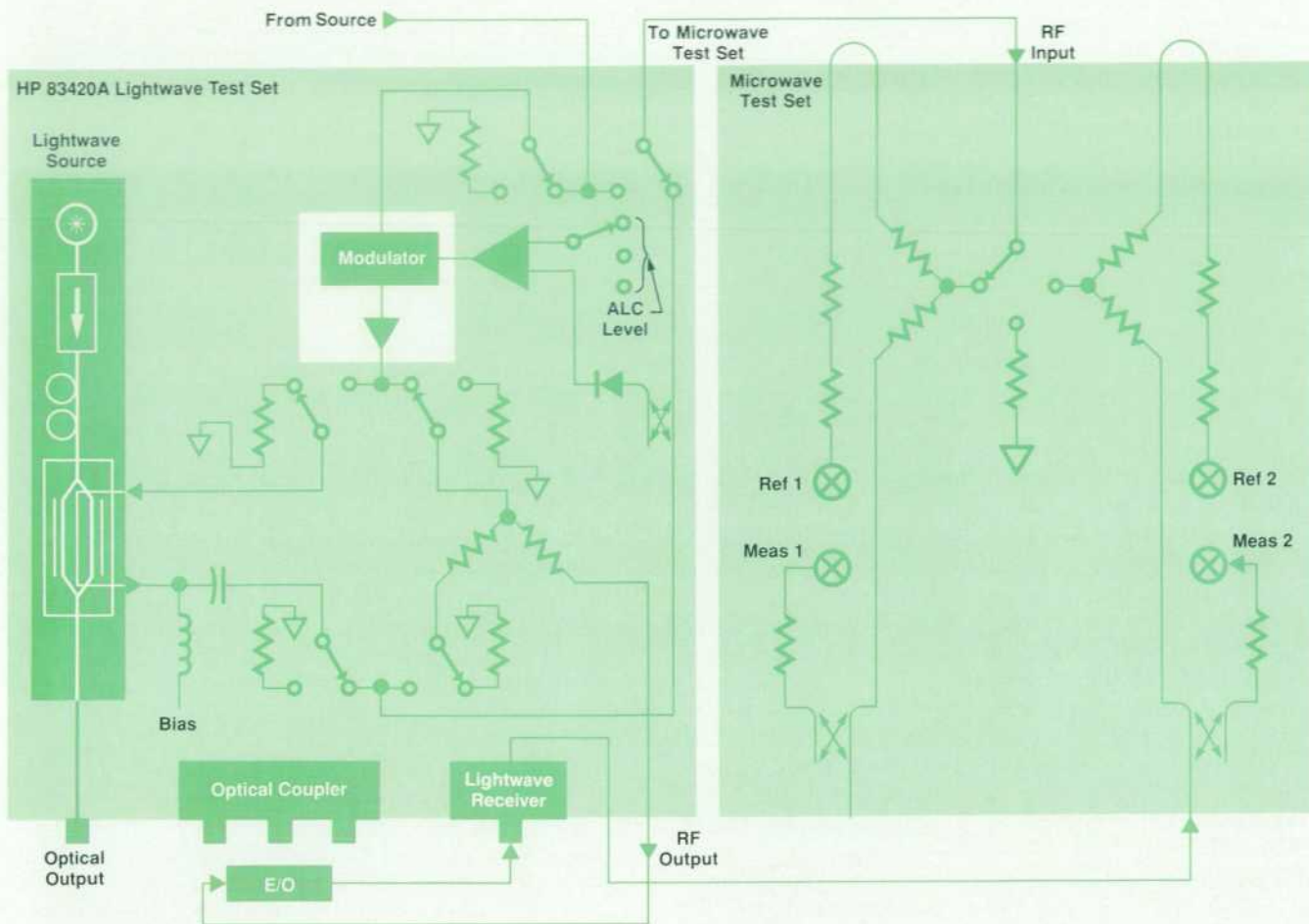
Fig. 8. *Signal paths for electrical-to-optical device measurements.*

$$(ES)(ECABLE1)(E/ODUT)(LWCABLE)(OR)(ECABLE2)(ER),$$

where: OR = optical receiver response
E/ODUT = E/O DUT response.

The calibration measurement is combined with the optical receiver response data contained on the data disk to form a calibration response:

$$\text{Calibration Response} = (\text{Calibration Measurement})(\text{ORCAL}),$$

where ORCAL = optical receiver calibration data. Therefore,

$$\frac{(\text{Device Measurement})}{(\text{Calibration Response})} =$$

$$\frac{(ES)(ECABLE1)(E/O\ DUT)(LWCABLE)(OR)(ECABLE2)(ER)}{(ES)(ECABLE1)(ECABLE2)(ER)(ORCAL)}$$

$$= (E/ODUT)(LWCABLE).$$

Note here we have assumed that (OR)/(ORCAL) = 1. Also, notice that the lightwave cable between the DUT and the optical receiver is not accounted for in the calibration, but contributes to the DUT response. The frequency response of this lightwave cable is negligible, but the phase response must be accounted for if the proper phase of the E/O DUT is to be displayed. The phase response is very linear and can be removed using the port extension capability of the network analyzer. Using this, the electrical delay of the cable is entered and is subtracted from the DUT response by the network analyzer.

Hardware Implementation

The four major hardware portions of the lightwave test set are described below. The details of the optical source and receiver have been reviewed in other papers, so comments on these portions pertain to their specific implementation in the lightwave test set.

Lightwave Source. The lightwave source converts RF energy into modulated laser light. The source of light is an unmodulated (CW) semiconductor laser. This can be a 1300-nm Fabry-Perot laser, or a 1300-nm or 1550-nm distributed feedback (DFB) laser. The light is directed through a high-performance isolator (greater than 55-dB isolation) to prevent reflections from disturbing the semiconductor laser. Next, the light passes through a polarization controller. The light from the laser is polarized, but at an unknown angle. The polarization controller is simply a series of pad-

dles with fiber wrapped around them. Rotating the paddles changes the polarization of the light.

The key component of the lightwave source, the lithium niobate modulator, comes next in the lightwave path. This modulator consists of a coplanar RF transmission line on top of a LiNO$_3$ substrate. A light guide deposited in the LiNO$_3$ splits and recombines the light beam. This forms a Mach-Zehnder interferometer. An RF signal across the coplanar line changes the velocity of propagation in the light guides differentially, such that the two beams of light add and subtract coherently with the RF signal. The modulator has a preferred polarization, and the polarization controller is used to match the polarization of the laser to this preferred polarization.

From the modulator, the laser light is routed to the front-panel connector. For units with the optional external laser input, an optical switch is inserted in the light path just before the modulator. In this way, any laser source can be modulated by the internal modulator, giving dual-wavelength capability. The output connector is designed to be adapted to any one of several common optical fiber connector types.

Lightwave Receiver. The amplified lightwave receiver completes the lightwave path. The receiver consists of a very high-speed photodiode followed by over 30 dB of broadband gain. The photodiode has a bandwidth greater than 20 GHz. The gain stages consist of four stages of GaAs IC traveling-wave amplifiers, with a bandwidth of more than 130 MHz to 20 GHz. This lightwave receiver is the key component in calibration. The magnitude and phase of the frequency response of the lightwave receiver are carefully measured and saved on a data disk. This becomes the standard for both O/E and E/O calibrations.

In normal operation, when the lightwave source is connected to the lightwave receiver, the output RF power will be nearly 0 dBm, with about 15 dB of roll-off to 20 GHz. The maximum input power to the network analyzer is 0 dBm. When measuring lasers or lightwave receivers, care must be taken not to exceed the input power rating of the network analyzer. Adding an attenuator between the lightwave receiver and the analyzer will not affect the accuracy of the measurement, provided it is added before calibration.

RF Drive Portion. All the new technology is not in the lightwave portion of the instrument. State-of-the-art components are used in the RF drive portion to realize the full potential of the lightwave test set. The RF input signal is routed through a bypass switch to the RF modulator/amplifier microcircuit.

The power amplifier on this microcircuit consists of a broadband leveling GaAs IC followed by four stages of GaAs traveling-wave amplifiers. This microcircuit has over 20 dB of gain from 130 MHz to 20 GHz, greater than +20 dBm RF drive power, and more than 40 dB of leveling range. The output of the amplifier is routed to a pair of microwave switches.

In operation, the LiNO$_3$ modulator operates at best efficiency with about +12 dBm of RF power at the output. It has about 2 dB of loss at 130 MHz, and about 9 dB at 20 GHz. Therefore, a sample of the RF signal is routed out of the modulator to the leveling circuit. This is used to set the proper drive power level to the optical modulator.

Alternatively, when trying to measure E/O devices, high drive power is desired. Rather than incur the loss of the optical modulator, a pair of microwave relays switch the output of the power amplifier from the optical modulator to a power splitter. One branch goes to the front panel to provide about +12 dBm of drive power to E/O devices. The other branch is switched to the leveling circuit to provide leveled power at the front panel.

In all cases, the minimum power level is set to ensure reference phase lock in the microwave test set. Maximum power is set to a level just below compression in the modulator/amplifier microcircuit.

The Main Control Board. The main printed circuit board in the instrument serves the functions of providing proper drive voltages, controlling the ALC loop, controlling the optical modulator bias, and controlling the front-panel and rear-panel interfaces.

The power supply provides five voltages (±15, $+9$, $+6$, $+5$). The two largest power-consuming circuits are the GaAs amplifiers in the modulator/amplifier microcircuit and the lightwave receiver. These are turned off when the front-panel power is set to standby. Also, the laser turn-on circuit is disabled during standby. The laser temperature control and the optical modulator bias voltage remain on during the standby mode. Each of these components has a long warm-up time constant, and it is recommended to leave them in the operating state.

The ALC loop senses detected RF power from the directional detector. This signal passes through a logging amplifier, so the ALC loop responds linearly to dB changes in power. The detected RF signal is compared to one of four reference states (E/O minimum and maximum, and optical minimum and maximum), and the error signal is integrated and passed to the control circuit in the RF amplifier. This circuit is shown in Fig. 9. A circuit that detects when no RF input is present, called the autoblanking circuit, sets the modulator/amplifier attenuator to a middle value, preventing power spikes in the E/O drive signal during blanking or retrace. This circuit can be disabled by providing a TTL low level to the **RF BLANK** input.

The ALC loop level can be set with an external detector, with the detected signal passed back to the instrument through the **EXT ALC INPUT** connector. The rear-panel ALC control switch must be set to **EXT** to enable this function. Setting this switch to **EXT** with no input signal will cause the ALC loop to set the modulator/amplifier attenuator to minimum loss, thus giving maximum gain to the optical modulator. This might be useful in fiber link applications where AM modulation, which would normally be removed by the ALC loop, is present on the input signal. If the input signal is small (less than -10 dBm) the autoblanking circuit should also be disabled. In other applications where remote leveling is desired, a negative detector must be used. The value of the external level can only be changed between minimum and maximum with the front panel; if finer control is desired, an adjustable-gain amplifier can be used before the **ALC EXT INPUT**.

The bias to the optical modulator is controlled by the main printed circuit board. On units with no optical switch, only the bias appropriate to the internal laser is available. On units with an optical switch, the rear-panel bias select switch is active when the front-panel control has selected
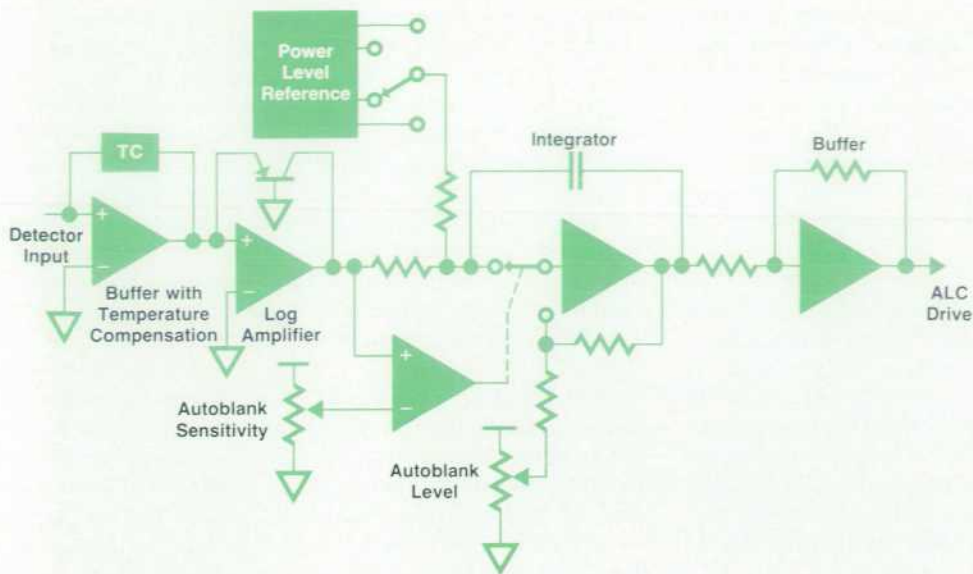
Fig. 9. *Main ALC loop.*

the external laser input. This switch changes the bias voltage to match the quadrature voltage on the modulator for the two most common wavelengths (1300 nm and 1550 nm).

The main printed circuit board also contains a programmable array logic device (PAL) which monitors the front panel switches, and performs the selected function when activated. The rear-panel remote programming connector will override the front panel and control the instrument state. This is the normal mode of operation when used with the control software.

Lightwave Test Set Software

For the HP 83420A lightwave test set to make accurate measurements in conjunction with a network analyzer, the characteristics of the receiver portion of the lightwave test set must be known and compensated for in the final results. Each test set is accompanied by a disk containing over 1600 data points characterizing the receiver from 45 MHz to 20 GHz along with an HP 9000 Series 200/300 program for downloading the disk data to the analyzer. This control software also sets up instrument states on the network analyzer and the lightwave test set and guides the user in calibration and measurement setup.

The following goals were set at the beginning of program development:

- The program was to work with the HP 8510B, 8720A/B, and 8719A network analyzers.
- Most of the analyzer's features were to remain functional for lightwave measurements.
- The program was to be designed for a sophisticated user.
- There was to be minimal user interaction with the computer.
- The program was to be easily modifiable by the user.
- The program was to be defined, written, and tested within five months.

To make the program easily modifiable by the user, HP BASIC was chosen as the operating language. Since both the user and the instrument were to have minimal interaction with the computer, operating speed was not a major concern. A windows environment would have consumed too much memory and would not have produced a significant gain in

ease of use, so a softkey-driven display was chosen. HP BASIC also provides usability with IBM-compatible computers via the HP 82300C Basic Language Processor Card.

The first task was to find an overhead program to handle display and softkey selection. A subset of STE-9000, a program developed by the HP Product Support Division, was chosen because it was well-tested and well-documented and consumed little memory.

The next task was to develop a routine that would interpolate the 1610 points of factory-supplied calibration data (in real and imaginary pairs) to any number of user-defined points over any defined frequency range. This interpolation routine also had to produce accurate phase information, thus eliminating any straight-line interpolation. The routine chosen was the circular interpolation described later.

The program supports O/O, O/E, and E/O transmission and reflection measurements as well as E/O reflection sensitivity measurements (E/E measurements are not supported since no lightwave test set is required). In addition, error corrected measurements can be made using either a response calibration or a response and isolation calibration. With these variations and more, it quickly became obvious that a simple method to guide the user in calibration and measurement was needed. While the program was originally designed for use by a knowledgeable user, it was determined that the addition of guided setup made the program easy to use even for a first-time user. The guided setup, patterned after that used by the HP 8703A (see article, page 13), provides a quick visual indication of all connections for both calibration and measurement setups.

The amount of interaction between the user and the computer was originally planned to be minimal. The computer's main job is to read the error correction terms from the analyzer, modify them, and then download the terms back into the analyzer. This sequence must be performed whenever the frequency range of the analyzer is changed. Until it is changed, the computer does little and can even be disconnected. This allows almost all built-in functions of the analyzer to be used for lightwave analysis (the major exception being log sweeps and frequency list sweeps) and

simplifies the program dramatically. However, it does require a small amount of user interaction with the computer. Since the lightwave test set has no microprocessor, switching of its several functions was originally to be performed manually. However, the addition of a few TTL logic lines allowed for simple automatic control via a GP-IO interface. This quickly became so popular that the GP-IO interface card and cable are now included with every HP 83420A shipment.

One of the largest obstacles for the software to overcome was the fact that optical dB calculations differ from those calculated in the network analyzer. The network analyzer multiplies the log of a voltage ratio by 20 to obtain an electrical dB reading. Optical dB must be calculated by multiplying by 10. Since this is performed in the analyzer, it requires a firmware upgrade of the analyzer to display dB measurements properly. The program will still work without this modification but a warning message is displayed on the analyzer's CRT indicating that the actual results are one-half the displayed results.

The software also handles many other minor functions so that the user can concentrate just on making measurements. Some of the overhead items it handles are averaging, plotting, titling, and storing and recalling of previous calibrations.

Circular Interpolation

The accuracy of the lightwave measurement system is based on the precise characterization of the lightwave receiver, as previously described. This characterization results in a finite number of characterized frequencies over the frequency range of the product. To use this information in a measurement calibration, the information must be interpolated to derive the calibration coefficients for the exact frequencies measured. The interpolation technique used is modeled after the technique employed in lightwave component analyzers such as the HP 8702B and 8703A. The algorithm is called circular interpolation.

The task of interpolating complex frequency-domain in-

formation requires careful attention to the interaction of the real and imaginary portions of the data. Two techniques were considered for the interpolation algorithm. The technique used, circular interpolation, takes the real and imaginary information together and interpolates between consecutive data points by assuming that the complex vector rotates through a circular path whose center and radius are determined by three consecutive data points. The other technique considered was the commonly known cubic spline. The cubic spline interpolation employs independent interpolation of the real and imaginary data according to a cubic polynominal fit determined by three consecutive data points.

Circular interpolation was chosen after experimental trials revealed that the circular algorithm showed lower interpolation errors than the cubic spline. The higher performance of the circular algorithm is attributed to the fact that the interpolation mechanism reflects a basic characteristic of complex, frequency-domain data: the data vector tends to rotate clockwise in a roughly circular path as frequency is increased.

Fig. 10 illustrates an example interpolation. The data shown represents a typical spiral of the complex transmission coefficient as frequency increases. The frequency at which the data is interpolated lies between the sixth and seventh data points. To perform the interpolation, the last three points are used to determine a circle in the complex plane. Then, the angle c between the sixth and seventh points is determined ($c = a + b$ in Fig. 10). The interpolated point is assumed to lie on this circle. To calculate the angle a of the interpolated point, F, the difference in frequency between the sixth and seventh points, F_1, is calculated.
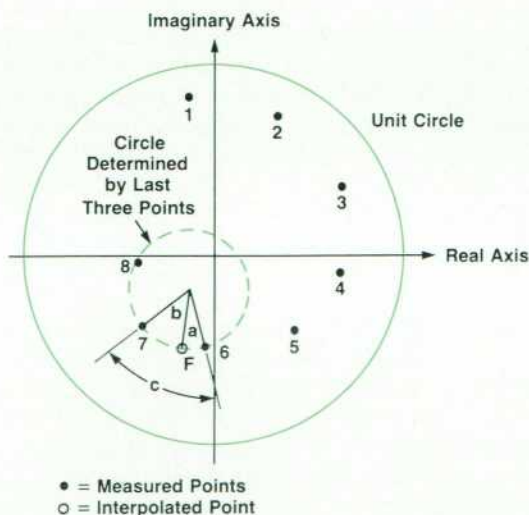

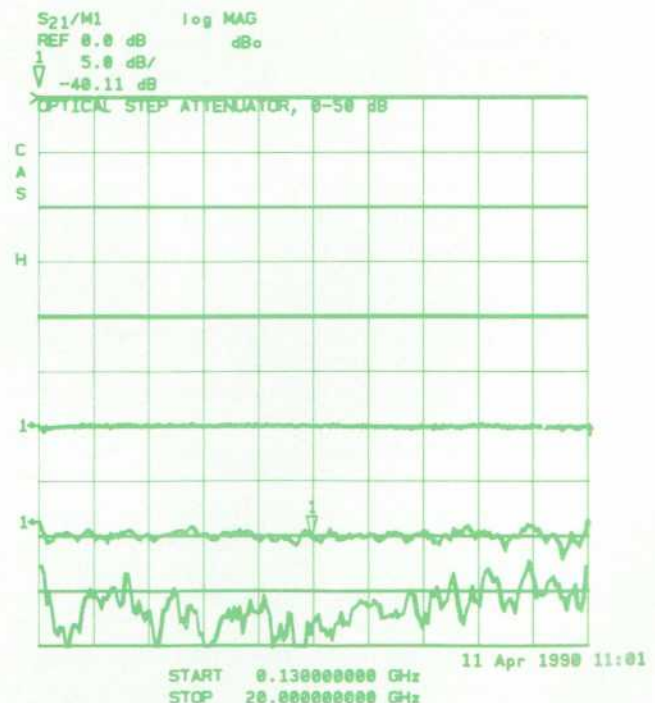Fig. 10. Example data (representational) and circular interpolation.

Fig. 11. Measurement of an optical step attenuator using the HP 83420A lightwave test set with the HP 8510B microwave network analyzer.

Then F_2, the difference in frequency between the interpolated point and the sixth point, is calculated. Finally, angle a is calculated using:

$$a = c \frac{F_2}{F_1}.$$

Given the center of the circle, the radius of the circle, and the angle a, the calculation of the real and imaginary parts of the interpolated data point is straightforward.

The performance of the algorithm is significantly enhanced by removing the constant linear phase term from all the data points. This obviates the problem of missing a 360-degree rollover because of rapidly changing phase with frequency, and ensures less than 180 degrees of phase change between frequency points (required for the interpolation routine to function.)

One of the attractive features of circular interpolation is that much of the calculation can be done beforehand, so that the calculation of specific interpolated points is relatively fast. In this implementation, the center and radius of the circle corresponding to each set of three points are calculated only when the program is first run. Subsequent measurement calibrations, performed whenever start or stop frequencies are changed, require significantly less computational effort, because the precalculated data is used.

Measurement Results

Fig.11 shows an example measurement of an optical step attenuator using the HP 83420A/HP 8510B lightwave compo-

nent analysis system. The optical attenuator was tested over 10-dB steps from 0 dB to 50 dB of optical attenuation. The HP 83420A system is able to measure to below 40 dB of optical attenuation. The −50-dB trace is a measure of noise and crosstalk. The noise floor of the system is a combination of the added noise in the amplified lightwave receiver and the noise floor of the microwave analyzer. The crosstalk floor is usually set by the microwave analyzer crosstalk.

Fig. 12 shows a comparison between the HP 83420A system and the HP 8703A lightwave component analyzer. Both systems were used to measure the same photodiode receiver. The frequency response variations from the two measurements agree within 0.25 dB over the active region of the photodiode. However, the two measurements are offset by about 1 dB. This is most likely because of the repeatability of fiber connections. To put this in perspective, the differences between the two different systems are of the same order of magnitude as the differences between the HP 8703A systems.

Acknowledgments

```
S12 & M1       log MAG
REF −15.0 dB    A/W
↑  2.5 dB/
∇ −7.9102 dB
HP 83420 / HP 8703 COMPARISON
```

```
START    0.130000000 GHz
STOP    20.000000000 GHz
```
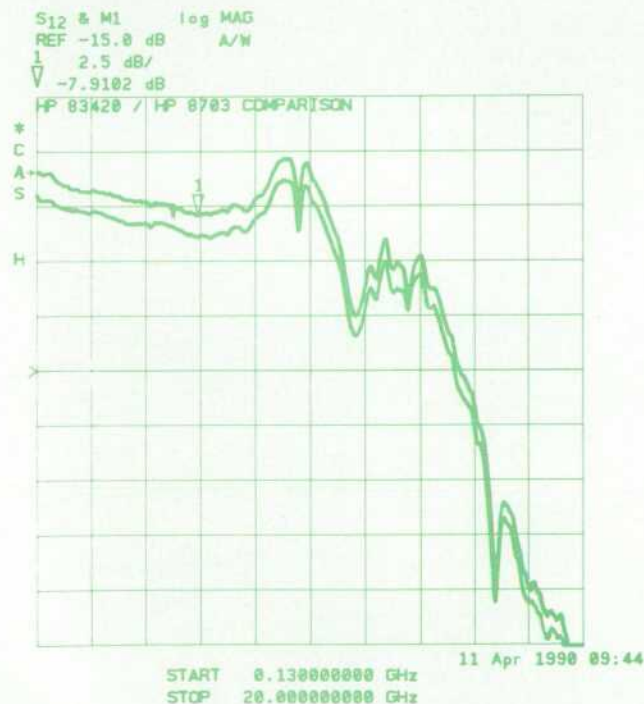
11 Apr 1990 09:44

Fig. 12. *Measurements of the same photodiode receiver by an HP 8703A lightwave component analyzer and by an HP 83420A/HP 8510B system. The differences are similar to these between HP 8703A analyzers.*

Accuracy Considerations and Error Correction Techniques for 20-GHz Lightwave Component Analysis

An understanding of factory calibration techniques, system capabilites, and device-under-test sensitivities can result in more accurate and repeatable measurements using the HP 8703A lightwave component analyzer.

by Daniel R. Harkins and Michael A. Heinzelman

THE ACCURACY OF MEASUREMENTS made with a lightwave component analyzer is the result of instrument performance, measurement technique, and consideration of the particular device being measured. To ensure the most accurate characterization of wide-bandwidth components, it is important to understand the measurement capabilities of the instrumentation, decide on the optimum configuration and calibration for a particular measurement, and be aware of potential impact the test device can have on the resulting measurement. The accuracy of the result is a combination of multiple sources of errors that must be carefully considered.

Factory Calibration

The measurements made by the HP 8703A lightwave component analyzer can be divided into four categories: optical-to-optical (O/O), electrical-to-electrical (E/E), optical-to-electrical (O/E), and electrical-to-optical (E/O). Optical and electrical calibrations are done in an HP standards laboratory using state-of-the-art equipment. This laboratory has NIST (U.S. National Institute for Standards and Technology) traceability for all of these measurements. However, there are no E/O or O/E standards that are directly traceable to NIST. The accuracy of these calibrations is based on theoretically derived performance of electrooptical devices as described below. Although the techniques are not directly traceable to NIST, the measurements used in the calibrations (optical power, RF power, etc.) are traceable.

One technique used at Hewlett-Packard for calibrating O/E devices is known as heterodyne calibration. The outputs from two temperature-tunable YAG (yttrium aluminum garnet) lasers are combined in an optical coupler and applied to a photodetector under test. The YAG lasers are tuned so that the difference between their frequencies sweeps the microwave band of interest. The output of the photodetector is measured on a calibrated receiver such as an HP 71210C spectrum analyzer. The optical power output of each YAG is measured and the sum of the two is computed. From this information the frequency response of the photodetector can be derived. Transfer standards calibrated on the HP heterodyne system are used to calibrate

the HP 83410/11A receivers and the HP 83400/01/02/03A sources.[1] Although this method does not directly calibrate the HP 8703A, 20-GHz photodiode receivers measured on HP's heterodyne system are used as a second verification of the frequency response of the HP 8703A.

The technique used to calibrate the HP 8703A's E/O frequency response is known as the two-tone technique (Fig. 1).[2] This technique applies two microwave signals (tones) to the optical modulator, which is biased off quadrature. It can be shown that the magnitude of the tones' mixing product (difference frequency) is proportional to the square of the modulator's response times the product of the magnitudes of the tones. If the tones are swept across the frequency band of interest (difference frequency kept constant) and the output of the modulator is monitored with a low-frequency detector, the square root of the ratio of the detector output to the tones' magnitudes will be a measure of the modulator's frequency response. The modulator can then be used to measure the frequency response of an optical receiver. Some advantages of this method are that it does not require accurate frequency response calibration of the detector (the detector only sees one frequency), it
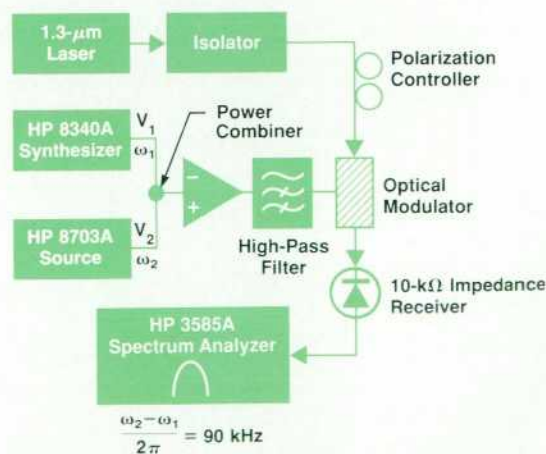

Fig. 1. *Two-tone calibration system for calibrating the E/O frequency response of the HP 8703A lightwave component analyzer.*

can be performed at any wavelength within the range of the optical modulator simply by changing the laser, and with the addition of the low-frequency photodetector it can be performed with equipment found in most microwave test stations. For the HP 8703A calibration this method provides improved accuracy over measuring a transfer receiver calibrated on the HP heterodyne YAG system. It also eliminates the need for a calibrated E/O source transfer standard.

There are also no standards for measuring the phase of E/O or O/E devices. For phase calibration, a 20-GHz photodiode receiver was modeled on an HP 85150B microwave design system. To model the device, its signal path was divided into sections: optical, optical-to-electrical, and RF (see Fig. 2). The known physical properties or theoretical properties of each section were converted to a model which was entered into the computer. In addition to phase response, the computer predicted several characteristics of the device that could be measured, such as the magnitude of the response and electrical parameters such as s_{22}. Comparing the predicted values to measured values gave information that was used to refine the model. When good correlation between the measured and predicted values was obtained for measurable parameters, we had high confidence that the model would also predict correct phase information. As a final check, an optical modulator was also modeled and the receiver and modulator were measured together. Their combined phase response was compared to the sum of the models (this is an E/E measurement for which standards exist). Agreement was within 5 degrees above 5 GHz and within 15 degrees at lower frequencies. The latter is nearly all attributable to the optical modulator, whose rapidly changing response at low frequencies is more difficult to model. The receiver has a smoother response, and therefore its phase response is more predictable.

Factory Calibration Sequence

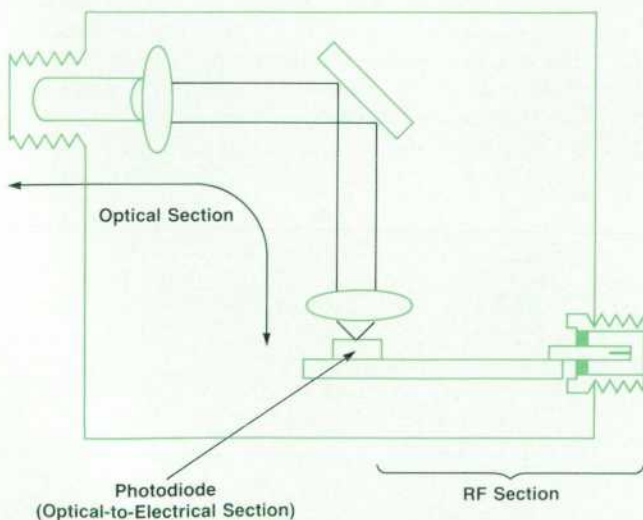Fig. 3 shows simplified signal paths for O/E and E/O measurements. For accurate measurements the HP 8703A RF and optical paths including the RF and optical cables must be calibrated out. To eliminate the need for an expensive reference receiver and source at the customer site, the HP 8703A is calibrated for these measurements at the factory and calibration constants are stored in the HP 8703A memory. The customer need only connect the measurement cables to the HP 8703A front-panel ports during calibration and the HP 8703A will automatically correct for systematic errors including the cables.

From Fig. 3 we see that the responses of four paths need to be corrected inside the HP 8703A: the port 1 electrical output, the port 2 electrical input, the optical output, and the optical input. The sequence of factory calibration for these paths is as follows:

Step 1. The HP 8703A's built-in synthesizer signal is combined with an external synthesizer and applied to the optical modulator via a rear-panel port to perform the two-tone calibration described above. The difference frequency is measured with a low-frequency detector and a spectrum analyzer at each frequency point and stored. This measures the frequency response of the optical output.

Step 2. The optical output is connected to the optical input through a previously calibrated optical cable and this path is measured and the data stored.

Step 3. Port 2's electrical response is measured with a previously calibrated source and stored. This gives a measure of Port 2's absolute response.

Step 4. Port 2 is connected to Port 1 with a previously calibrated RF cable and the measured response is stored. Port 2's response and the RF cable's response are subtracted from this measurement to compute the absolute response
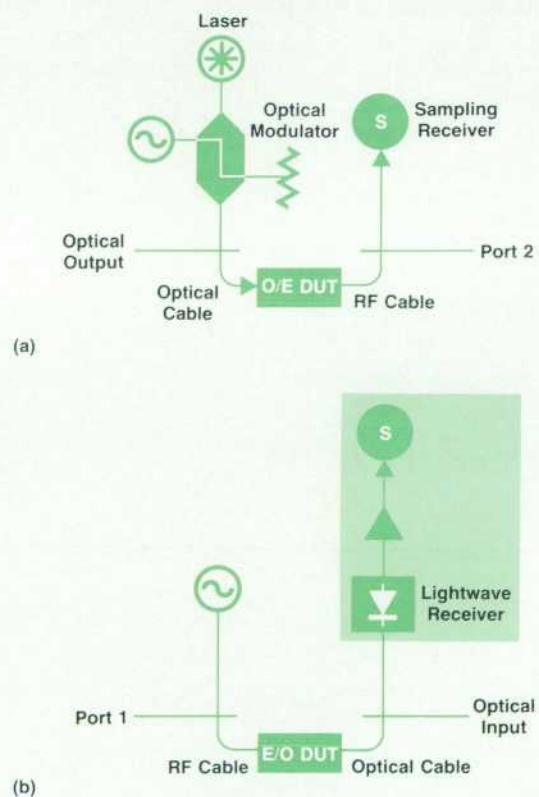

Fig. 2. *Reference receiver sections modeled.*

Fig. 3. *Simplified signal paths for (a) O/E measurements and (b) E/O measurements.*

of Port 1's output.

Step 5. A reference receiver is connected between the optical output and Port 2 and measured. This receiver has had its absolute responsivity calibrated at 130 MHz and has been phase modeled as outlined above.

Step 6. From the above data the computer generates calibration constants which are then stored in the HP 8703A's memory.

Step 7. As a final check a photodiode receiver that was previously calibrated on the HP heterodyne YAG system is measured with the HP 8703A and the results of the two systems are compared. Correlation between the systems is typically better than ± 0.5 electrical dB (see Fig. 4).

User Calibration

As an example of how the HP 8703A corrects E/O measurements, let us look again at Fig. 3. Four parameters need to be corrected to measure the DUT accurately: the port 1 response (PORT1), the optical input response (OPTIN), the RF cable response (RFCBL), and the optical cable response (OPTCBL). To calibrate the system the operator connects the measurement cables to the HP 8703A input ports as shown in Fig. 5a. Pressing the appropriate front-panel keys will cause the HP 8703A to calibrate the system automatically by measuring the following signal paths:

$$CAL1 = (PORT1)(RFCBL)(PORT2)$$
$$CAL2 = (OPTOUT)(OPTCBL)(OPTIN).$$

The factory-stored E/O constants are:

$$FACTE/O = (OPTOUT)(PORT2).$$

The HP 8703A combines this data to form correction constants

$$CORRECTION = \frac{(CAL1)(CAL2)}{FACTE/O}$$

Fig. 4. *Measurements of a reference receiver with the HP standards laboratory's heterodyne YAG system and with an HP 8703A.*

$$= \frac{(PORT1)(RFCBL)(PORT2)(OPTOUT)(OPTCBL)(OPTIN)}{(OPTOUT)(PORT2)}$$

$$= (PORT1)(RFCBL)(OPTCBL)(OPTIN).$$

The operator then connects the cables to the DUT as shown in Fig. 5b and the HP 8703A measures the DUT.

$$MEASURE = (PORT1)(RFCBL)(E/ODUT)(OPTCBL)(OPTIN).$$

The displayed data is:

$$\frac{MEASURE}{CORRECTION} = \frac{(PORT1)(RFCBL)(E/ODUT)(OPTCBL)(OPTIN)}{(PORT1)(RFCBL)(OPTCBL)(OPTIN)}$$

$$= E/ODUT.$$

A similar correction process occurs for O/E, O/O, and E/E measurements.

Verification

With the calibration stored in the instrument for E/O or O/E applications, the measurement of a device under test is accomplished by a process of substituting the DUT for system calibration data. Each instrument makes its measurements accurately because the factory calibration process generates absolute calibration data unique to that set of hardware. The quality of measurement provided is a direct result of the calibration performed at the factory. The long-term stability and repeatability and therefore the integrity of the product are direct results of the stability of the system hardware and the original calibration. For user verification of the system performance, the customer is provided with a measurement of the absolute characteristics of the critical instrument measurement paths made at the time of calibration. The integrity of the measurement system is then monitored over time by testing its ability to reproduce the original absolute characteristics measured at the factory. This provides the user with a simple measurement that monitors the system's status and is linked directly to its original calibration.

Specifically, at the time of the factory calibration of an HP 8703A, a measurement is made on the hardware that represents an absolute measurement of the optical and electrical portions of the measurement system that are used in E/O or O/E measurements. In each case, the only external connections to the instrument are RF and optical through
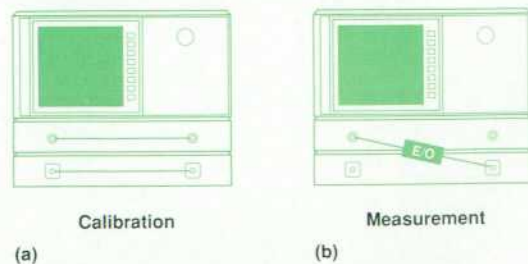
Calibration   Measurement

(a)   (b)

Fig. 5. *HP 8703A calibration and measurement connections for E/O device measurements.*

connections to close the measurement paths. The absolute measurement data along with instrument setup information and prescribed limit lines (which account for the allowable drift and repeatability of the measurements) are stored on a verification disc and shipped with the instrument. To verify the instrument, the customer makes the simple through connections, the data and limit lines are recalled, and a new measurement is compared to the original. If the new measurement is outside the allowable limits, verification has failed and the customer will be advised to check the quality of the cable and connections being used. If that does not alleviate the out-of-limits condition, the instrument will be considered out of specification and must be returned for repair and/or recalibration.

It is important that this process does not require special electrooptical verification reference devices. The only key elements besides the instrument are appropriate interconnect cables. This avoids the need for an expensive optical verification kit. In addition, the simplicity of the procedure makes it easy for the user to test the integrity of the system upon receipt and at frequent intervals during its use.

In addition to the frequency response verification, a full performance verification of the HP 8703A must also include absolute optical measurements of power and wavelength. All E/E microwave performance verification is done with a standard verification kit similar to other microwave analyzers.

System Capabilities

A thorough understanding of the HP 8703A's hardware characteristics and limitations is essential to achieving the best measurement results.[3]

The electrical stimulus is a 130-MHz-to-20-GHz synthesized microwave source with 1-Hz frequency resolution. The synthesizer's frequency accuracy and repeatability play a key role in achieving accurate and stable calibrations. A +5-dBm output power level provides a high signal level (compared to other microwave network analyzers) to achieve typical drive levels used for laser sources. Since the analyzer receiver is tuned to the source drive frequency, relatively high source harmonics (<10 dBc) are not a cause of measurement error. The typical source match varies over the frequency range from 20 dB at 130 MHz to only 10 dB at 20 GHz. This can result in measurement mismatch errors that may require user calibration.

The electrical receiver is a microwave sampler tuned to the source frequency. Its typical operating range is between

0 dBm—the largest signal input before receiver compression begins—and typically −105 dBm—the noise floor in a 10 Hz bandwidth. The receiver bandwidth can be increased in steps to 3 kHz. This allows faster response measurements but increases the noise floor of the receiver accordingly. Similar to the source, the receiver has an input return loss that varies from 26 dB to 12 dB (typically) over the operating frequency range. Fig. 6 shows the error of the receiver detection capability as a function of input power level. The high-power errors occur as a result of compression in the receiver samplers. The low-level errors occur as the detected signals approach the noise of the system. The detection response over the middle region from 0 to −80 dBm is very linear.

The optical output signal is intensity modulated at the measurement frequency rate. It has an average optical power of 250 microwatts and operates at a fixed modulation level of approximately 130 microwatts peak-to-peak intensity change. Laser options result in different optical source linewidths ranging from 3 nanometers for the Fabry-Perot structure to less than 50 MHz for the DFB sources. The optical output match is determined by the output match of the lithium niobate modulator and typically corresponds to greater than 15 dB of return loss. All the laser sources are isolated to avoid problems caused by sensitivities to reflections at the source output port.

The optical receiver is an amplified photodiode receiver in front of a tuned electrical receiver. Fig. 7 is a curve of the typical dynamic accuracy of the optical detection path. The high-level distortion comes from compression in the receiver samplers. The low-level noise is about 15 dB higher than in the electrical receiver because of noise added by the amplifiers in the photodiode structure. Also, since the photodiode is a power sensing device, the electrical detected output signal varies by 2 dB for every 1-dB optical change. Thus the optical levels shown represent an electrical detection dynamic range that is twice as large.

In conjunction with optimization of the basic measurement hardware, several levels of user calibration are provided to allow correction for some aspects of the system. Table I shows the various user calibrations available for each type of measurement.

The response calibration is the process of transferring the stored calibration of the reference receiver or source to the current measurement (in E/E or O/O measurements it is a simple through calibration). The port calibrations and
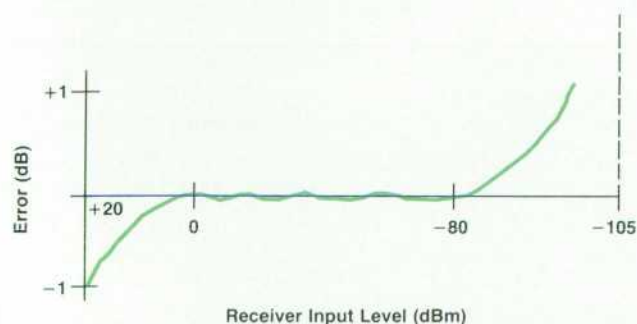

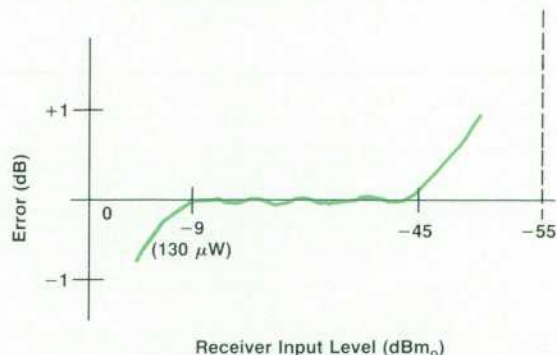**Fig. 6.** *Dynamic accuracy of the HP 8703A electrical receiver.*

Fig. 7. *Dynamic accuracy of the HP 8703A optical receiver.*

Table I
Selectable User Calibrations

E/E Measurements	E/O or O/E Measurements	O/O Measurements
Response	Response	Response
Response and Isolation	Response and Match	Response and Isolation
One-Port	Response and Isolation	
Two-Port		

match calibrations improve equivalent electrical source and load matches to greater than 30 dB. This is particularly important when test port and device port matches are of such a level that their multiple mismatch errors could be a significant source of error (typically for low-return-loss devices). Calibration of electrical ports for reflection measurements results in an equivalent directivity of >36 dB. Isolation calibration removes measurement system crosstalk to ensure full access to the system dynamic range.

Device-Under-Test Sensitivities

Besides understanding the primary characteristics of the measurement hardware, it is also important to pay careful attention to any device-under-test characteristic that could impact measurement accuracy or cause unstable or non-repeatable measurements.

First, the primary DUT characteristics (gain, match, distortion, etc.) must be considered in setting the measurement signal levels for maximum dynamic range and accuracy. These characteristics may establish a need for extra padding in the measurement path or determine the initial choice of user calibration. Not a small issue is the choice of connectors for the DUT. Optical connectors in particular can have match characteristics (for a mated pair) that vary from less than 10 dB return loss for noncontacting connectors to 40 dB for precision connector types.[4] Similarly, 3.5-mm RF connectors can vary from 20-dB-match, industrial-quality connectors to >45-dB-match instrument-grade connectors. In addition to the right choice of connector type, the proper use and care of the test port and DUT connectors are essential for making good and repeatable measurements. The cleanliness of optical connections is

Fig. 9. *Reflection sensitivity measurement of a Fabry-Perot laser.*

very frequently the source of significant repeatability difficulties.

More interesting than these issues are some of the more subtle sensitivities optical portions of the DUTs tend to display. One such characteristic that can often lead to confusing and unrepeatable measurements is the sensitivity of laser sources' responsivity-versus-frequency characteristics to optical load characteristics. A particular optical load can couple back into the laser and alter the modulation response of the structure. The diagram in Fig. 8 shows a test configuration used to measure reflection sensitivity. A low-coupling-factor coupler is used to monitor the modulated output of a laser while the main coupled path at the test laser output is exposed to various load conditions. Fig. 9 is a polarization sensitivity measurement of a Fabry-Perot laser with a high-reflection load that has been set with a polarization controller for maximum and minimum sensitivities. The responses change from 1.5-dB peak-to-peak ripples to greater than 4-dB peak-to-peak ripples. While this configuration can be used to measure such sen-

Fig. 8. *Laser reflection sensitivity test setup.*

Fig. 10. *Setup for a measurement of two lengths of fiber.*

sitivities, in other measurement configurations the same phenomenon can be the source of unexplained fine-grain variations in a device measurement. The sources used in the 20-GHz lightwave component analyzer products all have optical isolators to avoid any measurement system sensitivity of this type.

Another interesting device characteristic that can influence measurements is that of interferometric "noise" effects. These result when optical reflections in a system interact i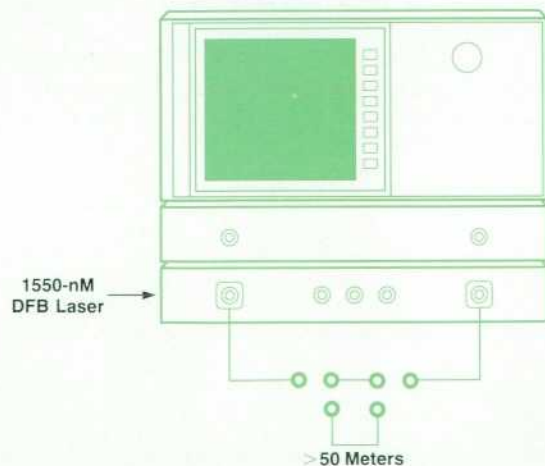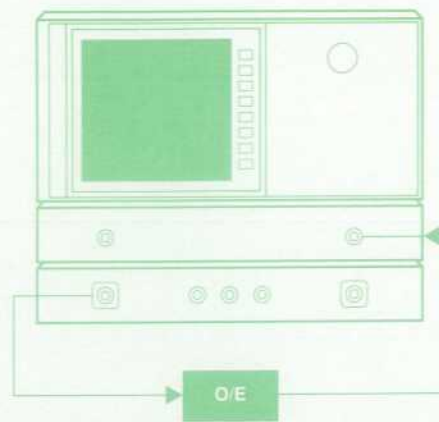n a time varying manner. Since the wavelengths of light are so small, a fiber can easily change length by many wavelengths with small changes in temperature. Such changes will cause the vector sum of the various light components in the system to vary over time. A method of reducing this condition is to add a length of fiber between the sources of optical reflections that is longer than the coherence length of the source spectrum. This will cause the multiple reflections in the system to be uncorrelated so that they no longer add or subtract coherently. Fig. 10 shows a simple fiber measurement with two different lengths of fiber. The longer length is greater than the coherence length of the 50-MHz-linewidth DFB laser source in the measurement system. Fig. 11 is a plot of the fiber measurements at a fixed modulation frequency of 1 GHz. The two traces are for the different lengths of fiber: the top trace is for 1 meter and the bottom trace is for 50 meters. The drift is somewhat random with time and the long-line trace shows about half that of the shorter line. The remainder of the effect is caused by multiple reflections in other parts of the system that were not separated by the longer line.

Measurement Example

Consider a typical device measurement as shown in Fig. 12. This is a photodiode receiver with a slope responsivity of approximately −10 dBe (0.316 A/W). Its electrical input match and optical output match both correspond to approximately 14 dB of return loss.

Table II shows estimates of the expected measurement accuracy for the sample receiver. The sources of error identified relate to the accuracy factors discussed. One term or factor not discussed is the measurement calibration error term. This represents the errors introduced during the user

Slope Responsivity = −10 dB
RF, Optical Return Loss = −14 dB

Fig. 12. *Photodiode receiver measurement setup.*

Table II
HP 8703A Measurement Accuracy (Typical)
Frequency Response of a Lightwave Receiver

	Non-RSS Estimate		RSS Estimate	
Factory Calibration	0.125	1.0 dB	0.053	0.65 dB
Laser Stability	0.012	0.1 dB	0.012	0.1 dB
Connector Repeatability	0 (Offset Error Ignored)			
Measurement Calibration	0.023	0.2 dB	0.023	0.2 dB
Optical Reflections	0.041	0.35 dB	0.041	0.35 dB
Electrical Reflections	0.020	0.17 dB	0.020	0.17 dB
Measurement Accuracy		1.7 dB		0.75 dB

CH1 MEM1   log MAG   .02 dB/   REF −.12 dB
CH2 MEM2   log MAG   .02 dB/   REF −.74 dB

dBo Cor

1-m Fiber

50-m Fiber

dBe Cor

START D e   CW 1.000 000 000 GHz   STOP 10 e

Fig. 11. *Time variations of the attenuation of two lengths of fiber.*

CH1 O/E   log MAG   4 dB/   REF −27.5 dB   1: −21.547 dB
E−2 x
dBe
H1d

.130 000 000 GHz

START .130 000 000 GHz   STOP 20.000 000 000 GHz
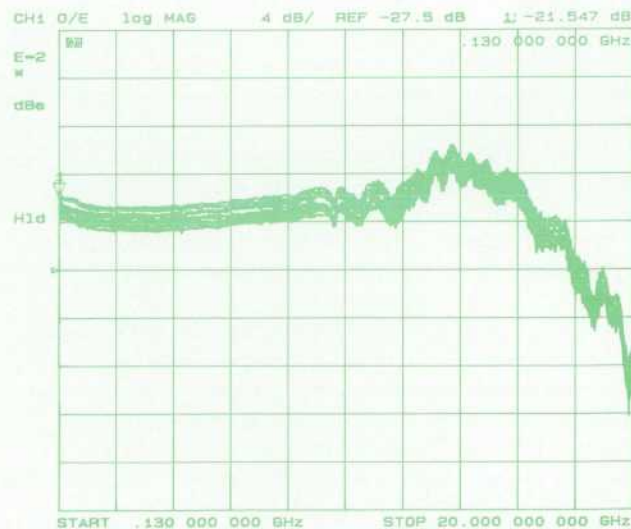
Fig. 13. *Measurements of the same lightwave receiver with ten different HP 8703A analyzers.*

CH1 O/E/Mllog MAG   1 dB/   REF 1.5 dB

E=2
 *

dBm

HId

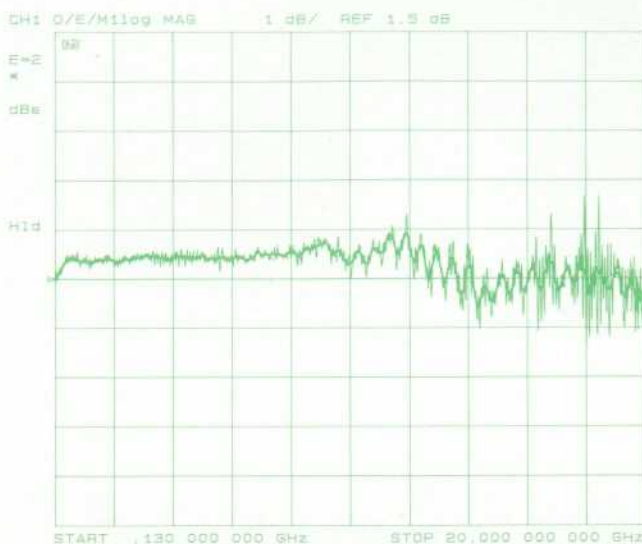START .130 000 000 GHz   STOP 20.000 000 000 GHz

Fig. 14. *Ratio of the maximum and minimum measurements in Fig. 13.*

calibration; the user calibration step is equivalent to measuring a device with no error-inducing characteristics.

The non-RSS estimate is a classical estimate of overall accuracy obtained by adding the systematic terms linearly to the RSS (root sum square) combination of all of the random terms. Since the accuracy of this system is influenced by numerous sources of error that have similar magnitudes and independent distributions, a better estimate of the *typical* expected performance is given by the RRS combination of all of the error terms, both systematic and random. In this case, the classical (non-RSS) value of expected accuracy is 1.7 dB and the typical (RSS) value is 0.75 dB.

Fig. 13 shows the measurement repeatability of a single lightwave receiver measured on ten different HP 8703A systems. There are two aspects that should be discussed: (1) the offset repeatability observed, which relates to the difference in the device's slope responsivity (i.e., conversion efficiency), and (2) the modulation frequency response flatness differences observed. In some cases measurements on any two systems agree to within tenths of a dB. The ten measurements all fall within about a 2-dB band over the frequency range.

A comparison of the two extreme measurements is shown in Fig. 14. The minimum trace was stored in memory and the maximum trace in the data register. A Data/Memory function was performed on the two traces to show the fine-grain agreement. The offset difference between the two measurements is about 2.0 dB, which means that the low-frequency slope responsivity for the two extreme cases varied between -21.5 dB and -23.5 dB. The frequency flatness difference between these two extreme measurements is about ± 0.5 dB if the fine-grain ripple or noise is neglected. If the fine-grain ripple is included in the measurement, the frequency flatness is no longer ± 0.5 dB but almost ± 1.5 dB. The multiple measurements represent a sampling of the distribution of potential random measurement error.

In the accuracy calculations using the non-RSS and RSS methods, the RSS method yielded a typical flatness uncer-

tainty of ± 0.6 dB, which agrees well with the measurement results when the fine-grain ripple is ignored, and the non-RSS method yielded a flatness uncertainty of ± 1.7 dB, which agrees well when the fine-grain ripple is included.

Acknowledgments

References

1. R. Wong, P. Hernday, M. Hart, and G. Conrad, "High-Speed Lightwave Component Analysis," *Hewlett-Packard Journal*, June 1989, Vol. 40, no. 3, pp. 35-51.
2. R. Wong, P. Hernday, and M. Hart, "Technical Innovations for the Design of a New 20-GHz Lightwave Component Analyzer," *Hewlett-Packard RF and Microwave and Lightwave Measurement Symposium*, October 1989.
3. D. Harkins, P. Hernday, and R. Wong, "Accuracy Considerations and Error Correction Techniques for 20-GHz Lightwave Component Analysis," *Hewlett-Packard RF and Microwave and Lightwave Symposium*, July 1990.
4. C. Hentschel and I. Muller, "Single-Mode Fiber Optic Connector Technology and Performance," *Hewlett-Packard RF and Microwave and Lightwave Symposium*, August 1988.

Development of an Optical Modulator for a High-Speed Lightwave Component Analyzer

The design and characterization of the first integrated optic modulator for commercial instrument application are described, including the advantages of titanium in-diffused lithium niobate, device geometries for both phase modulators and Mach-Zehnder intensity modulators, stability considerations including bias drift and acoustic resonances, wavelength sensitivity, packaging and pigtailing, reliability, and testing.

by Roger L. Jungerman and David J. McQuate

FOR HIGH-SPEED FREQUENCY-DOMAIN instrument applications, an efficient, large-bandwidth, calibrated modulated optical source is required. Our primary interest was in developing a source for a 20-GHz lightwave component analyzer, the HP 8703A. This application requires the maximum modulated power at all frequencies for a given drive power (to give the greatest dynamic range) and a stable, repeatable frequency response that can be calibrated out by the instrument. In addition, the phase of the optical modulation response must be known for group delay measurements and inverse Fourier transforms of the frequency-domain data into the time domain.

No commercially available sources had a 20-GHz modulation capability. Research papers indicated several possibilities for obtaining a wide modulation bandwidth. Direct laser diode current modulation[1,2] could achieve the desired bandwidth. However, the laser drive current required to obtain broad frequency operation is large and the long-term reliability of the devices under these conditions has not been demonstrated. Also, many wide-bandwidth fiber optic systems employ narrow-linewidth distributed feedback (DFB) lasers, which minimize dispersion effects in the system. Wide-bandwidth direct modulation of DFB lasers has been demonstrated,[3] but the frequency response of the DFB lasers is not as wide as conventional Fabry-Perot diode lasers, and the DFB linewidth broadens under modulation.

Optical heterodyne techniques, in which two narrow-linewidth lasers slightly offset in frequency are combined in a fiber to produce a difference-frequency signal, can be used to produce very wide-bandwidth intensity modulation.[4,5] The heterodyne laser frequencies are typically temperature tuned. Temperature tuning is slow and the temperature cannot be precisely controlled. This temperature variation produces frequency drift in the modulation so that the modulation phase is not well-characterized. Hence, the heterodyne system cannot be easily used in the HP 8703A where the phase of the optical modulation is critical.

External Modulators

The modulation method used in the lightwave component analyzer is external modulation.[6] A high power laser diode is run CW and input into a lithium niobate external modulator.[7,8] Direct and external modulation of a diode laser are compared in Fig. 1. With external modulation, the laser diode itself is unmodulated and the linewidth of the source can be very narrow if a DFB laser is used. The same modulator can be used with a variety of laser sources over the wavelength range of 1300 nm to 1550 nm. Tunable external cavity lasers[9] can also be input into the modulator. The HP Microwave Technology Division has years of experience processing $LiNbO_3$ surface acoustic wave filters,
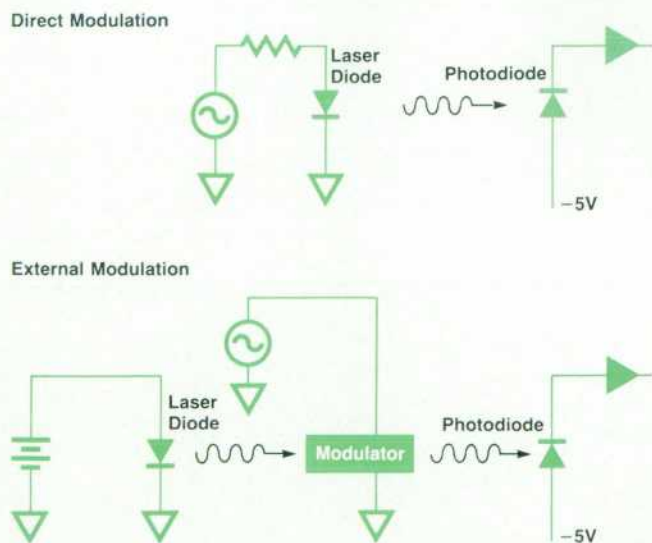
Direct Modulation

External Modulation

Fig. 1. *Direct versus external intensity modulation of a laser diode.*
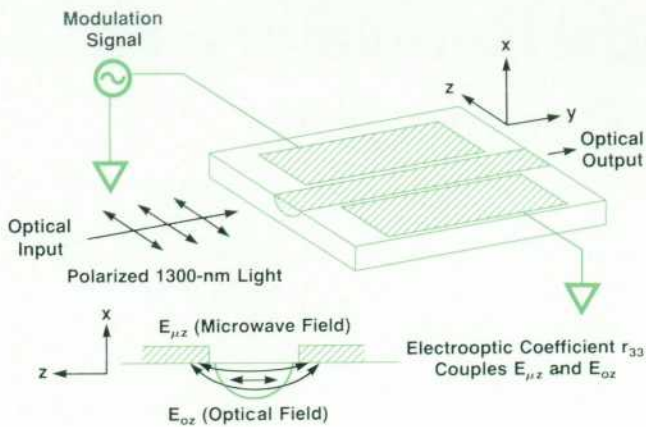
Fig. 2. *An integrated Ti:LiNbO₃ phase modulator.*

Fig. 4. *Velocity mismatch between the microwave modulation and the optical carrier limits the bandwidth.*

which we were able to leverage in developing the optical modulator. The primary disadvantages of using an external modulator are the added complexity (both a laser and a modulator are required), polarization sensitivity, and additional optical insertion loss.

External modulation can be accomplished with several schemes. Efficient modulation over a large bandwidth is realizable with integrated optic waveguide devices on substrates such as lithium niobate (LiNbO₃), lithium tantalate (LiTaO₃), and gallium arsenide (GaAs). These anisotropic substrates all exhibit the electrooptic (Pockels) effect, in which the phase velocity of light through the substrate is altered by an applied electric field.

Lithium niobate is an optically transparent dielectric with a low loss tangent for microwaves. An optical waveguide can be formed in LiNbO₃ by diffusing a strip of titanium into the wafer at elevated temperature.[7] Electrodes are plated onto the substrate to form a coplanar microwave waveguide. In x-cut LiNbO₃, as shown in Fig. 2, the microwave waveguide straddles the optical waveguide to exploit the largest electrooptic coefficient r_{33}. The z component of the optical field and the z component of the applied microwave field are coupled by this coefficient of the electrooptic tensor. The device shown is an optical phase modulator. Light traveling through the guide will emerge with its optical phase modulated by the applied microwave signal. Phase modulators are of interest in coherent optical communications,[10] where a narrow-linewidth laser is phase

modulated and the resulting signal can be detected using a tuned local oscillator laser. Coherent lightwave systems offer advantages in sensitivity and the number of channels that can be multiplexed on a single fiber.

An optical intensity modulator based on the Mach-Zehnder interferometer configuration is shown in Fig. 3. The input light is split in a Y branch. The two parallel optical waveguide arms form two phase modulators, which operate push-pull when the coplanar microwave waveguide is deployed as shown. When the light from the upper and lower waveguides recombines in the output Y branch, there is alternating constructive and destructive interference as the applied microwave signal changes polarity, resulting in intensity modulation of the output light. The high dielectric constant of LiNbO₃ (approximately 40) results in a low characteristic impedance of 22 ohms for the coplanar transmission line.

Several factors limit the response of these traveling-wave modulators at high microwave frequencies. The main limitation is a mismatch of the velocities of the two copropagating waves (optical and microwave) as shown in Fig. 4. The optical signal travels about twice as fast as the microwave signal. If the difference in time of propagation through the modulator is great enough, the microwave signal will get out of phase with the microwave modulation on the optical

Fig. 3. *An integrated Ti:LiNbO₃ Mach-Zehnder interferometer optical modulator.*

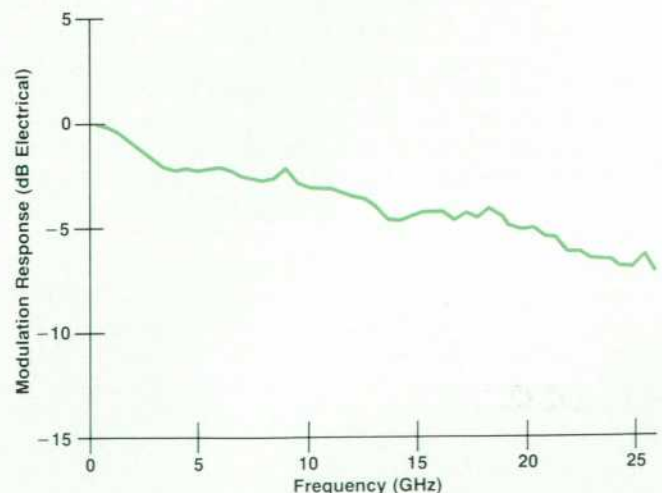**Fig. 5.** *Frequency response of the HP modulator.*

signal and begin to reverse the effect. By keeping the device length short, velocity mismatch can be reduced and broadband operation obtained. We use a 5-mm-long active electrode to achieve a frequency response that rolls off approximately 5 dBe (electrical dB) at 20 GHz as shown in Fig. 5. The response shown here uses a resistive circuit to match to the low modulator impedance. In the HP 8703A, an impedance-transforming taper is used, which gives more modulated power but also more ripple at low frequencies.

Microwave loss in the coplanar electrode also contributes to reduced modulation efficiency at high frequencies. If the plated gold electrodes are sufficiently thick the loss will be mainly because of the skin effect and will increase as the square root of frequency. Typically, the electrodes are several micrometers thick. Microwave power transmitted through the modulator coplanar line, s_{21}, measured on a network analyzer (Fig. 6) shows the square root dependence, in this case reaching about 12 dB at 25 GHz.

Modulator Fabrication

Fig. 7 shows how modulators are fabricated on x-cut $LiNbO_3$. Optical waveguides are produced by the in-diffusion of titanium. Narrow stripes of titanium are patterned using standard photolithographic and lift-off techniques. The wafers are then placed in a 1000°C furnace and diffused for several hours. The in-diffused titanium raises the index of refraction and confines light to the guide. Following the diffusion, a buffer layer of SiO_2 is deposited on the surface of the wafer. This is followed by a gold-plating base. After photoresist patterning, the gold electrodes are plated on. The plating base and SiO_2 are then etched away in the electrode gap. After wafer fabrication the ends of the waveguides must be polished to ensure good coupling of the light into the guide. Strips of $LiNbO_3$ are glued onto the top of the wafer to protect it. The end faces are then polished and the wafer is separated into individual chips, as shown in the photograph, Fig. 8.

To be useful off the optical bench, integrated optic modulators must be pigtailed with single-mode fiber. After fabrication, the modulator is firmly mounted on a carrier, which protects the modulator from mechanical shock and

Fig. 7. *Modulator cross section.*

breakage. The carrier has two RF connectors to provide an input and an output for the modulation signal and a thin-film circuit to match to the modulator impedance. Input and output pigtails are then attached. Pigtails are a mechanical joint between the optical fiber and the waveguide, which if properly aligned, provide a low-loss optical path through the modulator. The optical fiber is placed in a glass capillary to provide a more robust joint, and then polished. Optical pigtails are precisely aligned to minimize optical loss and then are permanently attached to the modulator with an adhesive. Small lateral or longitudinal misalignments increase the insertion loss. A lateral alignment of better than 1 μm must be maintained to keep the loss of two pigtails to a few tenths of a dB.

Modulator Characteristics

A measurement of a modulator's optical transmission as a function of the bias voltage yields the transfer function shown in Fig. 9. The dc bias is swept and the optical transmission is measured. From the transfer curve we can obtain

Fig. 6. *Microwave power transmitted through the HP modulator decreases as the square root of frequency.*

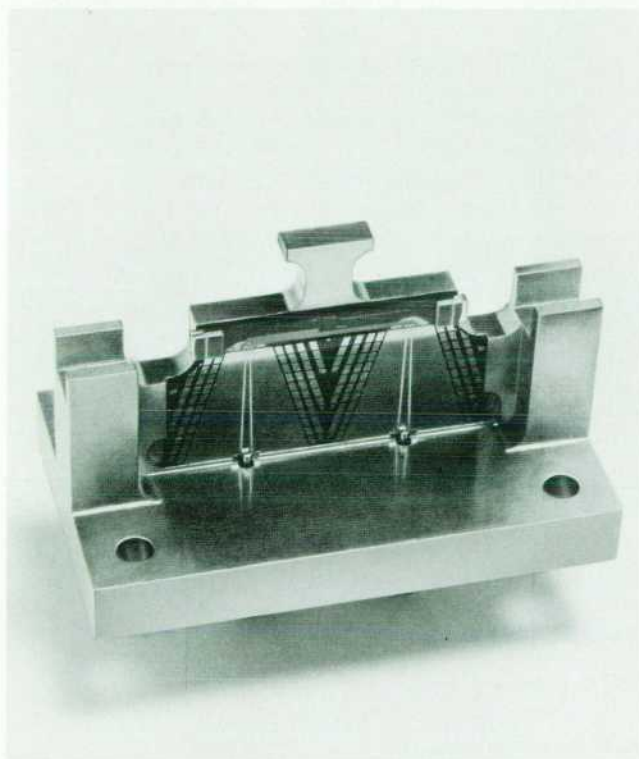**Fig. 8.** *Photograph of the HP optical modulator.*

four parameters:

- The insertion loss is the optical transmission at the peak of the curve.
- The switching voltage, V_π, is the difference in bias voltages at the minimum and maximum transmission points.
- The extinction ratio is the ratio of maximum to minimum optical transmission.
- The normal operating point is the bias voltage that results in optical transmission half-way between minimum and maximum.

The modulator is linear for small deviations from the normal operating bias point. The bias point of LiNbO₃ modulators can change because of a variety of factors. Temperature changes create pyroelectric surface charges which bias the modulator. As shown in Fig. 10, x-cut LiNbO₃ has better temperature stability than z-cut LiNbO₃. Other factors can also change the bias point. Stress in the modulator—caused, for example, during packaging—is one factor. The bias point of the modulator can be adjusted electrically by applying a dc voltage to the device. However, there are memory effects in the LiNbO₃ that cause drift after a large electrical bias is applied.[11] Modulator drift does not adversely affect instrument operation. The total instrument drift of the HP 8703A including the modulator is 0.03 dB over one hour after a standard instrument warm-up period.

Reliability and Testing

In addition to meeting bias drift requirements, the modulator chip, package and pigtail must withstand rigorous environmental qualification. Modulators have been subjected to the environmental tests listed in Table I and remain within specifications.

Table I
Modulator Environmental Tests

Test	Standard	Strife
Temperature cycling	10 cycles −45°C to +85°C	−55°C to +125°C
Vibration	Swept sine 20 Hz to 2 kHz, +15g, 30 min	Random 20 Hz to 2 kHz, 7.75g rms, 0.3 g²/Hz, 15 min per axis
Mechanical shock	1000g three times, each of six axes	1500g
Humidity	10 days 65°C 95% R.H.	Same but with bias applied
Optical damage	7mW 30 days	20mW 30 days
Electrostatic discharge	3000V	

Acknowledgments

The authors wish to thank the other members of the modulator development team: C.A. Johnsen, J.L. Hender-
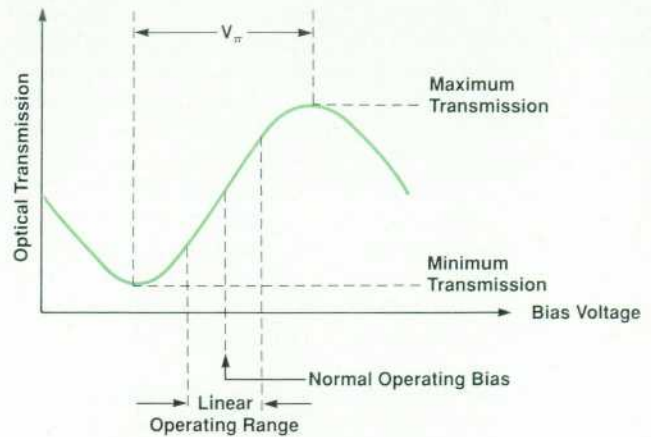
Fig. 9. *Mach-Zehnder interferometer transfer curve, showing the linear region.*

References

1. J.E. Bowers, B.R. Hemenway, A.H. Gnauck, and D.P Wilt, "High-Speed InGaAsP Constricted Mesa Lasers," *IEEE Journal of Quantum Electronics*, Vol. QE-22, 1986, p. 833.
2. R. Olshansky, W. Powazinik, P. Hill, V. Lanzisera, and R.B. Lauer, "InGaAsP Buried Heterostructure Laser with 22 GHz Bandwidth and High Modulation Efficiency," *Electronics Lettres*, Vol. 23, 1987, p. 839 (1987).
3. K. Kamite, H. Sudo, M. Yano, H. Ishikawa, and H. Imai, "Ultra-High Speed InGaAsP/InP DFB Lasers Emitting at 1.3 μm Wavelength," *IEEE Journal of Quantum Electronics*, Vol. QE-23, 1987, p. 1054.
4. S. Kawanishi and M. Saruwatari, "Wideband Frequency Response Measurement of Photodetectors Using Optical Heterodyne Detection Technique," *Electronics Lettres*, Vol. 22, 1986, p. 337.
5. T.S. Tan, R.L. Jungerman, and S.S. Elliott, "Optical Receiver and Modulator Frequency Response Measurement with a Nd:YAG Laser Heterodyne Technique," *IEEE Transactions on Microwave Theory and Techniques*, Vol. MTT-37, 1989, p. 1217.
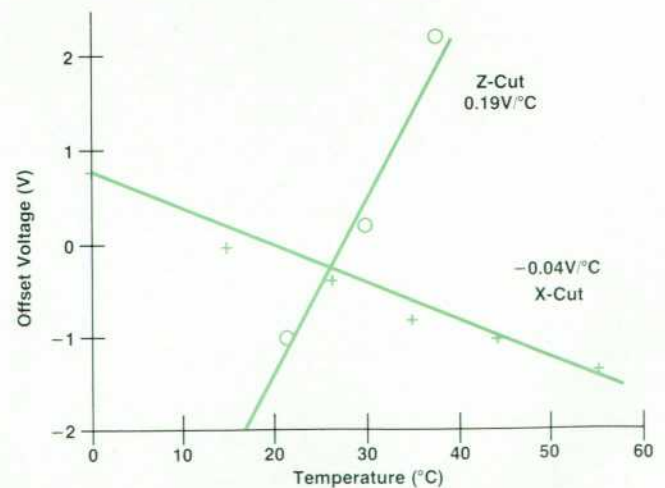
Fig. 10. *Temperature stability of the bias point.*

6. R.L. Jungerman, C.A. Johnsen, D.J. McQuate, K. Salomaa, M.P. Zurakowski, R.C. Bray, G. Conrad, D. Cropper, and P. Hernday, "High-Speed Optical Modulator for Application in Instrumentation," *Journal of Lightwave Technology*, Vol. 8, 1990, p. 1363.
7. R.C. Alferness, "Waveguide Electrooptic Modulators," *IEEE Transactions on Microwave Theory and Techniques*, Vol. MTT-30, 1982, p. 1121.
8. D.W. Dolfi, "Travelling-Wave 1.3 μm Interferometer Modulator with High Bandwidth, Low Drive Power, and Low Loss," *Applied Optics*, Vol. 25, 1986, pp. 2479-2480.

9. J. Mellis, S.A. Al-Chalabi, K.H. Cameron, R. Wyatt, J.C. Regnault, W.J. Devlin, and M.C. Brain, "Miniature Packaged External-Cavity Semiconductor Laser with 50 GHz Electrical Tuning range," *Electronics Lettres*, Vol. 24, 1988, p. 998.
10. J. Salz, "Coherent Lightwave Communications," *AT&T Technical Journal*, Vol. 64, 1988, p. 2153.
11. R.A. Becker, "Circuit Effect in LiNbO$_3$ Channel-Waveguide Modulators," *Optical Letters*, Vol. 10, 1985, p. 417.

A High-Performance Optical Isolator for Lightwave Systems

This compact, rugged, two-stage design uses birefringent rutile crystals and Bi-YIG films to achieve high isolation, low insertion loss, high return loss, and polarization independence.

by Kok-Wai Chang, Siegmar Schmidt, Wayne V. Sorin, Jimmie L. Yarnell, Harry Chou, and Steven A. Newton

OPTICAL ISOLATORS are playing an increasingly important role in fiber optic systems. Their purpose is to protect optical sources from reflections and backscattering that cause output instabilities or unwanted changes in the output spectra. Isolators can do this because they are nonreciprocal devices, that is, their transmission characteristics depend upon the direction of light through them. Isolators act as one-way light valves that allow the efficient injection of optical signals into a system while preventing unwanted feedback from returning to the optical source.

Reflections in optical systems can come from a variety of sources, including Fresnel reflections at connectors, splices, fiber ends, bulk optics interfaces, and detector surfaces (Fig. 1). Even Rayleigh backscattering from the fiber may add up to a substantial return signal. It is the job of an isolator to minimize the amount of this reflected and backscattered power that returns to the source.

Optical feedback can cause serious degradations in laser performance, including undesirable spectral changes and instabilities as well as increases in both intensity and phase noise. Secondary effects can include reduction in modulation bandwidth, environmental tolerance, and lifetime. Fig. 2 illustrates how the modulation frequency response
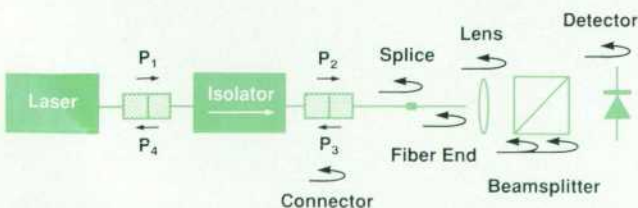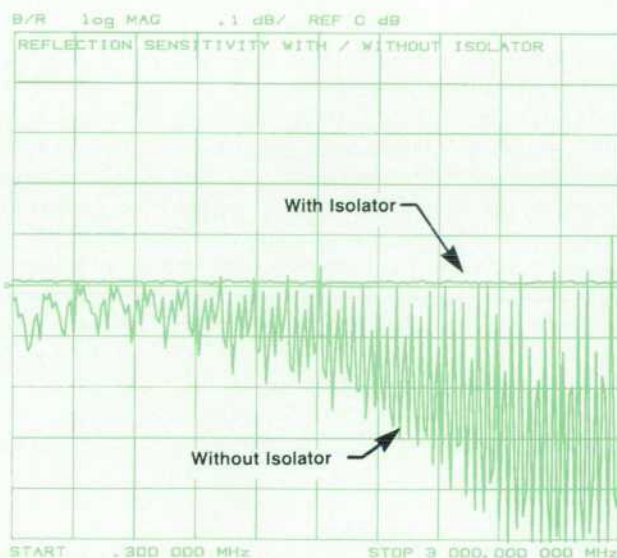

Fig. 1. *An optical isolator prevents downstream reflections from degrading laser performance.*

Fig. 2. *The modulation characteristics of a semiconductor laser can be greatly affected without the use of an isolator.*

of a Fabry-Perot laser diode changes with and without the use of an optical isolator. The feedback levels at which these effects occur can be remarkably low. For example, disabling perturbations have been observed in the spectra of certain distributed feedback (DFB) lasers as a result of reflections as small as -90 dB (i.e., 10^{-9} relative to the output power). In such cases, it is not uncommon for a user to need several cascaded isolators to provide complete protection for the laser. While this is an extreme example, it is clear that every optical source—from a single-frequency laser to a superluminescent diode (SLD)—will perform better when used in conjunction with a high-quality isolator.

In addition to source protection, isolators also play an increasingly important role within fiber optic transmission systems. Reflections between components or interfaces within such systems can result in serious degradations in system performance. For example, multiple reflections within a transmission system can cause the interferometric conversion of laser phase noise to intensity noise. In systems containing optical amplifiers, reflections can produce increased noise and can even cause lasing, thus limiting the levels of amplifier gain and component reflectivity that can be allowed. Clearly, then, there is a need for isolators to control reflections throughout optical transmission systems to avoid degraded performance.

Isolator Description

Magnetooptic isolators can provide solutions for most of the feedback problems that may be encountered in an optical system. Fig. 3 shows a conventional magnetooptic isolator in its simplest form. This single-stage isolator consists of two polarizers surrounding a piece of Faraday material, such as a YIG crystal. When placed in a magnetic field, such materials exhibit the Faraday effect—the nonreciprocal rotation of the polarization of the light that passes through them.

In a conventional isolator, the first polarizer transmits only a linearly polarized component of the incident light. The orthogonal component is absorbed, reflected, or otherwise discarded. The Faraday material rotates the polarization of the light by 45 degrees. The light is then transmitted through the second polarizer, which is oriented at 45 degrees with respect to the first.

In the reverse direction, the second polarizer passes only one linear component of the light that is reflected from points beyond the isolator. However, because of the non-reciprocal nature of the Faraday effect, the sense of rotation in the reverse direction (e.g., clockwise) is different from the sense of direction in the forward direction (e.g., counter-clockwise). As a result, the polarization plane is not rotated back to its original position, but is rotated another 45 de-

grees, or 90 degrees with respect to the original input polarizer, which therefore strongly attenuates the reflected signal.
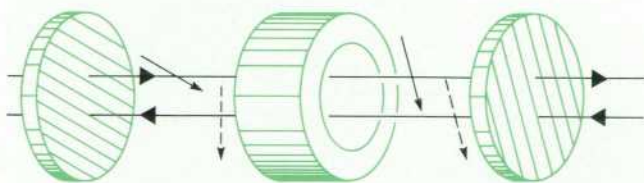
Unfortunately, conventional magnetooptic isolators have limitations that are particularly undesirable for use in fiber optic systems. The most significant limitation is that they are polarization dependent. The component of the input light whose polarization is orthogonal to the input polarizer is simply lost. In addition, conventional isolators are often bulky because of the size of the Faraday crystal and/or the magnetic field required to produce a 45-degree rotation. However, both of these limitations can be removed through the use of birefringent walk-off crystals as polarizers and bismuth substituted YIG films as the Faraday material.

Birefringent crystals do not have isotropic propagation characteristics. Instead, the optical refractive index (and therefore the propagation speed) depends upon the input polarization and the direction along which the light propagates.

When light is incident upon such a crystal at an angle to its optic axis, orthogonally polarized components of the light will be split into separate beams propagating in slightly different directions. If the crystal is a plane-parallel plate, two parallel, orthogonally polarized beams will emerge, one having "walked-off" from the other by an amount proportional to the crystal thickness. Therefore, unlike other kinds of polarizers which absorb, deflect, or otherwise discard one of the polarization components, birefringent crystal polarizers provide access to both polarizations in the form of separate parallel beams. This feature is critical in the manufacture of polarization independent isolators.

Recently developed bismuth substituted YIG films offer the advantage of providing ample Faraday rotation in a very small physical space. These films, which can be used for the 1300-nm and/or 1550-nm wavelength bands, can achieve 45 degrees of Faraday rotation in film thicknesses less than 500 micrometers. This can be accomplished using a relatively modest magnetic field that can be provided by a small permanent magnet. As a result, the use of Bi-YIG films can make compact, high-performance isolators possible.

HP Isolator

The HP isolator incorporates both rutile birefringent walk-off crystals and Bi-YIG films into a proprietary design whose primary goals are to achieve high isolation, low
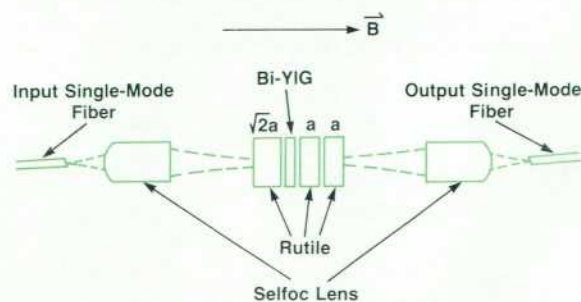

Fig. 3. *Conventional magnetooptic isolator consisting of a Faraday material surrounded by two polarizers.*

Fig. 4. *Components used in a single-stage, polarization independent isolator.*

insertion loss, high return loss, and polarization independence in a compact, rugged package. The design employed in HP products incorporates two isolating stages in series to obtain high performance in each of these important areas. However, to explain more clearly the design of the isolator and its operating principles, we will focus on an earlier, single-stage version of this device.

Fig. 4 illustrates the single-stage version of the isolator design. This design uses Selfoc lenses to couple the light from single-mode fibers into and out of the body of the isolator. At the center of the isolator is a Bi-YIG film. Although it is less than 500 μm thick, this film can provide 45 degrees of Faraday rotation at design wavelengths of either 1.3 or 1.5 μm when placed in the field of a small permanent magnet. The birefringent walk-off crystals are made of TiO_2 (rutile). Since the diameter of the beam waist for this design is 60 μm, a walk-off separation of about 200 μm was chosen to ensure that the beams would not overlap. This requires rutile crystal thicknesses of about 2 mm. As a result, the overall length of the rutile-YIG arrangement at the core of the isolator is less than 1 cm.

Fig. 5 shows how the isolator works. In this figure, the spatial position of each polarization is indicated as the light travels in both the forward and backward directions. The birefringent crystals are cut such that the forward traveling e-ray (extraordinary polarization) walks off in the + direction while the backward traveling e-ray walks off in the − direction. The o-ray (ordinary polarization) does not experience a spatial walk-off. Consider first what happens to the forward traveling signal. Incident to the first birefringent crystal (position 1), both polarization components can exist in a single input beam. After this first crystal (position 2), the vertical polarization (e-ray) walks off in the + direction. The two beams then pass through the Faraday film (position 3), where both polarizations are rotated by 45 degrees in the counterclockwise direction. The signal then passes through the second birefringent crystal, where the previously walked-off polarization experiences a second walk-off (see position 4). Since the thickness of the second and third rutile crystals is $1/\sqrt{2}$ times that of
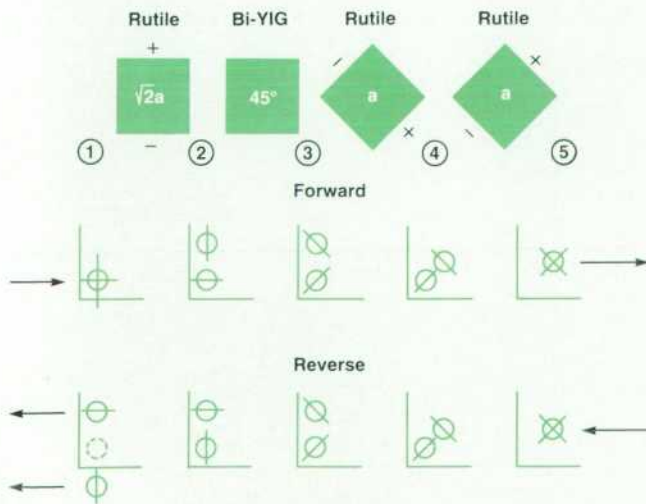
the first crystal, the two polarizations can be recombined into a single beam by orienting the third crystal at 90 degrees with respect to the second (see position 5). This arrangement of crystals allows any incoming state of polarization to be transmitted efficiently through the isolator in the forward direction.

It is easier to follow the path of reflected signals through the isolator in the reverse direction by noting that the components between position 5 and position 3 are reciprocal. This means that light traveling in the reverse direction must follow exactly the same path as it did in the forward direction. Therefore, at position 3, the spatial walk-off and polarization states must be identical for both the forward and backward traveling signals. As the beams propagate in the reverse direction through the Faraday film (from position 3 to position 2), they undergo a nonreciprocal (clockwise) rotation of 45 degrees. This causes the two beams traveling in the reverse direction to have orthogonal polarizations with respect to forward traveling beams. The first rutile crystal again causes the vertical polarization to walk off, but now this results in the spatial separation of both returning beams from the position of the input beam. Therefore, these backward traveling beams do not couple to the single-mode fiber at the input. As a result, the input is highly isolated from any signal returning from the output fiber.

These principles were incorporated into a more complex, two-stage isolator design which is presently used in HP products. After the first of these isolators was designed, assembled, and tested at HP Laboratories, the isolator technology was transferred to both the Böblingen Instruments Division (BID) and the Network Measurements Division (NMD). BID further developed the isolator and is presently offering it as a pair of fiber-pigtailed, polarization independent isolator products, the HP 81210LI and the HP 81310LI, for use at wavelengths of 1310 and 1550 nm, respectively. The technology was also transferred to NMD, which developed a slightly different version of the isolator and incorporated it into the lightwave section of the HP 8703A lightwave component analyzer.

The final versions of the HP isolator have met or exceeded all of the performance goals for which they were designed. The important performance characteristics are described in more detail in the following sections.

Isolation

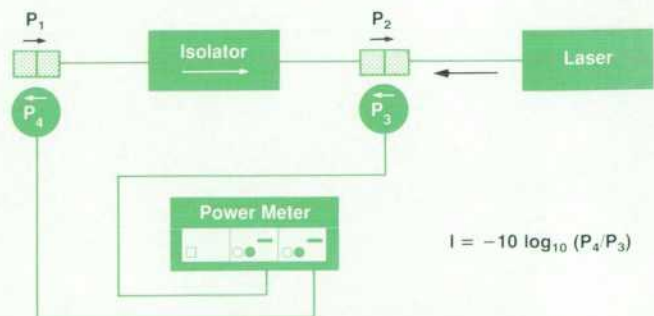Isolation is obviously one of the most important specifi-

Fig. 5. *Description of how spatial walk-off is used to provide isolation and polarization independent transmission.*

Fig. 6. *Method used for isolation measurement.*

$$I = -10 \log_{10} (P_4/P_3)$$

cations for any isolator. It is a measure of the amount of light reflected from points beyond the isolator back through the isolator and toward the source. If P_3 is the power reflected from points downstream of the isolator, and P_4 is the amount of this reflected power returning through to the input side of the isolator, then the isolation I can be expressed in dB by

$$I = -10\log(P_4/P_3).$$

An accurate way of measuring isolation is to inject power into what would normally be the output end of the isolator (see Fig. 6) and then measure and determine the ratio of the injected and transmitted powers using a sensitive dual-head power meter, such as the HP 8152A.

Fig. 7 shows a histogram of a production run of HP 81210LI and HP 81310LI isolators. The average HP isolator provides isolation of greater than 56 dB. This is sufficient protection for the vast majority of semiconductor laser sources. Two HP isolators can be used in series to provide greater protection for the most sensitive single-frequency lasers, or a single HP isolator can be used in conjunction with lasers that are packaged with their own integrated isolators.

Return Loss

Return loss refers to the amount of reflection, not from sites downstream of the isolator or from its connectors, but rather from the isolator itself. Such reflections can arise from one or more of the several optical surfaces within the body of a typical isolator.

To measure the return loss, the fiber on the output end of the isolator must be well-terminated (such as by index matching or knotting) to ensure that all reflections beyond the isolator are completely suppressed. The return loss can then be measured as shown in (Fig. 8). A 3-dB (50-50 splitting ratio) directional coupler is used to tap off equal fractions of the light that is being transmitted to and reflected from the isolator, and to transmit those fractions to a dual-head power meter for measurement and comparison. If the light power transmitted to the isolator is P_1 and the light power reflected from it is P_4, the return loss is expressed in dB as

$$RL = -10 \log_{10} (P_4/P_1)$$
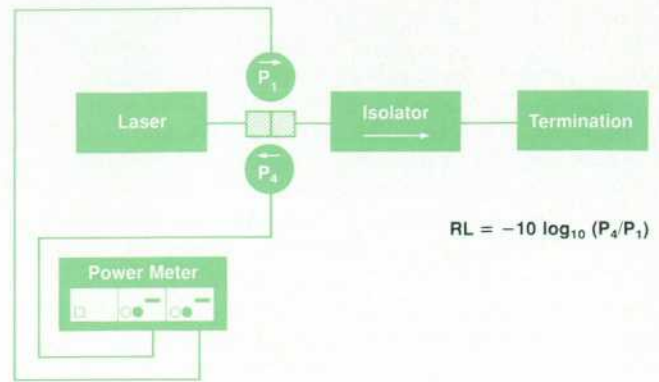
Fig. 8. *Method used for measurement of isolator return loss.*

$$RL = -10\log(P_4/P_1).$$

This result can be read directly from a dual-head power meter.

Even an isolator having excellent isolation specifications may be of only limited usefulness if its return loss is too low. For example, if an isolator is specified for 60 dB of isolation but has a return loss of only 30 dB, it will do an excellent job of protecting the laser source from strong reflections beyond the isolator. However, the 0.1% of the source light that is always reflected back to the source from the isolator itself may cause serious perturbations.

As Fig. 9 indicates, the HP isolator exhibits high return loss of more than 60 dB, exclusive of the connector end face. This means that with the use of low-reflection connectors or a fusion splice the user can enjoy the full advantage of the HP isolator's excellent isolation specification.

Insertion Loss

Insertion loss is a measure of the attenuation suffered by an optical signal when it passes through an isolator in the forward direction. It is expressed in dB by

$$IL = -10\log(P_2/P_1),$$

where P_1 is the input power and P_2 is the output power.
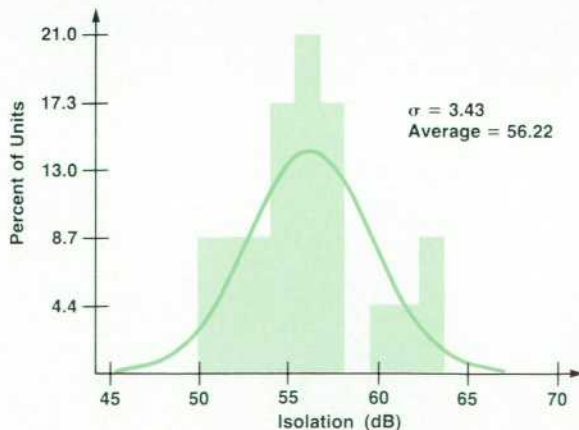
Fig. 7. *Histogram showing variation in isolation for an early production run of HP 81210IL and HP 81310IL isolators.*
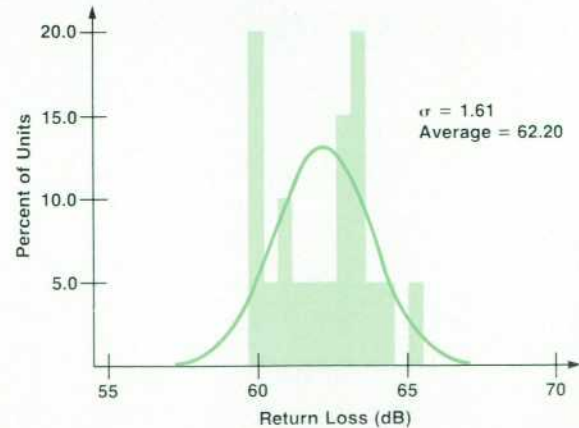
Fig. 9. *Histogram showing return loss for the HP 81210IL and HP 81310IL isolators.*

The insertion loss is easily determined by power meter measurements of the input and transmitted powers (Fig. 10). If a dual-head power meter and identical coupler taps are employed, these powers can be monitored simultaneously and the insertion loss can be read out directly.

As with most components, it is desirable that the insertion loss of an isolator be as low as possible. Isolator insertion loss tends to be particularly important, however, since systems that employ isolators typically have limited power budgets. The HP isolator has low fiber-to-fiber insertion loss of less than 2.5 dB over a wide range of temperatures and wavelengths. As Fig. 11 indicates, the average insertion loss for the HP 81210LI and HP 81310LI is only 1.75 dB.

Polarization Dependence

Polarization dependence is a critical issue for any fiber-pigtailed isolator, since the exact state of polarization at the isolator input is almost always uncertain because of unknown amounts of environmentally induced birefringence in the connecting fiber. Furthermore, the polarization can vary in time because of changes in temperature, pressure, bending, or other factors. As a result, it is essential that all aspects of a fiber-pigtailed isolator's performance be as independent of polarization as possible. In particular, an isolator whose insertion loss is dependent on polarization would be a severe liability if used in a fiber circuit or link.

Isolator polarization dependence is measured using a polarization control device to vary the input state of polarization while measuring the power levels that are relevant for the parameter of interest (Fig. 12). For example, the polarization dependence of the insertion loss is determined by measuring P_1 and P_2 as the polarization is varied.

The HP isolator exhibits transmission variations of less than ± 0.2 dB over a complete range of input polarization states. In fact, as Fig. 13 shows, the average polarization dependence of the insertion loss for the HP 81210LI and HP 81310LI is only 0.06 dB. Such low polarization dependence qualifies these devices as polarization independent isolators according to performance standards established by leading telecommunications companies.

Depolarizing Effects

Most isolators work well when very narrowband sources are used. However, many important applications make use of highly polarized multifrequency or broadband sources.
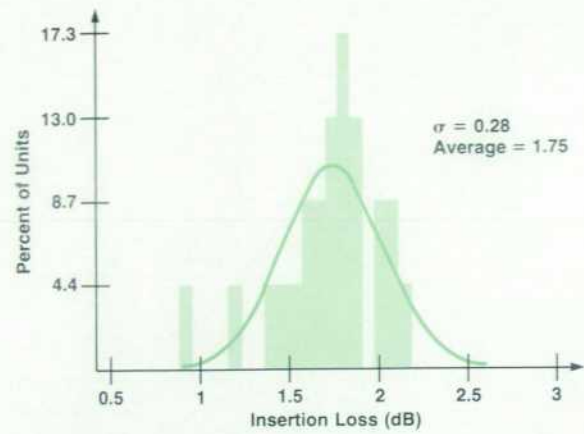
Fig. 11. *Histogram showing insertion loss for the HP 81210IL and HP 81310IL isolators.*

For example, the input to a polarization-sensitive intensity modulator should have a high degree of polarization. Unfortunately, many isolators depolarize such sources, necessitating the lossy repolarization of the light and thus making them undesirable for many applications.

The HP isolator preserves the degree of polarization of any optical source regardless of its spectrum. This means that the performance of the HP isolator is maintained not only when using external cavity or distributed feedback lasers, but also when an application requires a Fabry-Perot laser or a superluminescent diode as the source.

Wavelength and Temperature Dependence

The performance of an isolator can be degraded by changes in either wavelength or temperature. One of the main causes for this is that the 45-degree Faraday rotation is a function of both of these parameters. Errors in this rotation angle result in degradation of isolation and insertion loss. By using a two-stage design, the effect of rotation angle error is significantly reduced. Wavelength variation can also affect coupling efficiencies because of the focal length change of the lenses. Temperature changes can effect coupling efficiencies because of thermal expansion or contraction of the isolator package. Care must be taken to minimize the effects of both of these parameters.

The wavelength dependence of an isolator is determined
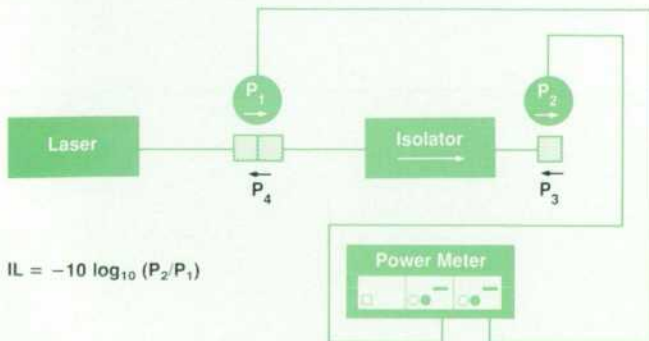
Fig. 10. *Method used for measurement of isolator insertion loss.*
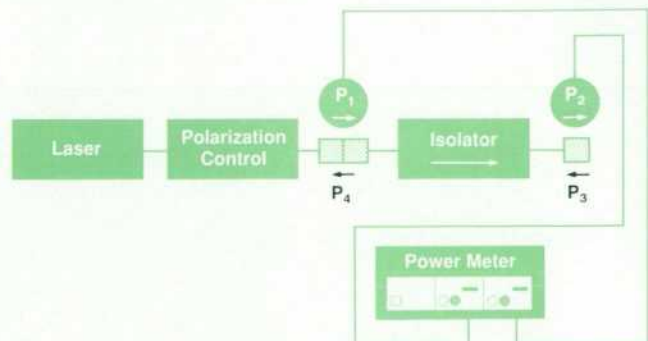
Fig. 12. *Method used for determining polarization dependence of isolator insertion loss.*
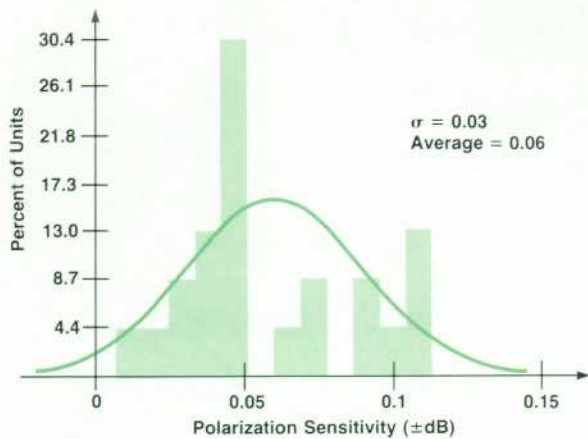
Fig. 13. *Histogram showing insertion loss variation caused by changes in the input polarization state.*

Fig. 14. *Measurement of isolation at different wavelengths and temperatures.*

by measuring its performance using a tunable laser as the source. In practice, this is important because the wavelength of the source may not coincide with the design wavelength of the isolator. The HP isolator provides high performance over a wide wavelength range of ± 30 nm around either of two center wavelengths: 1310 nm or 1550 nm.

Environmental Considerations

The HP isolator also offers outstanding performance over a wide range of operating temperatures: 0 to 55°C. It is also designed to withstand storage temperatures ranging from $-40°C$ to $+75°C$. Fig. 14 shows typical isolation as a function of wavelength at three different operating temperatures.

Environmental humidity, vibration, and shock tests have confirmed the ruggedness of the isolator design. One set of representative measurements was taken on a small sample of isolators used in the HP 8703A lightwave component analyzer. Placed in a humidity chamber at 95% relative humidity and 65°C for 10 days, the isolators showed no measurable change in isolation or insertion loss when returned to ambient conditions. In the vibration test, isolators were subjected to a broadband random vibration of 6.2g rms between 50 and 2000 Hz with a peak spectral density of 0.02 g^2/Hz for 15 minutes on each axis. Insertion loss changes were less than 0.4 dB and the isolation remained between 62 and 67 dB for all input polarization states. In

the shock test, isolators were subjected to a half-sine-wave shock of 1000g for 0.5 ms three times on each of their six sides. Insertion loss changes were not measurable and isolation values varied between 61 and 66 dB for all input polarization states.

Summary

The specifications and cost of commerically available isolators were not adequate for the stringent requirements of HP products. This led to the development of the high-performance isolators described in this paper using a proprietary design developed at HP Laboratories. In summary, the major specifications achieved for the HP 81210LI (1310 nm) and HP 81310LI (1550 nm) fiber-pigtailed, polarization independent optical isolators are summarized as follows:

- Peak isolation typically greater than 60 dB with isolation greater than 40 dB over a combined temperature and wavelength range of 0 to 55°C and ± 20 nm
- Insertion loss less than 3 dB with a polarization sensitivity not greater than ± 0.2 dB
- Return loss less than 60 dB.

Acknowledgments

Contributions were made by many people throughout the development of the HP isolator. Specific recognition should go to Gerry Conrad, Don Cropper, Roger Jungerman, Paul Hernday, Bernd Maisenbacher, Waguih Ishak, Peter Aue, and Roger Wong for their support and useful discussions.

A Broadband, General-Purpose Instrumentation Lightwave Converter

Converting lightwave signals with wavelengths of 1200 to 1600 nanometers to electrical signals, this device serves as an optical front end for spectrum analyzers, network analyzers, bit error rate testers, and oscilloscopes.

by Christopher M. Miller and Roberto A. Collins

APPLICATIONS OF HIGH-SPEED fiber optic transmission systems continue to grow. Digital lightwave telecommunication systems that can operate at rates of many gigabits per second are being developed. Currently, researchers are exploring fiber optic cable television (CATV) transmission to provide the gigahertz bandwidth required for all the channels and services, including high-definition television (HDTV), contemplated for future systems. Meanwhile, subcarrier modulated optical links are being investigated as alternatives to microwave links.

Special lightwave test instrumentation is required to test these high-speed systems. Often the systems and their components, such as laser diode transmitters, need to be characterized in both frequency and time domains. The HP 11982A amplified lightwave converter combines a high-speed pin photodetector with a low-noise preamplifier to provide a general-purpose instrumentation front end for lightwave frequency-domain and time-domain measurements on optical signals over the 1200-nm-to-1600-nm wavelength range. It can be used with spectrum analyzers, oscilloscopes, bit error rate testers, and network analyzers. Combining the dc-coupled HP 11982A with an HP 54120 Series oscilloscope, shown in Fig. 1, allows measurements of optical waveform characteristics such as pulse width, rise and fall times, extinction ratio, and eye diagrams. When this lightwave converter is operated with a spectrum analyzer, optical modulation characteristics such as signal strength and distortion, modulation bandwidth, and inten-

sity noise can be measured. The HP 83810A portable lightwave signal analyzer, shown in Fig. 2, is formed when the HP 11982A is combined with the HP 8593A microwave spectrum analyzer and a downloadable lightwave personality stored on a credit-card-size ROM. The downloadable program includes frequency response corrections that allow calibrated measurements over the frequency range of 9 kHz to 22 GHz.

Converter Design

The primary design goals of the HP 11982A lightwave converter were that it be dc-coupled and that it have sufficient conversion gain, broad bandwidth, and good flatness. Only by simultaneously achieving all of these design objectives could the converter be considered truly general-purpose. Dc-coupled response is required to display the absolute levels of a time-domain waveform and to be able to determine the extinction ratio. In addition, the average optical power can be determined from the dc level.

Ensuring sufficient conversion gain, bandwidth, and flatness for the converter involved making trade-offs. The highest-bandwidth photoreceiver would just be a broadband pin photodiode, which would convert the photons of light to an electrical current without any amplification. However, a photodiode-only converter often does not have sufficient conversion gain to see low-level signals, particularly when used with spectrum analyzers that have relatively large noise figures. Too much gain, however, would degrade flatness and introduce additional gain slope, reducing the
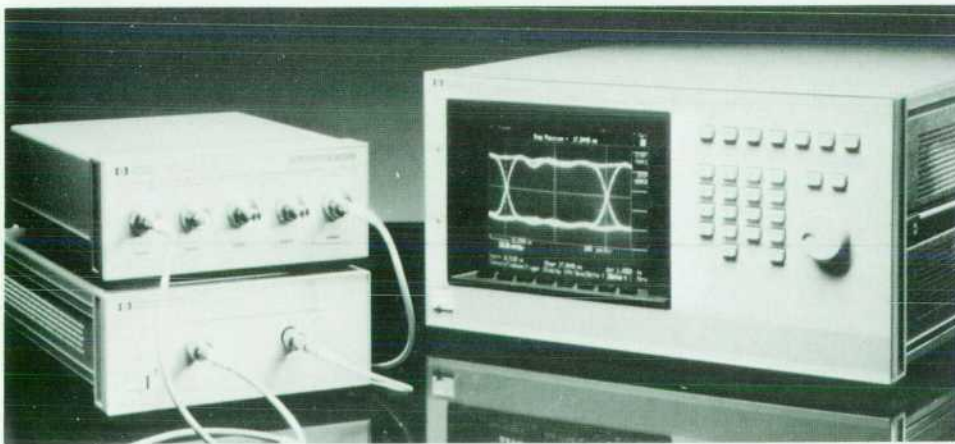

Fig. 1. *As an optical front end for an HP 54120 Series digitizing oscilloscope, the HP 11982A lightwave converter allows measurements of optical waveform characteristics such as pulse width, rise and fall times, extinction ratio, and eye diagrams.*
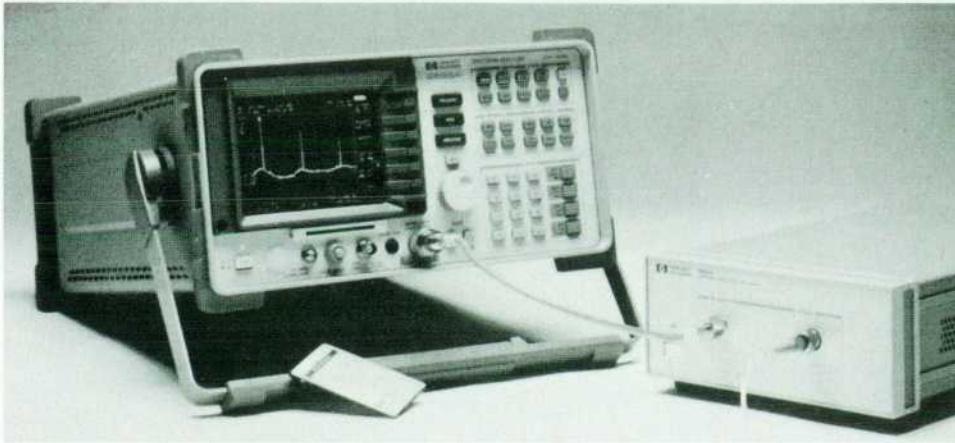
Fig. 2. The HP 83810A lightwave signal analyzer consists of the HP 11982A lightwave converter and the HP 8593A microwave spectrum analyzer.

benefits of the amplification at frequencies up to 22 GHz.

The basic design of the HP 11982A was leveraged from the HP 70810A lightwave receiver in the HP 71400A lightwave signal analyzer.[1] That design consisted of a pin photodiode followed by four microwave monolithic distributed amplifiers cascaded to provide a nominal 32 dB of amplification. However, the HP 70810A was not dc-coupled and its uncorrected frequency response was not acceptable for time-domain measurements. To provide the dc capability in the HP 11982A, a low-frequency dc-coupled amplifier is placed in parallel with a two-stage microwave amplifier in a split-band receiver configuration, as shown in Fig. 3. In the split-band approach, the low-frequency amplifier amplifies the detected signals from the photodiode below the crossover frequency, while the microwave amplifier amplifies signals above the crossover frequency. The outputs of the two amplifiers are resistively summed. The crossover frequency at approximately 2 MHz is formed by the parallel combination of output resistors and coupling capacitor according to the following formula:

$$\text{Crossover Frequency } f_c = 1/2\pi(C_2(r_o + (R_5 \| R_{Load})))$$

where r_o is the output impedance of the microwave amplifier and R_{Load} is the input impedance of the electrical measurement instrument.

The ideal operation of the two amplifiers in the neighborhood of the crossover is shown in Fig. 4. Well below the crossover, the high-frequency path has 90 degrees of phase lead and essentially zero amplitude, while the low-frequency path has zero degrees of phase and unity amplitude. At the crossover frequency, both paths have vectors that are complex conjugates and sum to produce a vector of unity with zero degrees of phase. Well above the crossover frequency the low-frequency path has 90 degrees of phase lag and essentially zero amplitude, while the high-frequency path has zero degrees of phase and unity amplitude. The low-frequency path also includes a zero about an octave above the pole at the crossover frequency. This zero is cancelled by adjusting the pole produced by C_3.

A well-behaved crossover frequency response characteristic is important for good time-domain performance for signals that have spectral content in the neighborhood of the crossover frequency. Fig. 5 shows a measurement of the crossover frequency reponse characteristic of the HP 11982A, indicating that there is less than 1 dB amplitude variation through the crossover band.

To provide a reasonable compromise between sensitivity and frequency response, the microwave amplifier is designed to provide about 18 dB of gain. As shown in Fig. 6, this requires two stages of amplification with only a single interstage network. The interstage coupling is provided by
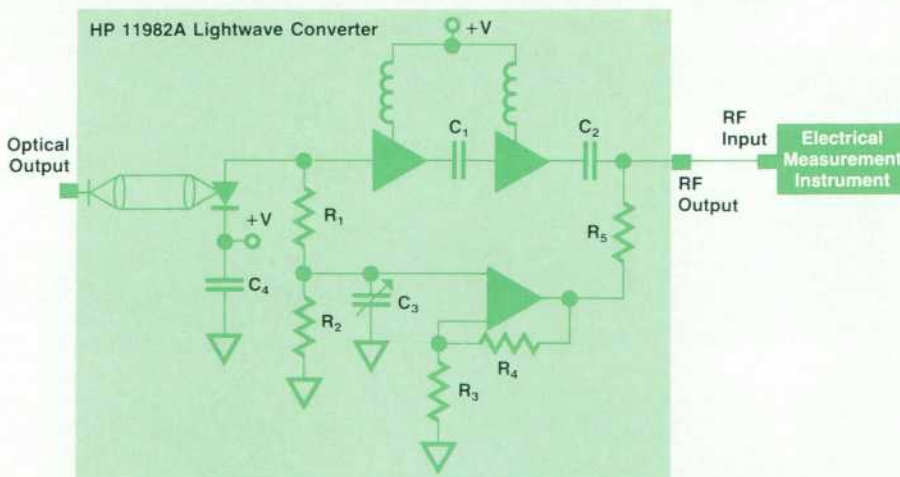
Fig. 3. Block diagram of the HP 11982A lightwave converter.
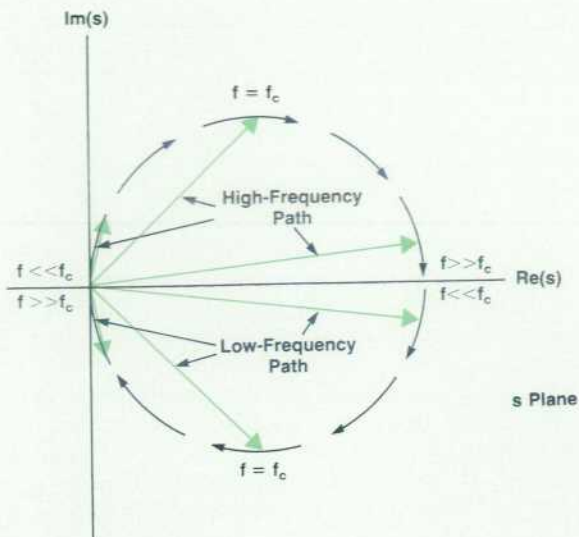
Fig. 4. *Ideal operation of the low-frequency and high-frequency amplifiers near the crossover frequency for the split-band configuration shown in Fig. 3.*

Fig. 5. *Crossover frequency response of the HP 11982A lightwave converter has about 1 dB variation through the crossover band.*

a 1000-pF TaO_5 thin-film integrated capacitor in parallel with a 0.047-μF ceramic capacitor. The integrated capacitor has good microwave performance and the large ceramic capacitor extends the low-frequency cut-off to 34 kHz, almost two decades below the crossover frequency. To reduce parasitics to ground, the interstage network is constructed

with a short suspended-substrate transmission line segment. The capacitor that determines the crossover frequency is also a 1000-pF integrated capacitor.
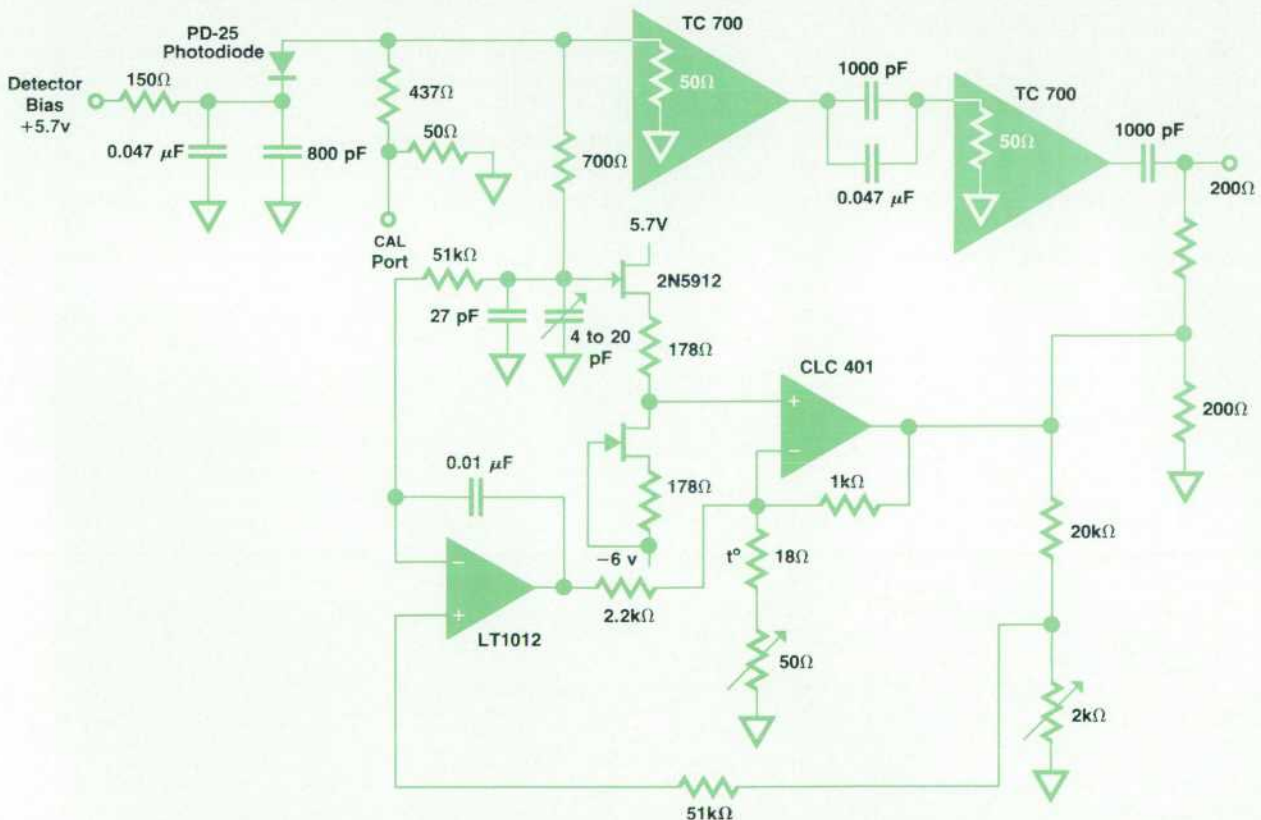
Fig. 6. *Split-band photoreceiver schematic diagram. The converter nominally has 18 dB of gain and 300 volts/watt responsivity.*

(Electrical dB)

Freq (MHz)	Ampl (dB)	Freq (MHz)	Ampl (dB)	Freq (GHz)	Ampl (dB)	Freq (GHz)	Ampl (dB)
.10	0.0	3.16	.4	.1	.9	11.5	-1.4
.13	0.0	3.98	.5	.6	1.0	12.0	-2.0
.16	.1	5.01	.3	1.1	.9	12.5	-2.3
.20	.1	6.31	.3	1.6	1.1	13.0	-2.7
.25	0.0	7.94	.3	2.1	.9	13.5	-2.4
.32	.1	10.00	.2	2.6	.7	14.0	-2.6
.40	.1	12.59	.2	3.1	.3	14.5	-2.4
.50	.2	15.85	.3	3.6	.2	15.0	-2.5
.63	.2	19.95	.3	4.1	-0.0	15.5	-3.1
.79	.2	25.12	.3	4.6	-.1	16.0	-3.6
1.00	.3	31.62	.4	5.1	-.1	16.5	-4.3
1.26	.3	39.81	.4	5.6	-0.0	17.0	-5.0
1.58	.4	50.12	.5	6.1	-.4	17.5	-5.7
2.00	.4	63.10	.7	6.6	-.6	18.0	-6.4
2.51	.4	79.43	1.0	7.1	-.9	18.5	-7.0
				7.6	-1.1	19.0	-7.4
				8.1	-1.1	19.5	-7.8
				8.6	-1.0	20.0	-7.8
				9.1	-1.0	20.5	-8.6
				9.6	-1.0	21.0	-9.8
				10.1	-1.2	21.5	-10.5
				10.6	-1.3	22.0	-11.4
				11.1	-1.4		

DC Responsivity into 50 ohms
(V/W)

1300 nm	285
1550 nm	292

Fig. 7. *Each HP 11982A comes with an individually generated calibration chart.*

The amplification in the low-frequency path is provided by a Comlinear CLC401 operational amplifier. This integrated circuit uses current feedback to provide high-speed operational amplifier performance. Because of the resistive divider network formed at the output by the 50-ohm input impedance of the receiver, the gain in this amplifier circuit has to be five times greater than the high-frequency path.

A FET follower is placed at the input to eliminate input offset voltage contributions from the input bias current of the CLC401. In addition, an LT1012, an amplifier with very low dc offset voltage, monitors the output and input voltages. This amplifier determines the output offset voltage, which is less than 1 mV. The thermistor shown is used to vary the gain of the low-frequency path to track temperature induced gain variations in the microwave amplifiers.
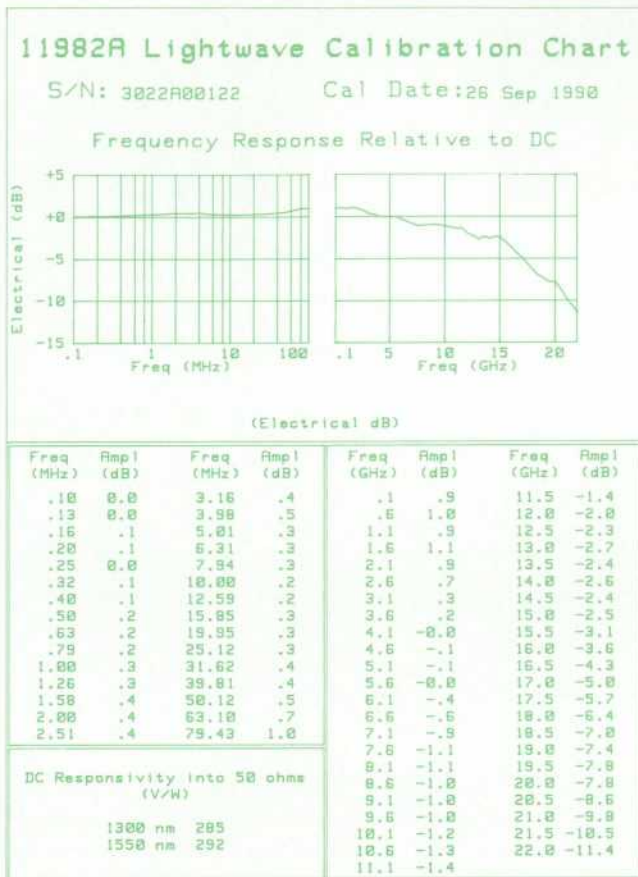
For maximum converter sensitivity, the photodetector is not back-terminated in 50 ohms. To mimimize the effects of mismatch loss at the higher frequencies, the detector is placed as close as possible to the microwave amplifier. The combination of the photodetector and the split-band amplifier provides conversion gain of typically 300 volts/watt. The overall frequency response roll-off of the HP 11982A is about 3 dB electrical at 11 GHz and 6 dB electrical, or 3 dB optical, at 15 GHz. The roll-off characteristic is gradual, as shown in the HP 11982A calibration chart (Fig 7). Each HP 11982A comes with its individually generated calibration chart, making it extremely useful for a number of frequency-domain lightwave measurements. The calibration is referenced to a Hewlett-Packard heterodyne laser system which produces a constant-amplitude optical modulation frequency.[1] In addition, the gradual roll-off of the lightwave converter is beneficial in displaying time-domain waveforms without excess overshoot and ringing. Assuming that the roll-off is Gaussian, the full-width-at-half-maximum (FWHM) impulse response of the HP 11982A can be calculated using the following relationship:[2]

$$FWHM = 0.44/(\text{Optical 3-dB Bandwidth}).$$

This would predict an FWHM of approximately 30 picoseconds for a 15-GHz optical bandwidth.

Optical-Mechanical Design

The optical-mechanical design of the lightwave converter shown in Fig. 8 consists of two parts: the optoblock and the optical microcircuit. The function of the optoblock is to collimate the light at the input connector and refocus it onto the photodetector. The input to the optoblock uses
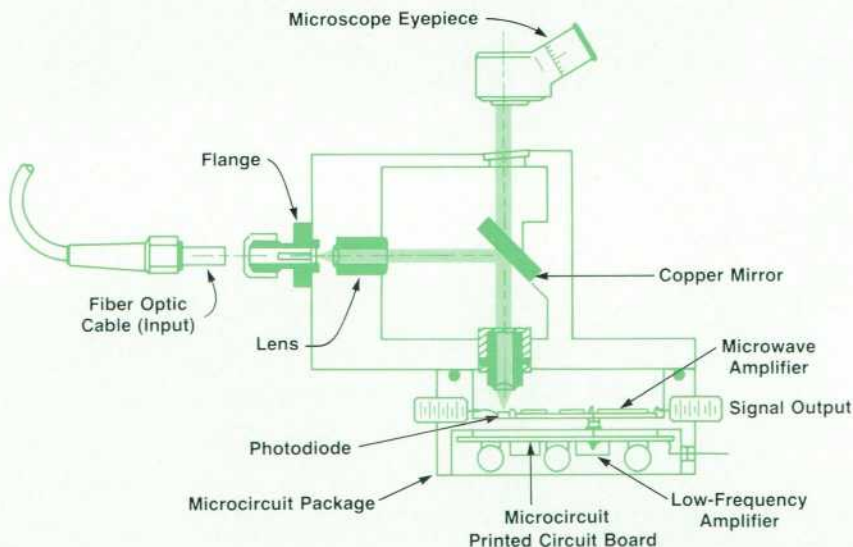
Fig. 8. *Optical-mechanical design and method of alignment of the lightwave converter.*
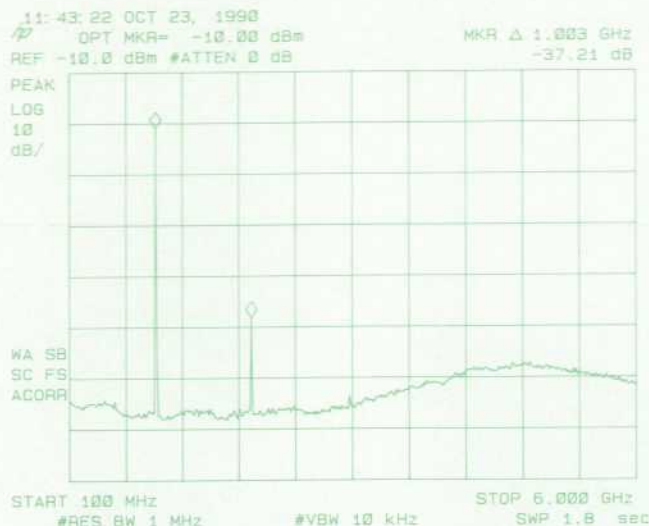
11:43:22 OCT 23, 1990
OPT MKR= -10.00 dBm   MKR Δ 1.003 GHz
REF -10.0 dBm #ATTEN 0 dB   -37.21 dB

PEAK
LOG
10
dB/

WA SB
SC FS
ACORR

START 100 MHz   STOP 6.000 GHz
#RES BW 1 MHz   #VBW 10 kHz   SWP 1.8 sec

Fig. 9. *Modulation response of a 1300-nm DFB semiconductor laser measured with the HP 83810A lightwave signal analyzer.*

10:52:10 OCT 23, 1990
OPT MKR= -72.13 dBm (1 Hz)   MKR 1.000 GHz
REF -30.0 dBm #ATTEN 0 dB   -145.16 dBm (1 Hz)

SMPL
LOG
10
dB/

WA SB
SC FS
ACORR

START 100 MHz   STOP 6.000 GHz
#RES BW 1 MHz   #VBW 10 kHz   SWP 1.8 sec

Fig. 10. *Laser intensity noise spectrum.*

the Hewlett-Packard fiber optic connector adapter system.[3] This adapter design allows mating to any of five different connector systems: HMS-10/HP, FC/PC, ST, biconic, and DIN. It also allows easy access to the ferrule for cleaning. The connector is designed to provide a physical, low-return-loss contact to the input fiber. Internally, it contains a short piece of fiber that is cleaved at a small angle to prevent reflections at the glass-to-air surface from propagating back out of the connector. Exiting the rear of the input connector, the light passes into air. The diverging beam is first collimated into an expanded parallel beam. Next, it is reflected off a mirror positioned at a 45-degree angle, which directs the light to the output lens. The light is then focused onto the detector. As shown in Fig. 8, the mirror is partially transmissive, which allows the light to be aligned to the detector by viewing the reflected light from the illuminated detector with a microscope eyepiece.

The optical microcircuit containing the pin photodiode and the amplifier is mated to the optoblock. The pin detector and microwave amplifier are placed in one half of the package. This half is sealed with a rubber O-ring gasket at the microcircuit-optoblock interface. A spiral-wound gasket is also placed at this interface to reduce the likelihood
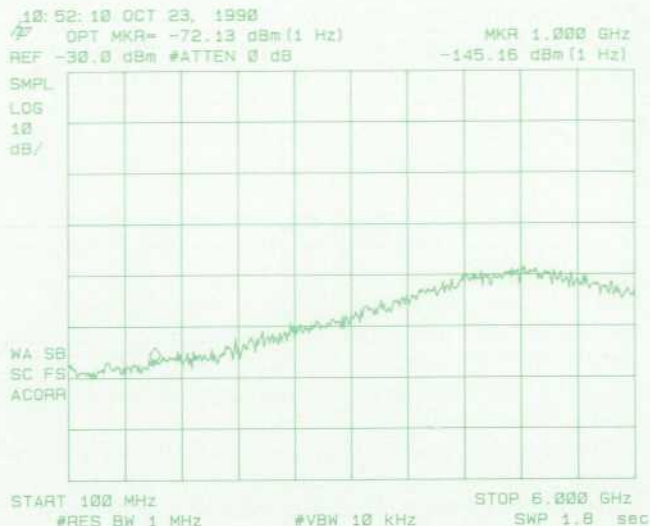
of any radiated electromagnetic interference (EMI) pickup. The low-frequency amplifier is constructed on a printed circuit board in the other half of the microcircuit package and is connected to the microwave amplifier with non-capacitive dc feeds.

Frequency-Domain Measurements

The HP 11982A can be used with an electrical spectrum analyzer to make a number of useful measurements on laser transmitters, such as modulation bandwidth, harmonic distortion, intensity noise spectrum, and linewidth, among many others.[4] These measurements can be made most conveniently when the HP 11982A is configured as the HP 83810A lightwave signal analyzer or with an HP 8593A microwave spectrum analyzer when the lightwave corrections are downloaded into the analyzer.

The modulation response and harmonic distortion of a laser can be measured easily using the HP 83810A. Using a microwave generator to provide an electrical modulation stimulus for the laser under test, the optically modulated fundamental and harmonic components can be observed, as shown in Fig. 9. With the lightwave personality the modulated power levels can be measured electrically referenced to the input of the spectrum analyzer, or optically referenced to the optical input of the lightwave converter.
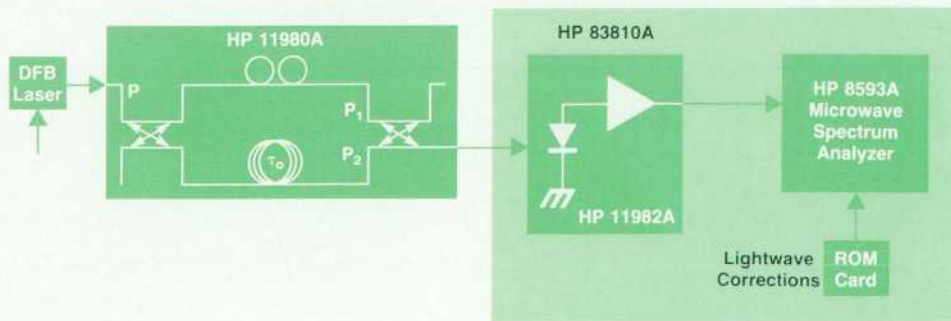
Fig. 11. *Linewidth measurements of single-frequency lasers can be done with the HP 11980A fiber optic interferometer and the HP 8310A lightwave signal analyzer.*

This 1300-nm distributed feedback (DFB) semiconductor laser was producing second-harmonic distortion of approximately −37 dB electrical at an optical modulation level of −10 dBm. By varing the electrical modulation frequency to the laser, both its modulation bandwidth and its harmonic distortion as a function of frequency can be determined.

Low harmonic distortion is required for the transmission of video on fiber optic systems. However, this is only one of many important measurements that need to be made on CATV systems. In addition, the HP 83810A lightwave signal analyzer has the ability to make composite-triple-beat and carrier-to-noise measurements on fiber optic systems when the CATV personality is downloaded along with the lightwave personality.

Often very low-noise performance from the laser is necessary to meet the required signal-to-noise ratio for these transmission systems. A measurement of a laser intensity noise spectrum is shown in Fig. 10, revealing the characteristic noise peak at the relaxation oscillation frequency,[5] which occurs at approximately 5 GHz for this laser. An important quantity used as a figure of merit for lasers is the relative intensity noise (RIN). It is the ratio of the mean square intensity fluctuation spectral density of the optical signal, P_n, to the square of the average optical power, P_{avg}. This ratio is equivalent to the ratio of the electrical noise power referenced to a 1-Hz bandwidth measured on the spectrum analyzer to the average electrical power. Because the HP 11982A is dc-coupled, this latter quantity can be determined by measuring its output voltage into a 50Ω load with a voltmeter, then equating it to $(V_{dc})^2/50$. Using this technique, the dc voltage was measured to be 200 mV and the electrical noise to be −145.2 dBm at the noise peak. Thus, the RIN for this laser can be determined to be −144.2 dB/Hz at 1 GHz.

Many future systems, especially those requiring coherent optical transmission techniques, will require lasers that operate in a single longitudinal mode and exhibit narrow linewidths. The linewidths of these single-frequency lasers, whose wavelength range is from 1250 nm to 1600 nm, can be measured with the lightwave signal analyzer when a fiber optic interferometer, such as the HP 11980A,[6] is connected in front of it as shown in Fig. 11. The interferometer functions as a frequency discriminator, convert-

Fig. 12. Linewidth measurement of a single-frequency distributed feedback laser.

ing optical phase or frequency deviations into intensity variations, which can be measured by the HP 83810A. A measurement of the linewidth of a single-frequency distributed feedback (DFB) laser is shown in Fig. 12. A linewidth of 40 MHz is indicated by the marker placed 3 dB down from the peak. This same basic technique can be used to measure frequency chirp (dynamic linewidth broadening under modulation) of lasers.[6]

Time-Domain Measurements

A number of very useful time-domain measurements can be made with the HP 11982A lightwave converter when it is combined with a high-speed oscilloscope such as an HP 54120 Series digitizing oscilloscope. The lightwave converter's broad bandwidth with gradual roll-off minimizes the amount of instrumentation-introduced aberrations, such as overshoot and ringing, in the displayed waveform.

This amplified converter is especially useful in observing eye diagrams produced by pseudorandom binary sequence (PRBS) intensity modulation. Since these waveforms are produced by the time superposition of the pseudorandom
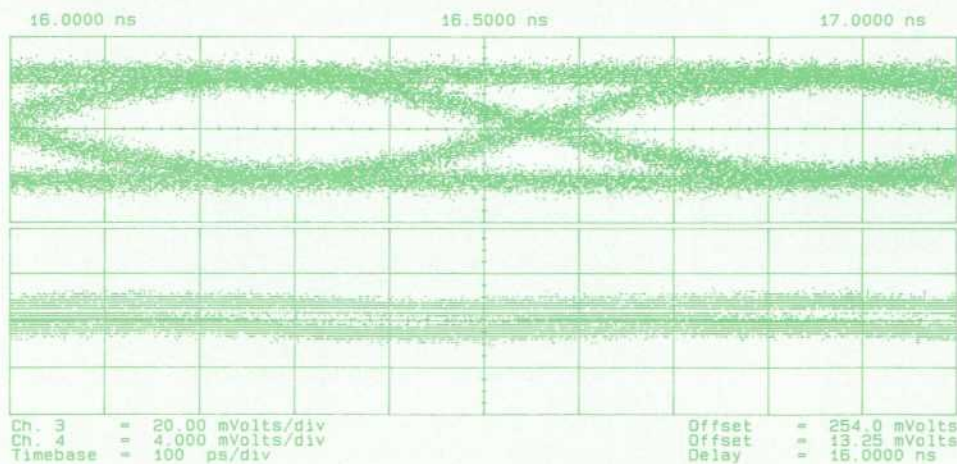

Fig. 13. (top) Eye diagram for a modulated lightwave carrier detected by the HP 11982A lightwave converter. (bottom) Eye diagram detected by a photodiode without amplification.
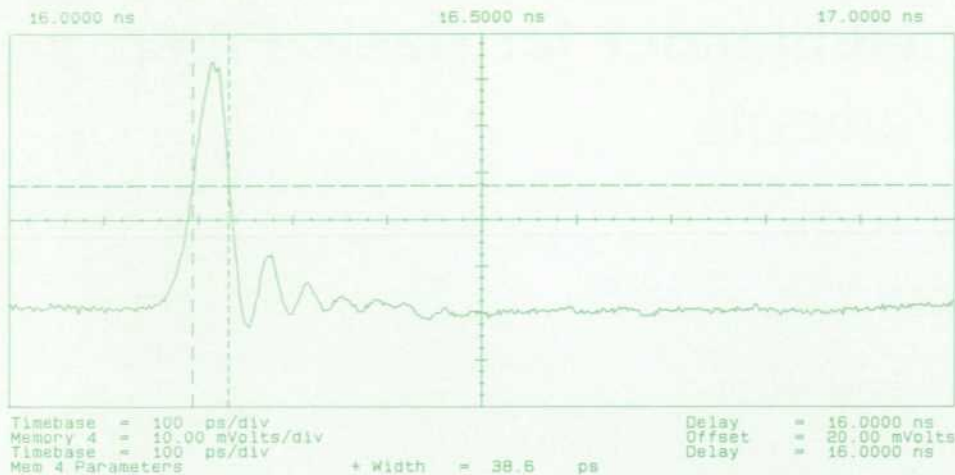
```
16.0000 ns                      16.5000 ns                      17.0000 ns
```

```
Timebase   =  100   ps/div                        Delay    =   16.0000 ns
Memory 4   =  10.00 mVolts/div                     Offset   =   20.00 mVolts
Timebase   =  100   ps/div                         Delay    =   16.0000 ns
Mem 4 Parameters              + Width  =  38.6   ps
```

Fig. 14. *Laser pulse width measurement using the lightwave converter and a digitizing oscilloscope.*

bit stream triggered at the bit rate, persistence mode must be used. Thus, low-level signals cannot be averaged and pulled out of the noise. Fig. 13 shows an eye diagram comparison of a laser, intensity modulated with a 1.7 Gbit/s PRBS, whose output has been detected with the HP 11982A and a photodiode without amplification.

The broad bandwidth of the HP 11982A is helpful in the measurement of high-speed laser pulse characteristics. Typically, the pulse width of a laser is given by its FWHM. Shown in Fig. 14 is the measured FWHM of a mode-locked semiconductor laser producing pulses at a 1-GHz repetition rate. The measured FWHM was 39 picoseconds. From this, it is necessary to subtract the contributions of the lightwave converter and the HP 54120 Series digitizing oscilloscope using the following relationship:

$$FWHM^2_{laser} = FWHM^2_{measured} - FWHM^2_{HP\ 11982A}$$
$$- FWHM^2_{HP\ 54120A}$$

$$= (39\ ps)^2 - (30\ ps)^2 - (16\ ps)^2.$$

Therefore,

$$FWHM_{laser} = 19\ ps.$$

This calculation assumes a Gaussian pulse shape and agrees with the result determined from an autocorrelation measurement of the laser pulse width.

References
1. C. Miller, "High-Speed Lightwave Signal Analysis," *Hewlett-Packard Journal*, Vol. 41, no. 1, February 1990, pp. 80-91.
2. *Fiber Optics Handbook*, Hewlett-Packard publication no. 5952-9654.
3. W. Radermacher, "A High-Precision Optical Connector for Optical Test and Instrumentation," *Hewlett-Packard Journal*, Vol. 38, no. 2, February 1987, pp. 8-11.
4. Application Note 371, *Lightwave Measurements with the HP 71400 Lightwave Signal Analyzer*, Hewlett-Packard Publication No. 5954-9137.
5. C. Miller, D. Baney, and L. Stokes, "Enhanced Intensity Noise and Spectral Measurements on Lasers Using Lightwave Signal Analysis," *Hewlett-Packard RF, Microwave, and Lightwave Measurement Symposium*, 1990.
6. D. Baney and W. Sorin, "Linewidth and Power Spectral Measurements of Single-Frequency Lasers," *Hewlett-Packard Journal*, Vol. 41, no. 1, February 1990, pp. 92-96.

A Lightwave Multimeter for Basic Fiber Optic Measurements

This new instrument can replace separate optical power meters, dedicated loss test sets, and stable light sources for measurements of absolute power, relative power, and loss.

by Bernd Maisenbacher and Wolfgang Reichert

INTRODUCED IN 1986, THE HP 8152A lightwave power meter made measurement contributions with the accuracy and repeatability of its measurements and the flexibility of its interfaces to various fiber connectors, fiber types, and open beams. The objectives for the new HP 8153A lightwave multimeter (Fig. 1) were to design a successor to the HP 8152A with more flexibility and better performance for a lower price.

Incorporating a mainframe with two plug-in slots and a number of different plug-ins for various applications (see Figs. 1 and 2), the modular architecture of the HP 8153A lightwave multimeter extends its usability to a wide range of basic fiber optic measurement tasks. It can replace a number of stand-alone instruments such as optical power meters, dedicated loss test sets, and stable lightwave sources. The HP 8153A is intended to cover the following measurement tasks:

- Absolute power measurements (one or two channels) of light from active optical components such as LEDs and lasers, either in fiber-guided or open-beam form, for the entire wavelength range from 600 to 1650 nm.
- Relative power measurements (one or two channels), that is, power ratio measurements, applied to active or passive optical components such as fibers, connectors, and waveguides, over the full near-infrared wavelength range.
- Loss measurements, that is, insertion or return loss mea-

surements requiring a source and a sensor, on passive optical components.

Absolute Power Measurements

The critical specification in absolute optical power measurements is the uncertainty of the displayed power. The more accurate the measurements of optical power, the higher is the confidence in component verification during incoming inspection, production, installation, and maintenance. In these areas, a more accurate power meter will increase yield and reduce cost.

Today, few engineers are concerned with the uncertainty of voltage measurements, because today's precision voltmeters are much more accurate than required for the majority of applications. However, in the optical domain there are still opportunities to contribute. The new HP 8153A lightwave multimeter improves the uncertainty of power measurements to ±2.2%, traceable to national standards laboratories such as NIST or PTB. A major engineering effort was required to achieve this improvement in measurement accuracy. More details about the uncertainty chain are described in the article on page 70.

To cover the required measurements for the entire fiber optic wavelength range, three detector materials are used. Silicon detectors are responsive from 450 to 1020 nm, germanium from 900 to 1650 nm, and indium gallium arsenide
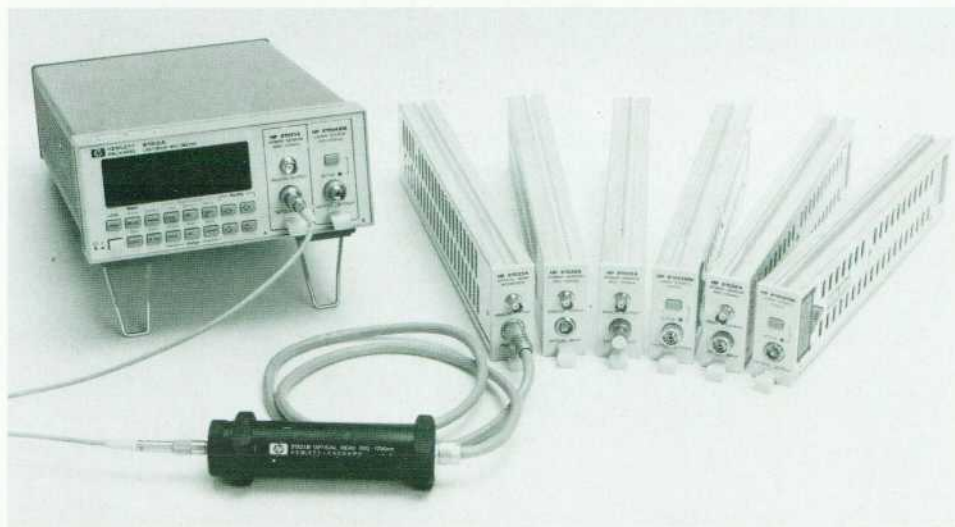

Fig. 1. *The HP 8153A lightwave multimeter with different modules for different applications.*
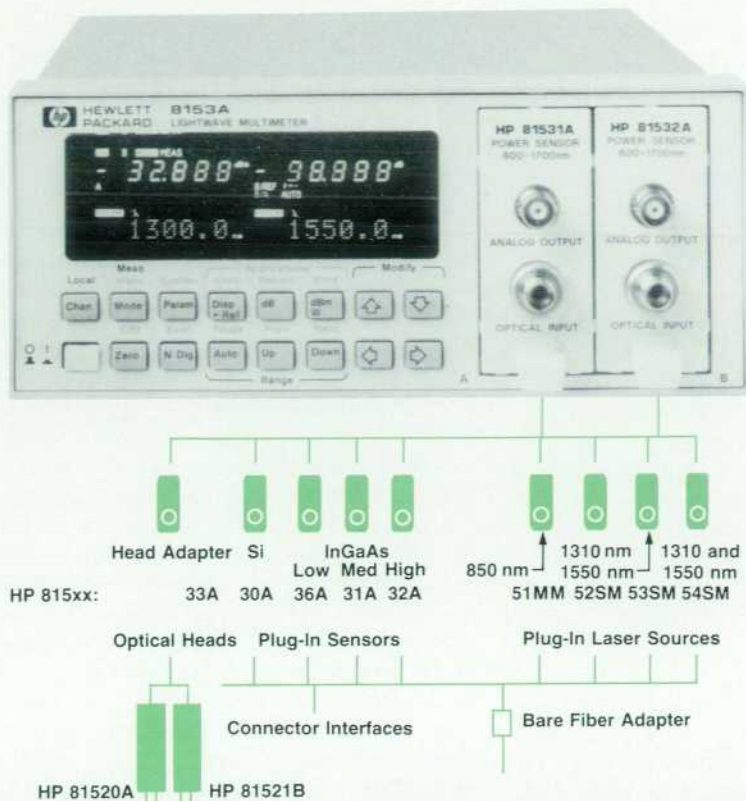
Fig. 2. *The HP 8153A lightwave multimeter system consists of a mainframe, optical heads, and plug-in modules.*

(InGaAs) from 800 to 1700 nm. For measurements at short wavelengths, silicon detectors are the best choice in terms of quantum efficiency, noise equivalent power (NEP), and cost. For the longer wavelength windows at 1300 and 1550 nm, two materials—InGaAs and germanium—compete. Germanium has a higher NEP and a strong variation in responsivity around 1550 nm, but is lower in cost, especially at larger detector diameters. InGaAs, on the other hand, exhibits a nearly flat responsivity over wavelength, especially at 1550 nm. Its NEP much lower than germanium's, but its cost is considerably higher.

For short-wavelength fiber applications, HP offers the HP 81530A power sensor with a 1-mm silicon detector. For long-wavelength fiber applications, three models—the HP 81531A, HP 81532A, and HP 81536A—are available, based on 500-μm InGaAs detectors. The main difference between the three InGaAs plug-ins is the noise performance of the detector/amplifier circuitry and therefore the measurement range.

For collimated-beam applications, the HP 81520A detector (5-mm silicon) and the HP 81521B detector (5-mm germanium), which were introduced with the HP 8152A power meter, have become well-established with many standards laboratories. The HP 8153A with the HP 81533A interface plug-in allows the use of these detectors. They combine the superior optical performance of the detectors with the improved electrical performance of the HP 8153A mainframe.

A major design goal for the detectors was to achieve maximum detector sensitivity. Therefore, the lowest possible noise and drift are required. Whereas most other manufacturers of sensitive lightwave power sensors are using optical choppers to achieve very high sensitivity and

minimize drift, we opted to avoid optical chopping, thereby avoiding the inherent disadvantages of chopper sensors, which include drastically reduced bandwidth, slow sampling rate, and possible strong interference with lightwave sources because of changing reflections created by the chopper device. Instead, we chose to mount the detector chip and transimpedance amplifier stage on a thermoelectric cooler inside a hermetically sealed package. Since the temperature of this assembly is kept extremely constant, we are able to cancel out the biggest source of error, the temperature dependence of the quantum efficiency of the detector. By cooling the detector, we are able to reduce the noise equivalent power to a minimum. Furthermore, the temperature stabilization of the transimpedance amplifier reduces the amplifier drift by many orders of magnitude and leads to drift performance similar to chopper sensors.

The new power sensors improve the power linearity by a factor of three over the HP 8152A, yielding ±0.35% maximum nonlinearity. The total uncertainty specification for fiber-guided applications is ±5% (±4% for parallel beam). Unlike some optical power meter specifications, which apply at only one power level (usually 10 μW or −20 dBm), the HP 8153A total uncertainty specification applies over most of the input power range and includes every realistic operating condition. To achieve this level of accuracy, it is necessary to calibrate the wavelength characteristics of each individual module. In addition, the nonlinearities of the electronic circuitry had to be eliminated. Details of these improvements are described in other articles in this issue.

Relative Power Measurements

In relative power or power ratio measurements, one mea-

surement result is used as a reference and subsequent results are compared against it. For example, in determining the insertion loss of fiber connectors, the light out of one connector is taken as the reference, then the connectors are mated and the measurement is taken at the far end of the second fiber. The relative measurement mode is used to characterize active or passive components over time or temperature or in terms of repeatability—for example, of an optical connector.

Instead of measuring relative to a previous measurement result, it is often necessary to take a simultaneous measurement relative to the power level at a different part of the setup. The HP 8153A allows the user to plug in a second power meter module and then measure the power of one channel relative to the other channel. For example, to measure the loss of a component independent of fluctuations of the applied power, a power splitter can be used to monitor the input power to the DUT with the first power meter and the output power with the second. If the input and output measurements are taken at the same time, the ratio of output to input is independent of the applied power level.

To detect very small changes in loss, very high power meter resolution is required. For example, to measure the repeatability of optical connectors or the output stability of lasers, users want to resolve changes on the order of 0.001 dB. Before the HP 8153A was introduced, many customers connected the analog output of the HP 8152A to a five-digit voltmeter to achieve the necessary higher resolution. Now, 0.001-dB resolution is available in the HP 8153A in relative as well as in absolute power measuring mode.

A large dynamic range is essential for attenuation measurements—for example, to characterize very long fibers or components with high loss. In these applications, linearity becomes very important. Although pin detectors are extremely linear over many orders of magnitude, careful design of the electronic circuitry is necessary to avoid nonlinearities. The gain of the amplifier chains must be carefully matched to avoid nonlinearities during range switching. In the HP 8153A, the total nonlinearity in relative power measurements is less than 0.015 dB worst-case and less than 0.005 dB in typical applications. These values are independent of the applied reference input power. For example, with a reference of 0 dBm, the HP 8153A with an HP 81532A power sensor can measure 80 dB of attenuation with a total error less than 0.015 dB.

Loss Measurements

To characterize passive components in terms of their insertion loss or return loss, a test setup must contain a light source as well as a sensor. Suitable sources are mostly semiconductor lasers, but some LEDs will do. For such tests, the most important source characteristic is output power stability. For the HP 8153A, several semiconductor laser source plug-in modules are available. They all have excellent output power stability characteristics and allow the user to configure the HP 8153A as a self-contained high-performance loss test set by plugging in one of the highly linear power sensors and a laser source module.

One of the source modules contains a 1310-nm laser and a 1550-nm laser together with a wavelength division mul-

tiplexer in a single plug-in module. This module works with the built-in firmware such that the instrument simultaneously measures and displays loss at two wavelengths: 1310 and 1550 nm.

Design Features

During the earlier parts of the investigation phase of the HP 8153A project, the R&D team aimed towards an HP 8152A replacement with higher resolution, faster HP-IB, and lower production cost. The potential advantages of a modular design became obvious very quickly, but there was strong concern whether the team would be able to design a modular system and keep the production cost low. Nevertheless, the design team opted for a modular system and finally came through with a very cost-efficient mechanical design, which is described later in this article.

The performance of all lightwave test equipment depends very much on the performance of the optical ports. Instead of standard fiber connectors and sleeves, HP uses a proprietary interface adapter scheme, which offers performance and flexibility advantages. This scheme is used wherever technically possible on HP lightwave test instruments and gives the user access to the front face of the internal fiber connector without the use of any tools for easy cleanability. Unfortunately, the importance of regular connector cleaning is not yet fully understood by many users of lightwave test instrumentation. HP offers interface adapters for most common fiber connectors, which can easily be exchanged by the user.

One of the biggest challenges of the project proved to be the design of the human interface. As a result of the goal of keeping the HP 8153A fully compatible with the HP 8152A, there was very limited space on the front panel, because the footprint of the new instrument could not be larger than that of its predecessor. The front-panel space on the HP 8152A was quite small, and this space is further reduced on the HP 8153A because of the use of plug-ins (separate sensor heads are used on the HP 8152A). The front-panel space reserved for these plug-ins cannot be used for human interface tasks. A custom-designed vacuum fluorescence display provides the necessary information density for four six-digit displays and the necessary units and instrument status information. The keyboard functions of the HP 8153A are not only fully compatible with the HP 8152A but include a substantial number of new functions and enhanced capabilities.

These new functions are available on a second keyboard layer, which is accessible through the **MODE** key, and are marked in blue on the front panel. While the casual user of the HP 8153A can access all necessary functions on the first keyboard layer, the second layer is aimed more towards the expert user. To conduct measurements that include some form of data logging, such as the output power drift of a laser or the settling behavior of laser power after power-on, it was previously necessary to use an external computer with the lightwave power meter to handle the data collection. The HP 8153A now offers data logging capabilities and, in addition, allows the user to print or plot the results directly without a computer and without writing a single line of software. With a few keystrokes on the second keyboard layer, the user has access to a number of advanced

functions like stability, manual logging, and alignment. These functions are described in detail in the article on page 77.

For remote control over the HP-IB (IEEE 488, IEC 625), the HP 8153A uses the IEEE 488.2 protocol with the HP Test and Measurement System Language (TMSL). TMSL is HP's version of the industry-standard SCPI—Standard Commands for Programmable Instrumentation. The use of this protocol is contradictory to the goal of design for compatibility, because several HP 8152A commands are explicitly incompatible with the new standard. To protect the customer's investment in software, the HP 8153A offers a compatibility mode in addition to TMSL, which allows the use of software written for the HP 8152A.

All of the HP 8153A firmware is designed to handle today's modules as well as future plug-ins. Each module contains its own firmware in ROM and a variable set of data in EEPROM. The EEPROM stores module identification and individual calibration data such as sensor responsivity as a function of wavelength. After module identification, the mainframe firmware boots the ROM content and links it with the other firmware. This modular firmware concept and a digital module interface are designed to facilitate the integration of new lightwave multimeter modules in the future.

The very high packaging density of the modules and the mainframe required the use of two application-specific integrated circuits (ASICs) and surface mount technology. One ASIC is on the microprocessor board and includes most of the digital hardware, keyboard, and display handling and the interface with the module hardware. The second ASIC is primarily designed for use in power sensor modules. It contains all digital hardware for the 8-bit device bus interface, some I/O ports, and the main parts of the high-resolution integrating analog-to-digital converter. The A-to-D converter concept permits gate times between 20 ms and one hour, thus allowing as many as 50 measurements per second for remote operation. The longer gate times allow a reduction in the noise floor and increase the measurement resolution up to 0.0001 dB (in remote operation).

Each laser source module contains temperature and current control circuitry for either one or two lasers. The output of each laser diode is monitored to keep the laser power within the safe levels of Laser Safety Class 1 for the U.S.A. and Canada and the new IEC Class 3A for the rest of the world.

Mechanical Design

One of the major design goals for the new lightwave multimeter was to come up with a small, highly flexible and reliable, yet very low-cost mechanical design.

To be compatible in size with its predecessor, the HP 8152A optical power meter, the dimensions of the new multimeter were to be identical to the HP 8152A's: 88.1 mm high, 212.3 mm wide, and 345.4 mm deep. The first thought, using standard HP cabinet parts, quickly proved to be unsuccessful because such a frame neither met the production cost goals nor could provide the necessary space for the electronics. It was clear that the project goals could only be met by designing a number of molds for custom plastic parts and custom aluminum extrusions for the plug-in modules. A way had to be found to avoid high

overhead costs in procurement and assembly wherever possible. An outside vendor now supplies the complete front frame and front-panel assembly ready for final integration of the mainframe.

The three major mechanical blocks of the instrument are the mainframe housing, the front insert assembly, and the plug-in modules.

Mainframe

Whereas the HP 8152A optical power meter is a dedicated instrument with separate sensor heads, the new HP 8153A lightwave multimeter is a modular design and incorporates two slots for plug-in modules. Although no HP standard cabinet parts are used, the instrument is fully compatible with HP standards in design and mechanical dimensions. Standard rack-mount kits and handle kits can be added.

The parts count was reduced by 35% compared with the HP 8152A and the new mainframe consists of only thirteen different parts (MP, MP1 through MP11, and A100 in Fig. 3). Sliding and snapping techniques are used extensively, reducing the number of screws and rivets from roughly 60 to only 26. This helped reduce assembly time and cost substantially.

While the front and rear frames are molded plastic, the chassis of the mainframe is made of sheet aluminum. This chassis serves as a card cage for the microcomputer board, the ac power supply board, and the optional dc power supply board. It also holds the motherboard and serves as the housing and guide for the plug-in modules. Designing this chassis so that the mechanical tolerances would allow the free exchange of plug-in modules and meet HP cosmetic requirements proved to be a major challenge for the mechanical designers.

One of the design goals was to keep the temperature rise anywhere in the instrument well below 15°C to increase reliability. Because of the high package density and limited rear-panel space, it was difficult to find a suitable, efficient location for the dc fan. Cool air now enters the instrument on the right side, flows through the plug-in modules and the fan, which is mounted in the middle of the frame, and cools the power supply and microcomputer boards before exiting on the left side. The maximum temperature rise inside the instrument is 12°C at the ac power supply board.

Further cost reductions were achieved by drastically reducing the wiring in the instrument. The only remaining wires are chassis grounding for safety reasons, the wires of the fan, and a flat ribbon cable to connect the front insert to the microcomputer. All other interconnections are provided by the multifunctional motherboard, which carries signal and power lines to the plug-in modules and contains the rear-panel HP-IB connector and related lines. Primary wiring was totally eliminated and the power inlet is soldered directly to the power supply board. Since the power supply covers all common line voltages in one range, a line voltage selector is not necessary. The power on/off switch is soldered onto the power supply board and activated by a molded plastic rod.

Front Insert Assembly

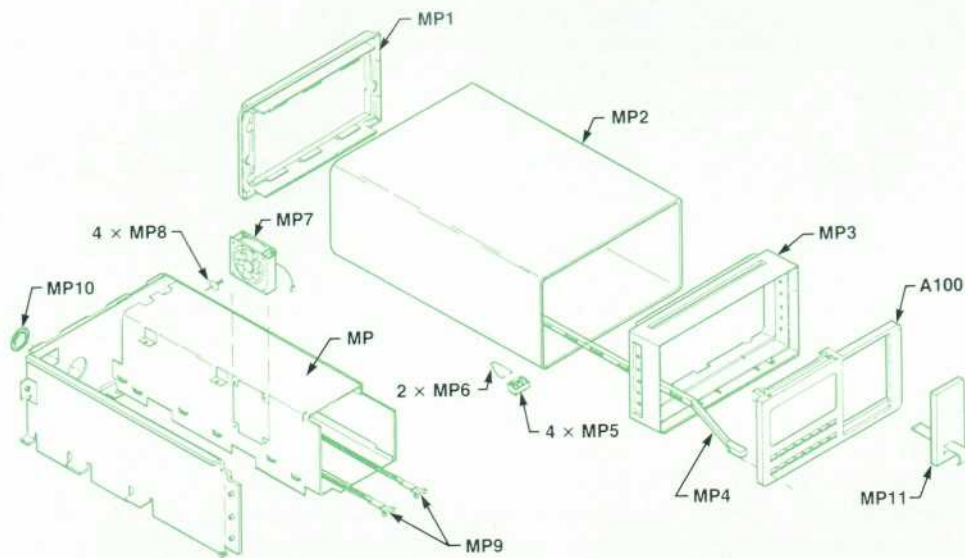The front insert assembly includes two subassemblies:

Fig. 3. *HP 8153A mainframe as-sembly.*

the front panel and the display board. The display board holds a number of surface mount components, the display driver IC, and the vacuum fluorescence display. The display was custom designed to provide the necessary high information density. It has two display sections, one for each plug-in slot. This board snaps into the front panel and is held by two catches, which are part of the front-panel molding. The front-panel molding is made of a parchment-white polycarbonate/ABS blend, includes a transparent window for the display area, has two-color silkscreened nomenclature, and needs no additional surface treatment. The backside of the front-panel molding is coated with aluminum to meet HP EMI/RFI specifications. The rubber keypad and the switching foil are ultrasonically welded to the front panel. The switching foil is a multilayer design with two contact layers separated by a third layer to keep the contacts open when no key is activated. This foil connects directly to a connector on the display board.

Plug-in Modules

A main advantage of power sensor heads over plug-in modules is the ability to move the sensor easily to the device under test (DUT). Based on feedback from users of the HP 8152A optical power meter, the design team concluded that the vast majority of all applications are fiber-based measurements. In this case it is very easy to bring the fiber ends to the test equipment, separate sensor heads are not necessary, and plug-in modules offer substantial technical and economical advantages. Therefore, the team decided to focus their design efforts on plug-in modules for laser sources and power sensors and avoid the expensive machined parts of sensor heads. For applications where customers need a parallel beam interface or want to move the sensor to the DUT, HP continues to offer the HP 81520A and HP 81521B optical sensor heads with the new HP 81533A head adapter interface to the HP 8153A mainframe (Fig. 2).

Mechanically, each plug-in module consists of a U-shaped aluminum extrusion, an L-shaped sheet aluminum cover, a plastic front panel, and a locking mechanism. The extruded part functions as the chassis on which the elec-

tronic circuitry is mounted, as a heat sink for detector assemblies or laser diodes with Peltier coolers, and as a cover. A major benefit of extrusions is that it is possible to get precise, complex shapes for little money. The sheet aluminum cover slides into the extrusion and is fixed with a single screw. For cooling purposes, the extruded chassis and the cover are partially perforated. The plug-in module front panels are made of the same plastic material as the mainframe front insert to match in color and appearance. The front panels are welded to a sheet aluminum subpanel which is screwed to the extrusion.

One of the design goals was to come up with a low-cost locking mechanism that would allow quick exchange of plug-in modules without the use of tools. All available plug-in schemes were evaluated but they all were too complex and too costly. Again a multifunctional part was designed. It is a flexible molded plastic latch that doubles as a locking mechanism to keep the module in place in the mainframe and as a small handle to pull it out if necessary. It keeps the module in place while it is in the mainframe. To remove the plug-in module, the handle must be lifted up to release a hook at the bottom of the plug-in from a recess in the mainframe. The module can then be pulled out.

To guarantee full interchangeability of all mainframes and plug-ins required careful mechanical design and tolerancing. The length of each individual plug-in and the position where the hook of the latch meets the recess in the mainframe were very critical design parameters. A molded plastic bar in each mainframe slot guides the plug-in connector precisely into the connector on the motherboard. This bar also provides the recess for the latch in the mainframe so that the tolerancing in the mainframe is reduced to just one part.

Acknowledgments

Much credit needs to be given to our section manager Peter Aue for his creative ideas and his support, and to Rudi Vozdecky, who designed a lot of the mechanical parts. Before he became the responsible materials engineer for all optical components, Michael Goder worked on the description of the human interfaces and on the layout of the

vacuum fluorescence display. Manfred Wacker and Reinhard Becker as the responsible production engineers supported us in the transfer to production and by setting up the calibration and test software.

Design of a Series of High-Performance Lightwave Power Sensor Modules

The power sensor modules for the HP 8153A lightwave multimeter feature a new optical interface, new detectors, an analog-to-digital converter based on a voltage-to-frequency converter, and a custom gate array. They offer excellent absolute accuracy and fast autoranging.

by Jochen Rivoir, Horst Schweikardt, and Emmerich Müller

LIGHTWAVE POWER SENSOR MODULES for the new HP 8153A lightwave multimeter had to meet a number of design requirements. Among these were a compact, low-cost fiber interface, excellent absolute accuracy traceable to national standards, improved sensitivity down to −110 dBm for all important wavelengths, low wavelength dependence near 1550 nm, nonlinearity better than 0.015 dB, a transducer output with fixed scaling in V/μW, resolution of 0.001 dB at 5% of full scale, 50 measurements per second, and fast autoranging.

With its inherently high dynamic resistance and its wavelength characteristics, InGaAs is the only possible detector material that meets the sensitivity and wavelength dependence requirements. Because this material is extremely expensive, a small-area detector (500 μm diameter) was chosen. Fortunately, the small size is accompanied by a high dynamic resistance, which improves the sensitivity even more.

In most applications, power is measured at the end of a fiber, where a small-area detector is sufficient. For parallel beam measurements and laser chip measurements, a head interface module, the HP 81533A, allows the use of the large-area optical heads of the earlier HP 8152A optical power meter.

The major challenge in the design of the small-area optical interface was the coupling of the fiber power to the small-area detector. Another challenge was the development of a new reference standard for the calibration of these power meter modules. No fiber-coupled standards are provided by the national standards laboratories (see article, page 70).

Small-Area Optical Interface

A GRIN (graded-index) lens forms an image of the radiating spot of a fiber optic connector on the plane rear side of the lens, where a 200-μm step-index fiber is attached and index matched. At the end of this fiber a radiating spot diameter of 200 μm is generated. This diameter is nearly independent of the core diameter of the input fiber. The beam path ends on the detector chip in the hermetically sealed detector module (see Fig. 1).

Since the GRIN lens accepts a numerical aperture (NA) up to NA = 0.46, all power from fibers with NA < 0.3 is coupled into the lens. Antireflective coating at the input surface of the GRIN lens minimizes back reflections and optical interference with the fiber end.

A graded-index lens has an index of refraction n(r) that is function of the radial distance r from the fiber axis:

$$n(r) = n_0(\lambda)(1 - \frac{A(\lambda)}{2} r^2) \qquad (1)$$
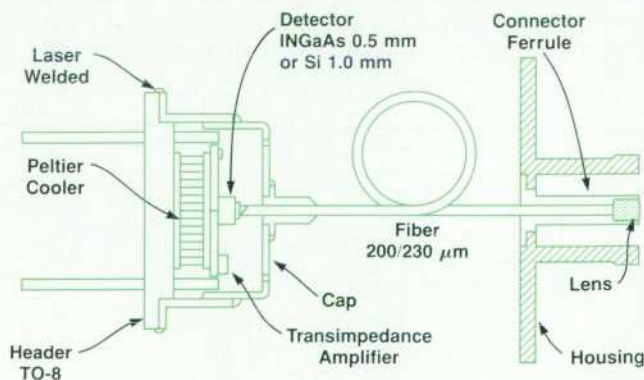

Fig. 1. *The optical interface concept used in the small-area power sensor modules for the HP 8153A lightwave multimeter.*

where both the refractive index on the axis n_0 and the quadratic gradient constant $\sqrt{A}$ are wavelength dependent.

The geometry and the profile n(r) define the beam path in the GRIN lens (see Fig. 2). The manufacturer's ray matrix formulas[1] for the GRIN lens are, in addition to equation 1:

$$\begin{bmatrix} r_2 \\ \theta_2 \end{bmatrix} = \begin{bmatrix} \cos(\sqrt{A}\,Z) - \dfrac{Q}{n_0\sqrt{A}}\sin(\sqrt{A}\,Z) & \dfrac{1}{n_0\sqrt{A}}\sin(\sqrt{A}\,Z) \\ -Q\cos(\sqrt{A}\,Z) - n_0\sqrt{A}\sin(\sqrt{A}\,Z) & \cos(\sqrt{A}\,Z) \end{bmatrix} \begin{bmatrix} r_1 \\ \theta_1 \end{bmatrix} \quad (2)$$

$$Q = \frac{n_0 - 1}{R} \quad (3)$$

We can use equations 1, 2, and 3 and the lens geometry (Fig. 2) to find the relation between the input distance L_1 and the spot diameter D of the image at the flat end surface of the lens. (The input distance L_1 is the distance between the end of the fiber and the curved front surface of the lens.) This yields L_1 = 388 μm and D = 112 μm at λ = 1307 nm for a step-index fiber with 100-μm core diameter and NA = 0.3 for minimum spot size. Measured and calculated values are in good agreement, as shown in Fig. 3.

The pitch is P = $Z\sqrt{A}/2\pi$ = 0.47 for this design. The length Z of the lens depends on the quadratic gradient constant, which is specified as $\sqrt{A}$ = 0.327/mm ±2.5% at 1300 nm over all fabricated batches. Within one batch $\sqrt{A}$ varies only within a range of 1.8%. For every batch, the length Z is fabricated according to the largest $\sqrt{A}$ within the batch.

Because of this variation of $\sqrt{A}$, the spot size D will be less than 150 μm at L_1 = 380 μm ±20 μm, and therefore the total power radiated from a fully excited 100-μm step-index fiber will be coupled into the 200-μm fiber with this GRIN lens.

The output end of the 200-μm fiber is cut at an angle of 5.3° so that reflections from the detector surface cannot be fully coupled back into the 200-μm fiber core and from there back into the input fiber.

The detector element is an InGaAs pin photodetector with a photosensitive area of 0.5-mm diameter. Spaced 0.3 mm from the fiber end, a maximum spot of 390-μm diameter is illuminated.

For a center wavelength of λ_c = 850 nm, silicon was selected as the detector material for the HP 81530A power sensor module. The different wavelength needs a different GRIN lens with a shorter length Z because the value of
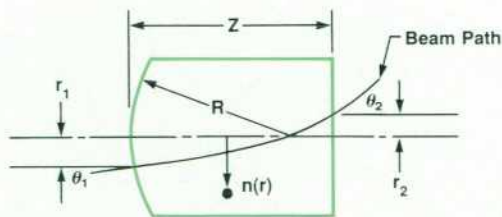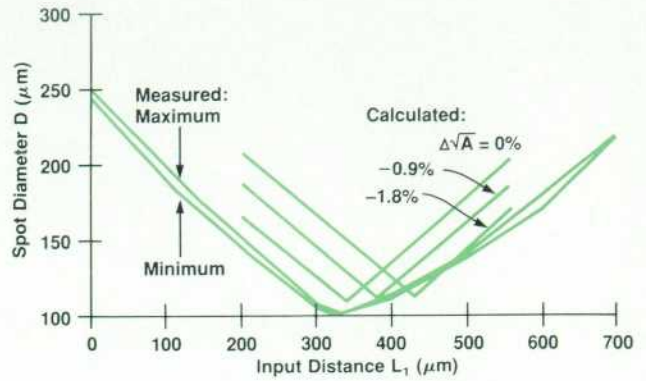
Fig. 3. *Spot diameter D versus input distance L_1 for a GRIN lens at 1307 nm.*

$\sqrt{A}$ is higher. A different antireflective coating is also needed. Since Si has a higher dynamic resistance R_D than InGaAs, a larger detector with a diameter of D = 1 mm was chosen to guarantee a more forgiving alignment process. This yields $R_D > 1\Omega$ at +20°C. To generate the same illumination conditions as in the InGaAs case, the distance between the detector surface and the 200-μm fiber end was increased by a factor of two, equal to the change in diameters. Thus, the maximum spot diameter on the Si detector is 780 μm.

The detector chip and the transimpedance amplifier are mounted on a ceramic carrier which is temperature stabilized with a Peltier cooler to +20°C (see Fig. 4). This effectively eliminates the temperature dependence of the detector's responsivity and the offset drifts of the amplifier.

Electrical Signal Path

Once the optical power has been coupled onto the detector, it is the task of the electrical signal path to amplify

Fig. 4. *Detector assembly.*

Fig. 2. *Beam path in the GRIN lens.*

and measure the signal. The main requirements are linearity, scaled transducer output, resolution, speed, and fast ranging. Fig. 5 shows the electrical signal path.

The photodetector is an extremely linear device. It converts the optical input power P into an electrical current I_D. However, the conversion factor or responsivity $r_D(\lambda)$ is strongly wavelength dependent. The relation between P and I_D is:
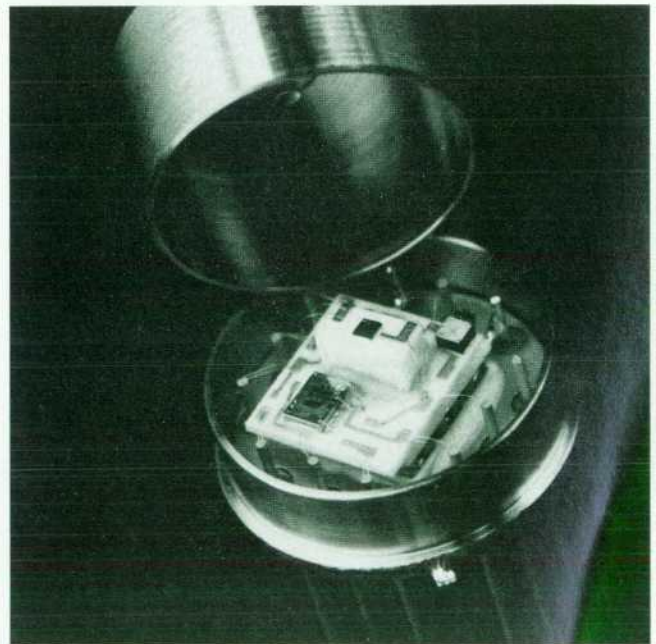
$$I_D = r_D(\lambda)P. \tag{4}$$

The transimpedance amplifier converts I_D to a voltage, which is amplified by a programmable-gain amplifier and a multiplying digital-to-analog converter (DAC). The resulting voltage is finally fed both to the analog-to-digital converter (ADC) and to the transducer output. To maintain a fixed conversion factor for the transducer output, for example 2V/200 nW, the multiplying DAC compensates for the wavelength dependency of the responsivity and for individual ranging errors, which are the main contributors to nonlinearity.

Based on a voltage-to-frequency converter (VFC) and a custom gate array, the ADC combines low cost, extremely high resolution, and selectable measurement speed.

Transimpedance Amplifier

Ideally the output of the transimpedance amplifier is:

$$V_{ximp} = R_f I_D = R_f r_D(\lambda)P, \tag{5}$$

where R_f is a range dependent feedback resistance in the transimpedance amplifier. However, both dc drift and noise limit the lowest detectable power.[2]

The dc offset is generated by the temperature dependent offset current and offset voltage of the amplifier IC. A dedicated 10-bit coarse-offset DAC subtracts these offsets at their origin and thus guarantees an offset-free transimpedance amplifier output. Because the amplifier is located inside the temperature stabilized detector assembly, drift can be kept well below 100 fW. To determine the appropriate coarse-offset DAC value, a zeroing operation is performed about one minute after power-on, when the temperature in the detector assembly has settled.

In the HP 81532A InGaAs-based power sensor module, the predominant noise source is the temperature noise of the detector's dynamic resistance, which is specified as $R_D > 100$ MΩ at $+10°C$. Other noise sources are the voltage and current noise of the operational amplifier used in the transimpedance amplifier and the temperature noise of R_f.[2] A typical temperature dependence of R_D is $\alpha = -0.065/K$ (see Fig. 6). With an estimated worst case value of $\alpha = -0.1/K$ and modeled by

$$R_D(T) = R_D(T_0)e^{\alpha(T-T_0)} \tag{6}$$

this yields a worst-case value of $R_D > 35$ MΩ at the actual detector temperature of 20°C.

For minimum noise and maximum signal, R_f is chosen as large as possible such that the specified full scale voltage $V_{ximp,FS}$ is not exceeded even for the highest responsivity ($r_D = 1.1$ A/W). For the most sensitive -70 dBm range (full scale power $P_{FS} = 200$ pW), the choice was $R_f = 400$ MΩ ±10% because $V_{ximp,FS}$ is 0.1V in this range. A detailed noise analysis shows a total rms noise power of $P_{rms} =$
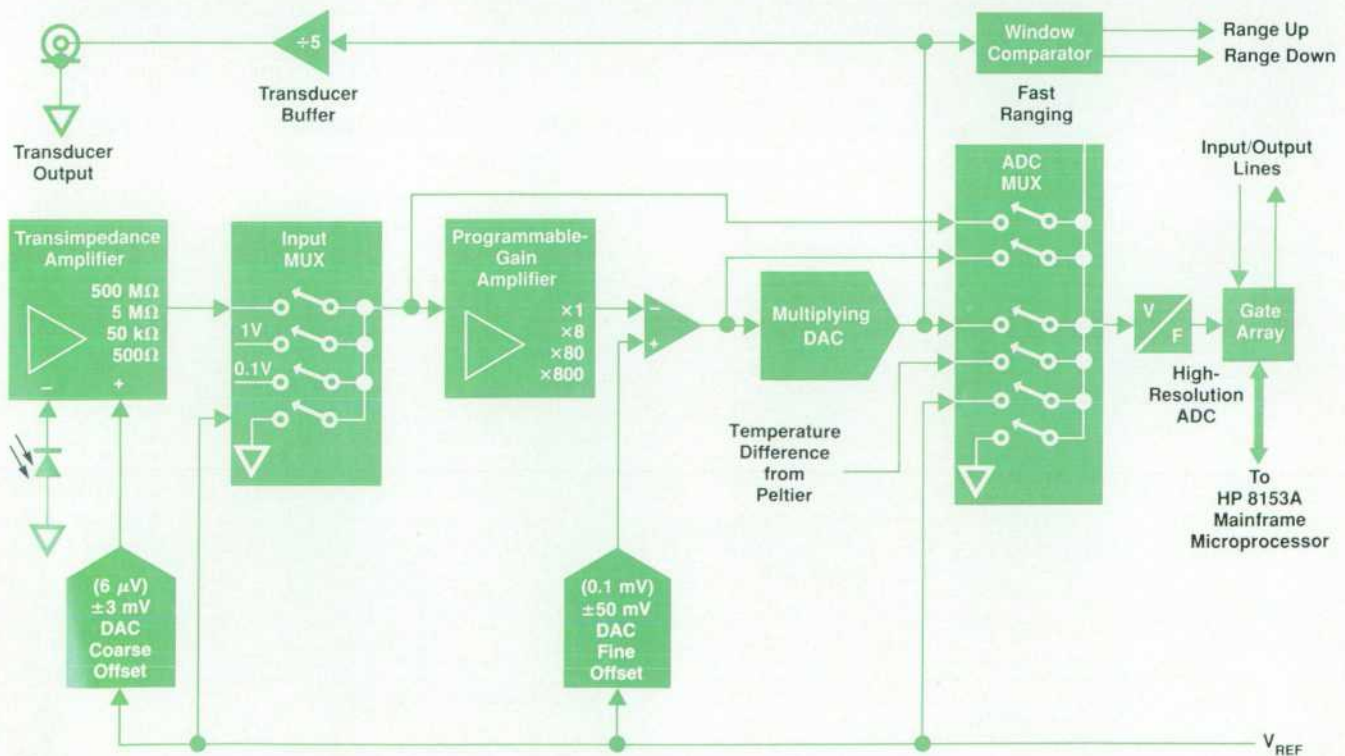

Fig. 5. *Electrical signal path of a power sensor module.*

0.029 pW at 1300 nm (r_D = 0.8 A/W). With a crest factor less than 8, the peak-to-peak noise is less than 0.3 pW, well below the specified 0.5 pW (see Table I).

Table I
Noise Analysis
RMS Noise in pW

	Si 81520A	Ge 81521B	Si 81530A	InGaAs 81531A	InGaAs 81532A
R_D	0.036	2.200	0.004	0.060	0.019
R_f	0.038	0.100	0.007	0.006	0.006
V_{nA}	0.002	6.200	0.002	0.016	0.016
I_{nA}	0.027	0.016	0.018	0.013	0.013
Total	0.058	6.600	0.018	0.064	0.029

Note: The V_{nA} and I_{nA} contributions are the voltage and current noise of the operational amplifier. The total is the root sum square (RSS) combination of the contributions.

For the Si-based HP 85130A power sensor module, the peak responsivity of the chosen diode is 0.75 A/W. This led to a feedback resistor R_f of 500 MΩ ±10%. Noise analysis for this design reveals an even better performance than the HP 81532A (see Table I).

For less-sensitive ranges, additional feedback resistors of about 5 MΩ, 50 kΩ, and 500Ω are available.

Programmable-Gain Amplifier

Depending on the selected range, the transimpedance amplifier delivers a full scale output voltage of 0.1V, 1V, or 10V at the highest responsivity (1.0 A/W). The programmable-gain amplifier is inserted to make best use of the ADC's 10V full scale voltage. Table II shows the feedback resistor R_f and the gain of the programmable-gain amplifier G_{PGA} for all ranges.

The design principle shown in Fig. 7 uses standard components. Thus, cost could be minimized without sacrificing performance in terms of offsets and drifts, which are most important for this application.

Because any operational amplifier offset voltage will be amplified by the maximum gain of the programmable-gain
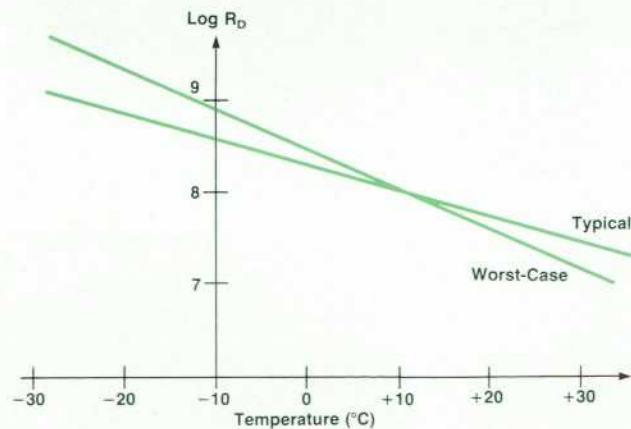
Table II
Ranging Table for the HP 81532A

Range	P_{FS}	R_f	$V_{ximp,FS}$	G_{PGA}
0 dBm	2 mW	500 Ω	1 V	8
−10 dBm	200 μW	50 kΩ	10 V	1
−20 dBm	20 μW	50 kΩ	1 V	8
−30 dBm	2 μW	5 MΩ	10 V	1
−40 dBm	200 nW	5 MΩ	1 V	8
−50 dBm	20 nW	5 MΩ	0.1 V	80
−60 dBm	2 nW	400 MΩ	0.8 V	8
−70 dBm	200 pW	400 MΩ	0.08 V	80

amplifier (80), an amplifier with good offset voltage properties was chosen. Offset and leakage currents flowing through the on resistance of the multiplexer generate an additional offset at the output of the programmable-gain amplifier. Because the on resistance of the multiplexer is the most critical parameter, the multiplexer is selected for minimum $R_{DS(on)}$ only. Leakage currents from the output side of the multiplexer see a relatively low impedance, and thus generate little offset.

To avoid a mix of annoying offset dependencies, the residual programmable-gain amplifier offset is corrected just after the amplifier with a 10-bit fine-offset DAC. To separate the programmable-gain amplifier offset from any previous offset the input multiplexer is inserted (see Fig. 5). Again, offset correction values for all programmable-gain amplifier gains are determined during zeroing.

In contrast to off-the-shelf programmable-gain amplifiers, no effort and expense were needed to guarantee exact gain factors such as 1.000, 10.00, and 100.0 for this design. Because of the wavelength dependent responsivity, the gain of the total signal path is an inexact number anyway, and has to be adjusted by the multiplying DAC. The only requirement on the programmable-gain amplifier is that the gain be stable over temperature and time.

Multiplying DAC

As indicated earlier, the purpose of the multiplying DAC is to correct the total gain of the signal path to the transducer output such that the full scale voltage at the transducer
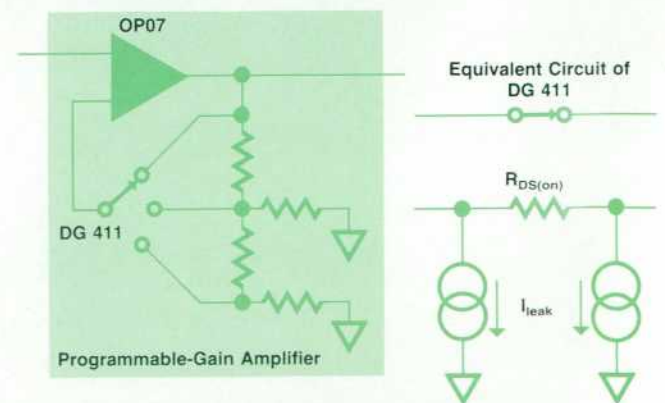

Fig. 6. Temperature dependence of the dynamic resistance R_D of a 500-μm InGaAs detector.

Fig. 7. Programmable-gain amplifier design.

output is exactly 2V for all ranges:

$$P_{FS}r_D(\lambda)R_fG_{PGA}G_{MDAC}G_{XDCR} = 2V,$$ (7)

where P_{FS} is the full scale power, G_{MDAC} is the gain of the multiplying DAC, and G_{XDCR} is the gain of the transducer buffer amplifier. Even in the uncalibrated power meter, typical resistances and gains in the signal path are taken into account by the measurement software to set the multiplying DAC. During calibration, additional correction factors for the actual gains of all ranges are measured (c_{range}). Furthermore, a correction factor for the wavelength dependency of the responsivity, c_λ, is calibrated in steps of 10 nm over the specified wavelength range.

$$G_{MDAC} = \frac{2V}{P_{FS}} \frac{c_\lambda\, c_{range}}{r_{D,typ}R_fG_{PGA}G_{XDCR}}.$$ (8)

Because the responsivity r_D drops drastically at the ends of the wavelength range, $|G_{MDAC}|$ has to range from about 1.0 to at least 10.0. Therefore, a design with a 12-bit multiplying DAC in the current-steering mode[3] was chosen. This design has almost no gain limitations:

$$|G_{MDAC}| = \frac{2048}{n} = 1.001, \ldots, \quad 0 < n \le 2047 \quad (9)$$

Because the hardware gain is set according to the requirements of the transducer output, the full scale voltage at the ADC deviates from 10.000V to the extent that G_{XDCR} is not equal to 0.2000. Since G_{XDCR} is measured during calibration, this can be taken into account. To improve the range accuracy over the resolution limitations of the multiplying DAC, the quantization error c_{qu} of the multiplying DAC gain is corrected by software.

$$c_{qu} = \frac{\text{Wanted Gain}}{\text{Real Gain}}$$ (10)

This is one of the ways in which the low nonlinearity of 0.015 dB maximum is obtained. A typical example for the range accuracy of a power sensor module is shown in Fig. 8.
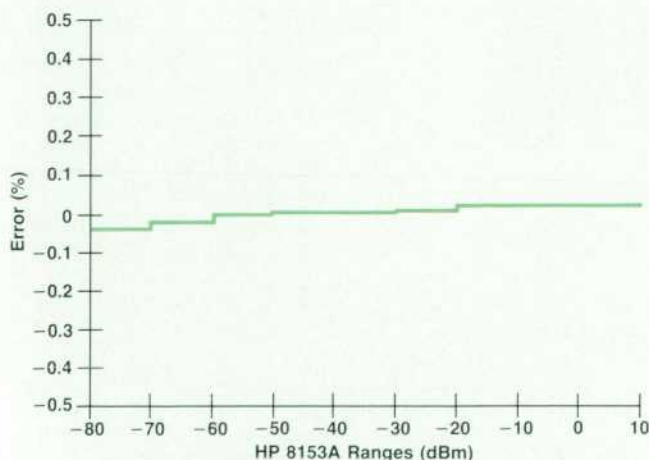

Fig. 8. *Measured range accuracy of an HP 81532A lightwave power sensor module relative to −40 dBm.*

Once all these correction factors are measured or calculated, the ADC voltage V_{ADC} can be used to compute the optical power P_{OPT}:

$$P_{OPT} = \frac{V_{ADC}}{10V} c_{qu} \frac{0.2}{G_{XDCR}} P_{FS}(\text{range}).$$ (11)

High-Resolution ADC

For the power meter readout, a resolution of 0.001 dB is required even at only 5% of the full scale power. This is equivalent to a resolution of at least 10^{-5}, or 17 bits. Commercial 17-bit ADCs are extremely expensive, because they also feature 17-bit linearity, which is much too precise for an optical power meter. A nonlinearity of 0.1% (13 bits) for the ADC is by far good enough.

These special requirements of the optical power meter can be met by a voltage-to-frequency converter (VFC) and some digital hardware that counts the frequency during a selectable measurement time. The principle of a conventional VFC ADC is shown in Fig. 9.

The VFC produces a frequency directly proportional to its input voltage, which is biased slightly in the positive direction to guarantee a minimum frequency of 100 kHz.

$$f_{VFC} = f_{VFC,0} + (f_{VFC,FS} - f_{VFC,0}) \frac{V_{ADC}}{V_{ADC,FS}}$$

$$= 100\text{ kHz} + (900\text{ kHz}) \frac{V_{ADC}}{10V}.$$ (12)

Here the subscript 0 indicates that the input is zero and the subscript FS indicates full scale.

A synchronous VFC was chosen over an asynchronous VFC because its full scale frequency is determined by a quartz oscillator and not by an external one-shot capacitor, which always exhibits temperature drifts and dielectric absorption. The linearity is limited by the VFC to about 14 bits, while resolutions of 20 bits can be achieved with long enough measurement times.

The synchronous VFC can change its output only every $1/(8\text{ MHz}/4) = 500$ ns, so there is some inherent quantization in the output frequency, which limits the resolution for a given integration time.

The 28-bit time counter, which is preloaded by the processor with n_{OSC}, defines a measurement time $T_m = n_{OSC}T_{OSC}$, where T_{OSC} is the period of the oscillator. During this time, the period counter counts n_{VFC} periods of the
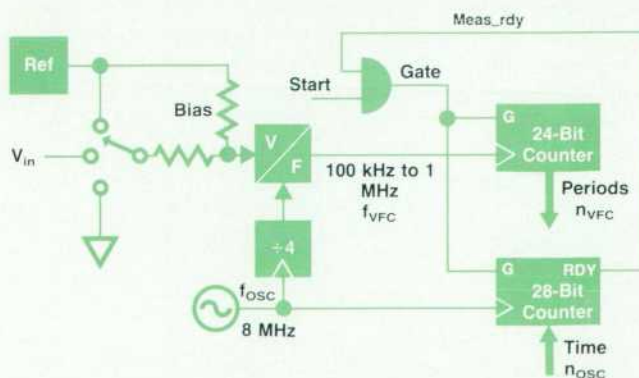

Fig. 9. *Conventional voltage-to-frequency converter ADC.*

VFC output. The measured frequency is:

$$f_{VFC} = f_{OSC} \frac{n_{VFC}}{n_{OSC}} = 100 \text{ kHz} \dots 1 \text{ MHz}. \quad (13)$$

An ADC voltage at 5% of full scale generates a total frequency of $f_{VFC} = 100$ kHz + (900 kHz)(5%) = 100 kHz + 45 kHz. Only 45 kHz contain information about the ADC voltage. During the 20-ms integration time this incremental frequency contributes $\Delta n_{VFC} = (20 \text{ ms})(45 \text{ kHz}) = 900$ periods, which are counted with an inherent uncertainty of one period, while n_{OSC} is exactly (20 ms)(8 MHz) = 160,000. This implies a resolution of 1:900, or 0.005 dB, which does not meet the requirements. Equation 14 shows that for this design the resolution depends on the measurement result.

$$\text{Resolution} = \frac{1}{\Delta n_{VFC}} = \frac{1}{T_m \left(f_{VFC,FS} - f_{VFC,o} \right)} \frac{V_{ADC,FS}}{V_{ADC}} \quad (14)$$

Because the result is mainly determined by the ratio of two integers n_{VFC} and n_{OSC} (see equation 13), with $n_{VFC} \ll n_{OSC}$, it is highly desirable that the number of periods n_{VFC} be exact and n_{OSC} have the unavoidable uncertainty of one count. Of course, this can easily be done by counting a large enough number of periods and finding out the time it took. Unfortunately, then the measurement time depends on the measurement result, which is not acceptable at all.

These considerations led to the modified VFC ADC concept shown in Fig. 10. An integration time is proposed by the HP 8153A mainframe processor, but the actual integration is synchronized with the closest multiple of VFC periods, that is, $T_m = n_{VFC}/f_{VFC}$. The actual measurement time T_m is measured by counting the number of clock cycles n_{OSC} of the oscillator with an uncertainty of one count.

As stated above, T_m is quantized in steps of 1 μs. This implies that now the resolution is limited by $f_{OSC}/4/2 = 1$ MHz, that is, effectively by the VFC's full scale frequency $f_{VFC,FS}$ instead of f_{VFC}. Therefore, the resolution is independent of the measurement result.

$$\text{Resolution} = \frac{1}{T_m f_{VFC,FS}}. \quad (15)$$

$T_m = 20$ ms yields a resolution of 5×10^{-5}, or 0.0002 dB, or 14 bits. A 1-s integration time yields a resolution of 10^{-6}, or 0.00005 dB, or 20 bits.

To compensate for offset drift and gain drift, an input multiplexer allows calibration at two voltages, V_{Ref} and GND. This is done during zeroing.

Besides selectable resolution, an integrating ADC with programmable measurement time makes it possible to trade off speed for noise reduction. In the frequency domain a VFC looks like a filter H(f) with selectable bandwidth.[4]

$$H(f) = \frac{\sin(\pi f T_m)}{\pi f T_m} \quad (16)$$

The effective noise bandwidth is

$$B_{eff} = \int_0^\infty H^2(f) df = \frac{1}{2T_m} \quad (17)$$

which means that noise reduction is proportional to $\sqrt{T_m}$,

that is, doubling T_m decreases the noise level by 1.5 dB. Thus, very low-level optical power can be measured by selecting a long enough measurement time. When the measurement time is chosen to be a multiple of the line period, for example 100 ms, theoretically an infinite power supply rejection ratio is obtained (see equation 16).

Another advantage of an integrating ADC is that it doesn't need an anti-aliasing filter, because the VFC itself acts as a filter with an appropriate cutoff frequency. Because there is no filter, there is no need to wait for its settling time when the range is changed.

Gate Array

The benefits of the VFC ADC can only be realized when the necessary huge digital counters are integrated into an IC. Therefore, we decided to design a custom gate array. We then decided to include all of the digital functions of the power meter in this gate array and make it as versatile as possible. For example, there are eight general-purpose pins that can be used as inputs outputs or interrupts. Used as interrupts, they can be programmed to be sensitive to a high level, a low level, a rising edge, or a falling edge. Twelve output lines are provided to select ranges, switch multiplexers, and so on.

Because of its flexibility, the gate array was able to adapt to some late design changes and is also used in the laser source modules and the head interface module.

Fast Autoranging

It was a design requirement that the power meter be able to change ranges very quickly. This is advantageous in autoranging mode and for fast remote progamming via the HP-IB. As mentioned above, fast ranging is possible because there is no filter in the signal path to wait for. A comparator at the ADC input detects when a range is exceeded even for a short time and issues a range-up interrupt, which
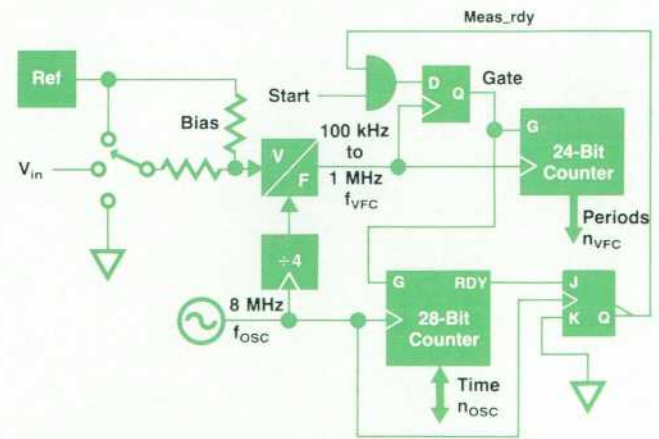
Fig. 10. *Modified voltage-to-frequency converter ADC.*

forces an immediate range change. The current measurement is aborted.

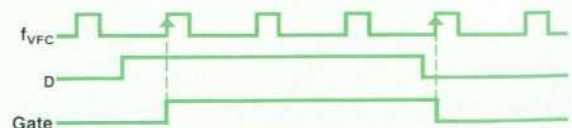If the comparator finds that the signal is low enough for a more sensitive range, it issues a range-down signal, causing an immediate range change. To avoid continuous up-down range switching in the case of pulsed power, only a single range-down interrupt is allowed until a valid measurement result has been shown on the display. From the averaged ADC result alone, momentary saturation caused by a pulsed signal cannot be detected. Therefore, the comparator is followed by a flip-flop, which stores even short violations of the range limits so the software can determine the proper range. Thus, this scheme combines fast autoranging for constant power levels with correct measurements even for pulsed power.

Because of the window comparator and the absence of a filter, a range can be changed in only 40 ms. This time is limited by the processor, which has to calculate a large number of correction factors for a new range.

Interface to Multimeter Mainframe

To guarantee maximum flexibility, the interface to the multimeter mainframe is purely digital. No analog information is exchanged. Characteristic data for the individual power meter module is stored in an EEPROM inside the module. This EEPROM contains information on the measurement capabilities of the module, calibration data such as wavelength correction data, range correction factors, and other information. It is programmed in the circuit during the calibration process.

Since the power meter relies on highly sophisticated interaction between hardware and software, the module-specific measurement software is located in an EPROM in the module. Thus, further improvements or changes can be handled within the module without affecting the mainframe software.

References

1. *Theory of the Selfoc® Lens*, Nippon Sheet Glass Co., Ltd.
2. J. Becker, "Detectors for Optical Power Measurements," *Hewlett-Packard Journal*, Vol. 38, no. 2, February 1987, pp. 16-21.
3. P. Burton, *CMOS DAC Application Guide*, Analog Devices, 1984, pp. 27-28.
4. *Analog-Digital Conversion Handbook*, Analog Devices, 1986.

Calibration of Fiber Optic Power Meters

This paper describes the proposed IEC standard and HP's implementation.

by Christian Hentschel

IN ADDITION TO PROVIDING high-performance lightwave measurement hardware, HP is also involved in contributing to a worldwide solution of the problem of calibrating fiber optic power meters. Presently, calibration and accuracy specifications are based on internal company standards, with the result that different vendors' specifications are not comparable. This is especially annoying to users, because instruments often don't meet their specified accuracies in practical measurements.

Calibration of optical power meters is difficult because the measurement results often depend on many parameters, such as the wavelength and the excitation conditions. Errors of 10% or more can occur when changing the type of fiber or connector.[1] Because the test meter's uncertainty usually depends on a number of subsequent calibrations (calibration chain), such errors can accumulate to unexpectedly large uncertainties. To accumulate the errors correctly, it is necessary to characterize meticulously all of the measurement conditions and the equipment used in the chain.

The problem of incompatible procedures in evaluating accuracy will soon be solved with the help of an international standard, the IEC document *Calibration of Fiber-Optic Power Meters*.[2] The aim is to make the calibrations traceable, comparable, and transparent to the user. To achieve this goal, the IEC document provides extensive help in categorizing, determining, and accumulating the individual uncertainties. A set of forms (Fig. 1) was developed to guide the calibrator (Forms B, C, D and E) and to provide the end user with detailed information about the calibration and its traceability (Forms A1 and A2).

In the following, let us discuss the IEC document with the help of an IEC-type calibration example: the production calibration of the HP 81532A InGaAs plug-in for the HP 8153A lightwave multimeter. This unit, like all HP power meters, is individually calibrated over its usable wavelength range. In this case, the calibration is performed from 1000 to 1650 nm in steps of 10 nm with 0.1-nm interpolation between calibration points. Within this range, HP specifies ±2.5% uncertainty at reference conditions, with a confidence level of 99.7%. How does HP arrive at such a low uncertainty?

Our calibration starts with selection of an appropriate light source. For continuous-wavelength calibration, the proper choice is a monochromator-type source. Fiber and connector coupling is necessary because the test meter is of the small-area type. HP uses a combination of a tungsten lamp, a monochromator and a 50-μm graded-index fiber. A mode filter is added to make the output power level less sensitive to fiber bending. The most important item in each calibration is an accurate, traceable standard (a second power meter). Our standard is a combination of an HP 81521B optical head (selected for best uniformity), an HP 81533A interface plug-in, and another HP 8153A multimeter. This instrument features 4½-digit resolution, which makes it well-suited for calibration purposes. Its traceability is discussed below.

As indicated in Fig. 2, the calibration is based on comparing the measurement results of the two meters and, in the HP case, writing correction factors into the nonvolatile memory of the plug-in. What is more demanding is calculating the uncertainty of the test meter. This process is based
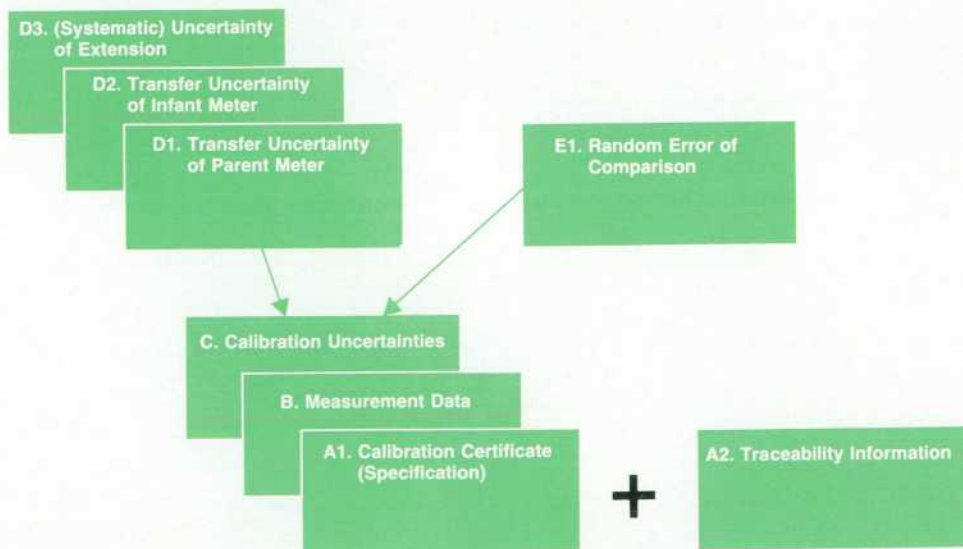

Fig. 1. *The IEC forms that guide the calibrator through the calibration.*
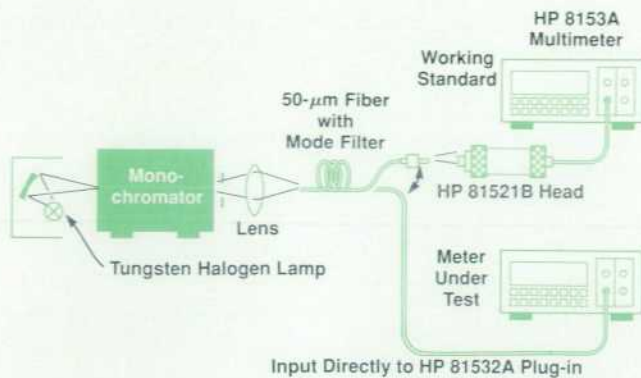
Fig. 2. *The calibration setup.*

on assessing individual errors and on accumulating them correctly. As usual in the world of standards laboratories, the IEC document distinguishes between the following individual uncertainties:

- Systematic uncertainties, expressed by a correction factor (if a deviation is known) and an uncertainty band. An assumed uncertainty band of width 2w can be expressed by a standard deviation of $\sigma = w/\sqrt{3}$.
- Random uncertainties, expressed by a standard deviation characterizing the reproducibility of the process. When the actual calibration is based on averaging more than one measurement sample, then the standard deviation can be divided by the square root of the number of samples.

Let us now start our paperwork.

Form A1. Calibration Certificate (Specification)

This form summarizes all measurements and calculations. It must accompany all IEC-compatible optical power meters. The form includes the conditions of the calibration (the reference conditions), the uncertainty at reference conditions, and the applicable confidence level. The reference conditions are to be supplied in the form of a standardized list. In our example, the list includes includes calibration date, temperature ($23 \pm 5°C$), power level ($10 \mu W$), beam geometry (fully excited 50-μm graded-index fiber), connector (HMS-10/HP), wavelength (1000 to 1650 nm), and spectral bandwidth (10 nm max). Before Form A1—the final result of the calibration—can be filled out, all of the remaining forms have to be completed first.

Form A2. Traceability Information

This form contains the name of the national standards laboratory and, if applicable, the name of the accredited calibration laboratory. It also lists all measurement equipment, all sets of reference conditions, and all relevant uncertainties in the chain. For our example, the calibration chain is as follows:

- Level 0. The lowest-level PTB (Physikalisch-Technische Bundesanstalt) standard, a thermopile radiometer, calibrated with a collimated beam.
- Level 1. A PTB-calibrated ECPR (electrically calibrated pyroelectric radiometer), also calibrated with a collimated beam, recalibrated by PTB every 9 months.
- Level 2. The working standard (HP 81521B), collimated-

beam calibration, recalibrated by PTB every two months.
- Level 3. The test meter (HP 81532A), to be calibrated with a fiber beam.

The traceability information must be made available upon request. All of the remaining forms are lab-internal.

Form B. Measurement Data

This worksheet collects the measurement data for the individual calibration and guides the calibrator through the calculation of the test meter's correction factor. To generate the data, the radiation source is consecutively measured with the working standard and the test meter. This cycle may have to be repeated several times, with the intention of reducing the random uncertainty (see Form E1). Each measurement pair is recorded in the form of a correction factor, and the final correction factor is calculated by averaging.

Form C. Calibration Uncertainties

This form contains the complete list of uncertainties of the specific calibration process and guides the calibrator through the uncertainty accumulation. It starts with the parent meter's uncertainty at reference conditions, which we extract from the working standard's calibration certificate. In our case, it is specified as:

Parent meter's uncertainty at reference conditions:	$\pm 1.9\%$ (confidence range)
Confidence level:	99.7% (means a $\pm 3\sigma$ confidence range)
Equivalent standard deviation $\sigma(C)$:	0.63% (from dividing 1.9% by 3).

The remaining part of the form deals with evaluating the cumulative transfer uncertainty, which accumulates all uncertainties from Forms D1 to E1.

Form D1. Transfer Uncertainty of Parent Meter (Working Standard)

This form collects the systematic transfer uncertainties of the parent meter, as caused by the difference between the parent meter's original reference conditions and the actual reference conditions. The IEC document suggests evaluating the individual uncertainties with the help of the standardized list of reference conditions. In our example, the main contribution to uncertainty comes from calibrating the working standard with an open beam (a nonreflective excitation) rather than a fiber-connector combination (a slightly reflective excitation). Altogether, these systematic uncertainties result in a standard deviation of $\sigma(D1) = 0.28\%$.

Form D2. Transfer Uncertainty of Infant Meter (Test Meter)

Similar to Form D1, this form contains the systematic transfer uncertainties of the test meter, as caused by the finite widths of the tolerance bands of the actual reference conditions. In our example, the largest uncertainties are the nonreproducibility of the beam geometry, causing an

estimated (systematic) uncertainty of ±0.2%, and the wavelength uncertainty of the monochromator, responsible for another uncertainty of ±0.2%. Summing all uncertainties and adding them geometrically yields $\sigma(D2) = 0.17\%$.

Form D3. (Systematic) Uncertainty of Extension

The new term "extension" applies when the test meter is to be specified at a set of reference conditions that are different from the calibration reference conditions. This can be done on the basis of relative measurements. Extension may be necessary, for example, if the calibration wavelength or power level does not coincide with the desired wavelength or power level. This situation does not apply in our example, so the uncertainty of extension is zero.

Form E1. Random Uncertainty of Comparison

The measurements suggested in Form E1 characterize the random uncertainties in the transfer process—for example, power level fluctuations and the uncertainty of reconnecting the fiber. The procedure goes through two steps. First, the reproducibility of the transfer process is characterized. To do this, a large number of consecutive measurements are taken with the standard and a test meter, and each measurement pair is recorded as a quotient. Then the standard deviation of the quotients is calculated as a measure of the randomness of the process.

In the second step, the normalized standard deviation (expressed in percent of average) is divided by the square root of the number of comparisons, n, carried out in the individual calibration; this is based on using the average as the final correction factor. In our example we used n = 1. The result is: $\sigma(E1) = 0.28\%$.

Uncertainty Accumulation

Most calibration authorities, such as NIST, BIPM, and PTB, agree with the IEC on accumulating these uncertainties with the so-called "PTB approach".[3] Such a common formalism is extremely important because otherwise the calculations can result in completely different uncertainty data. The IEC's algorithm is:

Cumulative standard deviation

$$\sigma_s{}^* = \left(\sum_{k=1}^{i} \sigma_{sk}{}^2 + \sum_{l=1}^{j} s_{rl}{}^2/n_l \right)^{1/2}$$

where: σ_{sk} = (calculated) standard deviation representing a systematic uncertainty, one of i

s_{rl} = (experimental) standard deviation characterizing a random uncertainty, one of j

i = number of systematic uncertainties

j = number of random uncertainties

n_l = number of measurement samples taken, one of j (averaging assumed).

For our example, Form C finally contains the following standard deviations:

Parent meter's uncertainty at reference conditions:	= 0.63% as listed in Form C
Transfer uncertainty of parent meter:	= 0.28% from Form D1
Transfer uncertainty of infant meter:	= 0.17% from Form D2
Systematic uncertainty of extension:	= 0.00% from Form D3
Random uncertainty of comparison:	= 0.28% from Form E1
Test meter's uncertainty at reference conditions:	= 0.78% from accumulating all above terms.

We can now conclude our calibration by going back to Form A1. To specify a confidence interval, the standard deviation is multiplied by 3, because our confidence level is 99.7% (the IEC document suggests a default confidence level of 95%). The multiplication results in an uncertainty at reference conditions of ±2.34%, which HP specifies as ±2.5%. Note that this specification only applies to the reference conditions, and that the document also provides guidelines in the calculation of the power meter's total uncertainty at operating conditions.

References

1. R. Gallawa and X. Li, "Calibration of Optical Fiber Power Meters: The Effect of Connectors," *Applied Optics*, Vol. 26, no. 7, April 1987, pp. 1170-1174.
2. *Calibration of Fiber-Optic Power Meters*, IEC Secretariat's Document IEC TC86, June 1990.
3. S.R. Wagner, "On the Quantitative Characterization of the Uncertainty of Experimental Results in Metrology," *PTB Mitteilungen* 89, 2/1979, pp. 83-89.

Semiconductor Laser Sources with Superior Stability for Optical Loss Measurements

Temperature stabilization and output power control provide excellent stability in the plug-in laser source modules for the HP 8153A lightwave multimeter.

by Frank A. Maier

LOSS MEASUREMENTS, one of the main applications of the HP 8153A lightwave multimeter, need two different kind of modules: accurate power meters and highly stable CW laser sources.

Corresponding to the important fiber optic wavelength bands, four different plug-in laser source modules have been developed:

- HP 81551MM 850-nm multimode
- HP 81552SM 1310-nm single-mode
- HP 81553SM 1550-nm single-mode
- HP 81554SM dual-wavelength (1310 and 1550 nm) single-mode.

This article discusses the design and stabilization of these laser sources.

Sources of Instability

First let us examine the parameters that limit the stability of a laser source and how their influence can be reduced or eliminated. Of course, the most important problem is ambient temperature deviations. Two parameters of a semiconductor laser are strongly temperature dependent: the central wavelength and the operating characteristic curve.

The central wavelength has a temperature coefficient of 0.1 to 0.5 nm/K, which leads to a wavelength shift of 7 to 35 nm over the operating temperature range of the plug-in laser sources. This is absolutely unacceptable.

Fig. 1 shows the temperature dependency of the laser curve. The laser curve at a certain temperature is given by

$$P_{opt} = P_{thr} + \epsilon (I - I_{thr}).$$

The laser threshold current can be modeled as:

$$I_{thr} = I_0 \exp(T/T_0),$$

where T_0 is the characteristic temperature of the laser material. For GaInAsP lasers, this leads to a temperature coefficient

$$\alpha_{thr} = dI_{thr}/dT$$

of about 1.2 to 2%/K. With

$$dP_{opt}/dT = \epsilon \alpha_{thr} I_{thr}$$

and typical values for the laser differential efficiency ϵ of 0.1 W/A and I_{thr} of 25 mA, we have:

$$dP_{opt}/dT = 50 \ \mu W/K = 0.2 \ dB/K!$$

Obviously, lasers are extremely sensitive to temperature deviations. Even with an excellent output power control circuit it is almost impossible to eliminate this effect. As a consequence, temperature stabilization is absolutely necessary.

Another source of instability is the laser chip-to-fiber coupling ratio, which is sensitive to temperature variations and even more sensitive to humidity deviations. These effects only can be avoided by thermal stabilization of the fiber-to-chip alignment and by providing a hermetic encapsulated housing.

Laser Source Design

Based on these considerations, a hybrid laser module, as shown in Fig. 2, was chosen. The module consists of the laser chip itself, a Peltier cooler with thermistor, and a back-facet diode to allow an output power control loop.

The resulting block diagram of a single source module is shown in Fig. 3. The circuitry consists of five main blocks:

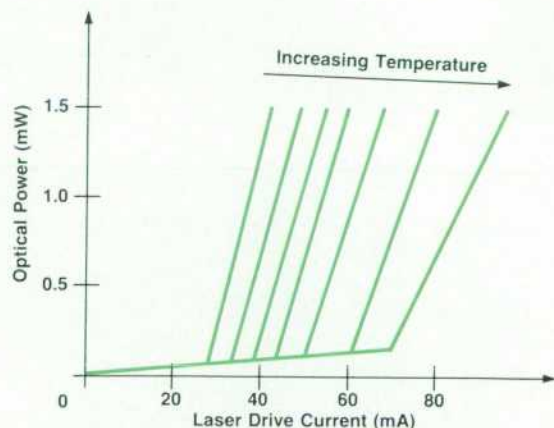- A device bus interface to communicate with the HP

Fig. 1. *Temperature dependence of the laser operating characteristic.*
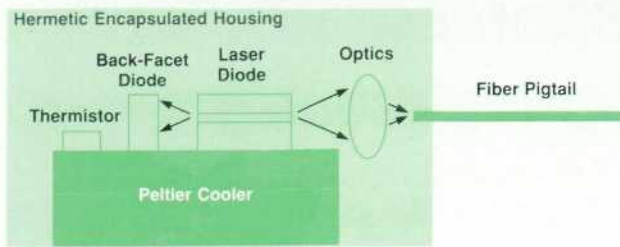
Fig. 2. *Hybrid laser module.*

8153A mainframe
- A temperature stabilization control loop
- An output power control loop
- A safety circuit to supervise the laser output power and prevent it from exceeding its maximum permitted value
- A modulation circuit to provide internal low-frequency chopping.

Temperature Stabilization

Fig. 4 shows the main features of the temperature control loop. This circuit consists of two different PI (proportional integral) control loops: a fast current control loop to stabilize the current through the Peltier element, and a slower temperature control loop.

A diode bridge protects the Peltier element from currents above its rating (especially during the settling time after turn-on). The transistor bridge in the current control loop allows bipolar temperature control from a unipolar Peltier supply. This is important because the HP 8153A doesn't provide a high-current bipolar power supply but only a universal 30V supply to produce every nonusual supply voltage on the plug-in level.

A Peltier element needs approximately 1A to pump 40K with a voltage drop of 2V maximum across the element. With a conventional 5V supply that would mean 5W for a single-wavelength source and 10W for a dual-wavelength source module. This was considered unacceptable. Therefore, a Peltier supply voltage of 2.2V was chosen. It is produced by a dc-to-dc buck converter as shown in Fig. 5. With a conversion efficiency of 75% this lowers the power consumption to 5.9W for the dual-wavelength module.

A ripple voltage of more than 10% across the Peltier element decreases its lifetime significantly. The switching frequency is about 40 kHz, so the current control loop is too slow to eliminate the ripple on the Peltier supply voltage. Therefore, the ripple is reduced using a simple LC filter (see Fig. 5).

To achieve a high conversion efficiency, the flyback diode in Fig. 5 must have a low turn-on voltage. Therefore, a high-current Schottky diode was chosen. The choke needs a low dc resistance, and the space available for it was restricted, so a 160-μH choke is used. The 180-μF, 50V
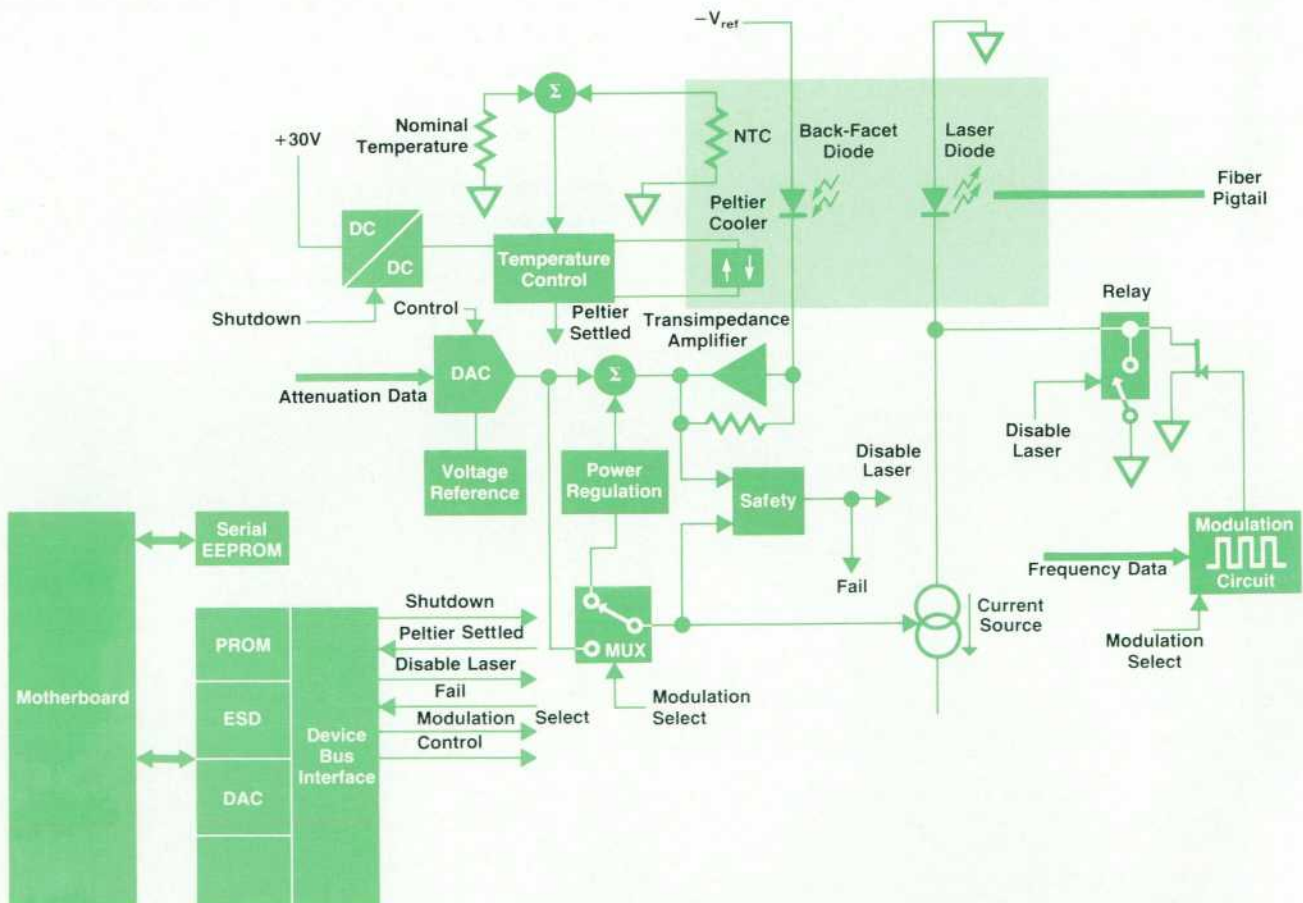

Fig. 3. *Block diagram of a single-wavelength plug-in laser source module.*
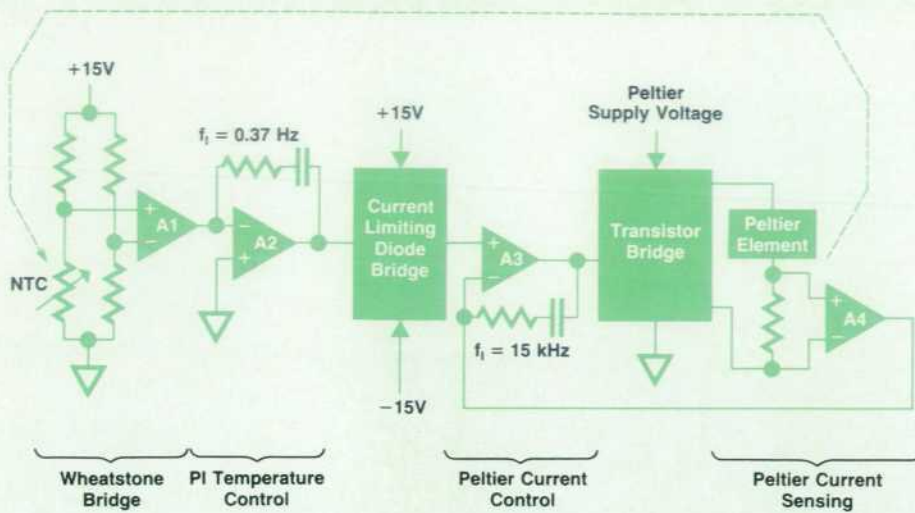
Fig. 4. Laser temperature control circuits.

filter capacitor has a current rating of 0.7A and a series resistance of 0.11 ohm. The resulting ripple voltage is 5% and the conversion efficiency is approximately 75%.

Output Power Control

To obtain excellent short-term performance and good stability in the noncontrolled chopping, a high-precision current source was implemented. Fig. 6 shows a simplified diagram. It is very important to eliminate the −15V devia-

tions by sensing the laser current directly across the sense resistor. To increase the current source output impedance, an enhancement MOSFET is used, thereby avoiding the base current uncertainties of bipolar transistors.

To improve the long-term stability and reduce laser diode aging effects, an output power control loop is necessary. The output power is sensed by a back-facet photodiode (see Fig. 2) to close the control loop as shown in Fig. 7. Because of the wide variations of laser diode curves and back-facet diode responsivities, a gain adjustment amplifier was implemented. To provide attenuation of the laser output power, the nominal value is produced by a DAC programmed by the mainframe. The attenuation can be set

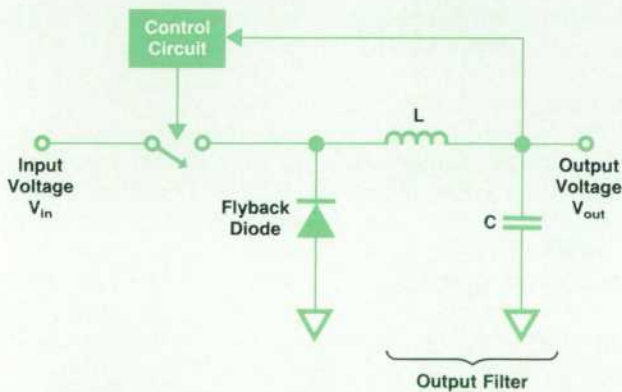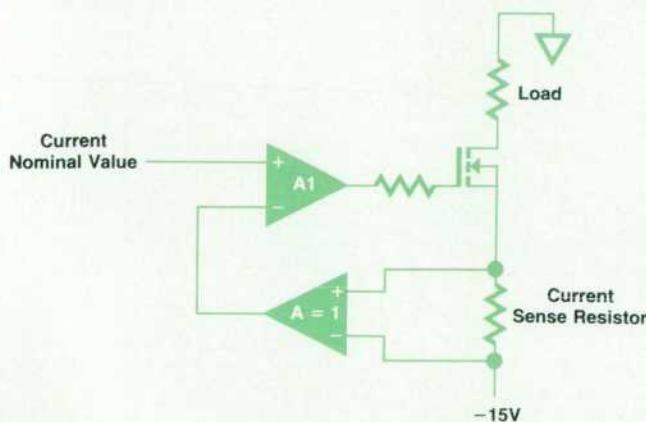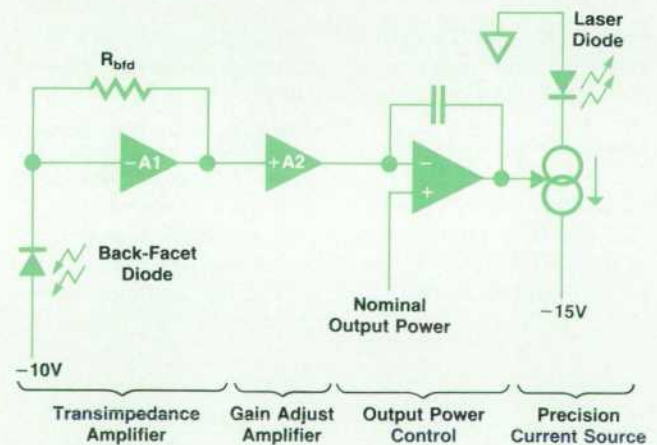**Fig. 5.** Positive dc-to-dc buck converter.

Fig. 7. Laser output power control.

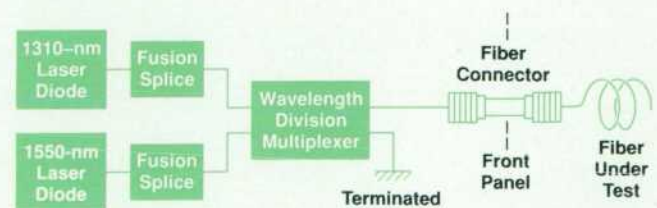**Fig. 6.** Precision current source.

Fig. 8. In the dual source module, a wavelength division multiplexer switches the two wavelengths to one optical output.

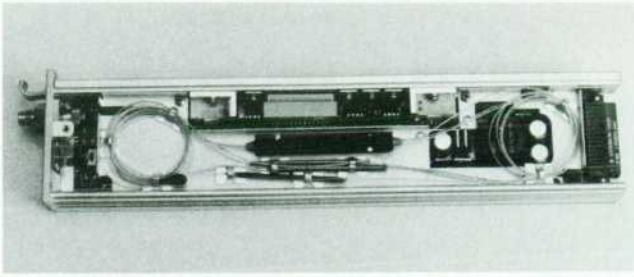**Fig. 9.** *Dual source module.*
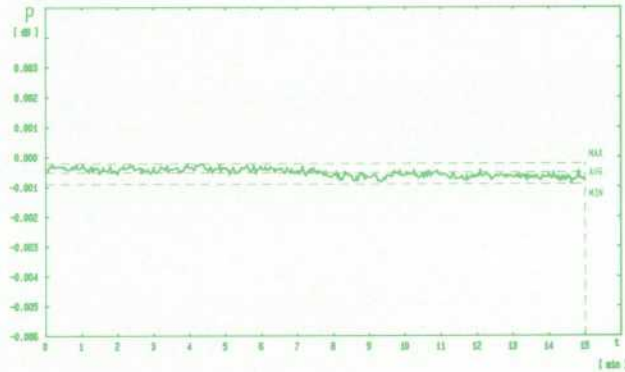
Fig. 10. *Fifteen-minute measurement at constant temperature with a 1310-nm single source (HP 81552SM). The total deviation is less than 0.001 dB.*

Fig. 11. *Six-hour measurement with varying temperature. The total variation is 0.0267 dB.*

from 0 dB to 6 dB in 0.1-dB steps. The necessary DAC value is taken from a table that stores calibration data on the laser and monitor diode curves.

Safety Circuit

It is required by law to guarantee that under single-fault conditions the laser source can't exceed its maximum permitted output power level. (These levels are also defined by law). The safety circuit in the laser source plug-ins (see Fig. 3) supervises both the laser drive current and the monitor diode current. If either exceeds its permitted value the laser is disabled and a message is sent to the mainframe microprocessor.

Dual Laser Source Module

For the HP 81554SM dual laser source, most of the electronic circuitry is simply duplicated, with the exception of the dc-to-dc converter and the device bus interface. To combine both wavelengths at one optical output, a wavelength dependent multiplexer is used (see Fig. 8). Fig. 9 shows a photograph of a dual laser source module.

Results

Fig. 10 and 11 show two different measurements made with a 1310-nm single source (HP 81552SM). Fig. 10 is a short-term measurement—15 minutes at constant temperature. The total deviation is below 0.001 dB. Fig. 11 shows a long-term measurement. During a six-hour period the temperature varied from 25°C to 27°C, then cycled twice between 27°C and 23°C, and ended at 21°C. The total deviation was 0.0267 dB, corresponding to a temperature coefficient of the laser output power of about 0.005 dB/K.

Lightwave Multimeter Firmware Design

Flexibility and modularity were challenges in the firmware development of the HP 8153A lightwave multimeter. Built-in applications software automates many commonly needed measurements.

by Wilfried Pless, Michael Pott, and Robert Jahn

MODULARITY ALLOWS AN INSTRUMENT to be tailored to the customer's needs, and is a major feature of the HP 8153A lightwave multimeter. Modularity can be thought of as design for the future. The HP 8153A mainframe is built to accept not only the power sensor and source modules that exist today, but also modules that will be built to meet tomorrow's needs.

If life were easy for the software engineer, a modular instrument would have a disc drive so that updates required by new modules could be installed easily, or at least would have EEPROMs so the software could be upgraded without the need to change ROMs. Unfortunately, size and price were issues for the HP 8153A and so neither of these options is available. Therefore, the software had to be designed to meet the needs of all possible combinations of sources and power sensors, including local and remote control of future modules.

This article will outline some of the measures undertaken to fulfill these needs for flexible and modular software. It will also describe an additional feature of the HP 8153A: the built-in application software. This application software allows the customer to perform the most frequently needed measurements without a controller and without writing any code.

Objectives and Constraints

The requirement that the software handle all present and future configurations was interpreted to mean that the customer must not be forced to set up the software in any way, either with a new set of EPROMs or by means of something like a setup menu, to work with the instrument either locally or remotely via the HP-IB (IEEE 488, IEC 625).

It was clear that the new instrument should use the new industry-standard HP-IB system language (called SCPI, Standard Commands for Programmable Instruments). However, we also wanted to offer compatibility in HP-IB programming with the language of the predecessor of the power meter modules, the HP 8152A, since we knew that customers had large investments in ATE software for that instrument. To help them preserve these investments, an HP 8152A compatibility mode was required.

In the research and development of fiber optic components and instruments, certain measurements, such as stability and loss measurements, are needed constantly. To help users automate these measurements without the need for either extensive HP-IB programming knowledge or an extra controller, it was decided to implement many commonly used applications in the firmware of the HP 8153A. One of the applications is the ability to print or plot data taken by another application.
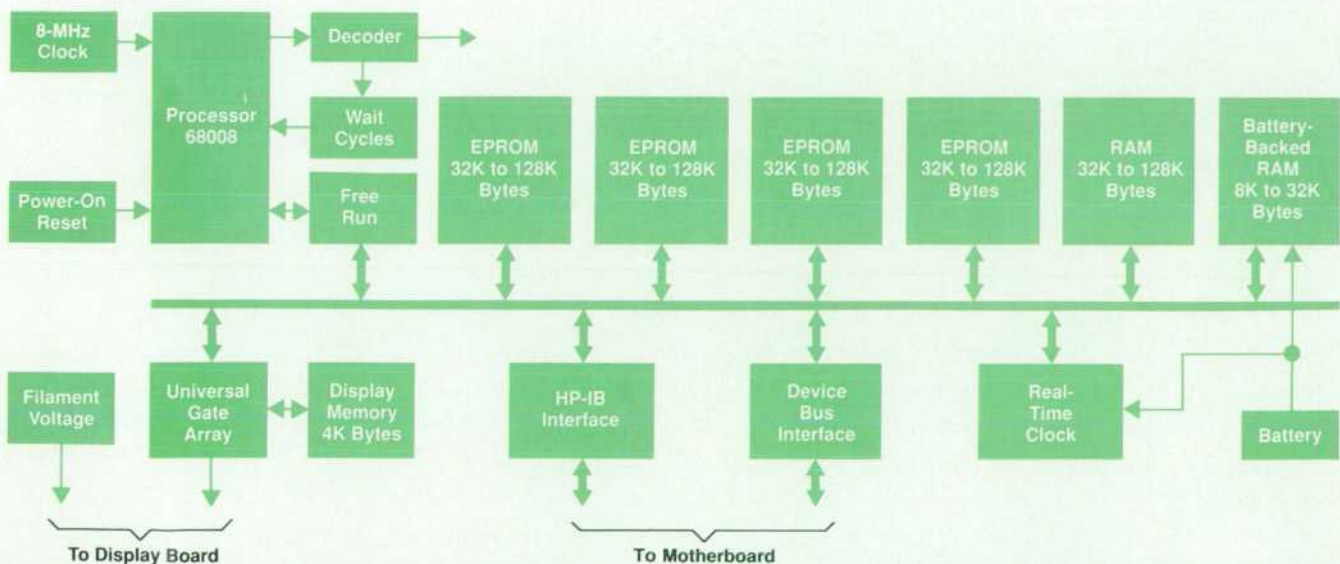
Fig. 1. *Block diagram of the microprocessor system of the HP 8153A lightwave multimeter.*
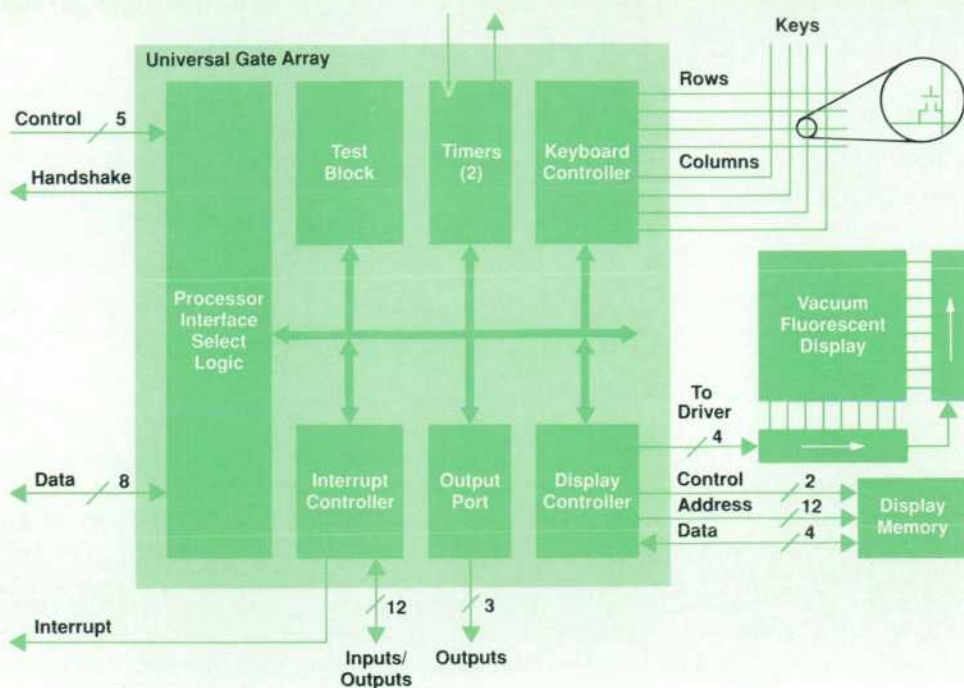
Fig. 2. Block diagram of the universal gate array for servicing the keyboard, display, and interrupts.

Hardware Platform

Fig. 1 is a block diagram of the microprocessor system of the HP 8153A mainframe. The system consists of a 68008 microprocessor, RAM and ROM, an HP-IB interface, a real-time clock, a device bus interface, a universal gate array for servicing the keyboard, interrupts, and the vacuum fluorescent display, and some miscellaneous logic.

The universal gate array helps reduce the size and cost of the microprocessor board. Fig. 2 shows the block diagram of this gate array. It contains a keyboard interface for servicing up to 32 keys, an interface for connecting a custom-designed vacuum fluorescent display and the associated display memory, free programmable lines that can be used as inputs and outputs, and two timers.

The mainframe communicates with the modules by way of digital interfaces. Fig. 3 shows the block diagram of a digital module interface. Via the device bus, the mainframe can read module-specific data out of the module's EEPROM, such as the module identifier, calibration data, and the number of the driver for downloading software. The EPROM contains the data and module-specific functions that are required to perform measurements and handle the local or remote operation of the module.

Software Platform

Fig. 4 shows the general structure of the HP 8153A software. The kernel of the software is pSOS-68K,* an operating system for embedded real-time system development. With pSOS, the problem of acting upon multiple asynchronous cyclic or noncyclic events is solved by multitasking capabilities.

Development time was saved by using an existing HP driver called the SCPI driver to handle all of the low-level HP-IB transactions. Using this software saved the time it would have taken to develop such things as communication protocols or a parser ourselves.

The software was developed on a local HP 9000 network. For debugging and testing, HP 64000 emulators were employed. Almost all of the code was written in C, except for a few low-level drivers, which were written in assembly language.

Instrument Data Base

The instrument data base shown in Fig. 4 contains the complete instrument setting and saves things like measurement values, physical parameters, and state variables. A well-defined interface (set of management functions) protects the data from direct access by other functions.

An important aspect of the data base is a set of dynamic data structures that hold the intrument configuration and change with different module configurations. Examples of the types of information stored in these structures are:
- Multilevel matrixes of function pointers for the keyboard layout
- Lists of possible (editable) input parameters with their characteristics, such as valid range, legal units, and

Fig. 3. Block diagram of the digital interface between a module and the mainframe.

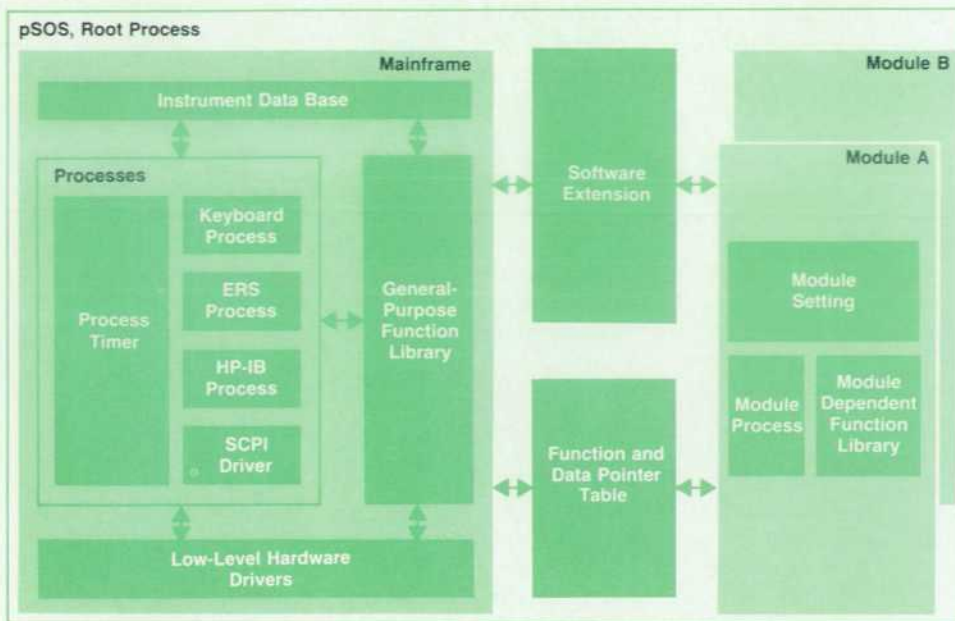* pSOS-68K is a trademark of Software Components Group, Inc.

Fig. 4. General software structure of the HP 8153A lightwave multimeter.

allowed edit actions
- Lists of legal HP-IB commands together with structures for future modules
- Lists of possible applications with complete execution environments (select application, edit parameter, start, show, interface for HP-IB, etc.).

Low-Level Hardware Drivers

The low-level hardware drivers make up the lowest software level. This level provides functions for accessing the instrument hardware (device bus, real-time clock, gate array, etc.). The main tasks are reading the keyboard, displaying data, and dispatching interrupts.

General-Purpose Function Library

In the general-purpose function library are some higher-level routines, including functions for converting values (e.g., from watts to dBm), functions for editing numbers, and functions for checking purposes (date, time, etc.).

Instrument Processes

The instrument processes are the heart of the software. Each process works on a well-defined, separate instrument task and communicates with the other processes via mailboxes or events.

The timer process is stimulated on every system clock tick and handles a set of software timers. It supplies the other processes with definable timers (timing rate, single, or continuous).

The keyboard process reacts to every key press. It resolves ambiguity, realizes vernier functions, and transforms the physical key information into a logical information structure for the ERS process.

ERS stands for external reference specification. The ERS process determines the presentation of instrument information to the user and reacts to key presses by executing the desired instrument functions.

The HP-IB process has nearly the same jobs as the ERS

process. It handles remote communication with the instrument by interpreting commands, reacting to them, and returning a response.

Mainframe-Module Software Interface

Ideally, the mainframe software and the module software would be as independent as possible. In the HP 8153A, because of the modules' limited ROM space, mainframe library functions and some basic mainframe functions have to be shared with the module software. Some data structures are also shared.

To get position independence, jumps (JMP) to commonly used mainframe functions and pointers to mainframe-resident data structures are put into a function table at a fixed location in the mainframe ROM. The modules can call the functions mentioned in this function table no matter where the code resides in the mainframe ROM. With this table,
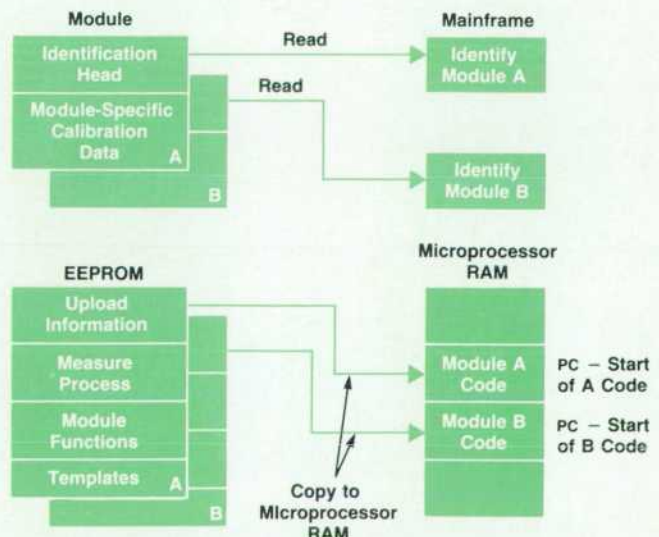

Fig. 5. Uploading module software to the mainframe.

the mainframe software and the module software can be linked independently, while all references to library functions are satisfied.

Because the number of pins on the motherboard connector is limited, the module EEPROM and EPROM couldn't be memory mapped into the address space of the mainframe microprocessor system. Another, more important reason for not memory mapping is to prevent address and data bus activities from interfering with subsystems outside the microprocessor board. Because the ROMs are not memory mapped, the contents of both ROMs need to be uploaded into dynamically allocated RAM on the mainframe microprocessor. As a result, the module software has to be PC-relative (PC = program counter), while accesses to mainframe functions and data are made by absolute addressing via the function table. Fig. 5 illustrates the process of uploading, and Fig. 6 illustrates how the module software accesses mainframe functions.

In the example shown in Fig. 6, the module needs to be able to compute the logarithm of a linear variable. Because of limited space, this function could not be resident in the module's ROM. The mainframe software includes a template—the mainframe function table—which is located at a fixed address and contains only JMPs to mainframe functions. The counterpart in the module software is a template consisting of an XDEF and a JMP dummy statement. This module template gets linked at the same address as the mainframe template, and calls to the functions in it are in absolute mode. Assuming that the mainframe template contains a JMP to the function log at address 300H, the module template will be linked at this address. When the module's software is uploaded to the mainframe, a call to the function log in the module code will cause the mainframe function to be executed.
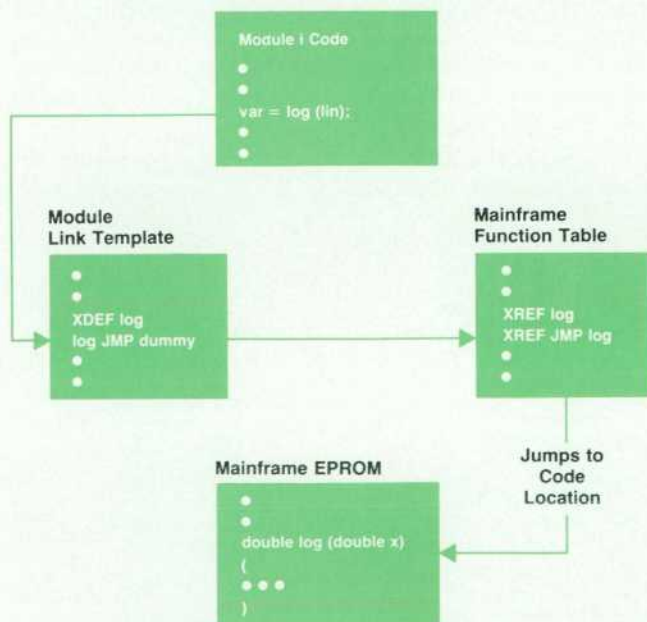

Fig. 6. *The module software accesses mainframe functions through a function table stored at a fixed location in the mainframe ROM.*

Expandability

The challenging objective in the design of the multimeter was the requirement that the firmware be expandable for local and remote control just by means of the module EPROM. The solution to this problem for the local software will be explained using a hypothetical future module, as an example. We will assume that this module has three parameters: calibration factor, reference factor, and speed.

At the time the software was released, there were modules that needed the following parameters:

- T_{avg} (the time constant of the averaging filter)
- Calibration factor
- Reference factor
- Wavelength (continuous entry for a power meter or discrete for the dual-wavelength source)
- Modulation
- Attenuation.

Entry functions for these parameters are part of the mainframe firmware. A power meter module needs only four of these entry functions as input parameters. Which of the entry functions offered by the mainframe are needed by a module and the order in which they will appear on the screen can easily be determined by the use of array indexes to entry function pointer arrays for the various parameters:

Pointers to Entry Functions for Parameters	Associated Indexes
T_{avg}	0
Calibration Factor	1
Reference Factor	2
Wavelength (Power Meter)	3
Wavelength (Double Source)	4
Modulation	5
Attenuation	6

An array with the values {3, 1, 0, 2} in the parameter template of the module means that the module has four input parameters: wavelength, calibration factor, T_{avg}, and reference factor, in that order. If an index greater than 6 appears in the module's parameter template, the mainframe software knows that the associated entry function must reside in the module and accesses this function by using a pointer to it that is found in the module's parameter item structure.

The expandability is implemented using a data type defined in C. Each module has a variable parameter of type item. The data type item is not only used for parameters, but the comments below apply to the variable parameter.

```
typedef struct
{  int8   act_item;           /* Index of the selected element of the   */
                              /* parameter array.                       */
   int8   nmb_of_items;       /* Total number of parameters.            */
   int8   *item_list;         /* Pointer to the array of parameter      */
                              /* indexes.                               */
   int8   last_int_index;     /* Index of last mainframe parameter.     */
                              /* It's 6 in this example.                */
```

```
ret_code (**int_fct)();      /* Pointer to the array of internal    */
                             /* parameter entry functions.          */
ret_code (**ext_fct)();      /* Pointer to the array of external    */
                             /* parameter entry functions.          */
} item;
```

During software initialization, the elements of this data structure for the module's variable parameter will be initialized by the ERS process and the module software. For the hypothetical module, there is an array of parameter indexes with the values {1, 2, 7}, corresponding to the parameters calibration factor, reference factor, and speed. For this module, the parameter variable of type item will be initialized as listed below:

```
i | parameter.act_item      = 0; /* Always start with first    */
                                 /* element.                   */
e | parameter.nmb_of_items  = 3; /* There are three items      */
                                 /* to select.                 */
e | parameter.item_list      = parameter_index_array;
                                 /* Start address of           */
                                 /* parameter index array.     */
i | parameter.last_int_index = 6;
i | parameter.int_fct        =  internal_parameter_function_array;
e | parameter.ext_fct        =  external_parameter_function_array;
```

The i means that the structure elements are initialized during boot-up by the mainframe software (ERS process). The e refers to initialization that is done by the module software.
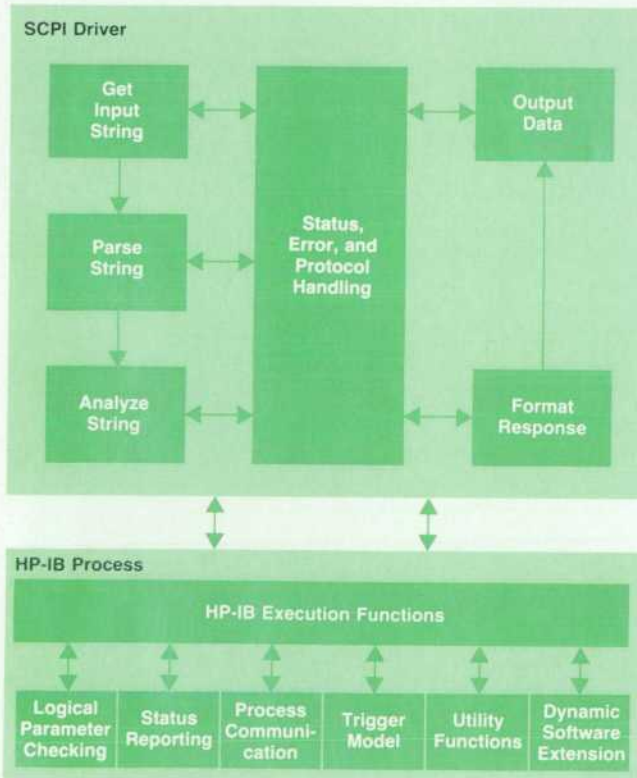

Fig. 7. *The HP-IB firmware in the HP 8153A combines the existing SCPI driver with instrument-specific execution routines.*

With the knowledge of these elements, the mainframe software can access mainframe-resident parameters as well as module-resident parameter entry functions.

SCPI Driver

Fig. 7 shows the parts of the HP-IB software that are implemented using the SCPI driver software. If an HP-IB interrupt is encountered, the driver software reads in the data from the HP-IB (always keeping track of the correct protocol mechanisms). The data is parsed and divided into its functional parts (program message header, parameter, etc.). All parsed message elements are analyzed to check whether the command exists and whether the parameters are all correct. If an is error found at any stage, it is reported. Otherwise, the corresponding execution function is called. The execution functions are run-time modules that had to be realized by the software team. The other work described so far is done by the SCPI driver software.

The execution functions take care of all command-specific tasks, such as logical parameter checking, communicating with other processes, and so on. In the case of a query, the response is returned to the SCPI driver, which formats it and outputs the formatted data. Fig 8 shows the process of realizing a simple command tree using the SCPI
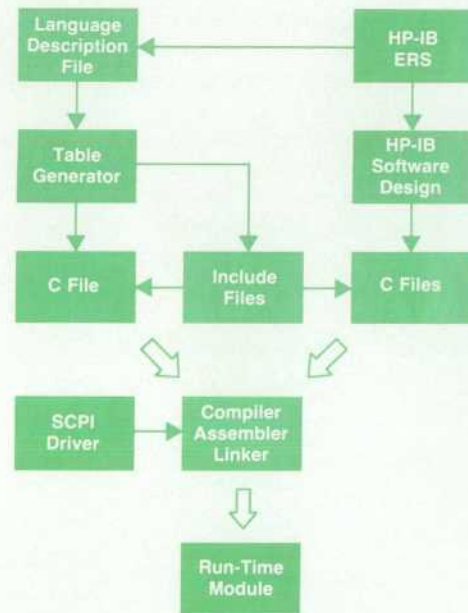
Example for a (very) small language description file:

```
HIERARCHY language
[
 SYSTem
  [
   DATE
    date_cmd()  in: int16, int16, int15
    date_qry()  out: int16 NR1, int16 NR1, int16 NR1;
  ]
]
```

Only the functions date_cmd() and date_qry() need to be realized by the software designer. The rest is done by the driver software. For example, date_cmd() is called when SYST:DATE 1990,1,1 is received.

Fig. 8. *Realizing a simple command tree using the SCPI driver and a language table generator.*

driver and a language table generator.

Although the SCPI driver already existed, there were some problems to solve. The HP 8153A had to be HP-IB compatible with the HP 8152A lightwave power meter. However, the syntax of the HP 8152A commands does not follow the IEEE 488.2 standard. Therefore, we had to modify the parser and the lexical analyzer of the driver software. Another problem was the lack of facilities for extending the language command tree at run time. How this was solved is described next.

HP-IB Run-Time Command Extension

The SCPI driver software supplied no facilities for extending the command table at run time. This difficulty was overcome by the use of the macro facility. A macro facility allows the customer to define a custom language tree by simply giving commands or sets of commands new names. For example, if the customer often wants to program the wavelength with

SENSE:POWER:WAVELENGTH x,

where x is the wavelength, but thinks this is too long to input repeatedly, a macro can be defined by inputting the following sequence once:

*DMC "W",#25SENSE:POWER:WAVELENGTH $1

Thereafter, only W x need be input to program the wavelength.

This feature is not implemented in the HP 8153A, but it is supported by the driver software and is used to solve the problem of dynamic command extension at run time.

For this purpose, every module available for the HP 8153A contains a data table that contains all of the informa-
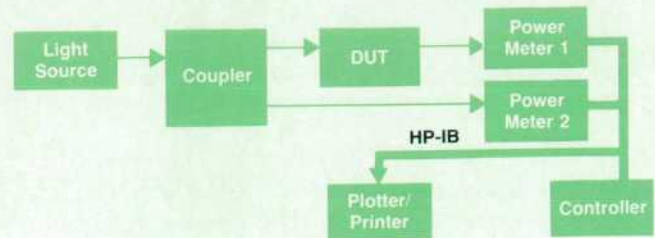
Fig. 10. *Conventional A/B stability measurement.*

tion needed for commands that are not implemented in the mainframe software. For the first general module types, all the commands are implemented in the mainframe software, so the corresponding tables are empty. Parts of this software (for sources and sensors) may later be used by new modules.

The basis for command extension is the following information, which fully characterizes a new command:

- The command name
- The number of parameters the command takes
- The types of parameters and their sequence
- The address of an accompanying execution function
- Whether the command has a response (e.g., a query).

This information is analyzed at boot-up and a command synthesizer is called, which builds the necessary macros after allocating memory for the new command set. To use the macro facility, the parser input is redirected to these synthesized macros. This procedure is repeated for every new command. When it is complete, the new commands are known by the instrument.

For defining macros, all parameters used in them must be known. Therefore, the mainframe software contains functions for passing all important input parameter types and for calling all important response formatter routines.
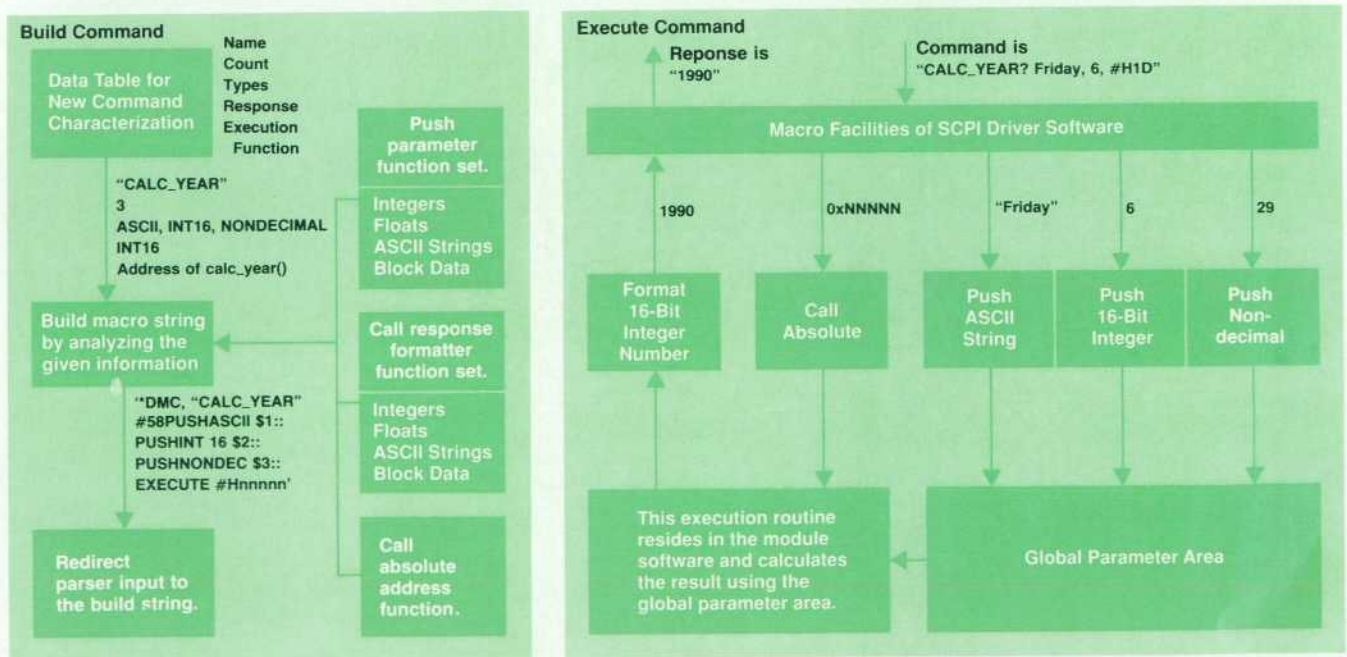
Fig. 9. *An example of building and executing a new HP-IB command.*

The execution routine for a new command is implemented in the module software. The mainframe software only needs to know its address.

The simplified procedures for building commands and executing them are shown in Fig. 9 using a simple example. This example is not worth implementing, but it shows the various aspects of command extension. The new command expects three parameters: a day of the week parameter as an ASCII string, a month of the year parameter as a decimal value, and a day of the month parameter as a nondecimal value. The response is an integer number (16-bit), which gives the latest year this condition was met.

Besides dynamic command extension at run time, the complete HP-IB environment is configured at boot-up by analyzing various information from the module data:

- Module dependent status reporting
- Configurable reset vectors
- Module dependent compatibility language mode
- Module-based application handling.

Applications Software

During the development of HP's fiber optic family of instruments and components, there was always the need for automated measurements to determine stability, power-versus-current characteristics, loss, loss-versus-time characteristics, polarization dependency, and more. We knew from our customers that these measurements are made very frequently by them, too. To eliminate the need for programming computers or knowing HP-IB commands, application programs for the most commonly used applications are built into the HP 8153A. Again, the ability to expand for future applications is taken into account in the design of the application software.

Fig. 10 shows a conventional setup for an A/B stability measurement. This kind of measurement is used to monitor the behavior of a device over time. Two power meters are needed to measure the reference and device outputs. A computer reads the results from the two power meters, calculates the ratio, and plots the results. A significant amount of programming effort is required.

Fig. 11 shows the setup for a stability measurement using the HP 8153A. To set up this application, the user only has to edit its parameters. In this case, the only parameter is the duration of the measurement, which can be up to almost 100 hours. The user can also set the application to start plotting or printing automatically when the measurements are finished. An application can be started with the
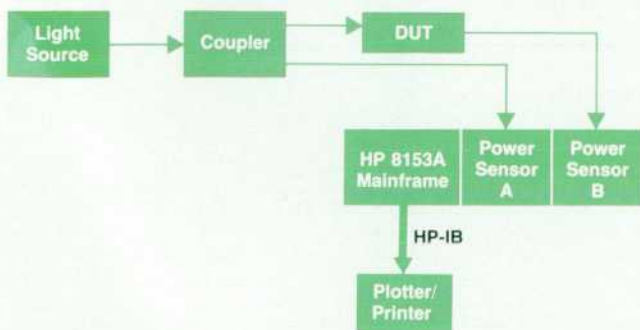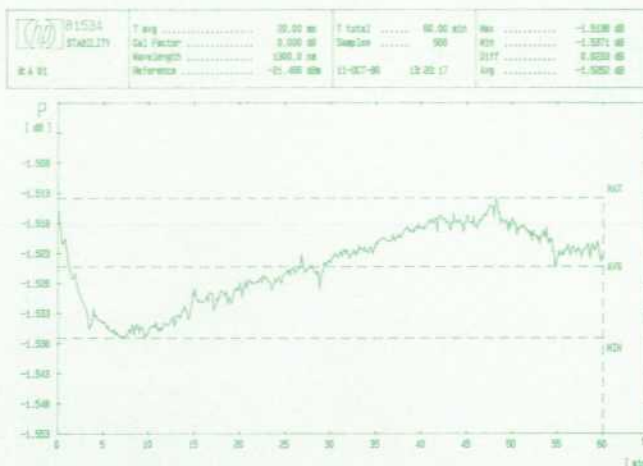
Fig. 12. *Plot showing the results of an HP 8153A A/B stability measurement, produced without programming.*

EXEC key and stopped by pressing **EXEC** again. To pause an application, the **PAUSE** key is provided; pressing it again causes the application to continue.

Fig. 12 shows a plot from such a measurement. It was drawn with the autoscaling feature activated. The user gets this plot without having written a line of code.

Another useful application is the logging application, which in the automatic mode stores up to 500 successive measurement values and can be used, for example, to measure and plot laser diode power as a function of current. The manual logging application can be used as a scratchpad memory for up to 500 measurement values. It is useful for storing data on temperature dependence, connector repeatability, polarization dependence, effects of bending radius, and so on. Documentation of the data can be done by a plotter or a printer.

Very often in optics one has to adjust optical components. The align application helps the user find a power maximum or check specifications by means of a large bar graph and acoustical feedback. Another use of the align application is in incoming inspection, where the objective is to find out quickly if the output power or the loss of a batch of components is within given limits.

Acknowledgments

Fig. 11. *HP 8153A A/B stability measurement.*

Authors

Columbia University in 1968. He is a member of the IEEE and the National Society of Professional Engineers. He has authored or coauthored a number of technical papers and articles on microwave transistor modeling, microwave amplifier design, and high-speed lightwave measurements. Two patents and four pending patents have resulted from his work. Roger was born in Honolulu, Hawaii, is married, has a son, and lives in Santa Rosa, California. His interests include gardening, swimming, cooking, and baking bread.

Paul R. Hernday

Paul Hernday is an R&D project manager at HP's Network Measurements Division. With HP since 1969, he has been involved in the development of sweepers, scalar and vector network analyzers, lightwave component analyzers, and a dual-laser heterodyne system for the calibration of lightwave receivers. Most recently he was project manager for the HP 8703A 20-GHz lightwave component analyzer. Two patents are pending as a result of his work on that project. Paul received his BSEE degree from the University of Wisconsin in 1968. Born in San Pedro, California, he now lives in Santa Rosa. He is married, has two children, and enjoys boardsailing, reading, and travel.

13 ══ 20-GHz Lightwave Component Analyzer

Michael G. Hart

Development engineer Mike Hart has worked on firmware development for the HP 8703A and HP 8702A lightwave component analyzers and the HP 8753A network analyzer. His work has resulted in two patents on HP 8702A technology. He attended Utah State University, earning his BSEE degree in 1983, and received a Master of Engineering degree from Cornell University in 1984. He joined HP's Network Measurements Division that same year. He is a member of the IEEE. Born in Sacramento, California, Mike is married and lives in Windsor, California. He plays piano and organ and enjoys travel.

Rollin F. Rawson

A development engineer with HP's Network Measurements Division, Fred Rawson has been with HP since 1960. Among the many products to which he has contributed are the HP 8753A and 8754A network analyzers, the HP 8756A scalar network analyzer,

6 ══ 20-GHz Lightwave Component Analysis ══

Daniel R. Harkins

Author's biography appears elsewhere in this section.

Roger W. Wong

R&D section manager Roger Wong had overall responsibility for development of the 20-GHz lightwave products. Formerly, he was program manager for the HP 8702A lightwave component analyzer. With HP since 1968, he has also had design responsibility for scalar network analyzer detectors, directional bridges and accessories, and microcircuits and associated components for microwave applications. He received his BSEE degree from Oregon State University in 1966 and his MSEE degree from

and the HP 8702A lightwave component analyzer. Most recently, he had design responsibilities for the power supplies, leveling loops, thermal loop, and digital interface circuits of the HP 8703A lightwave component analyzer. Fred was born in Laguna Beach, California. He served as a staff sergeant in the U.S. Air Force for four years, then enrolled at California State University at San Jose, graduating in 1961 with a BSEE degree. He is married and has four children and two grandchildren. A resident of Santa Rosa, California, he collects and refurbishes Studebaker automobiles and collects U.S. stamps.

Paul R. Hernday

Author's biography appears elsewhere in this section.

Geraldine A. Conrad

A development engineer with HP's Network Measurements Division, Gerry Conrad contributed to the design of the optical modulator and optical receiver microcircuits of the HP 8703A lightwave component analyzer and was involved in evaluation of the optical system. Previously, she worked on measurement accuracy and system performance analysis for the HP 8702A lightwave component analyzer, on verification and system evaluation for the HP 8753A network analyzer, and as a marketing engineer for sweep oscillators. Gerry originally joined HP as a summer intern in 1980, then accepted a permanent position two years later, after receiving her BSEE degree from the University of Florida. She has authored or coauthored four papers on lightwave and RF network analyzer topics, and is a member of the IEEE. Born in Trincomalee, Sri Lanka, Gerry is married, has a son, and lives in Santa Rosa, California. Her leisure interests include travel, cooking, camping, and quilting.

23 ══ 20-GHz Lightwave Test Set ══

Joel P. Dunsmore

As technical lead on the design of the system block diagram for the HP 83420A lightwave test set, Joel Dunsmore worked on the microwave circuit implementation and electrical design for the lightwave test set and accessories. Before joining HP in 1983 as a full-time R&D engineer, Joel worked as a summer intern at HP's Network Measurements Division during the summers of 1980 to 1982. He received his BSEE (1982) and MSEE (1983) degrees from Oregon State University. His other work at HP includes RF microcircuit design for the HP 8753 and

HP 8752 network analyzers and hardware design for the HP 85047 6-GHz test set. Joel's work has resulted in one patent and one pending patent on RF components, and he has authored a paper on RF measurement techniques. His professional interests include broadband RF components and systems. Joel was born in The Dalles, Oregon and currently resides in Sebastopol, California. He is married, has one son, and is expecting a new arrival soon. Leisure activities for Joel include woodworking, home remodeling, writing technical articles, Oakland A's baseball, and homebrewing beer.

John V. Vallelunga

A product support engineer at HP's Network Measurements Division, John Vallelunga joined HP in 1975. As a support engineer, he has worked on the HP 8350 series sweepers, most scalar products such as the HP 8757A scalar network analyzer, and many other products. He also served as a software engineer for the HP 83420A lightwave test set, working on all aspects of the software, particularly the user interface and interpolation routines. He studied engineering at San Francisco State University (1969-1973) and the University of California at Davis (1973-1974), and completed a diploma in electronic engineering technology from Healds Engineering College in 1975. John was born in San Francisco, California and currently resides with his three children in Santa Rosa, Calif. Besides his children, John's outside interests include camping, exploring, astronomy, and cooking.

34 ══ Lightwave Accuracy Considerations ══

Daniel R. Harkins

Dan Harkins is currently an R&D section manager for commercial network analyzers at HP's Network Measurements Division. Previously he was project manager for the HP 83420A lightwave test set and accessories. Dan joined HP in 1969 after receiving a BSEE that same year from Seattle University. He also holds an MSEE (1971) from Stanford University. In the past he was a project manager for the HP 8505 RF network analyzer, program manager for the HP 8757C scalar network analyzer, and section manager for the HP 3326A two-channel synthesizer and HP 3577A network analyzer. His work has resulted in a patent on lightwave components. He has authored papers for the HP Journal, the Microwave Journal, and the HP RF, Microwave, and Lightwave Symposium. His professional interests include RF design, network analysis, and communication theory. Dan was born in Snohomish, Washington and now lives with his wife and three children in Santa Rosa, California. His off-hours activities include coaching soccer, playing tennis, and bicycling.

Michael A. Heinzelman

Manufacturing development engineer Mike Heinzelman functioned as a new product introduction engineer for the HP 8703A lightwave component analyzer. Mike joined HP in 1976 after receiving a BSEE from the University of Wisconsin in 1975. In the past, he has been a production engineering supervisor, a new product introduction engineer for other HP lightwave products, and a production engineer for microwave spectrum analyzers. Mike is a member of the St. Vincent DePaul Society and a former director of the Sonoma County drug abuse council. He was born in Waukesha, Wisconsin and now lives in Santa Rosa, California. He is married, has six children and one grandchild, and has a foreign exchange student living at his house. Leisure activities for Mike include bowling, bridge, and playing bass guitar in a country band and a junior college jazz band.

41 ══ Optical Modulator ══

David J. McQuate

With HP since 1978, Dave McQuate was responsible for the development of the fiber pigtailing process and equipment, modulator modeling, and environmental and reliability tests for the optical isolator used in the HP 8703A lightwave component analyzer. He is currently working on a wide-bandwidth photoreceiver. Dave received his BS degree in physics in 1970 from Ohio University, and MS and PhD degrees in physics from the University of Colorado. His past assignments at HP include the design of microwave circuits and a microprocessor controller for a microwave spectrum analyzer, and the characterization and modeling of GaAS MESFETs. Dave was born in Bloomington, Indiana, and currently resides in Santa Rosa, California with his wife and two children. His outside interests include cross-country skiing, backpacking, bicycling, computer-controlled music synthesis, and gardening.

Roger L. Jungerman

Roger Jungerman's special interests are fiber optics, integrated optics, and acoustics. He contributed to the development of the high-speed optical modulator for the HP 8703A lightwave component analyzer. He received a BA degree in physics in 1978 from the University of California at Santa Cruz and an MS degree in applied physics from Stanford University. After receiving his PhD degree in applied physics from Stanford University in 1985, Roger joined HP's Microwave Technology Division. One of his initial assignments at HP was developing surface acoustic wave devices. His current responsibilities include developing laser sources for fiber optics and supporting production of the optical modulator. Roger was a member of the technical staff at Watkins-Johnson Company in Scotts Valley, California where he worked on thin-film coating development. He is the author of 20 technical journal articles and 20 conference papers on fiber optics, optical modulators, microscopy, and microwave acoustics. His work has resulted in two patents, one on an optical modulator and the other on a scanning optical microscope. He is a member of the IEEE, the SPIE, and the Optical Society of America. Roger was born in Sacramento, California and now resides with his wife in Petaluma, California. He enjoys bicycling and hiking.

45 ══ Optical Isolator ══

Kok-Wai Chang

After coming to HP in 1984, Kok-Wai Chang worked on the development of a magnetostatic-wave device for microwave signal processing. In his most recent assignment he worked on the optical isolator and the fiber-optic measurement system for the HP 8703A lightwave component analyzer. Before joining HP, Kok-Wai was a postdoctoral research associate at the University of Texas at Arlington. He earned a BSc degree in physics from the National Chung King University and a certificate of postgraduate study in physics from Cambridge University in 1978. He continued his education at Texas Christian University, receiving a PhD in physics in 1982. KoK-Wai has published several articles on magnetostatic-wave devices, molecular spectroscopy, optical isolators, and optical-fiber measurements. He is an inventor on five patents for magnetostatic-wave devices. Kok-Wai was born in Hong Kong and he now lives in Sunnyvale, California with his wife and two sons. He is an avid baseball fan, particularly of the Oakland A's.

Siegmar Schmidt

With HP since 1974, Siegmar Schmidt has a degree in physics from the Friedrich Schiller University at Jena. He's an optics specialist and worked in that field before coming to HP. He has contributed to the development of the HP 81210LI and HP 81310LI optical isolators, the HP 8158A/B optical attenuators, and the HP 81000AS/BS optical power splitters. Born in Jena, Thüringen, Siegmar is married, has two sons, and lives in Wildberg in the Black Forest region. His hobbies include fishing, boardsailing, and swimming.

Wayne V. Sorin

Wayne Sorin joined HP Laboratories in 1985 and has been developing new fiber optic measurement techniques and instrumentation. He contributed some of the initial concepts for the HP optical isolator. Previously, he contributed to the idea for the gated self-homodyne technique used in the HP 11980A fiber optic interferometer. His work has resulted in six patents on fiber optic components. He is a member of the IEEE and the Optical Society of America, and has authored 17 technical papers on fiber optic components and lasers. He teaches a fiber optics course at the California State University at San Jose. Born in New Westminster, British Columbia, Wayne earned a BS degree in physics in 1978 and a BS degree in electrical engineering in 1980 from the University of British Columbia, and MSEE and PhD degrees in 1982 and 1986 from Stanford University. At Stanford, he studied evanescent interactions in single-mode optical fibers. Married and the father of a son, he enjoys playing tennis and soccer in his hometown of Mountain View, California.

Jimmie L. Yarnell

Born in Klamath Falls, Oregon, Jimmie Yarnell worked as a product designer for the HP 8703A lightwave component analyzer. A graduate of Santa Rosa Junior College, Jimmie joined HP's Santa Rosa Division (now called Network Measurements Division) in 1973 when the division was still housed in temporary buildings. Jimmie has also worked as a product designer for the HP 11970 millimeter mixers and the HP 70810A lightwave receiver. Before joining HP, he worked for eight years at an optical coating laboratory. Jimmie is single and lives with his adopted son in Santa Rosa, California. His hobbies include gourmet cooking, collecting old cookbooks, pen-and-ink drawings of eggs, collecting fossil ivory artifacts, and restoring a 1941 Buick sedan.

Harry Chou

As an R&D engineer in the lightwave technology section of HP's Network Measurements Division, Harry Chou is responsible for the design and development of optoelectronic instruments and for the testing and characterization of fiber-optic systems. He carried out these responsibilities in the development of the HP 8703A lightwave component analyzer. Harry joined HP in 1989 after receiving his PhD from Massachusetts Institute of Technology that same year.

His PhD dissertation research was on spectroscopic studies of the properties of solid-state laser materials and modeling of laser behavior. He also received his BSEE (1981) and MSEE (1983) from Massachusetts Institute of Technology. His prior industry experience was at Codenoll Technology Corporation where he worked on the development of semiconductor light sources. Harry is the author or coauthor of five papers in the area of optically pumped solid-state lasers and wavelength stabilization of semiconductor light sources. His outside interests include cycling, sailing, and skating.

Steven A. Newton

As a project manager at HP Laboratories, Steve Newton managed the early development of the HP optical isolator and coordinated the transfer of this technology to two HP divisions. Previously, he directed the HP Laboratories contributions to the design of the HP 8145A optical time-domain reflectometer and helped conceive that instrument's signal processing system. Born in Teaneck, New Jersey, he received a BS degree in physics from the University of Massachusetts in 1976, and MS and PhD degrees in applied physics from Stanford University in 1978 and 1983. He came to HP on a part-time basis in 1978 and worked on optical design, optical data storage, and metal vapor lasers. Since joining HP Laboratories full-time in 1983, he has done research on single-mode fiber optic components, circuits, and measurement systems. He is now project manager of the fiber optics team in the Instruments and Photonics Laboratory. He is named inventor or coinventor on nine patents and has authored or coauthored 40 papers and articles. Steve and his wife live in Belmont, California. His outside interests include sports and music.

51 ══ Lightwave Converter ══════════

Christopher M. Miller

As a project manager for the past six years at HP's Signal Analysis Division, Chris Miller was responsible for development of the HP 11982A lightwave converter and the HP 83810A and HP 71400A lightwave signal analyzers. Before that, he was the project manager for the HP 71300A millimeter-wave spectrum analyzer. Earlier, he was with HP Laboratories, where he designed high-speed bipolar and GaAs integrated circuits. He came to HP in 1979 from Hughes Aircraft Company, where he designed electronic systems for laser target designators and cryogenic coolers for infrared sensors. He has coauthored papers on a high-speed photoreceiver and laser noise measurements and has written several symposium papers on RF and lightwave subjects. Born in Merced, California, he earned a BSEE degree in 1975 from the University of California at

Berkeley and an MSEE degree in 1978 from the University of California at Los Angeles. Married and the father of two sons, he lives in Santa Rosa, California and enjoys wine tasting, running, skiing, body surfing, and camping.

Roberto A. Collins

Roberto Collins designed the microwave preamplifier for the HP 11982A lightwave converter. He first joined HP's Signal Analysis Division in 1984 when he was a student at Cornell University. Graduating in 1986 with a BS degree in electrical engineering, he went on to earn an MEng degree in electrical engineering in 1988. He has also done digital circuit design for the HP 70810A lightwave receiver and is now doing RF and electronic circuit design for EMI instrumentation. Roberto was born in Santo Domingo, Dominican Republic. He enjoys Latin jazz, building loudspeakers and other audio gear, and dancing merengue, the music of the Dominican Republic.

58 ══ Lightwave Multimeter ══════════

Bernd Maisenbacher

Bernd Maisenbacher was project manager for the HP 8153A lightwave multimeter. He joined HP's Böblingen Instruments Division in 1981 and has been a project manager since 1986. He has contributed to the design of the HP 8112A pulse generator and various optical sources, attenuators, and power meters. His work has resulted in two patents on a variable optical attenuator and a fiber optic adjustment technique. He received his Diplom Ingenieur degree from the University of Stuttgart. Bernd was born in Pforzheim and now lives in Schömberg in the Black Forest region. He is married and enjoys tennis, skiing, stamp collecting, and hiking.

Wolfgang Reichert

Wolfgang Reichert is a mechanical designer at HP's Böblingen Instruments Division. He received his Diplom Ingenieur (FH) in mechanical engineering from the Engineering School of Esslingen and joined HP in 1982. He has done mechanical design for IC test systems, design and process engineering for fiber optic accessories, and mechanical design for the HP 8153A lightwave multimeter, serving as project leader on the HP 8153A. Born in Sindlefingen, Baden-Württemberg,

he is married, has two children, and lives in Aidlingen, Baden-Württemberg. He likes volleyball, downhill skiing, and woodworking, and is currently completing the construction of his family's home.

1981. He has coauthored several HP Journal articles and is a member of the International Society for Hybrid Microelectronics. Born in Villingen-Schwenningen, Emmerich is married, has two children, and lives in Aidlingen. His interests include woodworking, cycling, and skiing.

has also been responsible for the signal processing software of the HP 8145A optical time-domain reflectometer. Wilfried is interested in home musical recording and in the MIDI, an electronic interface for musical instruments. He is married and has five children, including a set of twins. Born in Westfalia (Haltern, Nord-Rhein-Westfalen), he lives in Grafenau, Baden-Württemberg.

63 ▭ Lightwave Power Sensors

Jochen Rivoir

Now a project manager at HP's Böblingen Instruments Division, Jochen Rivoir contributed to the design of the system architecture, power meter signal path, software, processor board, and gate arrays for the HP 8153A lightwave multimeter. With HP since 1985, he previously contributed to the design of the digital hardware of the HP 8145A optical time-domain reflectometer. He is particularly interested in system theory and has coauthored a paper on that subject. Jochen studied electronic engineering with an emphasis on system design at the University of Karlsruhe, receiving his Diplom Ingenieur degree in 1983. A resident of Magstadt, he is married and has a daughter. He is studying Japanese language and culture and sings in a choir.

Horst Schweikardt

An R&D project engineer at HP's Böblingen Instruments Division, Horst Schweikardt has been with HP since 1972. He contributed to the hardware design of the power meter modules for the HP 8153A lightwave multimeter. He has also served as a project leader for the HP 8152A optical power meter and the HP 81521B optical head, and has headed project teams for the HP 214B pulse generator and other products. He received his Diplom Ingenieur in electrical engineering from the University of Stuttgart in 1972. A native of Schwäbisch Gmünd, Baden-Württemberg, he is married, has two children, and lives in Gültstein, Baden-Württemberg. His hobbies include photography, mountaineering, and bowling.

Emmerich Müller

With HP since 1981, Emmerich Müller has designed fiber optic connectors and interfaces and contributed to the design of the HP 81519A optical receiver and the HP 81520A and HP 81521B optical heads. He was project manager for the detector modules and lens interfaces for the HP 8153A lightwave multimeter. He received his Diplom Ingenieur (FH) from the Engineering School of Furtwangen in

70 ▭ Optical Power Meter Calibration

Christian Hentschel

Christian Hentschel is lightwave standards laboratory manager at HP's Böblingen Instruments Division. He studied communications engineering at the University of Aachen, graduating with a Dr. Ing. degree in 1971. He joined HP in 1972, and has since then served in various R&D positions: as project leader for a 1-GHz pulse generator, as project manager for a family of custom bipolar integrated circuits, as project manager for HP's first-generation fiber optic instrumentation, and most recently as technology consultant, specializing in fiber optic instrumentation and international standards for calibrating fiber optic measurement equipment. He is the author of the HP Fiber Optics Handbook. His outside interests include sports, the mountains, and travel.

73 ▭ Semiconductor Laser Sources

Frank A. Maier

Frank Maier studied electrical engineering at the University of Stuttgart, specializing in high-frequency telecommunications. He received his Diplom Ingenieur in 1988 and joined HP's Böblingen Instruments Division in 1989. He designed the laser sources for the HP 8153A lightwave multimeter and did RFI and ESD work on the mainframe. He's a member of VDE. Frank comes from Waiblingen, Baden-Württemberg and now lives in Schönaich, Baden-Württemberg. His interests include food and wine, literature, classical music, theater, opera, and backpacking.

77 ▭ Lightwave Multimeter Firmware

Wilfried Pless

Senior engineer Wilfried Pless was responsible for the definition of the software for the HP 8153A lightwave multimeter and led the software team. He received his Diplom Ingenieur degree from the Ruhr University at Bochum in 1982 and joined HP in 1983. He

Michael Pott

Michael Pott received his Diplom Ingenieur degree from the University of Dortmund and joined HP's Böblingen Instruments Division in 1989. He contributed to the design, development, implementation, and testing of the HP-IB software for the HP 8153A lightwave multimeter. A native of Hamm, Westfalen, he is married, lives in Schönaich, Baden-Württemberg, and is interested in music, computers, photography, and travel.

Robert Jahn

Software engineer Robert Jahn contributed to the firmware design of the HP 8153A lightwave multimeter. He received his Diplom Ingenieur degree from the University of Dortmund in 1989 and joined HP's Böblingen Instruments Division the same year. Personal computers are both his professional interest and one of his hobbies. Robert was born in Landsberg/Lech, Bavaria, and now lives in Stuttgart. He also likes to play billiards.

88 ▭ HP VUE

Mark A. Champine

Born in St. Louis Park, Minnesota, Mark Champine earned his BS degree in computer science from the University of Minnesota in 1982 and an MS degree in computer science from Boston University in 1987. Mark joined HP Apollo in 1988 and worked as a software engineer on HP VUE for the Domain operating system. Before joining HP Apollo, Mark worked on laser printer graphics at Digital Equipment Corporation, and on hypertext publishing software at Agfa/Compugraphic Corporation. He is a member of the New England branch of ACM SIGGRAPH and has professional interests in object-oriented programming, distributed programming, and hypermedia. Mark is married and lives in Methuen, Massachusetts. Hiking, home remodeling, and reading occupy his leisure time.

A Visual User Interface for the HP-UX and Domain Operating Systems

This graphical user interface provides a friendly and pleasant front end for the HP-UX and Domain* operating systems. It makes these subsystems less intimidating for new users and at the same time provides features that appeal to experienced users.

by Mark A. Champine

THE UNIX** OPERATING SYSTEM has a powerful but hard-to-learn interface, which limits its appeal among casual or less technical users. Both the HP-UX and the Domain operating systems are distinct implementations of the UNIX operating system. HP VUE provides an easy-to-learn and easy-to-use interface to these operating systems. Adherence to OSF/Motif[1] look and feel throughout gives a standard interface style to the various components of HP VUE. There is a point-and-click interface for direct manipulation of the file system, and a number of pull-down menus and dialog boxes that provide a friendly interface to many UNIX utilities (see Fig. 1).

The HP VUE project was initiated in late 1988 at Apollo Computer. After Apollo Computer became a division of Hewlett-Packard, software engineers from HP's Interface Technology Operation in Corvallis, Oregon and HP Apollo began working together to see if their graphical user interface projects could be shared. While much of the design and some of the code was shared, customer needs required that the projects continue in parallel. The result was HP VUE 1.0 for the Apollo Domain operating system, which was released first, and later HP VUE 2.0 for the HP-UX operating system. This article describes the features and design considerations for HP VUE 1.0. The box on page 97 provides a brief description of features available in HP VUE 2.0.

HP VUE Features

HP VUE is made up of many X client applications (see

*The Domain operating system, or Domain/OS, runs on the Apollo Series 10000, 4500, 3500, 3000, and 2500 computer systems, and the HP Apollo 9000 Series 400.

**UNIX is a registered trademark of UNIX System Laboratories, Inc. in the U.S.A. and other countries.
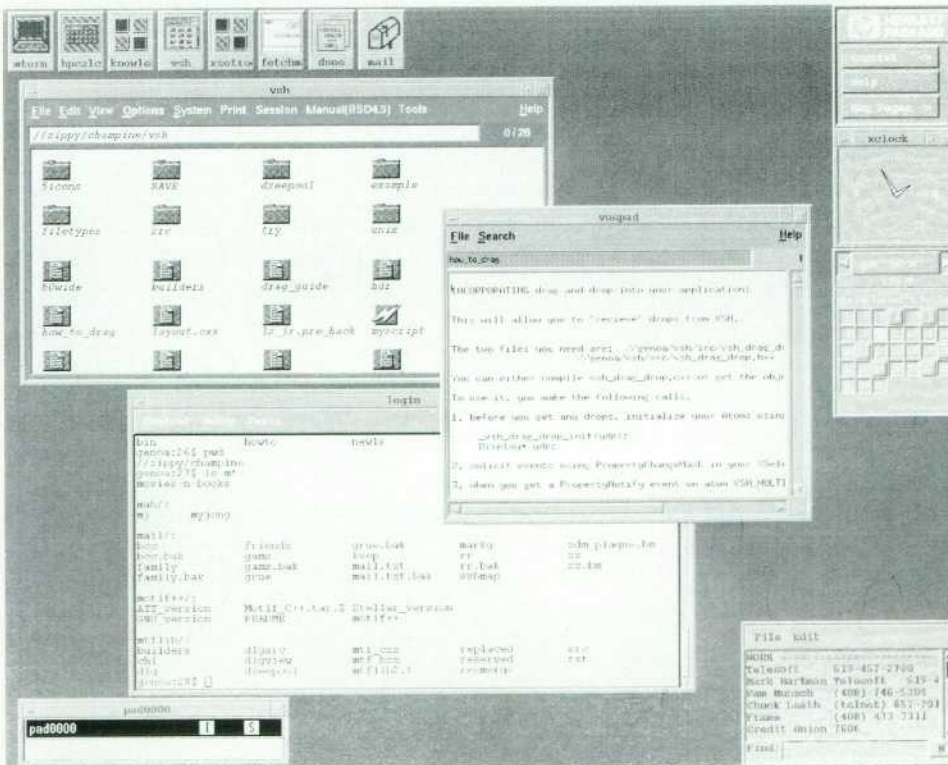

Fig. 1. *The HP VUE user interface. This interface uses the OSF/Motif interface style.*

Fig. 2). The clients were selected to form a useful working set of applications that emulate objects commonly found on a desktop. Each client contributes toward making the environment productive for a broad spectrum of users. The HP VUE components include:

- **Datebook.** A calendar and appointment manager. Datebook lets the user interactively describe periodic events like weekly meetings or one-time events like appointments. These events are signaled by a user-configurable pop-up window appearing on screen at the designated time.
- **Hpcalc.** A scientific calculator that uses postfix or infix notation.
- **Mterm.** An improvement on the X Window System terminal emulator xterm. Mterm provides OSF/Motif pop-up or pull-down menus.
- **Mwm.** The OSF/Motif window manager.[2]
- **Vsh.** The HP VUE visual shell. It provides the interface to the UNIX file system and command execution.
- **Vuepad.** A text file viewer that cooperates with the visual shell.
- **Xctrl.** A control panel that provides access to UNIX man pages, HP VUE help, and screen lock and logout.
- **Xdm.** An OSF/Motif interface for the Athena Xdm session manager. Athena Xdm is an X display manager developed by the Massachusetts Institute of Technology. Xdm presents the login screen, performs user authentication, and on login creates the HP VUE environment by loading X resources and starting clients.
- **Xicon.** A utility to manage program invocation via the desktop icons.
- **Xload.** A system load monitor.

These components have very different origins. The visual shell (vsh) and vuepad are based on Open Dialogue, a user interface management system that provides the OSF/Motif look and feel without having to make OSF/Motif calls (see the box on page 93 for more about Open Dialogue). The other components are based on the OSF/Motif widget set. Many of the OSF/Motif widgets had an earlier incarnation based on other widget sets such as Xaw from project Athena[3] and were converted to OSF/Motif by either the HP VUE team or others.

The command and file system interface to the UNIX operating system is built into HP VUE's iconic desktop application, the visual shell. HP VUE clients are accessible either directly by selecting their icon representation on the display, or by invoking them from vsh. The visual shell is the principal component of HP VUE 1.0.

The Visual Shell

Vsh provides a desktop metaphor for the UNIX file system and the facilities for controlling UNIX command execution. Unlike command line interfaces, such as the C shell (csh) or Korn shell (ksh), the visual shell provides an iconic, direct manipulation interface for files, and a menu and dialog driven interface for command execution.

The three main goals that guided the design of the visual shell were to:

- Provide a path to expertise for new users of a UNIX system
- Provide a powerful, highly customizable interface for experienced users
- Provide an effective look and feel to the user interface.

The UNIX system is quite daunting to newcomers. It features obscure command names, hard to remember command switches, complex regular expressions, pipes, filters, environment variables, and process control. A novice using HP VUE can very quickly learn how to select files, and use the menus to copy, move, and create files and links. Standard options for these commands are set by default and pop-up dialogs guide file manipulation by confirming certain actions and prompting for needed input. Both process control information and environment variables are presented in dialog boxes, with buttons controlling their display and modification.

As a user grows more confident, warnings can be disabled, command switches modified to alter the effect of commands, and commands added to the menu bar (perhaps after looking them up using the HP VUE help facility). This gradual presentation of UNIX facilities makes it more likely that more advanced UNIX functionality will be explored, and that the user will gain enough familiarity with UNIX commands and facilities to use a command line interface when necessary.
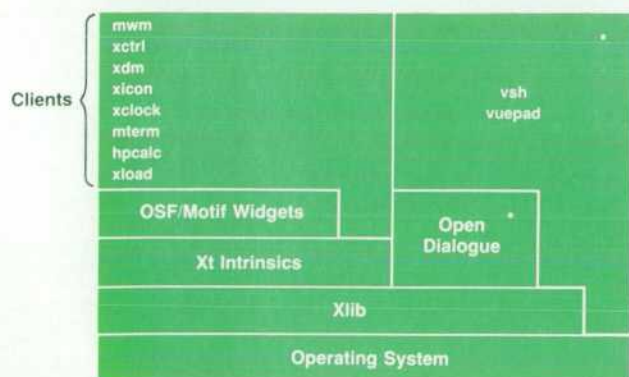
The second goal of building a highly customizable interface to the UNIX system is to avoid handcuffing people already proficient with the UNIX system. Any single-line UNIX command can be run from the command execution dialog box. Keyboard accelerators provide quick access to menus for common operations, and extensibility of the main menu lets the UNIX expert tailor the interface to access quickly and easily those functions particular to the current job.

Finally, addressing the many aspects of providing an effective user interface meant that the product must be visually appealing, have an integrated and complete set of features, be self-consistent, and provide an appropriate and powerful metaphor for the underlying application.

Meeting these goals required an approach to the design from several angles. The approaches to the visual design, the vsh features, the design choices, and the vsh implementation are summarized in the following sections.

Visual Design

Most of the visual appearance of HP VUE is determined

Clients {
mwm
xctrl
xdm
xicon
xclock
mterm
hpcalc
xload

vsh
vuepad

OSF/Motif Widgets

Xt Intrinsics

Open Dialogue

Xlib

Operating System

*Written in C++

Fig. 2. *Components and architecture of HP VUE.*

Fig. 3. *The main window of the visual shell.*

by OSF/Motif. Still, within OSF/Motif conformance there is plenty of room for both good and bad layout of dialogs, sizing, use of color, and use of controls. In the visual shell, much attention was paid to these aspects and to maintaining consistency and predictability throughout.

Main Window. The visual shell uses a typical OSF/Motif layout (see Fig. 3). There is a menu bar across the top, and a scrolled region at the bottom which shows the contents of the current directory. Between these areas is a line called the path bar that displays the current directory path name and two counters. One counter gives the number of objects displayed in the scrolled region, and the other shows how many of those objects are currently selected.

Directory Display Area. The scrolled region, which is called the directory display area, shows icon and filename pairs for each of the objects in the directory. Icon display can be turned off to save screen space, and file attribute information can be enabled to find out more about an object. Objects in the directory display area are laid out in rows and columns, with different object types grouped together (e.g., directories, text files, and links). Since the user generally knows the type of object searched for, grouping objects of the same type together aids a visual search.

Icons. The technique for producing the 3D icons for the directory display area was developed by the same design team that produced the OSF/Motif 3D appearance.[4] With their help, the icon set for the vsh was developed to give a pleasing and integrated look like other OSF/Motif implementations. Visual shell icons have the same simulated light source with the top-left edges highlighted and bottom-right edges shadowed, creating a beveled slab. A raised relief look for the image on top of the slab is created by dithering. The current object types and their associated vsh icons are shown in Fig. 4.

A suprisingly difficult problem was picking icons that represent abstract object types, such as a symbolic link or an executable file. Summing up a complex set of properties in a single, easily recognizable image cannot always be achieved, especially for a diverse user population.

Object count. At all times, vsh displays the number of objects in the directory display area and the number of objects currently selected. This is important because often only a subset of the objects fit into the scrolled region. Additionally, it is possible to have selected files scrolled out of the viewport, and the object counts offer the easiest way to see the selection status when this happens.

Dialog Boxes. Besides the visual aspects of the main window, there is a class of transient, pop-up windows, used to get user input, issue warnings, change configurations, and so on. These dialog boxes must have a readily understandable layout so that the user can quickly perform an action and return to the main window. Most of the visual shell's dialog boxes were redesigned several times, each time improving the layout and refining the set of controls. The layout of common interface components is consistent among all vsh dialog boxes.

Vsh Features

The following is an overview of the visual shell's main features and facilities, which were derived from a process of both original design and evolution during development. Although the need for the majority of the features was foreseen, it was only through actual use that the feature set could be refined to the degree necessary.

Drag and Drop. HP VUE allows the direct manipulation of file objects by using the visual shell's drag and drop
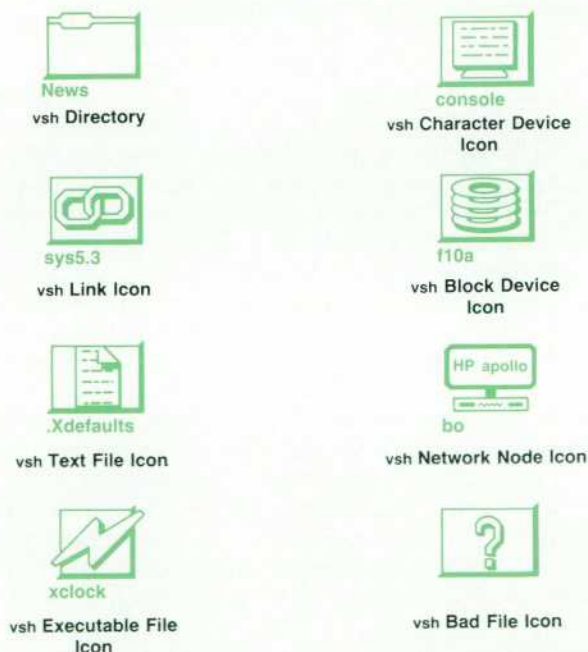

Fig. 4. *Visual shell icons.*

feature. Objects in a directory can be dragged from the visual shell to any application designed to accept vsh drops. This includes another visual shell and vuepad (the file viewer). Any X-based application can be modified to accept drops by incorporating code provided in the product documentation. Depressing the **Shift** key while dragging can modify the meaning of the drag. For example, when a file is dragged from one vsh to another, the **Shift** key changes the nature of the drag from a move operation to a copy.

Menus. One powerful feature of vsh is the capability for users to add menus to the menu bar. Users typically develop their own unique sets of commands. These operations can be made quickly accessible by putting them in the top-level menu. For example, if a user is making the transition from DOS to the UNIX system, a menu called DOS menu can be defined to contain a number of DOS commands like copy and type, which actually invoke their UNIX equivalents (cp and cat) when selected. Another common use is for printing files. The print menu could contain a list of printers and print options.

Command Execution. User commands can be executed quickly from the user-defined pull-down menus, or entered directly into a dialog box. Executed commands are saved in a common command history list.

Startup Configuration. Many aspects of the visual shell can be customized using the X Window System resource manager. The user can choose the format of file objects' display (sort order, with or without icon, etc.), which editor to use on text files, and options to edit menu commands, colors, fonts, and scrollbars.

Process Control. Information about processes running on the system can be viewed in a variety of ways and in different formats. Processes can be selected and sent a UNIX signal (e.g., halt, suspend, resume), which is selectable from a menu, to modify the state of the process.

Keypad Accelerators. Scrolling and selection in the directory display area can be done from the keypad as an alternative to using the mouse.

Vsh Design Choices

The design choices for vsh were the result of an iterative process of testing and refinement. The following is a description of the result of this process. The examples chosen represent the more interesting elements of the design, and what was learned in the process.

Drag and Drop. The goal for the drag and drop operation is to give the user the illusion of moving objects around on the desktop. The visual aspect of the drag operation is implemented by changing the X Window System cursor during the drag. As opposed to doing XOR screen blits* of icon bit maps, we found that this approach provided the advantages of performance, flexibility, and clarity.

- Performance. During heavy system loads and rapid mouse movement, the screen blit technique produces a flashing effect, indicating an insufficient update speed.
- Flexibility. We wanted to indicate, while dragging an icon, the state of a modifier key (e.g., to distinguish a copy operation from a move). Combining this modifier symbol with an arbitrary bit map might produce an awkward looking drag indicator.

*An operation performed on a rectangular area of pixels.

- Clarity. On multiple files, the approach taken by some systems is to show the outline of all files at full size during the drag. This produces an oddly shaped cluster, with the location of the cursor focus not immediately obvious. Some systems compensate for this by highlighting the destination object when it gains focus (i.e., when the cursor is moved into the object's area). With end users writing drop-compatible clients this could not always be expected.

To allow for end users who wish to write programs that cooperate with vsh (any application that acts on UNIX files can benefit), the X Window System's property mechanism is employed to achieve interclient communication.[5] Users can add a small code fragment (provided in source form with the release) to their applications that facilitates interaction between the client program and the vsh. The client can request a list of the objects dropped in one of its windows, along with any keyboard modifiers, the vsh version, and the window identifier of the vsh. This last item is provided so that a completion signal can be sent back to vsh, informing it to refresh the display area window. (The client may have changed or deleted one or more of the dropped files).

User-Defined Menus. Three modes of presenting program output were deemed necessary to cover the spectrum of needs for user-defined menus: foreground, background, and terminal emulation. The foreground mode provides a quick, simple pop-up for text output. The background mode is used for any program that is noninteractive (like daemons) or provides its own interface (like most X Window System clients). Finally, mterm provides terminal emulation for curses-based applications like more and vi.

Attributes of user-defined menus are specified with the keywords given in Table I.

Table I
Keywords for User-Defined Menus

Keyword	Specifies
Menu	The menu title to go in the main menu bar.
Alias	A label in the pull-down menu.
Output	The output mode of the command (foreground, background, or mterm).
Command	UNIX command to be executed when the alias is selected.

Menus can be created with a text editor or interactively through a pop-up dialog box in the vsh (see Fig. 5). In either case, the menus can be read from or written to a file at any time. The following is an example of a user-defined menu in the .vshrc file.

```
menu 'DOS'
{
    alias 'dir'
    {
        output    :  foreground
        command :  'ls'
    }
    alias 'copy'
    {
```
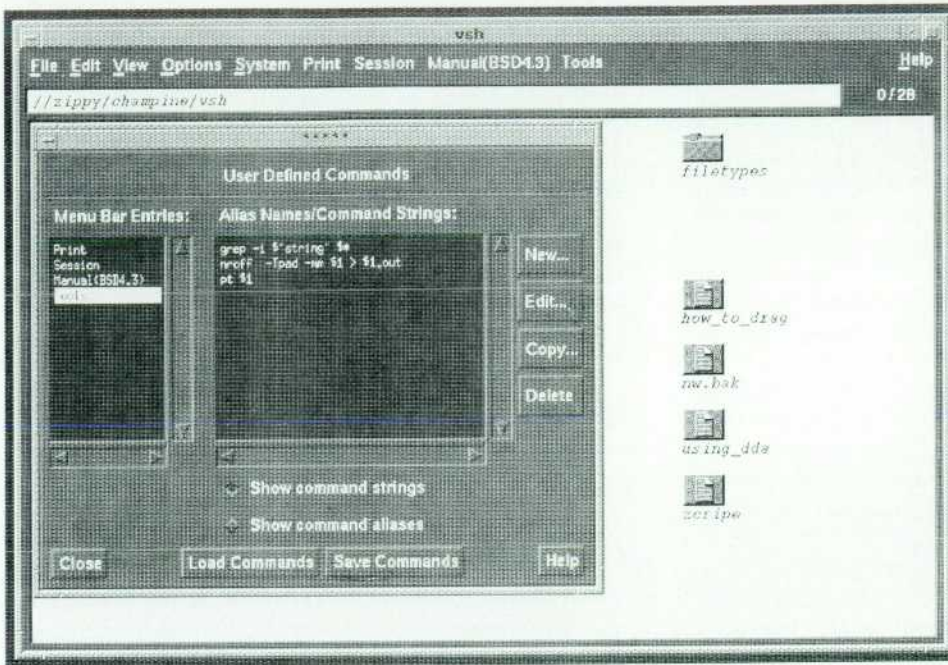
Fig. 5. *Dialog box for interactively creating user-defined menus.*

```
        output    :  foreground
        command  :  'cp'
    }
}
```

When executing user-defined commands, the user gains flexibility when allowed to specify arguments to the command, such as the files to operate on and command line switches. This ability to specify arguments is provided by a command syntax that allows arguments to be substituted into the command, as the following example shows.

```
menu 'Print'
{
    alias 'Print File'
    {
        output    :  foreground
        command  :  'lpr -p laserjet $*'
    }
    alias 'Show gif file'
    {
        output    :  background
        command  :  'xgif $"Print Options" $1'
    }
    alias 'compare'
    {
        output    :  xterm
        command  :  'diff $1 $2 | more'
    }
}
```

This example shows that different commands require different prompts, arguments, and output modes. For the Print File command, the output is foreground because the user will want to see any error and status messages that may be printed out. The parameter $* is replaced with the names of all currently selected files in the directory display area. For the Show gif file command, the output is background because xgif creates its own window. The parameter $"Print Options" causes vsh to pop up a dialog box with the prompt "Print Options" and a text input field (see Fig. 6). This input is then substituted into the command line. This way the command can be used differently each time it is executed. The $1 parameter is replaced by the first item selected in the vsh directory display area. Finally, for the compare command the output is an xterm because the output is piped through more which requires VT100 emulation. The $1 is replaced by the first selected item, $2 with the second.

If more than one $"prompt" field exists in a command then a separate dialog box pops up for each one. A possible extension of command execution would be to provide full dialog facilities for users to create their own custom dialogs to be used in building command strings, so that any number of fields could be satisfield with one pop-up, along with other user interface mechanisms such as radio buttons, scrolled lists, and so on. The drawbacks of adding this extension outweighed the advantage gained for this product. Adding the dialog facility would have taken a great deal of development time and increased the complexity of the menu syntax.

Command Execution History. Each user command executed is saved in a command history list, which enables the commands to be reexecuted at any time by double clicking the mouse on the command string. When commands are executed from the command history, they can be executed in one of two modes: raw or cooked. Raw mode refers to the command before it is interpreted. The result is that new file selections and user prompts are substituted into the command line each time it is run. This is the same as reexecuting the command from a pull-down menu. Cooked mode allows the command to be reexecuted exactly as it was previously using the original filenames and prompted values. Both modes are provided because neither one by itself satisfies the way users reuse commands. When
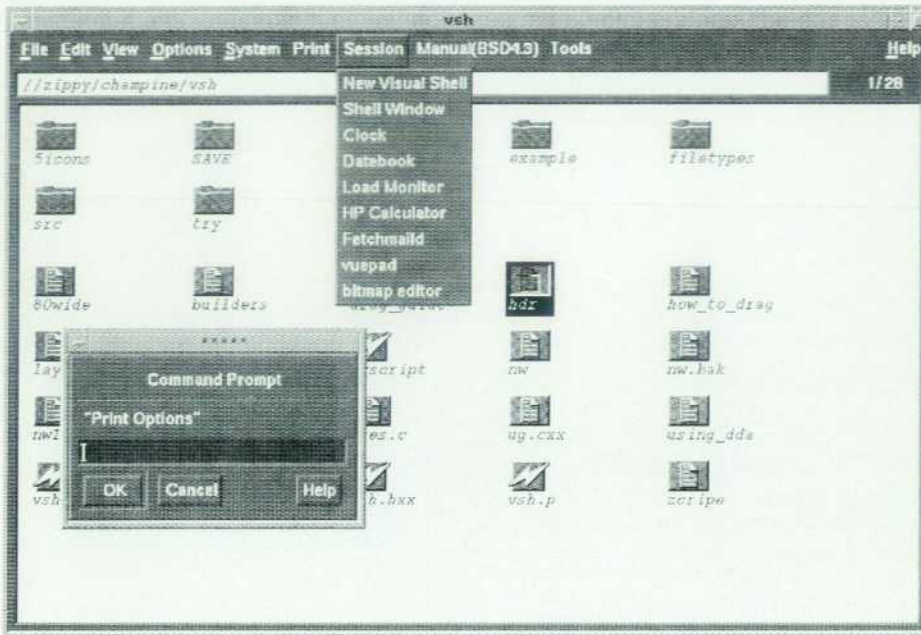
Fig. 6. *Command prompt caused by executing a user-defined command.*

a print command has some complex set of switches, raw mode can be used to substitute a new file selection. When a long path to some file has been specified from a prompt, cooked mode can be used to avoid having to remember or retype the path. Fig. 7 shows command history dialog boxes.

File System Navigation. Navigating through the file system is one of the most common uses of the visual shell. To make navigation as easy as possible and to account for the variety of user preferences, changing directories can be accomplished in several different ways.

- Double Click. A double click on a directory icon in the directory display area opens that directory, that is, makes that directory current and displays its contents.
- Path Bar. A double click in the path bar will navigate up the directory tree to that segment of the path where

---

Open Dialogue

Open Dialogue is an object-oriented user interface management system developed at HP Apollo in 1988. Using Open Dialogue to create an interface to an application allows a programmer to:

- Separate an interface definition from its underlying application code (the interface definition is written in a separate file using Open Dialogue's interface definition language)
- Specify both the presentation and the dialog as part of the interface definition.

An application's interface defines its appearance to the end user. For example, menus and scrollbars are part of an application's interface. The dialog of an interface is the mapping of user actions onto the underlying application. For example, help and error messages, transformation of user input, and calling application subroutines represent the dialog of an interface.

Because Open Dialogue allows the separation of the interface definition from its underlying application code, the application program is only responsible for:

- Calling the Open Dialogue event wait routines that start an interface and waiting for user input
- Processing the user input that is not handled by the interface
- Terminating the interface.

Open Dialog uses data structures called objects to contain the information related to an interface. The data fields in an object are called its variables. By manipulating the values of these variables, the programmer can give an application's interface an initial appearance and behavior and also change the appearance and behavior of an interface once it is running.

Open Dialogue includes a predefined set of classes for creating objects. One set of classes, called utility classes, are the foundation classes on top of which any interface style can be placed. The other two sets of classes can be used to create two distinct interface styles: OSF/Motif-style interfaces and open-style* interfaces.

As a user interface management system, Open Dialogue allows developers to:

- Use an interface previewer tool to prototype an interface separately from the application, providing an iterative approach to interface design
- Develop modular interfaces that are consistent in design from application to application
- Focus more time and attention on the interface than is possible when it is intertwined with the application code
- Develop a multiuser interface for an application, allowing the developer to choose the best style of interaction for a particular group of users
- Define interobject relationships that enable the interface to perform many types of actions without intervention from the application.

*Other available look-and-feel user interfaces that do not conform to OSF/Motif standards.
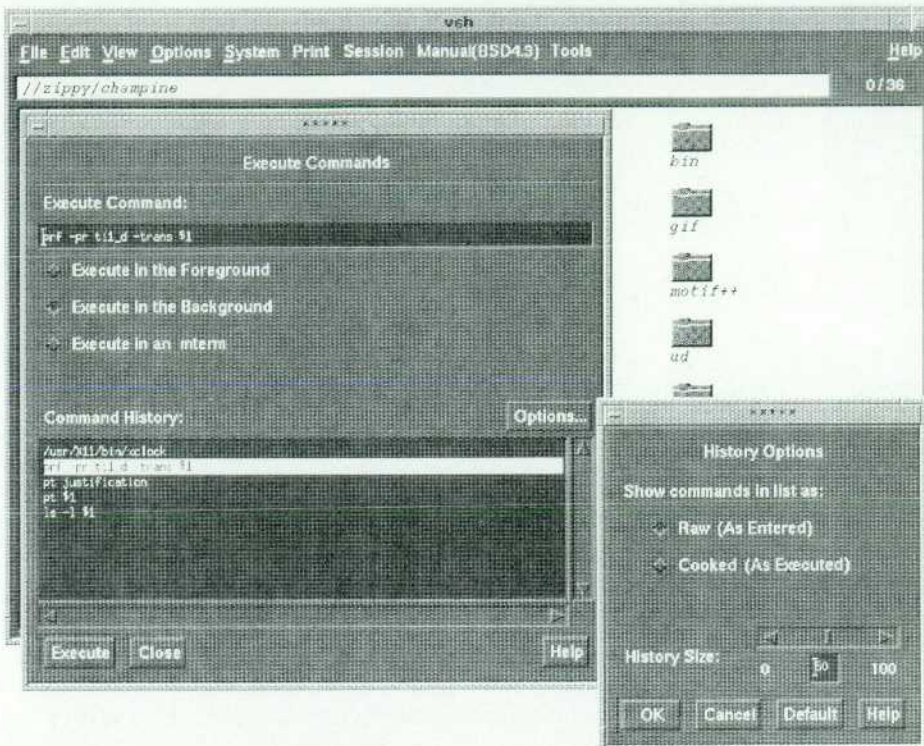
Fig. 7. *Command history dialog box.*

the click occurs. Highlighting on the first click provides feedback to show what the resulting directory will be.

- Dialog. In the Change Directory dialog box, the directory path can be entered directly into a text field, or selected from a history of previous directories. Three buttons allow the user to go up one level, to the home directory or to the node's root directory. The up and home functions also have keyboard accelerator equivalents.

Directory Layout. In the directory display area, files are displayed in a format that is different from the format obtained via a command line interface. For example, the output of the ls command with no options formats filenames into equal-width columns, alphabetically down from the top to the bottom of the leftmost column, continuing at the top of the next column (see Fig. 8a). This format works well when all the filenames can be displayed at the same time. However, when only a section of rows can be displayed and the user scrolls from top to bottom, that format causes a problem because two names that are next to each other alphabetically can be split, with one name at the bottom of a column, and the next name at the top of the next column. For vsh the sort order was changed to go from left to right, top to bottom, to eliminate wasted scrolling (Fig. 8b). Vsh allows directories to be sorted alphabetically, by file creation time, size, filename extension, time last modified, and file type. The default is file type, with directories first. This speeds file system navigation, with directories accessible to be clicked on.

One layout feature that is not included is the ability for the user to place icons interactively. Although a desirable feature, user placement presents many problems on a networked file system. The placement ideally would be specific to each user, so there would be multiple instances of the layout information. All this layout information clutters the file system and wastes space. Also, the files are likely to be manipulated by non-vsh users, leaving many files with no layout information. While there are solutions to most of these obstacles, this functionality was not considered key to the usability of the product.

Process Control. UNIX process information is somewhat cryptic to new users. There are many options to the ps command, and its output has many headings (e.g., PID,CP,PRI,NI, ADDR,SIZE,RSS,WCHAN). What the user usually wants to do with process information is find out what processes are running and which processes are parents of others. With this information the user typically determines which processes to send control signals like kill or suspend. The vsh process control dialog box (Fig. 9) makes available all the process information obtainable through the ps command. Unlike the output of ps, the process table presented by vsh is an indented list of processes with the children of a process displayed indented under their parent. To send control signals, the user need only select the process of interest with the mouse, then select the appropriate signal from a menu.

Edit Menu. Commands in the edit menu do not edit text files, they edit the file system. The edit commands move, delete, and copy apply to files in the current directory, and each command in the edit menu implements a UNIX command.

There are two approaches for implementing UNIX commands. One is to use the popen(3S)* facility to execute the command. This has the advantage of being portable to any UNIX system, and of course the code for the command is already written and stable, which would save development

---

*Popen creates a pipe between the calling program and the command to be executed.
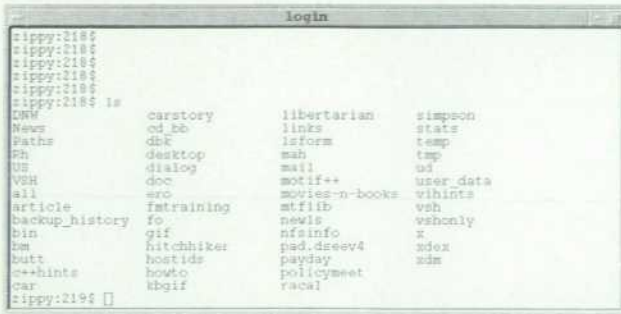
(a)
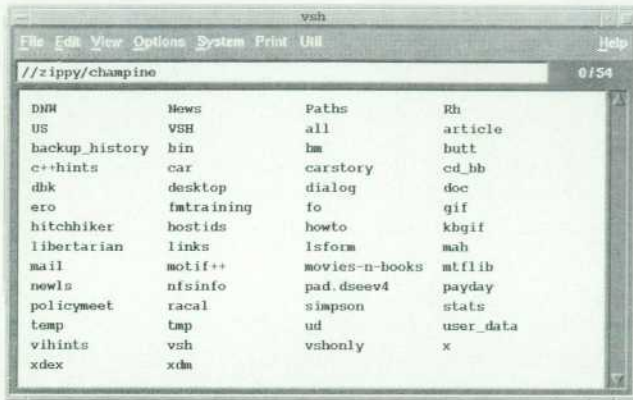
(b)

Fig. 8. *(a) Regular* ls *command output. (b)* Vsh *format for directory listing.*

time. The other approach is to rewrite the commands. The advantages here are performance (there is a delay for popen to start a process) and flexibility, especially for error handling.

We decided on the approach of rewriting the commands because it made it much easier to provide feedback during command execution—for example, getting confirmation on deleting a file many subdirectories below the current one during a recursive delete. The code to handle any prompts, errors, or other exceptions could be embedded right in the code. Using popen would have limited error handling to simply passing along the errors produced by the UNIX command, which would not be very user friendly.

Delete Leaves Holes. Initially, when files were deleted from the current directory, many users in our test groups commented on the temporary confusion caused by reformatting the directory display area after a delete. One of the strengths of iconic interfaces is the consistency of object position, which allows quick location by the user. When that consistency is disrupted, time is wasted while the user reorients to the new layout. Therefore, when objects are deleted, either by menu, keyboard accelerator, or drag and drop, the spaces where the objects existed are left open until the user initiates a refresh, or executes a command that causes a refresh (see Fig. 10).

When objects are added, we decided not to delay refreshing the display area window. The problem is that if the display area is not reformatted, the sort order is violated, and this outweighs the advantage of undisturbed display layout.

Fixed Set of Icons. Some of the reasons for using a fixed set of icons are clarity, consistency, and performance. If the user is allowed to provide icons for directory display,
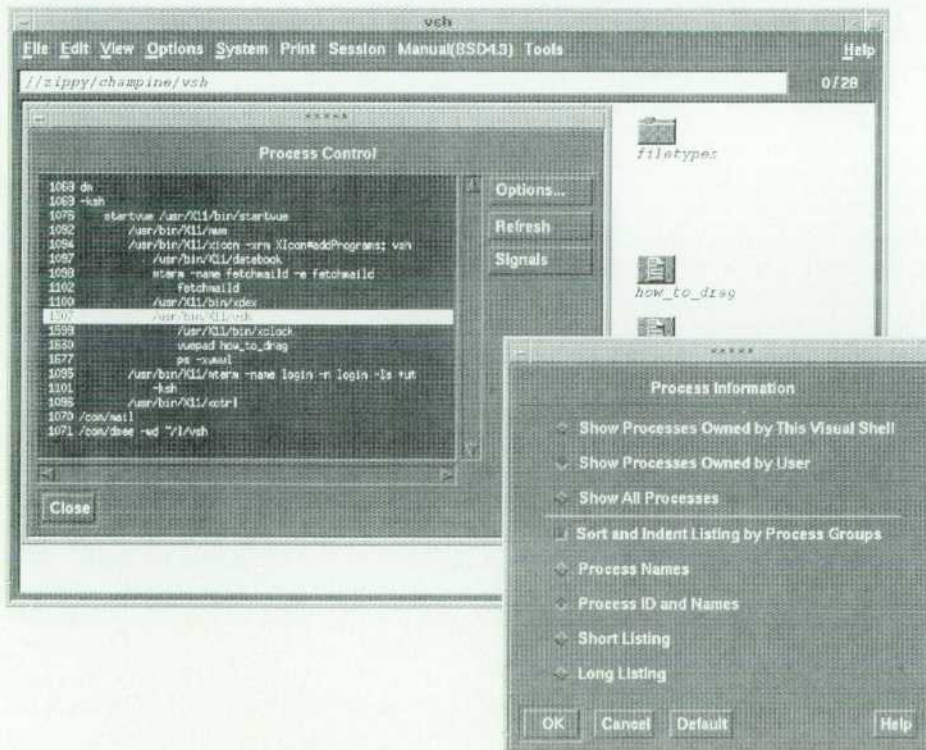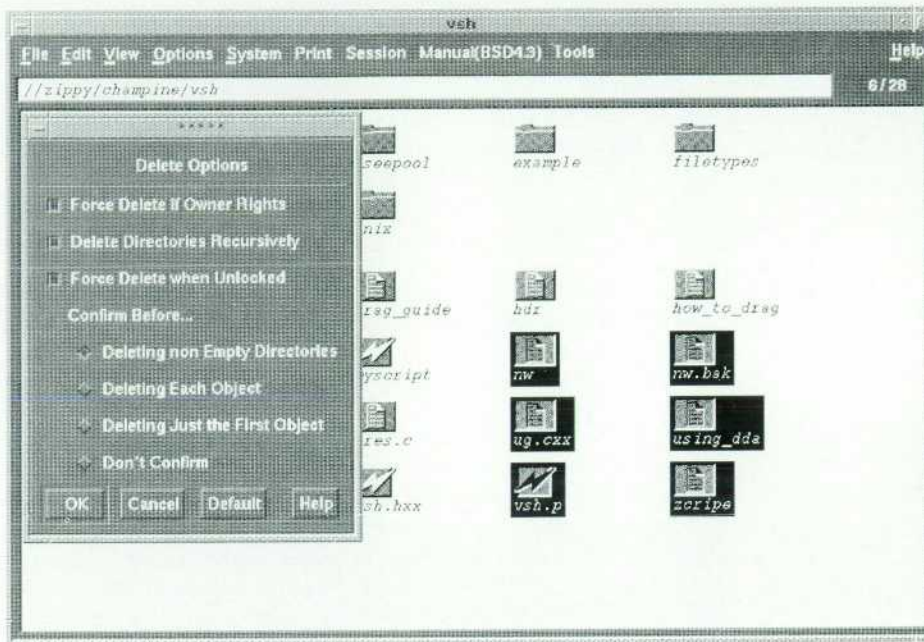

Fig. 9. *Process control dialog box.*

Fig. 10. *Delete options in* vsh.

there is the possibility of a loss of clarity because of the multiplicity of icon types and their possible lack of common style. Only by using built-in icons can a consistent 3D look be ensured, and only by limiting the total number of icons can the confusion of large numbers of icons be avoided.

Inconsistency can creep in when trying to associate certain filenames with the type of icon to display. Since the name of the file and its type may not have any correspondence, false information can easily be displayed. Filename extensions such as .c for C source and .o for object files are informal conventions at best.

Finally, the speed of displaying a directory can be slowed by the pattern matching required on every file name.

There is clearly a desire by many users to configure their own icon set. This issue presented trade-offs that were resolved on the basis of the overall design philosophy and expected client base.

Keyboard Accelerators. Although the mouse is easy and simple to use, and is invaluable for certain pointing operations, most users will move toward keyboard accelerators as they become more experienced with them. The reason is speed. It takes time moving the hand from keyboard, to mouse, and back. Vsh provides a set of accelerators for scrolling and pointing in the directory display area.

Unfortunately many mouse-based systems, while easy to learn, do not provide adequate keyboard substitutes. Expert users will become frustrated if they are required to pick through several menus or go to the mouse for something that can easily be done with a single keystroke.

Script and Text File Pop-up. When the user double clicks on an object in the directory display area, that object is opened. The meaning of open is different for each type of file object. Opening a directory navigates to that directory, and opening an executable file runs it as a program.

One interesting problem encountered was that for one class of file objects—shell scripts—there was a conflict about what the open action should be. A shell script is both a text file and an executable. Therefore, when a script is opened, the user is given a pop-up with a choice of what action to perform. The alternative to providing this one pop-up would be to let the user choose an open action before opening any object. Since this slows and complicates the open operation, and since the alternative open actions can be accessed through a user-defined menu, it was decided that the pop-up was the best compromise.

Displaying Links. UNIX links are something that takes some time for new UNIX users to get used to. For most purposes, the user doesn't care whether the file being edited is actually there or is just a link. The behavior is the same. By default, links in the vsh are not displayed as links. They appear as real files because of the way that the user interacts with them. The display mode can be changed to display the link itself if the distinction between links and files needs to be made. (For example, deleting a soft link does not destroy the original file).

Updating the File-System View. It is problematic to maintain total consistency between the file system and the view of the file system provided by vsh since they are not tightly coupled. There are many ways for the files in a directory to change that don't involve the vsh. One way to maximize consistency would be to check for a change in the modification time of the current directory periodically, say every second or so. This of course would cause wasted compute cycles and more important, the view could change and reorganize unexpectedly while operating on the directory. This would be very disconcerting and hard to use. The compromise reached for the vsh allows an update of the directory display area on any user-initiated action that brings up a dialog, changes files, or changes display attributes. This way, updates don't appear to be random, or out of nowhere. Updates are connected to user actions, but the directory display area is updated often enough so that the display and the directory seldom get far out of synchroni-

HP Visual User Interface, Version 2.0

While cooperation between HP's Interface Technology Operation (ITO) and HP Apollo allowed for many similarities between HP VUE 1.0 (for Domain/OS) and HP VUE 2.0* (for the HP-UX operating system), several differences exist. HP VUE 2.0 provides the same interface capabilities as HP VUE 1.0, but with additional features. The most significant additions in HP VUE 2.0 from a users perspective include:

- Use of HP OSF/Motif 1.1[1]
- A workspace manager
- File manager action and file typing capabilities
- Style manager interactive customization.

HP OSF/Motif 1.1

HP VUE 2.0 is built on HP OSF/Motif 1.1, which includes a style guide that defines a common user interface behavior consistent with Presentation Manager, a window manager to control graphical objects on the display screen, a software toolkit of widgets and intrinsics with which to build applications, and a user interface language to speed application prototyping. Since HP OSF/Motif 1.1 was developed at ITO, HP VUE 2.0 is the first product to use it. HP VUE 2.0 also makes extensive use of HP SoftBench's broadcast message server,[2] a dispatcher of messages between various tools in a user's software engineering environment.

Workspace Manager

The most visually distinctive attribute of HP VUE 2.0 is the workspace manager, the front panel located at the bottom of the screen (see Fig. 1). The workspace manager delivers the following capabilities.

Multiple Workspaces. The workspace manager extends the OSF/Motif window manager to provide multiple, virtual screens, or workspaces. The workspace can be used for organizing applications or projects, and the user can change from one workspace to another with the click of a mouse. The default number of workspaces is six, but this and all components of the workspace manager can be extensively customized using the vuemrc file, a resource file that describes each facet of the workspace manager.

Drop Zones. These front-panel areas accept file or directory icons as inputs in addition to their behavior as an HP OSF/Motif toggle or pushbutton. Drop zones included with the workspace manager are:

- Trash. Files or directory icons dropped on this drop zone are moved to a temporary holding directory for later permanent removal. Clicking on the trash button opens a view of the trash contents and a pull-down menu is provided to allow the user to restore or destroy the contents.
- Printer. Using the action data base, which is described below, icons dropped on the printer icon can be routed to different printers according to need. For example, PostScript® files can go to an HP LaserJet printer with a PostScript cartridge, and xwd files, which are full-color dump files, can be routed through the appropriate filters and then sent to an HP PaintJet printer. Clicking on the printer drop zone brings up a printer status window. The printer status indicates what jobs are in the queue for each printer on the system and what printers are on-line and running.

For visual feedback, a drop zone assumes a pushed-in status

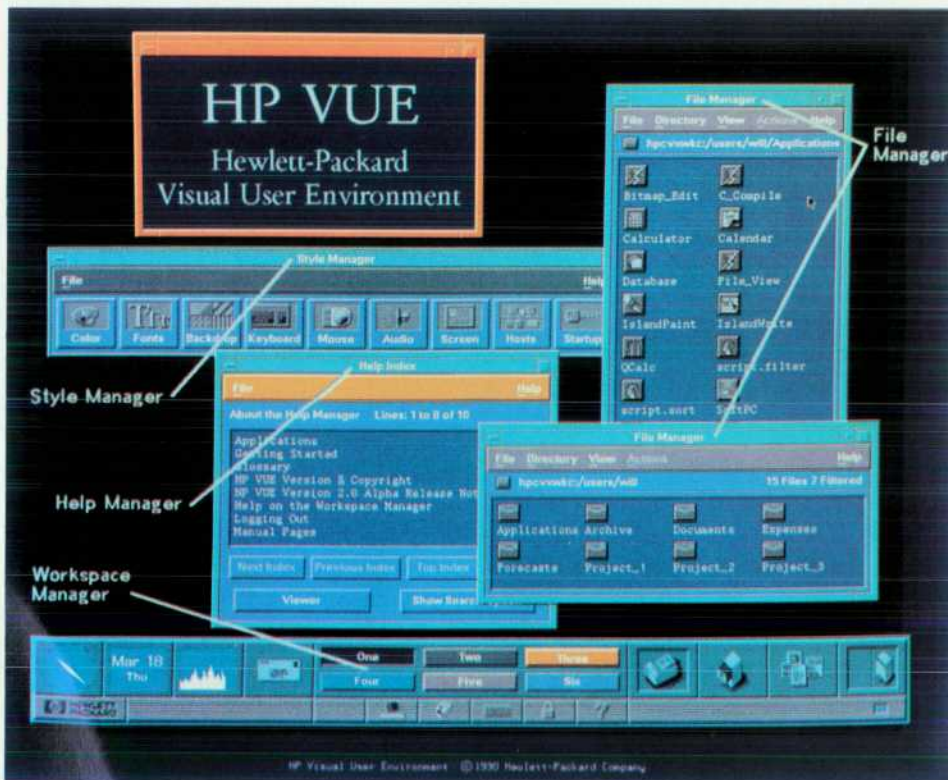*As of this writing HP VUE 2.0 is being ported to Domain/OS.

Fig. 1. *HP VUE 2.0 user interface features.*

when an icon is positioned over it. Additionally, a drop zone's bit map can be animated when an icon is dropped on it. The trash zone, for example, has doors that open to receive the trash, and a sheet of paper comes out of the printer. This is accomplished through a series of bit maps specified in the vuemrc file in conjunction with the animation capabilities of HP SoftBench.

Buttons in HP VUE 2.0. Buttons provide for opening the file manager, application directory, style manager, help manager, mail (elm), HPterm, workspace naming, and optionally the IconBox. The mail button also indicates when new mail has arrived.

System Indicators. HP VUE 2.0 uses the functions xload, which provides a histogram of CPU load, and xclock, which displays an analog clock.

File Manager's Action and File Typing Capabilities

Similar to HP VUE 1.0, HP VUE 2.0 provides an iconic view and manipulation of the file system. Additionally, HP VUE 2.0 provides a data base of file types and actions to perform on various file types. For example, HP VUE 2.0 can differentiate between using a bit-map editor on a bit-map file and a text editor on a text file. The file type and the action data base can be edited automatically or manually when installing an application (no changes need to be made to an application for it to work in HP VUE 2.0).

Interactive Customization

HP VUE's style manager allows easy customization of the X environment, with real-time changes to the colors of workspace backdrops, and various other HP VUE 2.0 features. These changes, along with the status of each workspace and what windows are in each workspace, are saved for the next time the user logs into the system.

David A. Williams
Product Manager
Interface Technology Operation

References

1. A.O. Deininger and C.V. Fernandez, "Making Computer Behavior Consistent: The OSF/Motif Graphical User Interface," *Hewlett-Packard Journal*, Vol. 41, no. 3, June 1990, pp. 6-12.
2. M.R. Cagan, "The HP Softbench Environment: An Architecture for a New Generation of Software Tools, *Hewlett-Packard Journal*, Vol. 41, no. 3, June 1990, pp. 36-47.

PostScript is a registered trademark of Adobe Systems, Inc. in the U.S. and other countries.

zation. Also, if the user is in any doubt, the display can be refreshed manually.

No Command Line Interface. Determining the best approach of allowing users access to a full command line interface was a difficult design decision. One option considered was the concept of a co-shell: a command line interface that is closely connected with the rest of the visual shell. The advantages of this approach are that it provides a powerful, proven interface for advanced UNIX users. It is familiar to many people, and would be useful for many one-time, complex commands. (Commands that are used regularly would be good candidates for the menu bar). However, this approach has some drawbacks. A command line interface is already provided in the mterm terminal emulator. If a co-shell had been used, the current directory would have had to be coordinated with that of the visual shell, possibly requiring any change directory commands, or any command that would change the current directory's contents, to be trapped and used to update the icon display. Also, it would have required a choice about what to do with command history for the command line—whether it should be merged with the main line history, and how to deal with the raw and cooked command history features. Therefore, instead of a co-shell, the visual shell provides a single-line command interface in a pop-up dialog, avoiding the problems mentioned above.

Implementing HP VUE

In its use of OSF/Motif, the HP VUE that runs on HP Apollo's Domain/OS is actually a hybrid. Most of the desktop clients are based on the OSF/Motif widget set, but two of the clients, vsh and vuepad, while visually and behaviorally identical to widget-based clients, are built using a tool called Open Dialogue, a user interface management system developed at HP Apollo that has been extended to create OSF/Motif interfaces.

Virtually all the routine components of the vsh interface are described using the Open Dialogue interface description language. This language allows the description of the layout hierarchy (interface components, subcomponents, and positional relationships) and the data flow (maintaining state and linkages between interface components). Open Dialogue enhanced productivity when minor changes were made to the interface. We were able to view a new interface without recompiling or relinking the application.

C++ was used as the implementation language for the visual shell. The advantages of using an object-oriented language for software development are beyond the scope of this article, but there are clear advantages in being able to treat graphical screen objects as self-contained entities.[6,7] An interesting result of the early design phases is a hierarchy of object classes used in the display of file objects. Directory objects contain two subclasses, data attributes and visual attributes. Data attributes are those items retrieved from the UNIX stat structure such as file size, type, and protection mode. Visual attributes are used to display the object in the directory display area, such as the icon bit map, filename, and highlight status. A layout class controls positioning, scrolling, and selection of objects in the directory display area. Another useful abstraction is the physical display area class. An instance of this is created for both the path bar and the directory display area. The physical display area maintains the X Window System window identifier and display and graphical context information, manages exposure events, and handles drags and drops. The physical display area also has a full set of graphics operations that insulate the rest of the application from making any direct X calls.

Conclusion

With the introduction of HP VUE, HP is providing a

complete user environment for the HP-UX and Domain operating systems. This is an end-user product that provides the power of a direct-manipulation interface to advance the usefulness of HP and Apollo desktop workstations. We have built this environment with a new login manager, session manager, visual shell, terminal emulator, advanced calendar and scheduling tool, and a variety of other desktop accessories.

The major advance in user interaction is the visual shell. It provides an icon-based view of the file system. The function of UNIX commands like cd, ls, and pwd is provided by the point-and-click interface. The most common UNIX commands are handled by pull-down menus. All of the common functions used for working with files and directories are built in. Copying or moving files involve a simple drag and drop action with the mouse. Viewing files is done the same way; drag a file to the file viewer (vuepad) and see it immediately.

To augment the UNIX commands, the visual shell is extensible. Users can add new pull-down menus and menu entries either from a simple text startup file, or dynamically via the built-in interface. This allows anyone to encapsulate the specific commands they use most often. The commands can either launch stand-alone applications or act on the objects in the directory display area.

Acknowledgments

References

1. A. O. Deininger and C.V. Fernandez, "Making Computer Behavior Consistent: The HP OSF/Motif Graphical User Interface," *Hewlett-Packard Journal*, Vol. 41, no. 3, June 1990, pp. 6-12.
2. B. C. Krizan and K. M. Taylor, "The HP OSF/Motif Window Manager," *Hewlett-Packard Journal*, Vol. 41, no. 3, June 1990, pp.12-26.
3. D. L. McMinds and B. J. Ellsworth, "The Evolution of Widgets," *Hewlett-Packard Journal*, Vol. 41, no. 3, June 1990, pp. 27-28.
4. S. R. Anderson and J. Chaffee, "Creating an Effective User Interface for HP IVIBuild," *Hewlett-Packard Journal*, Vol. 41, no. 5 October 1990, pp. 39-48.
5. B. C. Krizan and K. M. Taylor, "Interclient Communication Conventions," *Hewlett-Packard Journal*, Vol. 41, no. 3, June 1990, pp. 23-24.
6. J. A. Dysart, "The NewWave Object Management Facility," *Hewlett-Packard Journal*, Vol. 40, no. 4, August 1989, pp. 17-23.
7. T. F. Kraemer, "Product Development Using Object-Oriented Software Technology," *Hewlett-Packard Journal*, Vol. 40, no. 4, August 1989, pp. 87-100.

Hewlett-Packard Company, 3200 Hillview
Avenue, Palo Alto, California 94304

ADDRESS CORRECTION REQUESTED

CHANGE OF ADDRESS:

To subscribe, change your address, or delete your name from our mailing list, send your request to Hewlett-Packard Journal, 3200 Hillview Avenue, Palo Alto, CA 94304 U.S.A. Include your old address label, if any. Allow 60 days.

5091-0638E